

**THE STUDY OF A NEW AND  
SPECIFIC PROLINE CLEAVING  
PEPTIDASE FROM BOVINE SERUM**

**Thesis Submitted for the Degree of**

**Doctor of Philosophy**

**by**

**Patrick J. Collins B.Sc.**

**Supervised by**

**Dr. Brendan F.O'Connor**

**School of Biotechnology**

**Dublin City University**

**Ireland**

**August 2003**

**Declaration**

I hereby certify that the material I now submit for assessment on the program of study leading to the award of Doctor of Philosophy, is entirely my own work and has not been taken from the work of others save and to the extent that such work has been cited and acknowledged within the text

Signed: Patrick Collins  
Patrick Collins

ID No.: 95051201

Date: 5/9/03.

## Acknowledgements

I would like to thank the following

Brendan O'Connor, my supervisor who was always there throughout for advice and encouragement. Your great enthusiasm made the whole experience a lot easier and enjoyable.

My family, even though I believe they really didn't have a clue what I was actually at, for their encouragement and slugging for being a student for so long. I would like to give special thanks to my parents who were great to me during those write-up months at home- true greats.

The lab members past and present. To Yvonne who was great when I began my projects for advice and ideas. Seamus who I worked with for most of my postgraduate, I really enjoyed the scientific discussions and the craic we had (with mad dog) outside of our scientific life. You probably are the only cork man I like seeing as I am from Kerry. To the new recruit Pam for her help in the final months, good luck with your project.

Thanks to a few drinking buddies for an enjoyable time, Caroline, Sinead, Dave (we must go back to Praha!!!), Clarkey etc. It was a laugh at times.

My housemates and undergrad friends, Colm (candy), Darragh, Brian, James, Ado and Mike for the good few rips we had.

A special thanks to Paraic and Roman. Paraic my good mate and fellow lab rat since our early BT days. Those long chats on every topic possible were good and quite amusing, enough said. Roman for his help during the write-up and I think our knowledge on "kinetics" at this stage is unmatched!!!

And the most important, Orla ("Switch off Pat") who was without doubt so influential throughout my Ph.D. You were always there to listen, encourage and care when I needed it most. Simply the best- thanks for everything.

## Publications

### **Papers**

McMahon, G., Collins, P. and O'Connor, B. (2003) Characterisation of the active site of a newly discovered and potentially significant post proline cleaving endopeptidase called ZIP using LC-UV-MS. *The Analyst* **128**(6), 670-675.

Buckley, S.J., Collins, P. and O'Connor, B. (2003) The Purification and Characterisation of novel dipeptidyl peptidase IV-like activity from bovine serum. *The International Journal of Biochemistry and Cell Biology*. [Accepted for publication, February 2003].

Collins, P., McMahon, G. and O'Connor, B. (2003) Substrate Specificity Studies of a New Proline- Specific endopeptidase. [In preparation].

Collins, P. and O'Connor, B. (2003) A Highly Sensitive Fluorimetric Assay for the Detection of Seprase Activity. [In preparation for *Analytical Biochemistry*].

Collins, P. and O'Connor, B. (2003) The Prolyl oligopeptidase Family- A Review. [In preparation]

### **Poster Presentation**

"Neurotransmitter Transporters: Molecular Mechanism and Regulation", Neuroscience group. Biochemical Society Meeting, 11-13 July 2001, Trinity College Dublin.

### **Oral Presentation**

The Purification and Characterisation of a New Proline Specific Peptidase from Bovine Serum. Probiobdrug AG, Halle, Germany. November, 2002.

## Abbreviations

$\beta$ Na	$\beta$ -naphthylamide
2-NNAp	$\beta$ -naphthylamide
A $\beta$	Amyloid $\beta$ -protein
AA	Amino Acid
ACN	Acetonitrile
AEBSF	4-(2-aminoethyl)-benzenesulfonyl fluoride
AMC	7-amino-4-methylcoumarin
APMSF	4-amidino-phenylmethane-sulphonyl fluoride
BCA	Bicinchoninic Acid
Bisacryl	Bisacrylamide
BSA	Bovine Serum Albumin
BT	Benzothiazol
Bz	Benzoyl
CAPS	3[cyclohexylamino]-1-propanesulphonic acid
cDNA	copy Deoxyribonucleic acid
CN	2-nitrile
Conc.	Concentration
CPC	Calcium Phosphate Cellulose
DFP	Diisopropyl fluorophosphates
DPP IV	Dipeptidyl peptidase IV
DP IV	Dipeptidyl peptidase IV
DTT	Dithiothreitol
eds.	Editors
EDTA	Ethylenediaminetetra acetic acid
EH	Eadie-Hofstee
EtOH	Ethanol
Fmoc	9-fluorenylmethyloxycarbonyl
FPLC	Fast Protein Liquid Chromatography
HCl	Hydrochloric Acid
HIC	Hydrophobic Interaction Chromatography
HPLC	High Performance Liquid Chromatography

HW	Hanes-Woolf
IC <sub>50</sub>	Concentration at which enzyme is 50% inhibited
IgG	Immunoglobulin G
JTP-4819	(S)-2-[[[(S)-2-(hydroxyacetyl)-1-pyrrolidinyl]carbonyl]-N-phenylmethyl]-1-pyrrolidinecarboxamide
K <sub>i</sub>	Inhibition Constant
K <sub>m</sub>	Michaelis constant
LB	Lineweaver-Burk
LHRH	Luteinising hormone-releasing hormone
Log	Logarithm
MW	Molecular Weight
MeOH	Methanol
NaCl	Sodium Chloride
NaOH	Sodium Hydroxide
ND	Not determined
NEM	N-ethyl maleimide
PAGE	Polyacrylamide gel electrophoresis
PE	Prolyl Endopeptidase
PEP	Prolyl Endopeptidase
pH	log of the reciprocal of the hydrogen ion concentration
pI	Isoelectric point
PMSF	Phenylmethanesulphonylfluoride
PO	Prolyl oligopeptidase
POP	Prolyl oligopeptidase
PVDF	Polyvinylidene fluoride
Pyrr	Pyrrolidide
RCO	Acyl
RP	Reverse phase
S9	Prolyl oligopeptidase family of serine proteases
SDS	Sodium dodecyl sulphate
SE	Standard Error
S-S	Disulphide bridges
Suc-	Succinyl
TEMED	N, N, N, N'-tetramethyl ethylenediamine

TFA	Trifluoroacetic acid
TRH	Thyrotropin-releasing hormone
Tris	Tris (hydroxymethyl) amino methane
UV	Ultraviolet
v/v	Volume per volume
Xaa	Any amino acid
Yaa	Any amino acid
Z-	<i>N</i> -benzyloxycarbonyl
Zaa	Any amino acid
ZIP	Z-Pro-prolinal insensitive Z-Gly-Pro-AMC degrading peptidase

### Units

Da	Dalton
g	Gram
hr	Hour
k	Kilo
l	Litre
m	Metre
M	Molar
mM	Millimolar
min	Minute
sec	Second

### Prefixes

c	centi ( $1 \times 10^{-2}$ )
m	milli ( $1 \times 10^{-3}$ )
$\mu$	micro ( $1 \times 10^{-6}$ )
n	nano ( $1 \times 10^{-9}$ )
p	pico ( $1 \times 10^{-12}$ )

## Amino Acid Abbreviations

Ala	<b>A</b>	Alanine
Arg	<b>R</b>	Arginine
Asn	<b>D</b>	Asparagine
Asp	<b>N</b>	Aspartic acid
Cys	<b>C</b>	Cysteine
Gln	<b>Q</b>	Glutamine
Glu	<b>E</b>	Glutamic Acid
Gly	<b>G</b>	Glycine
His	<b>H</b>	Histidine
Ile	<b>I</b>	Isoleucine
Leu	<b>L</b>	Leucine
Lys	<b>K</b>	Lysine
Met	<b>M</b>	Methionine
Phe	<b>F</b>	Phenylalanine
Pro	<b>P</b>	Proline
Ser	<b>S</b>	Serine
Thr	<b>T</b>	Threonine
Trp	<b>W</b>	Tryptophan
Tyr	<b>Y</b>	Tyrosine
Val	<b>V</b>	Valine



<b>Declaration</b>	<b>I</b>
<b>Acknowledgements</b>	<b>II</b>
<b>Publications</b>	<b>III</b>
<b>Abbreviations</b>	<b>IV</b>
<b>Table of Contents</b>	<b>VIII</b>
<b>List of Figures</b>	<b>XV</b>
<b>List of Tables</b>	<b>XIX</b>
<b>Abstract</b>	<b>XXI</b>

### **Table of Contents**

<b>1.0. <u>Introduction</u> - The Prolyl Oligopeptidase Family</b>	<b>2</b>
<b>1.1. Proteolytic Enzymes: Serine Proteases</b>	<b>2</b>
<b>1.2. Prolyl Oligopeptidase</b>	<b>5</b>
1.2.1. Distribution	5
1.2.2. Purification	6
1.2.3. Activity Detection	7
1.2.4. Structural and Biochemical Aspects	8
1.2.5. Catalytic Classification	12
1.2.6. Catalytic and Structural Mechanism	14
1.2.7. Substrate Specificity	17
1.2.8. Inhibitors	21
1.2.9. Physiological Relevance	24
<b>1.3. Dipeptidyl Peptidase IV</b>	<b>26</b>
1.3.1. Distribution	26
1.3.2. Purification	27
1.3.3. Activity Detection	29
1.3.4. Structural and Biochemical Aspects	30
1.3.5. Catalytic Classification	35

1.3.6.	Catalytic and Structural Mechanism	36
1.3.7.	Substrate Specificity	40
1.3.8.	Inhibitors	41
1.3.9.	Physiological Relevance	43
<b>1.4.</b>	<b>Seprase</b>	<b>46</b>
1.4.1.	Distribution and Purification	46
1.4.2.	Activity Detection and Specificity	46
1.4.3.	Structural and Biochemical Aspects	47
1.4.4.	Catalytic Classification	48
1.4.5.	Catalytic and Structural Mechanism	48
1.4.6.	Inhibitors and Physiological Relevance	49
<b>1.5.</b>	<b>Oligopeptidase B</b>	<b>50</b>
1.5.1.	Distribution and Purification	50
1.5.2.	Biochemical and Structural Aspects	51
1.5.3.	Activity Detection	53
1.5.4.	Catalytic Classification	53
1.5.5.	Catalytic and Structural Mechanism	55
1.5.6.	Substrate Specificity and Inhibitors	57
1.5.7.	Physiological Relevance	58
<b>1.6.</b>	<b>Acylaminoacyl Peptidase</b>	<b>60</b>
1.6.1.	Distribution and Purification	60
1.6.2.	Biochemical and Structural Aspects	61
1.6.3.	Substrate Specificity and Activity Detection	62
1.6.4.	Catalytic Classification	62
1.6.5.	Catalytic Mechanism	63
1.6.6.	Inhibitors and Physiological Relevance	63

2.11.2.1. Native Polyacrylamide Gel Electrophoresis	88
2.11.2.2. UV Zymogram Assessment	88
2.11.2.3. Protein G Affinity Chromatography	88
2.11.2.4. Gelatin Sepharose Chromatography	89
<b>3.0. <u>Results</u></b>	
<b>3.1. Protein Determination</b>	<b>91</b>
<b>3.2. AMC Standard Curves and the Inner Filter Effect</b>	<b>93</b>
<b>3.3. Purification of ZIP Activity From Bovine Serum</b>	<b>96</b>
3.3.1. Serum Preparation	96
3.3.2. Phenyl Sepharose Hydrophobic Interaction Chromatography	96
3.3.3. Calcium Phosphate Cellulose Chromatography	96
3.3.4. Cibacron Blue 3GA Chromatography	96
3.3.5. Sephacryl S-300 Size Exclusion Chromatography	97
<b>3.4. Purity Assessment of ZIP</b>	<b>104</b>
3.4.1. Fluorimetric Assays	104
3.4.2. SDS Polyacrylamide Gel Electrophoresis	104
<b>3.5. Substrate Specificity Studies</b>	<b>106</b>
3.5.1. Effect of Residues Located NH <sub>2</sub> -Terminally from the scissile Bond	106
3.5.2. K <sub>m</sub> Determination for Z-Gly-Pro-AMC	108
3.5.3. Effect of Residues at the COOH-Terminal Site of the Scissile Bond	110
3.5.3.1. Amino Acid Preference After the Proline Residue	110
3.5.3.1.1. Determination of K <sub>i</sub> Values	110
3.5.3.1.2. Reverse Phase HPLC	115
3.5.3.1.3. LC-MS Analysis	125
3.5.3.2. Chain Length Elongation at the Carboxyl Terminal Site	133
3.5.3.2.1. Determination of K <sub>i</sub> Values	133
3.5.3.2.2. Reverse Phase HPLC Analysis	137

4.4.1.1.	Serum Preparation	178
4.4.1.2.	Phenyl Sepharose Hydrophobic Chromatography	179
4.4.1.3.	Calcium Phosphate Cellulose Chromatography	180
4.4.1.4.	Cibacron Blue 3GA Chromatography	180
4.4.1.5.	S-300HR Gel Filtration Chromatography	181
<b>4.5.</b>	<b>Purity Assessment</b>	<b>182</b>
<b>4.6.</b>	<b>Substrate Specificity</b>	<b>183</b>
<b>4.7.</b>	<b>Partial Purification of Prolyl Oligopeptidase From Bovine Serum</b>	<b>188</b>
4.7.1.	Phenyl Sepharose Hydrophobic Interaction Chromatography I	188
4.7.2.	Phenyl Sepharose Hydrophobic Interaction Chromatography II	188
4.7.3.	Cibacron Blue 3GA	189
<b>4.8.</b>	<b>Inhibitor Studies</b>	<b>189</b>
4.8.1.	Catalytic Classification	189
4.8.2.	Effect of Specific Prolyl Oligopeptidase Inhibitors	190
<b>4.9.</b>	<b>Immunological Studies</b>	<b>192</b>
<b>4.10.</b>	<b>Identification of Z-Pro-prolinal Peptidase</b>	<b>193</b>
<b>5.0.</b>	<b><u>Bibliography</u></b>	
<b>6.0.</b>	<b><u>Appendix</u></b>	

## List of Figures

### Introduction

<b>Figure 1.1.</b>	<b>Three-Dimensional Structure of Prolyl Oligopeptidase</b>	9
<b>Figure 1.2.</b>	<b>Structural Diagram of the <math>\beta</math>-Propeller Domain</b>	10
<b>Figure 1.3.</b>	<b>Schematic Representation of the Catalytic Mechanism of Serine Proteases</b>	14
<b>Figure 1.4</b>	<b>A View of the Active Site of Prolyl Oligopeptidase</b>	15
<b>Figure 1.5.</b>	<b><math>\beta</math>-Propeller Domain with Closed Velcro Topology</b>	16
<b>Figure 1.6.</b>	<b>Schematic Representation of an Enzyme-Substrate Complex</b>	18
<b>Figure 1.7.</b>	<b>Chemical Structure of Prolyl Oligopeptidase Inhibitors</b>	23
<b>Figure 1.8.</b>	<b>Secondary Structure of DP-IV</b>	30
<b>Figure 1.9.</b>	<b>Structure of Dipeptidyl Peptidase IV</b>	31
<b>Figure 1.10.</b>	<b>Structural Comparisons of DP-IV and Prolyl Oligopeptidase</b>	32
<b>Figure 1.11.</b>	<b>Active Site View of DP-IV</b>	37
<b>Figure 1.12.</b>	<b>Substrate Selectivity of Dipeptidyl Peptidase IV</b>	40
<b>Figure 1.13.</b>	<b>The Chemical Structure of Inhibitor Val-Pyrrolidine</b>	43
<b>Figure 1.14.</b>	<b>Catalytic Domain Homology of OpdB and PO</b>	54
<b>Figure 1.15.</b>	<b>A Model for <i>T. cruzi</i> Oligopeptidase B-Mediated Signalling In Mammalian Cells</b>	59

### Results

<b>Figure 3.1.1.</b>	<b>Biuret Standard Curve</b>	91
<b>Figure 3.1.2.</b>	<b>BCA Standard Curve</b>	92
<b>Figure 3.1.3.</b>	<b>Coomassie Plus Standard Curve</b>	92
<b>Figure 3.2.1.</b>	<b>AMC Standard Curve</b>	94
<b>Figure 3.2.2.</b>	<b>AMC Standard Curve</b>	94
<b>Figure 3.2.3.</b>	<b>Quenched AMC Standard Curve</b>	95
<b>Figure 3.2.4.</b>	<b>Quenched AMC standard Curve</b>	95
<b>Figure 3.3.2.1.</b>	<b>Phenyl Sepharose Elution Profile</b>	98
<b>Figure 3.3.2.2.</b>	<b>Differentiation of ZIP and PO Activities</b>	99

<b>Figure 3.3.3. Calcium Phosphate Cellulose Elution Profile</b>	100
<b>Figure 3.3.4. Cibacron Blue 3GA Elution Profile</b>	101
<b>Figure 3.3.5. S-300 Gel Filtration Elution Profile</b>	102
<b>Figure 3.4.2.1. Gelcode Blue Stained 10% SDS PAGE Gel</b>	105
<b>Figure 3.4.2.2. Silver Stained SDS PAGE Gel</b>	105
<b>Figure 3.5.1.1. HPLC Chromatogram of Z-Pro-Phe</b>	107
<b>Figure 3.5.1.2. HPLC Chromatogram of Z-Pro-Phe Incubate with ZIP</b>	107
<b>Figure 3.5.2.1. <math>K_m</math> Determination of ZIP (LB)</b>	108
<b>Figure 3.5.2.2. <math>K_m</math> Determination of ZIP (EH)</b>	109
<b>Figure 3.5.2.3. <math>K_m</math> Determination of ZIP (HW)</b>	109
<b>Figure 3.5.3.1.1.1. Kinetic Analysis of Z-Gly-Pro-Phe</b>	111
<b>Figure 3.5.3.1.1.2. Kinetic Analysis of Z-Gly-Pro-Met</b>	111
<b>Figure 3.5.3.1.1.3. Kinetic Analysis of Z-Gly-Pro-Tyr</b>	112
<b>Figure 3.5.3.1.1.4. Kinetic Analysis of Z-Gly-Pro-Ser</b>	112
<b>Figure 3.5.3.1.1.5. Kinetic Analysis of Z-Gly-Pro-Glu</b>	113
<b>Figure 3.5.3.1.1.6. Kinetic Analysis of Z-Gly-Pro-His</b>	113
<b>Figure 3.5.3.1.1.7. Kinetic Analysis of Z-Gly-Pro-Leu</b>	114
<b>Figure 3.5.3.1.1.8. Kinetic Analysis of Z-Gly-Pro-Ala</b>	114
<b>Figure 3.5.3.1.2.1. HPLC Chromatogram of Z-Gly-Pro-Phe</b>	116
<b>Figure 3.5.3.1.2.2. HPLC Chromatogram of Z-Gly-Pro-Phe with ZIP</b>	116
<b>Figure 3.5.3.1.2.3. HPLC Chromatogram of Z-Gly-Pro-Met</b>	117
<b>Figure 3.5.3.1.2.4. HPLC Chromatogram of Z-Gly-Pro-Met with ZIP</b>	117
<b>Figure 3.5.3.1.2.5. HPLC Chromatogram of Z-Gly-Pro-Tyr</b>	118
<b>Figure 3.5.3.1.2.6. HPLC Chromatogram of Z-Gly-Pro-Tyr with ZIP</b>	118
<b>Figure 3.5.3.1.2.7. HPLC Chromatogram of Z-Gly-Pro-Ser</b>	119
<b>Figure 3.5.3.1.2.8. HPLC Chromatogram of Z-Gly-Pro-Ser with ZIP</b>	119
<b>Figure 3.5.3.1.2.9. HPLC Chromatogram of Z-Gly-Pro-Glu</b>	120
<b>Figure 3.5.3.1.2.10. HPLC Chromatogram of Z-Gly-Pro-Glu with ZIP</b>	120
<b>Figure 3.5.3.1.2.11. HPLC Chromatogram of Z-Gly-Pro-His</b>	121
<b>Figure 3.5.3.1.2.12. HPLC Chromatogram of Z-Gly-Pro-His with ZIP</b>	121
<b>Figure 3.5.3.1.2.13. HPLC Chromatogram of Z-Gly-Pro-Leu</b>	122
<b>Figure 3.5.3.1.2.14. HPLC Chromatogram of Z-Gly-Pro-Leu with ZIP</b>	122
<b>Figure 3.5.3.1.2.15. HPLC Chromatogram of Z-Gly-Pro-Ala</b>	123
<b>Figure 3.5.3.1.2.16. HPLC Chromatogram of Z-Gly-Pro-Ala with ZIP</b>	123

<b>Figure 3.5.3.1.2.17. HPLC Chromatogram of Z-Gly-Pro Standard</b>	124
<b>Figure 3.5.3.1.2.18. Z-Gly-Pro Standard Curve</b>	124
<b>Figure 3.5.3.1.3.1. LC-MS Spectra of Z-Gly-Pro-Phe Digestion</b>	126
<b>Figure 3.5.3.1.3.2. LC-MS Spectra of Z-Gly-Pro-Met Digestion</b>	127
<b>Figure 3.5.3.1.3.3. LC-MS Spectra of Z-Gly-Pro-Tyr Digestion</b>	128
<b>Figure 3.5.3.1.3.4. LC-MS Spectra of Z-Gly-Pro-Ser Digestion</b>	129
<b>Figure 3.5.3.1.3.5. LC-MS Spectra of Z-Gly-Pro-Glu-Digestion</b>	130
<b>Figure 3.5.3.1.3.6. LC-MS Spectra of Z-Gly-Pro-His Digestion</b>	131
<b>Figure 3.5.3.1.3.7. LC-MS Spectra of Z-Gly-Pro-Ala Digestion</b>	132
<b>Figure 3.5.3.2.1.1. Kinetic Analysis of Z-Gly-Pro-Phe-His</b>	134
<b>Figure 3.5.3.2.1.2. Kinetic Analysis of Z-Gly-Pro-Phe-His-Arg</b>	134
<b>Figure 3.5.3.2.1.3. Kinetic Analysis of Z-Gly-Pro-Phe-His-Arg-Ser</b>	135
<b>Figure 3.5.3.2.1.4. Kinetic Analysis of Z-Gly-Pro-Met-His</b>	135
<b>Figure 3.5.3.2.1.5. Kinetic Analysis of Z-Gly-Pro-Met-His-Arg</b>	136
<b>Figure 3.5.3.2.1.6. Kinetic Analysis of Z-Gly-Pro-Met-His-Arg-Ser</b>	136
<b>Figure 3.5.3.2.2.1. HPLC Chromatogram of Z-Gly-Pro-Phe-His</b>	138
<b>Figure 3.5.3.2.2.2. HPLC Chromatogram of Z-Gly-Pro-Phe-His with ZIP</b>	138
<b>Figure 3.5.3.2.2.3. HPLC Chromatogram of Z-Gly-Pro-Phe-His-Arg</b>	139
<b>Figure 3.5.3.2.2.4. HPLC Chromatogram of Z-Gly-Pro-Phe-His-Arg with ZIP</b>	139
<b>Figure 3.5.3.2.2.5. HPLC Chromatogram of Z-Gly-Pro-Phe-His-Arg-Ser</b>	140
<b>Figure 3.5.3.2.2.6. HPLC Chromatogram of Z-Gly-Pro-Phe-His-Arg-Ser with ZIP</b>	140
<b>Figure 3.5.3.2.3.1. LC-MS Spectra of Z-Gly-Pro-Phe-His Digestion</b>	141
<b>Figure 3.5.3.2.3.2. LC-MS Spectra of Z-Gly-Pro-Phe-His-Arg Digestion</b>	142
<b>Figure 3.5.3.2.3.3. LC-MS Spectra of Z-Gly-Pro-Phe-His-Arg-Ser Digestion</b>	143
<b>Figure 3.5.3.2.3.4. LC-MS Spectra of Z-Gly-Pro-Met-His Digestion</b>	144
<b>Figure 3.5.3.2.3.5. LC-MS Spectra of Z-Gly-Pro-Met-His-Arg Digestion</b>	145
<b>Figure 3.5.3.2.3.6. LC-MS Spectra of Z-Gly-Pro-Met-His-Arg-Ser Digestion</b>	146
<b>Figure 3.5.4.1. Kinetic Analysis of Z-Gly-Leu-Phe-His</b>	148
<b>Figure 3.5.4.2.1. HPLC Chromatogram of Z-Gly-Leu-Phe-His</b>	149
<b>Figure 3.5.4.2.2. HPLC Chromatogram of Z-Gly-Leu-Phe-His with ZIP</b>	149
<b>Figure 3.5.4.2.3. HPLC Chromatogram of Z-Gly-Leu Standard</b>	150
<b>Figure 3.5.4.3. LC-MS Spectra of Z-Gly-Leu-Phe-His Digestion</b>	151
<b>Figure 3.6.1. Phenyl Sepharose I Elution Profile of PO</b>	154
<b>Figure 3.6.2. Phenyl Sepharose II Elution Profile of PO</b>	155

<b>Figure 3.6.3.</b>	<b>Cibacron Blue 3GA Elution Profile of PO</b>	156
<b>Figure 3.7.1.</b>	<b>Effect of Diisopropylfluorophosphate</b>	158
<b>Figure 3.7.2.1.</b>	<b>Inhibitor Profile Effect of Fmoc-Ala-PyrrCN on PO</b>	160
<b>Figure 3.7.2.2.</b>	<b>Inhibitor Profile Effect of Fmoc-Ala-PyrrCN on ZIP</b>	160
<b>Figure 3.7.2.3</b>	<b>Inhibitor Profile Effect of Z-Phe-Pro-BT on PO</b>	161
<b>Figure 3.7.2.4.</b>	<b>Inhibitor Profile Effect of Z-Phe-Pro-BT on ZIP</b>	161
<b>Figure 3.7.2.5.</b>	<b>Inhibitor Profile Effect of SR 063298 on PO</b>	162
<b>Figure 3.7.2.6.</b>	<b>Inhibitor Profile Effect of SR 063298 on ZIP</b>	162
<b>Figure 3.7.2.7.</b>	<b>Inhibitor Profile Effect of SR 063125 on PO</b>	163
<b>Figure 3.7.2.8.</b>	<b>Inhibitor Profile Effect of SR 063125 on ZIP</b>	163
<b>Figure 3.7.2.9.</b>	<b>Inhibitor Profile Effect of JTP-4819 on PO</b>	164
<b>Figure 3.7.2.10.</b>	<b>Inhibitor Profile Effect of JTP-4819 on ZIP</b>	164
<b>Figure 3.8.1.1.</b>	<b>Western-Blot Analysis of Bovine ZIP and PO</b>	165
<b>Figure 3.8.1.2.</b>	<b>Western-Blot Analysis of Rat Cortex and Bovine PO</b>	165
<b>Figure 3.9.1.1.</b>	<b>Coomassie-Stained PVDF Membrane Blot</b>	166
<b>Figure 3.9.1.2.</b>	<b>SDS PAGE Gel of Partial Purified ZIP Sample</b>	167
<b>Figure 3.9.2.1.</b>	<b>Native Page Analysis of ZIP Proteolytic Activity</b>	168
<b>Figure 3.9.2.2.</b>	<b>In Gel Assay (Zymogram) and Silver Stain of Native ZIP</b>	169
<b>Figure 3.9.2.3.</b>	<b>Peptides Sequenced for the Identification of ZIP</b>	170
 Discussion		
<b>Figure 4.1.</b>	<b>Chemical Structure of JTP-4819</b>	176
<b>Figure 4.2.</b>	<b>Progress Curve of an Enzyme-Catalysed Reaction</b>	177
<b>Figure 4.3.</b>	<b>Chemical Structure of Prolyl Oligopeptidase Inhibitors</b>	191



## List of Tables

### Introduction

<b>Table 1.1.</b>	<b>Members of the Prolyl Oligopeptidase (S9) Family</b>	4
<b>Table 1.2.</b>	<b>Biochemical Properties of Prolyl Oligopeptidase</b>	11
<b>Table 1.3.</b>	<b>Amino Acid Sequence Surrounding the Active Site Serine</b>	13
<b>Table 1.4.</b>	<b>Bioactive Peptides Hydrolysed by Prolyl Oligopeptidase</b>	20
<b>Table 1.5.</b>	<b>Prolyl Oligopeptidase Specific Inhibitors</b>	23
<b>Table 1.6.</b>	<b>Biochemical Properties of Dipeptidyl Peptidase IV</b>	34
<b>Table 1.7.</b>	<b>Peptides Cleaved By Dipeptidyl Peptidase IV</b>	45
<b>Table 1.8.</b>	<b>Biochemical Properties of Oligopeptidase B</b>	52

### Methods

<b>Table 2.1.</b>	<b>Fluorimetric Substrates Tested</b>	75
<b>Table 2.2.</b>	<b>SDS PAGE Gel Preparation</b>	76
<b>Table 2.3</b>	<b>Silver Staining Procedure</b>	78
<b>Table 2.4.</b>	<b>Peptide Preparation for <math>K_i</math> Determination</b>	79
<b>Table 2.5.</b>	<b>Substrate and Standard Preparation for HPLC and LC-MS</b>	81
<b>Table 2.6.</b>	<b>Preparation of Specific Inhibitors</b>	85

### Results

<b>Table 3.1.</b>	<b>Slopes of Quenched Standard Curves</b>	95
<b>Table 3.2.</b>	<b>Purification Table of ZIP from Bovine Serum</b>	103
<b>Table 3.3.</b>	<b>Purity Assessment using Fluorimetric Substrates</b>	104
<b>Table 3.4.</b>	<b>Effect of Peptides Extended <math>\text{NH}_2</math>-Terminally from the Scissile Bond</b>	106
<b>Table 3.5.</b>	<b><math>K_m</math> Value Obtained for ZIP</b>	110
<b>Table 3.6.</b>	<b><math>K_i</math> (<math>_{app}</math>) Values Obtained for Proline Containing N-blocked Tripeptides</b>	115
<b>Table 3.7.</b>	<b>Quantification of Z-Gly-Pro After Hydrolysis by ZIP</b>	125

<b>Table 3.8.</b>	<b>Kinetic Parameters of Peptides Extended COOH-Terminally From the Scissile Bond</b>	133
<b>Table 3.9.</b>	<b>Quantification of Z-Gly-Pro OF Peptides Extended COOH-Terminally After Hydrolysis by ZIP</b>	137
<b>Table 3.10.</b>	<b>Importance of a Proline Residue in the P<sub>1</sub> Position</b>	147
<b>Table 3.11.</b>	<b>Overall Substrate Specificity Results for ZIP</b>	152
<b>Table 3.12.</b>	<b>Purification Table of PO From Bovine Serum</b>	157
<b>Table 3.13.</b>	<b>IC<sub>50</sub> Values Determined for PO Inhibitors</b>	159

Discussion

<b>Table 4.1.</b>	<b>Comparison of Protein Determination Assays</b>	175
<b>Table 4.2.</b>	<b>Comparison of the Biochemical Properties of ZIP and Seprase</b>	196

## Abstract

*Prolyl oligopeptidase is a serine peptidase characterised by oligoendopeptidase activity. Definitive evidence for the discrete biological role of prolyl oligopeptidase remains unknown, though its role in the maturation and degradation of peptide hormones and neuropeptides has been implicated. A second activity that readily cleaves the specific prolyl oligopeptidase substrate Z-Gly-Pro-AMC was previously discovered in bovine serum. Due to its complete insensitivity towards the classic prolyl oligopeptidase inhibitor Z-Pro-prolinal, this peptidase was designated Z-Pro-prolinal Insensitive Peptidase (ZIP). The study of this new and specific proline cleaving endopeptidase from bovine serum is presented.*

*ZIP was separated from prolyl oligopeptidase by phenyl sepharose hydrophobic interaction chromatography. The enzyme was further purified 30,197-fold, to homogeneity, using calcium phosphate cellulose, cibacron blue 3GA and gel filtration chromatography in an overall recovery of 12% from bovine serum.*

*Substrate specificity studies using kinetic, HPLC and LC-MS analysis of proline-containing peptides suggest that ZIP has an extended substrate-binding region in addition to the primary specificity site  $S_1$ . This analysis revealed at least five subsites to be involved in enzyme-substrate binding, with the smallest peptide cleaved being a tetrapeptide. A proline residue in position  $P_1$  was absolutely necessary therefore showing high primary substrate specificity for the Pro-X bond, while a preference for a hydrophobic residue at the C-terminal end of the scissile bond ( $P_1'$ ) was evident. An affinity constant ( $K_m$ ) of  $270\mu\text{M}$  using Z-Gly-Pro-AMC was determined.*

*Diisopropylfluorophosphate inactivated ZIP resulting in an  $IC_{50}$  value of  $100\text{nM}$  suggesting catalytic classification as a serine peptidase. ZIP showed complete insensitivity to the prolyl oligopeptidase specific inhibitors, Fmoc-Ala-pyrrCN and Z-Phe-Pro-BT and showed no immunological cross-reactivity with an anti-human prolyl oligopeptidase antibody. Internal peptide sequence analysis of ZIP identified it as seprase, a member of the serine integral membrane peptidases. This protein is overexpressed by tumour cells and may possibly play a significant role in their invasion.*

## **INTRODUCTION**

## 1.0 Introduction - The Prolyl Oligopeptidase Family

### 1.1. Proteolytic Enzymes: Serine Proteases

Proteolytic enzymes or proteases represent a class of enzymes with important roles in physiological process. These enzymes are involved in essential biological processes like blood clotting, controlled cell death, and tissue differentiation. They catalyse important proteolytic steps in tumour invasion or in infection cycle of a number of pathogenic microorganisms and viruses, making them valuable targets for new pharmaceuticals. They also participate in protein catabolism in degradative or biosynthetic pathways and in the release of hormones and pharmacologically active peptides from precursor proteins. They are also well known to conduct highly specific and selective modifications of proteins such as activation of enzymes by limited proteolysis and collaborate with the transport of secretory proteins across membranes.

Proteases catalyse the cleavage of peptide bonds in proteins or peptides. They are enzymes of class 3, the hydrolases, and subclass 3.4, the peptide hydrolases or peptidases. They constitute a large family (EC 3.4) divided as endopeptidases (proteinases) or exopeptidases according to the point at which they cleave the peptide bond. These proteases can be ordered further, according to the reactive groups at the active site involved in catalysis.

Proteolytic enzymes dependent on a serine residue for catalytic activity are widespread and very numerous. Serine proteases are ubiquitous, being found in viruses, bacteria and eukaryotes and include proteins with endopeptidase, oligopeptidase, exopeptidase and omega-peptidase activity. These proteases conduct proteolysis using a serine side chain as the active site nucleophile. Over 20 families (denoted S1-S27) of serine proteases have been identified, these being grouped in 6 clans (SA, SB, SC, SE, SF and SG) on the basis of structural similarity and other functional evidence (Rawlings and Barrett, 1994). Structures are known for at least four of the clans (SA, SB, SC and SE) and appear to be totally unrelated, suggesting at least four evolutionary origins of serine proteases. There are, however, similarities in the reaction mechanisms of several proteases even with different evolutionary origins. They contain a common catalytic triad of three amino acids: serine (nucleophile), aspartic acid (electrophile) and histidine (base). The geometric orientations of the catalytic residues are similar between families, despite different protein folds. The

linear arrangements of the catalytic residues commonly reflect clan relationships. For example the catalytic triad is ordered HDS in clan SA, DHS in clan SB and SDH in clan SC, of which the prolyl oligopeptidase family is a member (Rawlings and Barrett, 1993; Rawlings and Barrett, 1994).

The prolyl oligopeptidase family represents a relatively new group of serine peptidases, unrelated to the well-known trypsin and subtilisin families. This group includes dipeptidyl peptidase IV, acylaminoacyl peptidase, prolyl oligopeptidase and oligopeptidase B (Rawlings *et al.* 1991; Rawlings and Barrett, 1994). The prolyl oligopeptidase group called family S9 is a member of the SC clan of serine proteases. Due to the structural relationship between these enzymes and lipases (Polgar, 1992a), on secondary structural studies (Goosens *et al.* 1995) and most recently on three-dimensional (3D) structures these enzymes are considered to be members of the  $\alpha/\beta$  hydrolase fold enzymes. The amino acid sequence homology of the four main peptidases is quite low but as shown with prolyl oligopeptidase and dipeptidyl peptidase IV they all possibly share a similar tertiary structure. They display distinct specificities and represent different types of peptidases. Prolyl oligopeptidase and oligopeptidase B are endopeptidases (oligopeptidases) which are found in the cytosol. Dipeptidyl peptidase IV and acylaminoacyl peptidase are exopeptidases; dipeptidyl peptidase IV is a membrane bound ectoenzyme, whereas acylaminoacyl peptidase is a cytoplasmic omega peptidase. The structural basis of these enzymes specificity, selectivity, which is restricted to oligopeptides, and catalytic functional regulation has recently been understood by the three-dimensional structures of prolyl oligopeptidase and dipeptidyl peptidase IV (Fulop *et al.* 1998 and 2000; Rasmussen *et al.* 2003; Engel *et al.* 2003).

The catalytic triad residues (Ser, Asp, His) of these enzymes are located in the peptidase domain within about 130 residues of the C-terminus with amino acid sequence homology more significant in this domain between proteins. The enzymes are much larger (about 80 kDa, greater for dipeptidyl peptidase IV due to the transmembrane domain) than the trypsin and subtilisin serine proteases (25-30kDa), and do not possess any zymogen form. The enzymes of this family are involved in important physiological processes (Polgar, 2002a).

<b>Subfamily</b>	<b>Peptidase</b>	<b>EC No.</b>	<b>Peptidase Type</b>
Subfamily S9A	Prolyl oligopeptidase	3.4.21.26	Endopeptidase
	Oligopeptidase B	3.4.21.83	Endopeptidase
Subfamily S9B	Dipeptidyl peptidase IV	3.4.14.5.	<b>Exopeptidase-</b> Dipeptidase
	Dipeptidyl aminopeptidase A	-	Aminopeptidase
	Dipeptidyl aminopeptidase B	-	Aminopeptidase
	Prolyl tripeptidyl peptidase	-	Tripeptidase
	Dipeptidyl peptidase 8	-	Dipeptidase
	Dipeptidyl peptidase 9	-	Dipeptidase
	Fibroblast activation protein $\alpha$ /Seprase	-	<b>Endopeptidase-</b> Gelatinase
Subfamily S9C	Acylaminoacyl peptidase	3.4.19.1	<b>Exopeptidase-</b> Omega peptidase
Subfamily S9D	Glutamyl endopeptidase (plant)	-	Endopeptidase

**Table 1.1. Members of the Prolyl Oligopeptidase (S9) Family of Serine Proteases**

## 1.2. Prolyl oligopeptidase

Prolyl oligopeptidase (EC 3.4.21.26) is a member of the new serine peptidase group, the prolyl oligopeptidase family, classified under family S9A of the clan SC (Barrett *et al.* 1998). This activity was first reported as an oxytocin-inactivating enzyme in human uterus (Walter *et al.* 1971). Further studies on this oxytocin-degrading enzyme (Walter, 1976; Koida and Walter, 1976) revealed a high specificity for the amino acid proline, cleaving the peptide bond on its carboxyl side. It was subsequently called post proline cleaving endopeptidase (PPCE). Several enzymes with similar specificity like thyrotropin-releasing hormone deaminase from rat brain (Rupnow *et al.* 1979), brain kinase B from rabbit brain (Oliveira *et al.* 1976) and endo-oligopeptidase B were previously described, which later proved to have been identical to prolyl oligopeptidase. The selectivity of the enzyme for oligopeptides was discovered in the nineteen seventies by Camargo *et al.* (1979). The name prolyl endopeptidase was first recommended by the Enzyme Nomenclature in 1981, but later was changed to prolyl oligopeptidase, emphasising the special characteristics of this enzyme.

### 1.2.1. Distribution

Although prolyl oligopeptidase is predominantly a cytosolic enzyme (Dresdner *et al.* 1982), the presence of prolyl oligopeptidase activity has been detected in the particulate fractions of brush border kidney cells (Sudo and Tanabe, 1985), N1E 115 (neuroblastoma) cells (Checler *et al.* 1986) and human and rat brain neurons (Irazusta *et al.* 2002). O'Leary and O'Connor (1995) reported the purification and characterisation of a novel membrane bound form of prolyl oligopeptidase from bovine brain. The synaptosomal membrane localisation and the higher affinity of this particulate form compared to cytosolic enzyme for certain peptide substrates (O'Leary *et al.* 1996) may be of potential physiological significance in relation to neuropeptide hydrolysis.

Localisation studies performed by Irazusta *et al.* (2002) compared rat tissular distribution of soluble and particulate prolyl oligopeptidase activity. The levels of activity in both cases was more than two-fold greater in the brain than in any other tissue studied. Similar localisation studies performed by Kato *et al.* (1980) and Orłowski *et al.* (1979) on human and rabbit tissues showed considerable species to



species variation. While uniformly high levels were reported in brain tissue, high prolyl oligopeptidase activity in humans was observed in skeletal muscle, testes and kidneys compared with rabbit tissue where high activity was seen in the small intestine, lung and spleen with lowest activity observed in skeletal muscle.

As previously mentioned, consistently high prolyl oligopeptidase levels are present in mammalian brain but Irazusta *et al.* (2002) found that both soluble and particulate prolyl oligopeptidase activities were higher in the human brain than the rat brain. Regional distribution of prolyl oligopeptidase activity was highest in the brain cortices and lowest in the cerebellum of human brain. These results agree with previous work by Kato *et al.* (1980). In the rat brain, regional distribution of prolyl oligopeptidase was different to that in human brain with homogenous soluble activity present in most regions but lowest in the cerebellum (Irazusta *et al.* 2002). Tate (1981) has also previously documented this species to species variation in the regional distribution of prolyl oligopeptidase in brain tissue regions.

Subcellular localisation studies showed highest prolyl oligopeptidase activity present in the cytosol with activities lower than those present in nuclear, microsomal and mitochondrial soluble fractions. Particulate prolyl oligopeptidase activity was enriched in the synaptosomes correlating well with previous work by O'Leary and O'Connor (1995) (Irazusta *et al.* 2002).

Prolyl oligopeptidase activity has also been reported in human bodily fluids, although the activities were much lower than that present in tissues (Goosens *et al.* 1996).

### **1.2.2. Purification**

Prolyl oligopeptidase was first isolated from human tissue (Walter *et al.* 1971) and has subsequently been isolated from tissue sources of other mammals (Yoshimoto *et al.* 1981 and 1983), fungi (Yoshimoto *et al.* 1988; Sattar *et al.* 1990), bacteria (Chevallier *et al.* 1992; Kanatani *et al.* 1993) and archaea (Harwood *et al.* 1997). Wide ranges of sources for isolation were initially available due to the enzymes ubiquitous distribution (Goosens *et al.* 1996) and consistently elevated enzyme levels in mammalian brain. The first steps usually employed for the isolation of prolyl oligopeptidase from tissue source involved homogenisation using mechanical and centrifugal forces (Polgar, 1994), followed usually by an ammonium sulphate precipitation step (Yoshimoto *et al.* 1981 and 1983; Kalwant and Porter, 1991).

Yoshimoto *et al.* (1983) employed an anion exchange resin twice for the purification of bovine brain prolyl oligopeptidase, while four DEAE cellulose steps were utilised for the purification of prolyl oligopeptidase from human erythrocytes, giving a 64,000-fold purification (Rosens *et al.* 1991).

Purification of the recombinant enzyme expressed in *Escherichia coli* provides much better yields than the isolation from various tissues (Szeltner *et al.* 2000). Prolyl oligopeptidase has been cloned from several sources such as porcine brain, bovine brain, human lymphocytes, *Flavobacterium meningosepticum* and *Pyrococcus furiosus* (Rennex *et al.* 1991; Yoshimoto *et al.* 1997; Shirasawa *et al.* 1994; Diefenthal *et al.* 1993; Robinson *et al.* 1995).

### 1.2.3. Activity Detection

When prolyl oligopeptidase was first discovered, its known substrates oxytocin and arginine-vasopressin were employed in native or radiolabelled forms for enzyme detection (Walter, 1976). Koida and Walter (1976) used Z-Gly-Pro-Leu-Gly as substrate, detecting cleavage product Leu-Gly with the ninhydrin assay. Since then assays of prolyl oligopeptidase have been performed spectrophotometrically and spectrofluorometrically utilizing N-blocked proline containing dipeptides linked to a cleaved molecule as synthetic substrate. Initially p-nitrophenylesters (Walter and Yoshimoto, 1978), p-nitroanilides (Yoshimoto *et al.* 1978) and naphthylamides (Yoshimoto *et al.* 1979) were used. In 1979, Yoshimoto *et al.* reported the first use of Z-Gly-Pro-AMC (7-amino-4-methylcoumarin), a fluorescent substrate with a  $K_m$  of 20 $\mu$ M for prolyl oligopeptidase from lamb kidney. As mentioned above many prolyl oligopeptidase assays incorporate 2-NNAp ( $\beta$ -naphthylamide), an alternative fluorogenic substrate and pNA (p-nitroanilide) that is a colorimetric substrate but Z-Gly-Pro-AMC shows enhanced sensitivity over these (Polgar, 1994). A succinyl group in the substrate Z-Gly-Pro-AMC has often replaced the benzyloxycarbonyl group making the substrate much more soluble and without requiring organic solvent for solubility. These compounds are poor substrates though, their specificity rate constants being lower by two orders a magnitude than those of the benzyloxycarbonyl derivatives (Polgar, 1994). In a study on the secondary specificity of prolyl oligopeptidase, a ten fold lower  $K_m$  was achieved using 7-amino-4-methyl-2-quinoline

(Meq) as an alternative to AMC. This lower affinity constant was due to glycine in the P<sub>2</sub> position being replaced by positively charged or bulky hydrophobic groups (Noula *et al.* 1997). An added advantage in these substrates is the reduction in solvent required for solubilisation. The discovery of a second peptidase activity in bovine serum (Cunningham and O'Connor, 1997a) capable of cleaving Z-Gly-Pro-AMC, questions its classification as a specific prolyl oligopeptidase substrate.

#### **1.2.4. Structural and Biochemical Aspects**

The first structural information about prolyl oligopeptidase was deduced from the cDNA of the porcine brain enzyme (Rennex *et al.* 1991). This study revealed a single chain protein having a molecular mass of 80,751 Da, calculated from the 710-residue sequence. The peptidase domain was located at the carboxyl terminus and exhibits a characteristic  $\alpha/\beta$  hydrolase fold (Goosens *et al.* 1995). The active site residues serine and histidine were the first to be identified as Ser<sup>554</sup> (Rennex *et al.* 1991) and His<sup>680</sup> (Stone *et al.* 1991) in the porcine brain enzyme. This order of the catalytic residues is the reverse of that found with the trypsin and subtilisin sequences, but corresponds to some lipase sequences (Polgar, 2002a). A structural relationship between lipases and the peptidase domain of oligopeptidases has been indicated. Comparison of the sequences of lipases and oligopeptidases identified Asp<sup>641</sup> as the third member of the catalytic triad (Polgar, 1992a). Goosens *et al.* (1995) also identified Asp<sup>641</sup> as the third member based on sequence alignment and secondary structure prediction of dipeptidyl peptidase IV, acylaminoacyl peptidase and prolyl oligopeptidase.

Fulop *et al.* (1998) revealed the three dimensional structure of prolyl oligopeptidase by x-ray crystallography, in complex with its inhibitor Z-Pro-prolinal. It consists of two domains, a peptidase and a seven bladed  $\beta$ -propeller (Figure 1.1.).

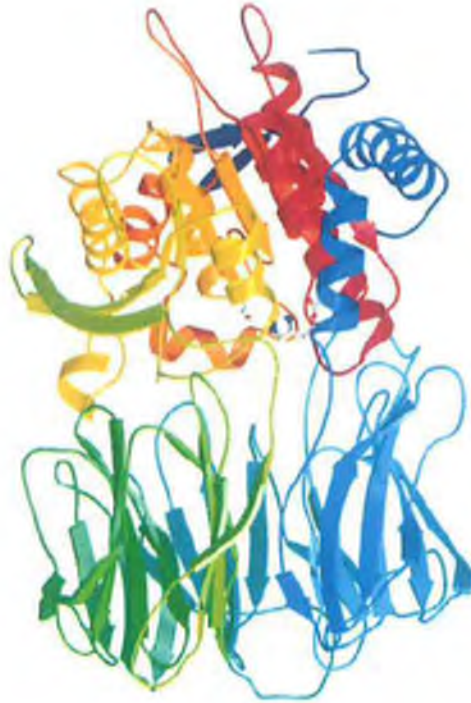


**Figure 1.1. Three-Dimensional Structure Representation of Prolyl oligopeptidase**

The ribbon diagram is colour-ramped blue to red from the N to the C terminus. The catalytic residues are shown in a ball-and-stick representation (Fulop *et al.* 1998).

The peptidase or catalytic domain is built up of residues 1-72 and 428-710. This region was observed to exhibit an  $\alpha/\beta$  hydrolase fold as predicted by Goosens *et al.* (1995). The peptidase domain contains a central eight-stranded  $\beta$ -sheet with all strands except the second one aligned in a parallel manner. The  $\beta$ -sheet is significantly twisted and it is flanked by two helices on one side and six helices on the other.

The  $\beta$ -propeller domain is located between residues 73-427 and is connected to the catalytic domain mainly by hydrophobic forces. The propeller domain is based on a sevenfold repeat of four-stranded antiparallel  $\beta$ -sheets, which are twisted and radially

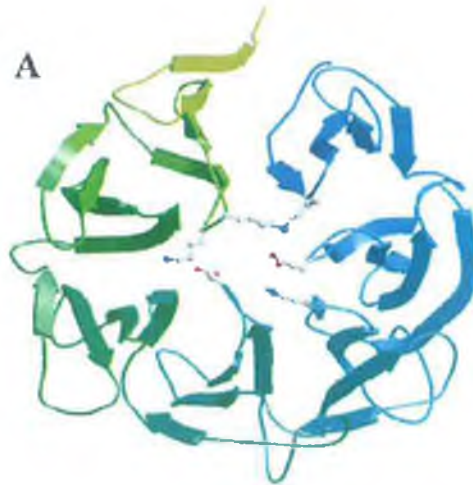


**Figure 1.2. Structural Diagram of the  $\beta$ -Propeller Domain**

The protein chain of the  $\beta$ -propeller domain of prolyl oligopeptidase is coloured as in Figure 1.1. The  $\beta$  sheets of the seven blades are joined in succession around the central axis. The “Velcro” is not closed; there are only hydrophobic interactions between the first (blue) and last (green) blades. Residues narrowing the entrance to the tunnel of the propeller are shown by ball-and-stick representation (Fulop *et al.* 1998)

arranged around their central tunnel. The central tunnel of this  $\beta$ -propeller covers the catalytic triad but unlike other  $\beta$ -propellers the Velcro is not closed between the first and last blades. This structural feature permits partial opening of the propeller and provides access via its tunnel to the active site (Figure 1.2.).

The structure and localization of the mouse prolyl oligopeptidase gene has been accomplished (Kimura *et al.* 1999). It is located at chromosome 10B2-B3, consists of 92 kilobases and contains 15 exons.

Preliminary studies of prolyl oligopeptidase reported this protein to have a dimeric structure with a possible molecular weight of 115-140kDa (Koida and Walter, 1976). It is now known that prolyl oligopeptidase is a monomeric protein ranging in molecular weight from 65-85kDa. Yoshimoto *et al.* (1981) reported a molecular weight of 74-77kDa for lamb brain, while prolyl oligopeptidase from human brain was reported to have a molecular weight of 76.9kDa (Kalwant and Porter, 1991). As mentioned previously, cDNA cloning of porcine brain prolyl oligopeptidase allowed deduction of a monomeric structure with a molecular weight of 80,751kDa. Studies on prolyl oligopeptidase from *Flavobacterium meningosepticum* (Yoshimoto *et al.*

1992) deduced a molecular mass of 78.71kDa for the 705 residues sequenced. This sequence was discovered to contain a signal peptide of twenty amino acids, loss of this peptide resulted in a molecular weight of 76.78kDa (Chevallier *et al.* 1992; Kanatani *et al.* 1993;).

pH optimum values of between 6.5 and 8.5 are reported for bacterial and mammalian prolyl oligopeptidase (Yoshimoto *et al.* 1980 and 1983). Isoelectric points of between 4.8 and 4.9 indicate an acidic nature of mammalian prolyl oligopeptidase (Yoshimoto *et al.* 1983; Goosens *et al.* 1995), while bacterial pI seem to be slightly higher with *Treponema denticola* having a reported pI of 6.5 (Makinen *et al.* 1994).

Source	MW kDa	pI	pH optima	Temp. optima (°C)	Reference
Human Brain	76.9	4.75	6.8	ND	Kalwant and Porter, 1991
Human Lymphocytes	76	4.8	ND	ND	Goosens <i>et al.</i> 1995
Bovine Brain	62-65	4.8	7.0-7.5	40	Yoshimoto <i>et al.</i> 1983
Bovine Serum	69.7	ND	8.0	37	Cunningham and O'Connor, 1998
Lamb Brain	74-77	4.9	7.0	45	Yoshimoto <i>et al.</i> 1981
Porcine Liver	72-74	4.9	6.5	37	Moriyama and Sasaki, 1983
Daucus carota	75	4.8	7.3	37	Yoshimoto <i>et al.</i> 1987a
<i>F. meningosepticum</i>	74	9.6	7.0	40	Yoshimoto <i>et al.</i> 1980
<i>A. hydrophilia</i>	76.4	5.5	8.0	30	Kanatani <i>et al.</i> 1993
<i>T. denticola</i>	75-77	6.5	6.5	ND	Makinen <i>et al.</i> 1994
<i>L. cinerascens</i>	76	5.2	6.8	37	Yoshimoto <i>et al.</i> 1988
<i>P. furiosos</i>	72	5.76	7.5	85-90	Harwood and Schreier, 2001

**Table 1.2. Biochemical Properties of Prolyl Oligopeptidase from Mammalian, Plant and Microbial Sources**

### 1.2.5. Catalytic classification

Prolyl oligopeptidase is an endopeptidase due to its ability to cleave at the carboxyl side of proline residues within oligopeptides (Camargo *et al.* 1979; Wilk, 1983). This enzyme has been classified as a serine protease due to its sensitivity to DFP, Z-Gly-Pro-CH<sub>2</sub>Cl and to a lesser extent PMSF (Rennex *et al.* 1991; Walter *et al.* 1980; Goosens *et al.* 1995). The classification of prolyl oligopeptidase as a serine protease was confirmed by the cloning of the prolyl oligopeptidase gene and subsequent deduction of its amino acid sequence (Rennex *et al.* 1991).

When the amino acid sequence of prolyl oligopeptidase was deduced, no similarity with proteases of known tertiary structure was observed. In 1992, it was first observed that a similarity existed between prolyl oligopeptidase and dipeptidyl peptidase IV (Polgar and Szabo, 1992). They noticed a 21.7% identity between these enzymes in their C-terminal regions. Rawlings *et al.* (1991) agreed with these observations but went on to show an even greater similarity between prolyl oligopeptidase and acylaminoacyl-peptidase based also on their C-terminal residues. This led to the general acceptance that a prolyl oligopeptidase family of serine proteases existed (Barrett and Rawlings, 1992).

The amino acids that surround the active site seryl residue are conserved in each family. With the sequencing of prolyl oligopeptidase by Rennex *et al.* (1991), the amino acids around the active site serine were discovered to be Gly-Gly-Ser-Asn-Gly-Gly. This sequence showed no homology to those from the subtilisin, trypsin or carboxypeptidase families (Table 1.3.). When Barrett and Rawlings (1992) postulated that the greatest similarity between members of the prolyl oligopeptidase family existed at the C-terminal end of the sequence, which contains the catalytic domain, the general consensus sequence GxSxGGzz (x = any amino acid, z = hydrophobic amino acid) was used for identifying other members of this family.

<b>Serine Protease (Family)</b>	<b>Sequence about active site serine</b>
Trypsin	Gly-Asn-Ser-Gly-Gly-Pro
Subtilisin	Gly-Thr-Ser-Met-Ala-Ser/Thr
Carboxypeptidase	Gly-Glu-Ser-Tyr-Ala-Gly
Prolyl oligopeptidase	Gly-Xaa-Ser-Yaa-Gly-Gly
<b>Prolyl oligopeptidase family</b>	
Porcine prolyl oligopeptidase	Gly-Gly-Ser-Asp-Gly-Gly
Rat dipeptidyl peptidase IV	Gly-Trp-Ser-Tyr-Gly-Gly
Porcine acylaminoacyl-peptidase	Gly-Gly-Ser-His-Gly-Gly
<i>E.coli</i> oligopeptidase B	Gly-Gly-Ser-Ala-Gly-Gly
Seprase	Gly-Trp-Ser-Tyr-Gly-Gly

**Table 1.3. Amino Acid Sequences Surrounding the Active Site Serine of Families of Serine Proteases**

Another distinguishing feature of prolyl oligopeptidase is the order of its catalytic triad residues. The linear arrangement of the active site residues of prolyl oligopeptidase, nucleophile-acid-base, differs from that of the established serine proteases but is similar to that of lipases (Polgar, 1992a). In 1995, Goosens *et al.* while studying the secondary structure of prolyl oligopeptidase reported Asp<sup>641</sup> as its third member and showed striking similarity in its secondary structure to dipeptidyl peptidase IV and acylaminoacyl-peptidase. This showed that the order of the catalytic triad of prolyl oligopeptidase (Ser-Asp-His) was unique compared to trypsin (His-Asp-Ser) and subtilisin (Asp-His-Ser) families. Based on the structural similarity between prolyl oligopeptidase and lipases (Polgar, 1992a) and reports on the secondary structure (Goosens *et al.* 1995) of this enzyme, prolyl oligopeptidase was the first known endopeptidase to adopt an  $\alpha/\beta$  hydrolase fold structure. It was also postulated that the prolyl oligopeptidase structure could be an evolutionary link between the exopeptidases and the endopeptidases.



## 1.2.6. Catalytic and Structural Mechanism

### Active site and substrate binding

The catalytic triad (Ser<sup>554</sup>, Asp<sup>641</sup>, His<sup>680</sup>) is located in a large cavity at the interface of the  $\beta$ -propeller and catalytic domains (Fulop *et al.* 1998). These three catalytic amino acids play an essential role in the catalysis. The histidine acts as a general acid-base catalyst activating the nucleophilic group, the hydroxyl group of the serine acts as a nucleophile in the attack on the peptide bond while the aspartic acid stabilizes charged tetrahedral intermediates formed in the reaction (Fink, 1987; Rennex *et al.* 1991).

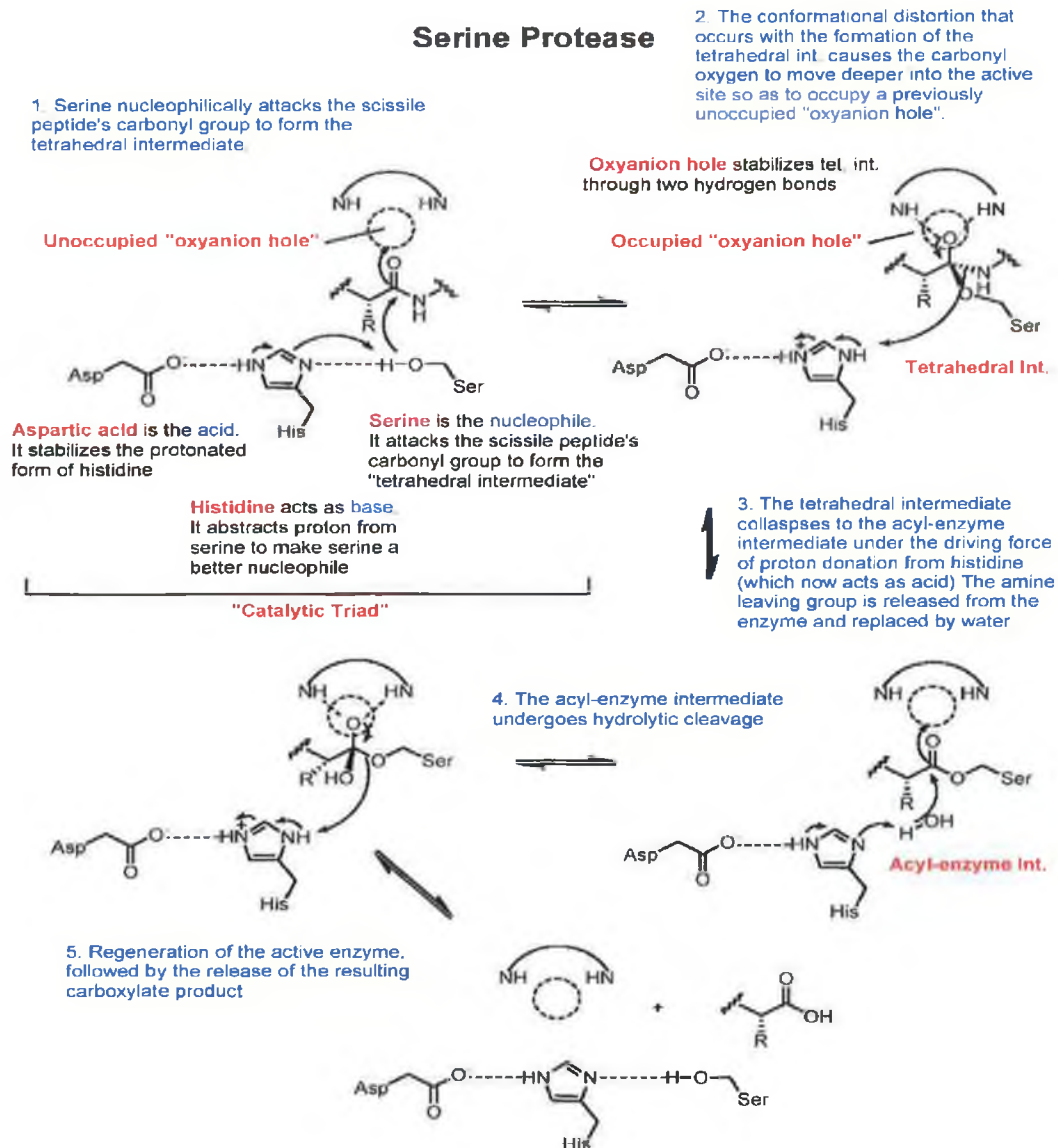


**Figure 1.3. Schematic Representation of the Catalytic Mechanism of Serine Proteases**

The mechanism of action of serine proteases (Figure 1.3.) involves an acyl-enzyme intermediate. Both the formation and decomposition of the acyl-enzyme proceed through the formation of a negatively charged tetrahedral intermediate (Polgar, 2002a).

Fulop *et al.* (1998) were the first to provide information on substrate binding during prolyl oligopeptidase catalysis (Figure 1.4.). Due to the serine OH group being well exposed and readily accessible to the catalytic imidazole group on one side and to the substrate on the other, Figure 1.4. shows that the catalytic serine side chain attacks the aldehyde carbon atom forming a covalent hemiacetal adduct. Proline is accepted well in the  $S_1$  specificity pocket, with specificity also being enhanced by ring stacking between the indole ring of Trp<sup>595</sup> and the inhibitor/substrate proline residue. The binding of the peptide main chain to the enzyme is different with prolyl oligopeptidase and the classic serine proteases. Proline as an imino rather than an amino acid does not possess the main chain NH group for  $S_1P_1$  hydrogen bonding which is essential for trypsin and subtilisin catalysis as they form antiparallel  $\beta$ -sheets with the NH groups of the substrate main chain. So in the binding to prolyl oligopeptidase the  $S_2P_2$  hydrogen bond is very significant. This shows that the architecture of the  $S_1$  binding site has evolved to be much more specific in prolyl oligopeptidase.

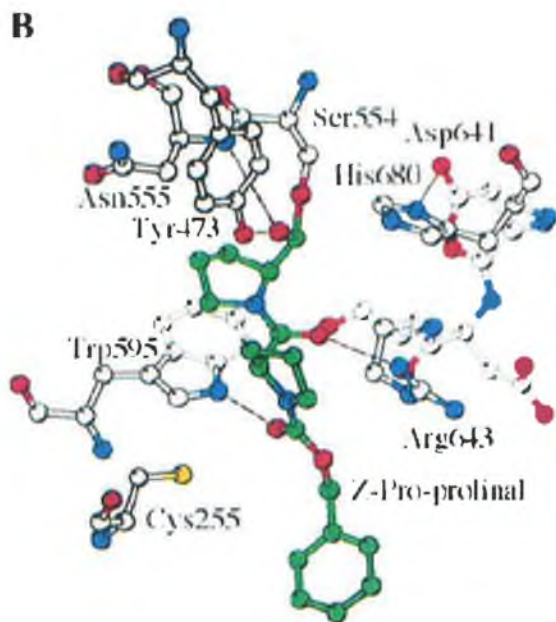


**Figure 1.4. A View of the Active Site of Prolyl oligopeptidase**

The carbon atoms of the enzyme and the covalently bound inhibitor, Z-Pro-prolinal, are coloured gray and green, respectively. Dashed lines indicate hydrogen bonds (Fulop *et al.* 1998).

The oxyanion-binding site, which stabilizes the oxyanion of the tetrahedral intermediate, is an essential feature of serine protease catalysis. The hydrogen bonds provided by the oxyanion binding site in order to stabilize the negatively charged oxyanion come from distinct groups in prolyl oligopeptidase compared to the classic serine proteases. The main chain NH group of Asn<sup>555</sup> provides one and the second, which is a special feature of prolyl oligopeptidase, is provided by the OH group of Tyr<sup>473</sup> (Fulop *et al.* 1998; Polgar, 2002a).

### Oligopeptide selection

The narrow opening at the bottom of the propeller tunnel that is opposite the entrance to the active site is much too small for entrance of an average peptide. It has been reported (Fulop *et al.* 2000) that prolyl oligopeptidase uses the partial opening between its propeller blades 1 and 7 (Figure 1.2.) for regulating entrance to its active site. This would prevent proteins and large structured peptides from hydrolysis. They verified this mechanism by engineering a disulfide bond between blades 1 and 7, thus closing the velcro (circular structure) with the effect of causing complete inactivation of the enzyme (Figure. 1.5.). So prolyl oligopeptidase shows a novel strategy of regulation in which oscillating propeller blades act as a gating filter mechanism during catalysis.



**Figure 1.5.  $\beta$ -Propeller Domain Representation With Closed Velcro Topology**

The protein chain of the  $\beta$ -propeller domain only, showing the engineered disulfide bond connecting blades 1 and 7 in red (Fulop *et al.* 2000).

### Effect of propeller domain on catalysis

The inhibition of mammalian and plant prolyl oligopeptidase by cysteine protease inhibitors is well documented (Polgar, 1991; Yoshimoto *et al.* 1987a). This effect was presumed to be due to a cysteine residue in close proximity to the active site. Szeltner *et al.* (2000) reported that the cys<sup>255</sup> side chain (Figure. 1.4.), which is located close to the S<sub>1</sub> and S<sub>3</sub> binding sites accounts for this effect. This finding has indicated that in addition to the regulatory effect the propeller domain, which is independent of the catalytic domain, provides a residue that can modify the catalytic action of the peptidase domain.

### Kinetic properties of catalysis

Polgar (1991) reported that kinetic analysis indicated that prolyl oligopeptidase is remarkably sensitive to ionic strength and postulated the existence of two catalytically active forms, which exhibit different activities and interconvert with changing pH. Usually the ionisation of the histidine residue in the active site of serine proteases governs the pH dependence of catalysis, exhibiting a pK<sub>a</sub> of 7.0. It has been noticed that a second ionisation event in the pH dependent kinetics was observed at pK<sub>a</sub> 5.0 (Polgar, 1991).

An additional difference between prolyl oligopeptidase and the classical serine proteases is the rate-limiting step of catalysis. Kinetic deuterium isotope effects of the chymotrypsin enzyme reaction show that the rate limiting step involves general base/acid catalysis, as the reactions proceed 2-3 times slower in deuterium oxide than water (Polgar, 2002a). No significant isotope effects were noticed in prolyl oligopeptidase catalysis of different substrates that, along with the lack of leaving group effects on K<sub>cat</sub>/K<sub>m</sub> indicate the possibility of a substrate induced conformational change being the rate-limiting step (Polgar, 1991; Polgar, 1992b; Polgar *et al.* 1993; Polgar 2002a). This conformational change induced by the substrate may be the opening of the propeller blades as mentioned earlier.

### 1.2.7. Substrate Specificity

The general substrate specificity of prolyl oligopeptidase from various sources is well documented (Koida and Walter, 1976; Walter and Yoshimoto, 1978; Yoshimoto *et al.* 1988; Kreig and Wolf, 1995). In general the ability of prolyl oligopeptidase to hydrolyse a peptide bond is dictated by the presence of a particular residue (proline or alanine), location of the residue and the length of the peptide. Prolyl oligopeptidase is a proline specific endopeptidase, cleaving peptides with a proline residue in the P<sub>1</sub> position (Pro-Xaa) in peptides consisting of an acyl-Yaa-Pro-Xaa sequence (Nomura, 1986). Cleavage will not occur if a free  $\alpha$ -amine exists in the P<sub>2</sub> position. Pro-Pro bonds and N-blocked peptides of the sequence Z-Pro-Xaa are also not hydrolysed. Nomura (1986) investigated the importance of the residue in the P<sub>1</sub> position and its effect on the S<sub>1</sub> subsite of the enzyme (Figure 1.6. for terminology). It was concluded that the S<sub>1</sub> subsite of prolyl oligopeptidase is designed to specifically fit proline residues but can tolerate residues carrying substituent groups, provided they do not exceed the size of the pyrrolidine ring of proline. There is a preference for a hydrophobic residue at the C-terminal end of the scissile bond (P<sub>1</sub>') with lower specificities observed for basic and acidic residues in this position.

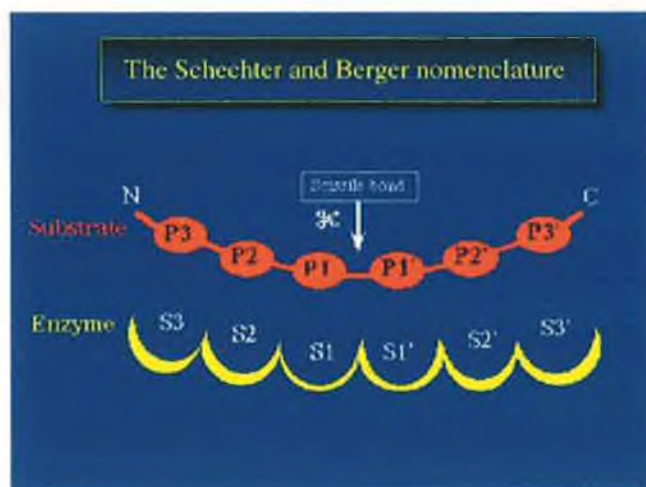


**Figure 1.6. Schematic Representation of an Enzyme-Substrate Complex**

Residues of the substrate and enzyme subsites are numbered according to their distance from the scissile bond and their location on the N- or C-terminal side of the cleavage site (Schechter and Berger, 1967).

The smallest peptide cleaved by prolyl oligopeptidase is an N-blocked tripeptide or a tetrapeptide containing residues in positions P<sub>3</sub>-P<sub>1</sub>'. Further studies showed that prolyl oligopeptidase has an extended substrate binding region in addition to the primary specificity site, S<sub>1</sub>. It is seemingly comprised of three subsites located at the amino-terminal site (S<sub>1</sub>, S<sub>2</sub> and S<sub>3</sub>) and two located at the carboxyl site from the scissile bond (S<sub>1</sub>' and S<sub>2</sub>'). High stereospecificity was observed for subsites S<sub>1</sub>, S<sub>2</sub> and S<sub>1</sub>' (Walter and Yoshimoto, 1978; Yoshimoto *et al.* 1988; Sattar *et al.* 1990). Fulop *et al.* 2001 by showing the binding of an octapeptide substrate to an inactive prolyl oligopeptidase active site, have clarified the above findings that were based on kinetic analysis. They concluded that their structure determination revealed that substrate binding is restricted to the P<sub>3</sub>-P<sub>2</sub>' region only.

As an oligopeptidase, prolyl oligopeptidase has a substrate size limitation that enables it to cleave low molecular weight peptides much faster than larger peptides. The enzyme is unable to cleave proteins or peptides greater than 25 amino acids in length (Koida and Walter, 1976; Walter *et al.* 1980; Moriyama *et al.* 1988). The presence of a gating filter mechanism by the β-propeller domain of prolyl oligopeptidase explains this substrate size limitation (see section 1.2.6.).

Most peptide hormones and neuropeptides comprise one or more proline residues. Seeing as prolyl oligopeptidase has a broad specificity for proline containing oligopeptides, its ability to degrade many bioactive peptides is well documented. *In vitro*, prolyl oligopeptidase is able to degrade several neuropeptides, such as substance P and arginine-vasopressin (Wilk, 1983; Mentlein, 1988; Makinen *et al.* 1994). Table 1.4. summarises some of the peptides reported to be degraded by prolyl oligopeptidase and their identified cleavage site.

<b>Peptide</b>	<b>AA</b>	<b>Sequence and cleavage point</b>	<b>Reference</b>
Substance P	11	Arg-Pro-Lys- <b>Pro</b> -Gln-Gln-Phe-Phe-Gly-Leu-Met	O'Leary <i>et al.</i> 1996
Oxytocin	9	Cys-Tyr-Ile-Gln-Asn-Lys- <b>Pro</b> -Leu-Gly-NH <sub>2</sub>	Walter <i>et al.</i> 1971
Neurotensin	13	Pyr-Leu-Tyr-Glu-Asn-Lys- <b>Pro</b> -Arg-Arg- <b>Pro</b> -Tyr-Ile-Leu	Camargo <i>et al.</i> 1984
Angiotensin I	11	Asp-Arg-Arg-Val-Tyr-Ile-His- <b>Pro</b> -Phe-His-Leu	Moriyama <i>et al.</i> 1988
Angiotensin II	8	Asp-Arg-Val-Tyr-Ile-His- <b>Pro</b> -Phe	Moriyama <i>et al.</i> 1988
Angiotensin III	7	Arg-Val-Tyr-Ile-His- <b>Pro</b> -Phe	Moriyama <i>et al.</i> 1988
Bradykinin	9	Arg-Pro-Pro-Gly-Phe-Ser- <b>Pro</b> -Phe-Arg	Tate, 1981
TRH	3	pGlu-His- <b>Pro</b> -NH <sub>2</sub>	O'Leary <i>et al.</i> 1996
Vasopressin	8	Cys-Tyr-Phe-Gln-Asn-Cys- <b>Pro</b> -Arg-Gly	Moriyama <i>et al.</i> 1988
Tuftsins	4	Thr-Lys- <b>Pro</b> -Arg	Tate, 1981
LHRH	10	Pyr-His-Trp-Ser-Tyr-Gly-Leu-Arg- <b>Pro</b> -Gly-NH <sub>2</sub>	Wilk <i>et al.</i> 1979
Arg-vasopressin	9	Cys-Tyr-Phe-Gln-Asn-Cys- <b>Pro</b> -Arg-Gly-NH <sub>2</sub>	Walter, 1976
Melanotropin	13	Ser-Tyr-Ser-Met-Glu-His-Phe-Arg-Trp-Gly-Lys- <b>Pro</b> -Val-NH <sub>2</sub>	Tate, 1981

**Table 1.4. Bioactive Peptides Hydrolysed by Prolyl Oligopeptidase**



### 1.2.8. Inhibitors

Specific inhibitors of prolyl oligopeptidase are typically substrate analogues, which interact with the enzyme in a substrate like manner and prevent enzyme catalysis. This mode of action of these inhibitors, which are very specific due to the proline residue in the P<sub>1</sub> position, will play a role in identifying the physiological role of the enzyme. Therefore, the continuing development of specific inhibitors that inactivate prolyl oligopeptidase *in vivo* and can readily cross the blood brain barrier is very important.

The first highly potent and specific inhibitor of prolyl oligopeptidase synthesised was the peptidyl aldehyde N-benzyloxycarbonyl (Z)-Pro-prolinal (Wilk and Orłowski, 1983), which is effective *in vivo* as well as *in vitro*. A K<sub>i</sub> of 14nM was reported for this non-competitive, transition state aldehyde inhibitor for rabbit brain prolyl oligopeptidase. After intraperitoneal administration Z-Pro-prolinal traverses the blood brain barrier to inhibit the brain enzyme (Friedman *et al.* 1984). Both the alcohol and acid derivatives of Z-Pro-prolinal were found to be 3000 times less inhibitory towards the rabbit enzyme than the aldehyde (Friedman *et al.* 1984; Wilk and Orłowski, 1983). In 1990, Bakker *et al.* proposed that Z-Pro-prolinal was in fact a competitive slow tight binding inhibitor of mouse and human prolyl oligopeptidase with K<sub>i</sub> values of 0.35nM and 0.5nM respectively. The potency of Z-Pro-prolinal is attributed to this transition state peptide aldehyde forming a hemiacetal adduct with the active site serine (Kahyaoglu *et al.* 1997).

Yokosawa *et al.* (1984) using Z-Pro-prolinal substituted the P<sub>2</sub> proline with various amino acids. Z-Val-prolinal was found to be the most potent with a K<sub>i</sub> of 2.4nM for prolyl oligopeptidase from ascidian (*Halocynthia roretzi*) sperm. Further studies reported that Z-Thiopropio-thioprolinal gave a K<sub>i</sub> of 10pM for bovine brain prolyl oligopeptidase. Replacement of the thioprolinal with thiazolidine also remained very potent giving a K<sub>i</sub> of 0.36nM (Tsuru *et al.* 1988). Although Z-Thiopropio-thiazolidine doesn't have an aldehyde group, it shows potent activity comparable to Z-Pro-prolinal. These studies on Z-Pro-prolinal and its derivatives indicate that the length of the main chain of the inhibitor corresponding with the subsites, S<sub>1</sub>, S<sub>2</sub> and S<sub>3</sub> is most suitable for inhibition. Also it showed that there seems to be a hydrophobic pocket at the S<sub>3</sub> subsite with bulkiness and length of the acyl group important for firm binding.



Many potent prolyl oligopeptidase inhibitors are variations of the N-blocked dipeptide chain. SUAM 1221, a phenyl butanoyl prolyl-pyrrolidine derivative has a reported  $IC_{50}$  of 190nM (Saito *et al.* 1991). Fmoc-aminoacylpyrrolidine-2-nitriles are also potent prolyl oligopeptidase inhibitors. Both Fmoc-Ala-PyrrCN and Fmoc-Pro-PyrrCN inhibition resulted in  $K_i$ 's of 5nM. They were also found to be stable, cell permeable and crossed the blood brain barrier (Li *et al.* 1996). Goosens *et al.* (1997) reported the inhibition of prolyl oligopeptidase ( $K_i$  of 0.8nM) by converting Z-Pro-pyrrolidine to Z-Pro-3-fluoropyrrolidine. A well-studied inhibitor, JTP-4819 that contains a benzylaminocarbonyl blocked dipeptide carboxamide (Toide *et al.* 1995a) shows an  $IC_{50}$  of 0.83nM. As can be seen most described low molecular weight prolyl oligopeptidase inhibitors contain an acyl-L-prolyl-pyrrolidine backbone, with the lipophilic acyl end group reported to be important for high inhibition. Most recent prolyl oligopeptidase inhibitors (Wallen *et al.* 2002) synthesised dicarboxylic acid bis (L-prolyl-pyrrolidine) amides and studied their inhibitory activity. These new compounds have in common an L-prolyl-pyrrolidine moiety, but the typical lipophilic acyl end group is replaced by another L-prolyl-pyrrolidine moiety connected symmetrically via a short dicarboxylic acid linker, they are a new type of peptidomimetic prolyl oligopeptidase inhibitor. The most potent new inhibitor gave an  $IC_{50}$  of 0.39nM.

Many compounds, which are bacterial and fungal in origin, were discovered to be potent inhibitors of prolyl oligopeptidase. Postatin that was isolated from *Streptomyces viridochromogenes* (Aoyagi *et al.* 1991) was a potent inhibitor resulting in an  $IC_{50}$  of 0.03 $\mu$ g/ml. A variety of derivatives of postatin have been chemically synthesised in an attempt to obtain a greater inhibitory potency and selectivity (Tsuda *et al.* 1996). Propeptin (Kimura *et al.* 1997) and Lipohexin (Heinze *et al.* 1997) were isolated from fungal origins and both reported to be inhibitors of prolyl oligopeptidase. A  $K_i$  of 0.70 $\mu$ M was obtained for propeptin. Many prolyl oligopeptidase inhibitors have been isolated from the mushroom *Polyozellus multiplex*. The most recent Kynapcin-24 was shown to non-competitively inhibit prolyl oligopeptidase, with an  $IC_{50}$  value of 1.14 $\mu$ M (Song and Raskin, 2002).

Inhibitor	Potency	Reference
Z-Pro-prolinal	$K_i = 14\text{nM}$	Wilk and Orłowski, 1983
Z-Val-prolinal	$K_i = 2.4\text{nM}$	Yokosawa <i>et al.</i> 1984
Z-Thiopropio-thioprolinal	$K_i = 0.01\text{nM}$	Tsuru <i>et al.</i> 1988
Z-Thiopropio-thiazolidine	$K_i = 0.36\text{nM}$	Tsuru <i>et al.</i> 1988
Z-Indolinylnyl-prolinal	$K_i = 2.4\text{nM}$	Bakker <i>et al.</i> 1991
SUAM-1221	$K_i = 190\mu\text{M}$	Saito <i>et al.</i> 1991
Y-27924	$\text{IC}_{50} = 0.95\mu\text{M}$	Nakajima <i>et al.</i> 1992
JTP-4819	$\text{IC}_{50} = 0.83\text{nM}$	Toide <i>et al.</i> 1995a
Fmoc-Ala-PyrrCN	$K_i = 5\text{nM}$	Li <i>et al.</i> 1996
Fmoc-Pro-PyrrCN	$K_i = 5\text{nM}$	Li <i>et al.</i> 1996
Z-Pro-3-fluoropyrrolidine	$K_i = 0.8\text{nM}$	Goosens <i>et al.</i> 1997
S-17092-1	$K_i = 1\text{nM}$	Barelli <i>et al.</i> 1999
Postatin	$\text{IC}_{50} = 0.03\mu\text{g/ml}$	Aoyagi <i>et al.</i> 1991
Propeptin	$K_i = 0.7\mu\text{M}$	Kimura <i>et al.</i> 1997
Lipohexin	$K_i = 3.5\mu\text{M}$	Heinze <i>et al.</i> 1997
Kynapcin-24	$\text{IC}_{50} = 1.14\mu\text{M}$	Song and Raskin, 2002

**Table 1.5. Prolyl Oligopeptidase Specific Inhibitors**

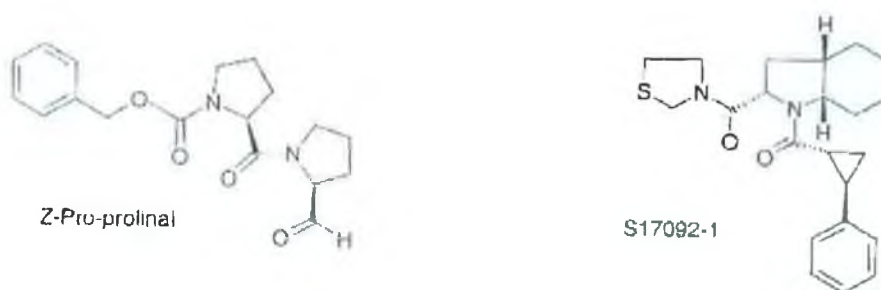


**Figure 1.7. Chemical Structure of Some Prolyl Oligopeptidase Inhibitors**

### 1.2.9. Physiological Relevance

On the basis that processing and degradation of peptide hormones and neuropeptides, which comprise one or more proline residues, require the use of proline specific peptidases it was important to study the contribution of prolyl oligopeptidase to a number of biologically important functions. The biology of prolyl oligopeptidase is consistent with a potential neuromodulatory role. They cleave peptides of less than 3kDa after proline residues, which include peptide hormones and neuropeptides such as substance P and  $\beta$ -endorphin (Cunningham and O'Connor, 1997b). It is still somewhat unclear though if these are physiologically relevant substrates because prolyl oligopeptidase activity appears to be predominantly cytosolic (Kato *et al.* 1980; Irazusta *et al.* 2002).

As an important brain enzyme, prolyl oligopeptidase is implicated in a variety of disorders of the central nervous system. Prolyl oligopeptidase activity has been associated with the mental disorders of unipolar and bipolar depression. Serum prolyl oligopeptidase activity is lowered during depression, but raised during mania and schizophrenia (Maes *et al.* 1994 and 1995). The antidepressant fluoxetine and the antimanic drug valproate restore prolyl oligopeptidase activity levels to normal (Maes *et al.* 1995). It is also worth noting that peptides involved in the pathophysiology of depression like thyroliberin, substance P and  $\beta$ -endorphin are all substrates of the enzyme. The most recent studies on depression, for which lithium is the oldest and simplest agent for treatment, have indicated that an inverse relationship between prolyl oligopeptidase activity and inositol (1,4,5)-trisphosphate (IP<sub>3</sub>) signalling is evident (Williams *et al.* 1999; Williams and Harwood, 2000; Williams *et al.* 2002). The low prolyl oligopeptidase activity may cause neurotrophic effects (depression) through elevation of IP<sub>3</sub>, the process being reversed by lithium. Schulz *et al.* (2002) also demonstrated an influence on IP<sub>3</sub> metabolism by prolyl oligopeptidase. They concluded that reduced prolyl oligopeptidase activity was found to amplify substance P mediated stimulation of IP<sub>3</sub>. This effect of reduced prolyl oligopeptidase activity on second messenger concentration indicates a possible novel intracellular function of this peptidase, therefore maybe having an impact on the reported cognitive enhancements due to prolyl oligopeptidase inhibition.

The effects of various prolyl oligopeptidase inhibitors have revealed a further physiological role of the enzyme. *In vitro*, substrates such as TRH, substance P and arginine-vasopressin (AVP) are known to exert neuroprotective effects like improving the performance of animals in learning and memory tasks (De Wied *et al.* 1984; Griffiths, 1987). The first effective inhibitor, Z-Pro-prolinal was shown to reverse scopolamine-induced amnesia in rats (Yoshimoto *et al.* 1987). These findings were confirmed for a number of other prolyl oligopeptidase inhibitors such as JTP-4819, Ono-1603 and S-17092-1 and they are known as cognitive enhancers (Toide *et al.* 1995a; Katsube *et al.* 1996; Barelli *et al.* 1999). For instance, JTP-4819 in rats with lesions of the nucleus basalis magnocellularis ameliorated memory impairment by increasing the levels of substance P, TRH and arginine-vasopressin (Shinoda *et al.* 1999).

More studies on the biological relevance of prolyl oligopeptidase show evidence that this enzyme could be linked with Alzheimer's disease, with specific inhibitors having a therapeutic value for its treatment (Toide *et al.* 1997a). It was reported (Shinoda *et al.* 1997) that the prolyl oligopeptidase inhibitor JTP-4819 was able to suppress *in vitro*  $\beta$ -amyloid protein ( $A\beta$ ) formation in neuroblastoma cells. This importance, due to the deposition of  $\beta$ -amyloid protein in brains being a hallmark of Alzheimers was studied but later findings indicate that specific inhibitors do not affect formation and degradation of  $\beta$ -amyloid peptides and  $\beta$ -amyloid precursor proteins. This would be expected, as prolyl oligopeptidase is known to only degrade small peptides. It is now accepted that low prolyl oligopeptidase activity is associated with neuronal degeneration rather than  $\beta$ -amyloid accumulation (Petit *et al.* 2000; Laitinen *et al.* 2001).

Prolyl oligopeptidase also possibly plays a role in the regulation of blood pressure through the metabolism of bradykinin and angiotensin I, thus participating in the renin-angiotensin system (Polgar, 2002b).

The protozoan parasite *Trypanosoma cruzi* also contains prolyl oligopeptidase. Using specific prolyl oligopeptidase inhibitors, the role of the enzyme in the invasion of target cells has been studied showing that these specific inhibitors can block the entry of the parasite into host cells (Grellier *et al.* 2001).

Although the enzymatic and structural properties of prolyl oligopeptidase are well known, its biological function is far from being fully understood.

### 1.3. Dipeptidyl Peptidase IV

The ectoenzyme dipeptidyl peptidase IV (DP IV, EC 3.4.14.5) is a serine exopeptidase catalysing the release of N-terminal dipeptides from oligo- and polypeptides preferentially with proline or to a lesser extent alanine in the penultimate position (Ikehara *et al.* 1994). Among the rare group of proline specific proteases, dipeptidyl peptidase IV was originally believed to be the only membrane-bound enzyme specific for proline as the penultimate residue at the amino-terminus of the polypeptide chain. However, recent studies have identified many proteins with DP IV-like enzymatic activity (Sedo *et al.* 2001). Dipeptidyl peptidase IV was first identified as glycylproline naphthylamidase by Hopsu-Havu and Glenner (1966) and also called dipeptidyl aminopeptidase IV (DAP IV) or postproline dipeptidyl peptidase IV in earlier work. It's cellular localization and enzymatic properties differ from those of the other dipeptidyl peptidases. Dipeptidyl peptidases I and II are localized in lysosomes, whereas dipeptidyl peptidase III is found in the cytoplasm. The specificity of dipeptidyl peptidase II is similar to dipeptidyl peptidase IV but neither dipeptidyl peptidase I or III can cleave post proline (Polgar, 2002a). Dipeptidyl peptidase IV is grouped in subfamily S9B of the peptidase family S9 (Prolyl oligopeptidase family), clan SC (Barrett *et al.* 1998). It is different from both prolyl oligopeptidase and oligopeptidase B in that it's a dimer, an exopeptidase, a glycoprotein and an ectoenzyme bound to the cell membrane. Dipeptidyl peptidase IV is reported to be identical to CD26 (Fleisher, 1994), a T-lymphocyte surface antigen and to adenosine deaminase (ADA) binding protein. Dipeptidyl peptidase is thus often referred to/called CD26 and ADA-binding protein.

#### 1.3.1. Distribution

Dipeptidyl peptidase is predominantly a cell membrane bound glycoprotein widely distributed in a variety of species and tissues. In addition to the integral membrane form, a soluble form of dipeptidyl peptidase occurs in serum (Iwaki-Egawa *et al.* 1998). Dipeptidyl peptidase IV is found in all organs, primarily on apical surfaces of epithelial and acinar cells, with lower levels on lymphocytes and capillary endothelial cells (Gorrell *et al.* 2001). Dipeptidyl peptidase IV was detected by enzyme cytochemistry using Gly-Pro substrates in human tissues such as kidney, placenta, gastrointestinal tract and on endothelia of all organs examined such as liver, spleen,

lungs and brain. Rat tissues produced identical data and showed that endothelial cells of capillaries in all organs including lymphoid organs, muscle and brain contain dipeptidyl peptidase activity. In the kidney, where the enzyme is exceptionally enriched, it is located primarily in the cortex and also found in the brush-border and microvillus fractions. In the liver, dipeptidyl peptidase IV activity is primarily located on hepatocytes at the plasma membranes around bile caniculi and on the bile duct epithelia.

Lojda (1977) showed for the first time dipeptidyl peptidase IV activity on human peripheral blood lymphocytes. Within the hematopoietic system, dipeptidyl peptidase IV is expressed on the surface of resting and activated T cells, activated B and activated NK cells (Reinhold *et al.* 2002).

Much work has been carried out on the soluble form of dipeptidyl peptidase IV. This activity was reported to be present in the cytoplasm of guinea-pig brain indicating the existence of a soluble form (Gilmartin and O’Cuinn, 1999). Dipeptidyl peptidase IV activity can be found in many mammalian bodily fluids, such as serum, urine and seminal fluid. Most reports are on the serum dipeptidyl peptidase IV that is derived from cell surface dipeptidyl peptidase IV but its cellular origin is still unclear (Gorrell *et al.* 2001).

Yoshimoto and Tsuru (1982) reported the presence of dipeptidyl peptidase IV in *Flavobacterium meningosepticum* although its biochemical properties differed to the mammalian enzyme.

### **1.3.2. Purification**

Since dipeptidyl peptidase was first isolated from rat liver by Hopsu-Havu and Glenner (1966), it has been isolated with various degrees of purity since due to its wide distribution in a variety of species and tissues. The enzyme has been purified to homogeneity from liver (Ikehara *et al.* 1994), Kidney (Kenny *et al.* 1976; Wagner *et al.* 1999) and serum (Shibuya-saruta *et al.* 1996; Iwaki-Egawa *et al.* 1998; Durinx *et al.* 2000). The intact membrane form can be prepared by solubilizing the enzyme with Triton X-100, while the soluble form is obtained by autolysis of microsomes incubated at low pH or by digestion of membrane form with papain, which cleaves a

peptide bond of the stalk linking the peptidase to the membrane. The intact membrane form is usually separated from the soluble form by centrifugation, if they both co-exist in that source.

Conventional column chromatographic techniques are usually employed with varying degrees of success for purification. DEAE anion exchange chromatography is a widely used step for dipeptidyl peptidase IV purification (De Meester *et al.* 1992 and 1996; Ohkubo *et al.* 1994) and the concept of re-chromatographing on this same resin is commonly employed (Yoshimoto and Walter, 1977; Puschel *et al.* 1982; Iwaki-Egawa *et al.* 1998). The cation exchange resin CM-cellulose has also been employed in tandem with anion exchange chromatography (Kenny *et al.* 1976; Yoshimoto and Walter, 1977). Hydrophobic interaction chromatography is not reported to be used often in dipeptidyl peptidase IV purification. The enzymes soluble form purification from guinea-pig brain (Gilmartin and O’Cuinn, 1999) and its isolation from human serum (Iwaki-Egawa *et al.* 1998) both employed hydrophobic interaction chromatography, the latter group obtaining an overall purification of 14,400 with its use. Gel filtration chromatography is also widely used, pore sizes ranging from G150 for *Flavobacterium meningosepticum* (Yoshimoto and Tsuru, 1982), an S200HR for guinea pig brain cytoplasm (Gilmartin and O’Cuinn, 1999) and an S300HR for human serum dipeptidyl peptidase IV isolation (Iwaki-Egawa *et al.* 1998).

The use of affinity resins in the purification of dipeptidyl peptidase IV report the greatest purification factors. Lectin affinity chromatography using concanavalin A-sepharose and wheat germ-agglutinin sepharose which exploit the glycoprotein characteristic of dipeptidyl peptidase IV were employed widely for its isolation (De Meester *et al.* 1992; Ikehara *et al.* 1994). Shibuya-saruta *et al.* (1996) employed Gly-L-Leu affinity chromatography along with the use of a monoclonal antibody, Tal bound to EAH sepharose 4B for dipeptidyl peptidase IV purification from human serum. They achieved an overall purification factor of 18,000 with their use. Durinx *et al.* (2000) also employed a monoclonal antibody recognising the adenosine deamidase-binding site for dipeptidyl peptidase IV purification from human serum. De Meester *et al.* (1996) exploited the adenosine deamidase-binding site of dipeptidyl peptidase IV by purifying it from human seminal plasma using immobilized adenosine deamidase (ADA) on CNBr-activated sepharose. The use of immobilized

metal affinity chromatography using  $\text{Cu}^{2+}$  as metal ligand was very successful in removing contaminating protein, which proved difficult to remove otherwise in dipeptidyl peptidase IV purification from ostrich kidney and human lymphocytes (De Meester *et al.* 1992; Wagner *et al.* 1999).

Recent studies have employed a two-step purification of the recombinant human dipeptidyl peptidase IV enzyme that was overexpressed in *Spodoptera frugiperda* (SF9) insect cells as a more readily achievable preparation compared with tissue isolation (Dobers *et al.* 2002).

### **1.3.3. Activity Detection**

Dipeptidyl peptidase IV cleaves N-terminal dipeptides from substrates consisting of three or more amino acid residues or dipeptides linked to C-terminal chromogenic or fluorogenic compounds. Gly-Pro- is normally the dipeptide attached C-terminally to a compound that can be measured and quantified either spectrophotometrically or fluorometrically. A number of dipeptide substrates such as p-nitroanilides (Nagatsu *et al.* 1976),  $\beta$ -naphthylamides (Hopsu-Havu and Glenner, 1966) and 4-methoxy- $\beta$ -naphthylamides (Puschel *et al.* 1982) have been used for characterisation of dipeptidyl peptidase IV. Gly-Pro-AMC is being increasingly used for detection of dipeptidyl peptidase IV activity due to its high sensitivity. The hydrolysis of the assay substrate selected is dependant on the enzyme source and the substrate choice should be optimised as such (McDonald *et al.* 1971).

Sensitive fluorogenic rhodamine 110-based substrates are becoming increasingly employed for the detection and quantification of dipeptidyl peptidase IV on the surface of immune cells. Rhodamine 110 (R110), a highly fluorescent xanthene dye was used to synthesise dipeptidyl peptidase IV substrates Gly(Ala)-Pro-R110-R, thus facilitating a stable binding of the fluorescent moiety on the cell surface. These substrates provide the opportunity to determine cell surface-associated dipeptidyl peptidase IV activity on single cells (Lorey *et al.* 2002).



### 1.3.4. Structural and Biochemical Aspects

The amino acid sequences of dipeptidyl peptidase IV have been determined from different species by complementary DNA (cDNA) cloning and sequencing. The human (Misumi *et al.* 1992; Darmoul *et al.* 1992), murine (Marguet *et al.* 1992), rat (Ogata *et al.* 1989) and porcine (Engel *et al.* 2003) enzymes contain 766, 760, 767 and 766 amino acid residues. The bacterial enzyme from *Flavobacterium meningosepticum* displays a shorter peptide chain of 711 residues (Kabashima *et al.* 1995). Each protein is anchored to the lipid bilayer by a single hydrophobic segment located at the N-terminus, and has a short cytoplasmic tail of six amino acids. A flexible stalk links the membrane anchor to a large glycosylated region, a cysteine rich region and a C-terminal catalytic domain. The extracellular domain contains several glycosylation sites, mostly in the amino-terminal half. This glycosylation accounts for the difference in the molecular mass between the predicted and the native forms (Ogata *et al.* 1989). The essential residues of the human enzyme are Ser<sup>630</sup>, Asp<sup>708</sup> and His<sup>740</sup>. This order of the catalytic triad is characteristic of the  $\alpha/\beta$  hydrolase fold secondary structure.

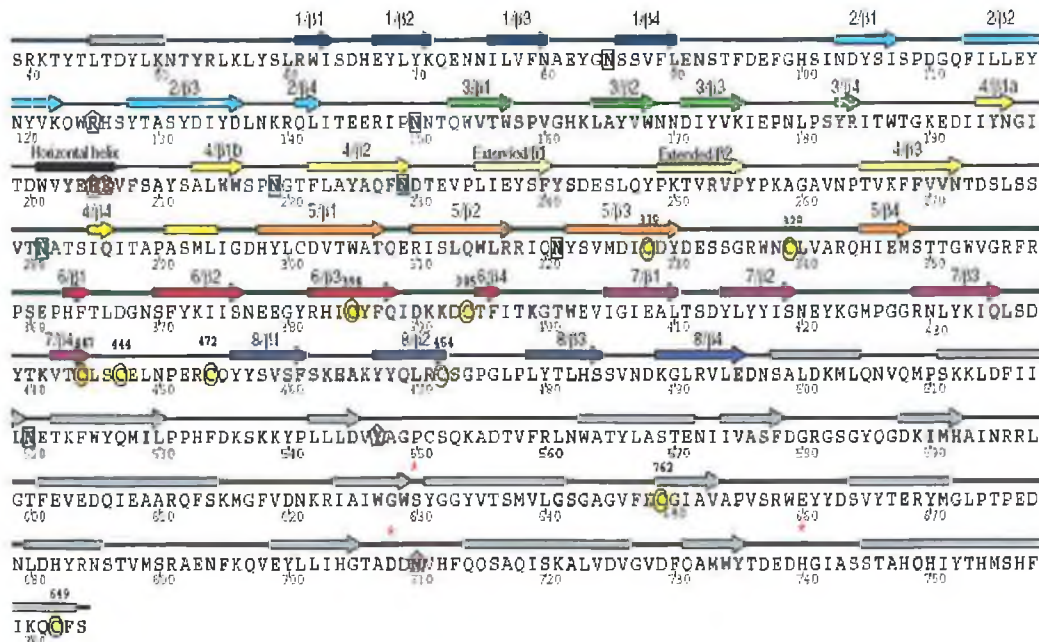


**Figure 1.8. Secondary Structure of DP-IV Shown Over the Amino Acid Sequence**  
 Arrows indicate  $\beta$ -strands, bars indicate helices. Colour code is as propeller blade numbers in Figure 1.10. Hydrolase domain is gray. Glycosylated residues are marked with a cyan square. Cysteines in S-S bonding are yellow circles. Catalytic residues are marked with a red asterisk (Rasmussen *et al.* 2003).

Recent crystal structures of human (Rasmussen *et al.* 2003) and porcine (Engel *et al.* 2003) have reported the most important three-dimensional structural information on dipeptidyl peptidase IV. The 2.5Å structure of the extracellular region of human dipeptidyl peptidase IV in complex with the inhibitor Valine-Pyrrolidide was elucidated. It consists of two domains, a peptidase and an eight-bladed  $\beta$ -propeller (Figure 1.10.). Dipeptidyl peptidase IV was seen as a dimer in the crystal structure, agreeing with reports that the active enzyme is a dimer (Gorrell *et al.* 2001). The N-terminus of each subunit is located at the same site of the dimer (Figure 1.9.), indicating that full length, membrane bound dipeptidyl peptidase IV could exist as homodimers at the cell surface. Interestingly, from this Engel *et al.* (2003) in their crystal structure indicated that tetramerization of dipeptidyl peptidase IV is a key mechanism for possible cell-cell contacts.

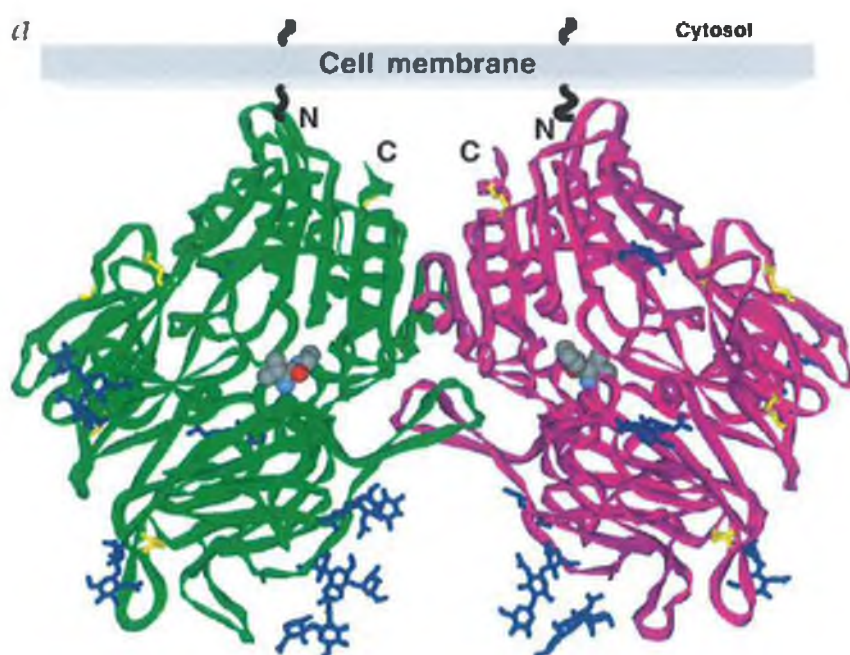


**Figure 1.9. Structure of Dipeptidyl Peptidase IV**

DP-IV forms a homodimer (subunit A in green, B in magenta). Each subunit consists of two domains: an  $\alpha/\beta$ -hydrolase domain, located closest to the membrane, and an eight-bladed  $\beta$ -propeller. The inhibitor Val-Pyr is shown and coloured by element: carbon (gray), nitrogen (blue) and oxygen (red). Five S-S bridges (yellow) have been identified in each molecule. Carbohydrates (blue) have been located at seven of the possible nine-glycosylated positions in both subunits. These sites are all situated in the  $\beta$ -propeller, except one (Rasmussen *et al.* 2003).

Each subunit consists of two domains, an  $\alpha/\beta$  hydrolase domain and an eight-bladed  $\beta$ -propeller (Figure 1.10a.). The C-terminal residues 506-766 and a short stretch of N-terminal sequence, residues 39-51, assemble the peptidase domain. It adopts a typical  $\alpha/\beta$  hydrolase fold with a central eight stranded  $\beta$ -sheet sandwiched by several helices. The  $\beta$ -propeller domain is formed from residues 55-497. It consists of eight-blades each containing four antiparallel  $\beta$ -strands (Figure 1.10b). The propeller is divided into two domains with blades 2-5 forming one subdomain and blades 1 and 6-8 forming the other.

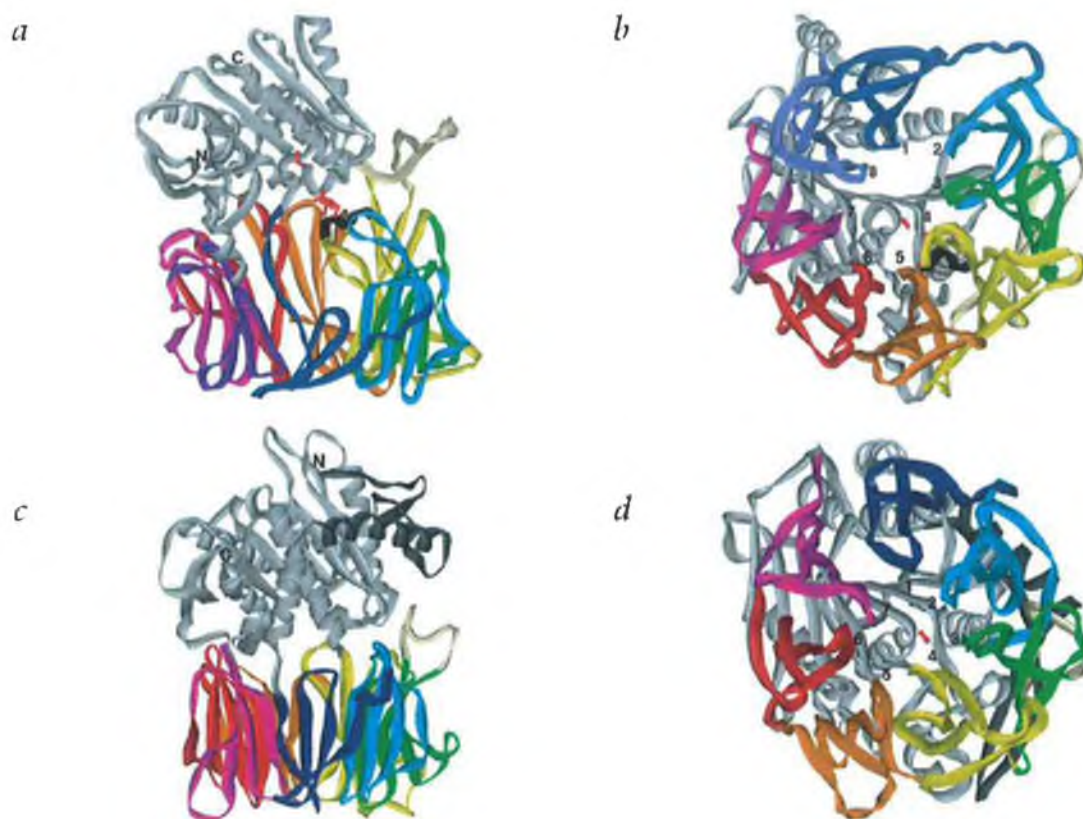


**Figure 1.10. Structural Comparison of DP-IV and Prolyl Oligopeptidase**

The eight (DP-IV) and seven (PO) bladed  $\beta$ -propeller domains are illustrated by solid ribbons and coloured by blade number (as shown in Figure 1.8. for a & b). The  $\alpha/\beta$  hydrolase domain is gray. a) Side view of DP-IV. The extended arm involved in dimerization is off yellow, while the black helix holds Glu<sup>205</sup> and Glu<sup>206</sup>. b) DP-IV viewed from bottom. c) View of PO from the side. The N-terminal extension relative to DP-IV and covering dimer contact area is shown in dark gray. d) PO viewed from the bottom (Rasmussen *et al.* 2003)

The  $\beta$ -propeller of dipeptidyl peptidase IV is similar to prolyl oligopeptidase in that it displays open “Velcro” topology. The inside of the propeller of dipeptidyl peptidase IV forms a funnel shaped tunnel between the active site and the bottom of the monomer. However, the funnel is not the only opening to the active site of dipeptidyl peptidase IV. A side opening to the active site is generated by the kinked arrangement of blades 1 and 2. On the basis of size and electrostatic characteristics, both the tunnel and side opening may serve as entrance/exit to the active site (Rasmussen *et al.* 2003).

The formation of cysteine bridges has an important impact on the correct folding of proteins. Incorrect folding leads to retention in the endoplasmic reticulum and the misfolded proteins are degraded (Dobers *et al.* 2000). With the exception Cys<sup>649</sup>-Cys<sup>762</sup> all disulfide bonds are located in the  $\beta$ -propeller domain where they form intrablade-stabilizing crosslinks (Figure 1.8.). This cysteine rich domain is responsible for binding of extracellular matrix components and extracellular adenosine deaminase. The structures reported by Rasmussen *et al.* (2003) and Engel *et al.* (2003) also offer an insight into the ADA-binding site of dipeptidyl peptidase IV. By using site-directed mutagenesis Leu<sup>294</sup> and Val<sup>341</sup> were identified as two ADA-binding sites (Abbott *et al.* 1999). The dipeptidyl peptidase IV structure shows that these amino acids are distant from both possible active site openings, which could explain the lack of interference of ADA-binding with dipeptidyl peptidase IV catalytic activity.

The gene structure of human dipeptidyl peptidase IV has been reported. It spans about 70kbp and contains 26 exons. The widely varying transcriptional activity of the gene may explain why the enzyme is expressed ubiquitously, but at different levels in different tissues (Abbott *et al.* 1994).

Source	MW (Mono) kDa	MW (Dimer) kDa	pI	Assay Temp. (°C)	pH Optima	Reference
Human Placenta	120	200	3-4	37	8.0	Puschel <i>et al.</i> 1992
Human Lymphocytes	ND	264	5.0	ND	8.7	De Meester <i>et al.</i> 1992
Human Serum	100	250	ND	37	8.5	Shibuya-Saruta <i>et al.</i> 1996
Porcine seminal Plasma	115	300	6.85	37	8.0	Ohkubo <i>et al.</i> 1994
Ostrich Kidney	133	270	4.7	45	8.0	Wagner <i>et al.</i> 1999
Lamb Kidney	115	230	4.9	ND	7.8	Yoshimoto and Walter, 1977
<i>F.meningosepticum</i>	75	160	9.5	45	7.4-7.8	Yoshimoto and Tsuru, 1982

**Table 1.6. Biochemical Properties of Dipeptidyl Peptidase from Mammalian and Bacterial Sources**

Human dipeptidyl peptidase IV is a 110kDa glycoprotein, which is only catalytically active as a dimer. The relative molecular mass of the membrane bound dimer is 220-264kDa by gel filtration (De Meester *et al.* 1992). Dipeptidyl peptidase IV also exists as a soluble circulating form of ~100kDa. Bacterial dipeptidyl peptidase IV seems to be smaller with a molecular mass of 160kDa, so 75-80kDa monomers (Yoshimoto and Tsuru, 1982; Koreeda *et al.* 2001).

Due to the presence of sialic acids in the carbohydrate structures, dipeptidyl peptidase IV has an acidic isoelectric point. pI values of 3-5 have been reported. A pI of 4.7 was reported for ostrich kidney enzyme (Wagner *et al.* 1999), while human lymphocyte dipeptidyl peptidase IV gave a pI of 5.0 (De Meester *et al.* 1992).

The pH optimum of dipeptidyl peptidase IV, though dependent to some degree on the substrate used, ranges from 8.0 to 9.0. Whether the enzyme is soluble or membrane bound has no apparent effect on its pH optimum. Lamb kidney dipeptidyl peptidase IV and soluble dipeptidyl peptidase IV from guinea pig brain both degraded their respective substrates optimally at pH 7.8 (Yoshimoto and Walter, 1977; Gilmartin and O'Cuinn, 1999). A pH optimum of 8.7 for human lymphocyte dipeptidyl peptidase IV using the substrate Gly-Pro-4-Methoxy-2-naphthylamide was also reported (De Meester *et al.* 1992). On the stability characteristics, human placenta dipeptidyl peptidase IV maintained activity at room temperature from pH 6-12, while been completely inactivated at pH 3 (Puschel *et al.* 1982).

Temperature optimum reported for ostrich kidney was 45°C (Wagner *et al.* 1999) with the same value been obtained for the bacterial enzyme from *Flavobacterium meningosepticum* (Yoshimoto and Tsuru, 1982). Ogasawara *et al.* (1996) confirmed this bacterial temperature optimum with a value of between 40-50°C for *Pseudomonas* dipeptidyl peptidase IV enzyme.

### **1.3.5. Catalytic Classification**

Dipeptidyl peptidase IV is a serine exopeptidase that cleaves dipeptides from a free NH<sub>2</sub>-terminal end of peptides. It has been classified as a serine protease due to its inhibition by diisopropylfluorophosphate (DFP) and its resistance to sulphydryl blocking agents and chelators (Ohkubo *et al.* 1994). A concentration of 100µM DFP resulted in an IC<sub>50</sub> on human placenta dipeptidyl peptidase IV activity (Puschel *et al.* 1982). De Meester *et al.* (1992) reported 47% inhibition using phenylmethane-



sulfonylfluoride (PMSF) on human lymphocyte dipeptidyl peptidase IV activity, whereas DFP resulted in 97% inhibition. This may be due to PMSF inhibiting serine proteases less potently or via a different mode to the organophosphate, DFP.

Although dipeptidyl peptidase IV lacks significant homology with chymotrypsin or subtilisin, it has a ~200 amino acid extracellular domain, which exhibits a high degree of sequence similarity with prolyl oligopeptidase and acylaminoacid hydrolase. Analysis of the similarity of secondary structures and amino acid sequences between these enzymes in their COOH terminal regions led to the identity of Ser<sup>624</sup>, Asp<sup>702</sup> and His<sup>734</sup> as the catalytic triad residues for murine dipeptidyl peptidase IV (Marguet *et al.* 1992; David *et al.* 1993). The identification of the serine protease Gly-X-Ser-X-Gly consensus motif, which is the consensus sequence proposed for serine proteases, for murine dipeptidyl peptidase IV, its significant structural and sequence similarities in the catalytic domain to prolyl oligopeptidase and the linear order of the catalytic triad Ser-Asp-His indicates that this enzyme is a member of the prolyl oligopeptidase family of serine proteases. All members of this family contain the active site residues within 130 amino acids of the C-terminus while the membrane bound members contain the membrane spanning domain at the N-terminus (Rawlings and Barrett, 1994).

### 1.3.6. Catalytic and Structural Mechanism

Serine protease catalysis as mentioned earlier (section 1.2.6.) follows a predefined mode. Catalysis generally involves an acylation reaction in which the acyl (RCO-) moiety of the substrate is transferred to the enzyme's serine group. This is the first half of the catalysis. The second stage involves deacylation, where the imidazole group of the histidine residue activates a water group molecule by general-base catalysis leading to the formation of an acid product and enzyme (Fink, 1987).

#### Active Dimer

Dimerization is mediated by the three C-terminal secondary structure elements on the catalytic domain namely, helix Met<sup>746</sup>-Ser<sup>764</sup>, helix Gln<sup>714</sup>-Asp<sup>725</sup> and strand Asp<sup>729</sup>-Thr<sup>736</sup>, and an extended arm from the  $\beta$ -propeller. The function of the arm is to stabilize the dimeric structure. An N-terminal extension of ~ 60 amino acids present

in prolyl oligopeptidase covers the dimeric contact area of dipeptidyl peptidase IV, explaining why prolyl oligopeptidase does not dimerize (Figure 1.10.). Besides participating in the dimerization of dipeptidyl peptidase IV, this extended arm if the dimer dissociated could move towards the side opening to the active site and close it. These structural observations raise the possibility that dipeptidyl peptidase IV may exist as an open, enzymatically active dimer or as a closed inactive monomer. This may suggest that dimerization-mediated arm movement may regulate activity (Rasmussen *et al.* 2003).

#### Active site and substrate binding

A complex of dipeptidyl peptidase IV with its substrate analog, the competitive inhibitor valine-pyrrolidide (Val-Pyr) gave the first insight into substrate binding (Rasmussen *et al.* 2003). Between the peptidase and  $\beta$ -propeller domain lies a large cavity. The Val-Pyr molecule is bound in a smaller pocket within the cavity, next to the catalytic triad, Ser<sup>630</sup>, Asp<sup>708</sup>, and His<sup>740</sup>. Residues from both the hydrolase and propeller domains take part in substrate analog inhibitor binding (Figure. 1.11.).

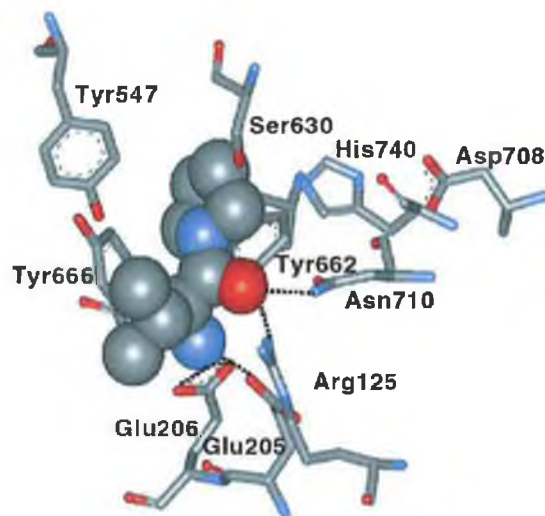


**Figure 1.11. Active Site View of DP-IV**

Val-Pyrrolidide is shown coordinated in the active site pocket, with selected residues shown in stick and coloured by element type as in Figure 1.9. Hydrogen bonds/electrostatic interactions are shown with dotted lines. Glu<sup>205</sup> and Glu<sup>206</sup> coordinate the N-terminus. Arg<sup>125</sup> and Asn<sup>710</sup> coordinate the carbonyl group of the peptide bond before the cleavage point, with the pyrrolidide ring stacked between Tyr<sup>547</sup>, Tyr<sup>662</sup> and Tyr<sup>666</sup> (Rasmussen *et al.* 2003).



The pyrrolidide moiety of Val-Pyr is buried in a hydrophobic pocket next to the active serine. The hydrophobic S<sub>1</sub> pocket fits proline as well as other small-uncharged residues such as alanine or serine. Tyr<sup>662</sup> and Tyr<sup>666</sup> stack at each side of the pyrrolidide ring of Val-Pyr. Tyr<sup>547</sup> and Tyr<sup>631</sup> probably form the oxyanion hole. Proper orientation of the proline in the P<sub>1</sub> position is achieved by its side chain interaction along with its binding to the oxyanion pocket.

Two glutamic acids, Glu<sup>205</sup> and Glu<sup>206</sup>, form salt bridges to the free amino terminus of the P<sub>2</sub> residue, which corresponds to the N-terminus of a peptide substrate. These two residues are situated in a small horizontal helix (residues 201-207, Figure 1.8.) in blade four of the propeller domain. This small horizontal helix narrows the active site, leaving room for only two amino acids before the peptide substrate/inhibitor reaches the active site serine. This novel feature is the reason for DPIV being a dipeptidyl peptidase. The spatial arrangement of Ser<sup>630</sup> with respect to Glu<sup>205</sup> and Glu<sup>206</sup> in dipeptidyl peptidase IV makes these two residues the most important feature for alignment of the peptide prior to catalysis. The carbonyl oxygen of the P<sub>2</sub> residue is stabilized and activated by Arg<sup>125</sup> and Asn<sup>710</sup>. The valine side chain of Val-Pyr points into the large cavity thus making no specific contact with dipeptidyl peptidase IV. This explains why dipeptidyl peptidase IV has no specific requirements for the N-terminal amino acid in the P<sub>2</sub> position.

As a post proline cleaving enzyme dipeptidyl peptidase IV has to meet an additional requirement for efficient catalysis. As known, proline-containing peptides can adopt cis- and trans- peptide bond conformations. Only a peptide in the trans conformation is able to productively bind to the active site (Fischer *et al.* 1983). In dipeptidyl peptidase IV catalysis the conformation of the peptide bond at the amino terminal side of the proline is important (P<sub>2</sub>-P<sub>1</sub>). Reports suggest a conformational two-step mechanism for substrate hydrolysis where a trans substrate binds to the active site, followed by a trans-cis isomerization to enable proteolytic cleavage. In dipeptidyl peptidase IV the Arg<sup>125</sup> residue is responsible for destabilizing the trans conformation (Engel *et al.* 2003).

#### Oligopeptide access and product release from the active site

As highlighted in section 1.3.6., Rasmussen *et al.* (2003) favoured access of substrate to the active site of dipeptidyl peptidase IV through the negatively charged side

opening, with product egress through the  $\beta$ -propeller. Functionally, the side opening only model fails to explain dipeptidyl peptidase IV's high substrate selectivity, as even secondary structured peptides could access the active site through the side opening. Also comparisons to prolyl oligopeptidase show that their open  $\beta$ -propeller is responsible for channelling substrates to and products away from the active site (Fulop *et al.* 1998). Engel *et al.* (2003) believe that the  $\beta$ 8-propeller of dipeptidyl peptidase IV provides substrate access to and its side opening product release from the active site. Passage through the  $\beta$ -propeller tunnel requires substrates to unfold. Once the peptides amino terminus approaches the active site, it is still held in place by the C-terminus interacting with the  $\beta$ -propeller. This may contribute to the bending of the substrate for cleavage. The product is then directly released through the side exit. This hypothesis could explain why degradation of glucagons by dipeptidyl peptidase IV is not processive but occurs sequentially in two independent steps (Pospisilik *et al.* 2001).

#### Catalytic cavity and $\beta$ -propeller architecture comparisons

The eight-bladed  $\beta$ -propeller widens from the surface towards the active site of dipeptidyl peptidase IV, this was also a feature of the prolyl oligopeptidase structure (Fulop *et al.* 1998). The residue in prolyl oligopeptidase structurally and functionally equivalent to Asn<sup>710</sup> and Arg<sup>125</sup> of dipeptidyl peptidase IV is Arg<sup>643</sup>. The side chain of Tyr<sup>662</sup> in dipeptidyl peptidase IV aligns structurally with the side chain of Trp<sup>595</sup> of prolyl oligopeptidase, whereas the backbone of Trp<sup>595</sup> aligns structurally with Tyr<sup>666</sup> of dipeptidyl peptidase IV. The Cys<sup>255</sup> residue of prolyl oligopeptidase shows no homologous counter residue in dipeptidyl peptidase IV. So dipeptidyl peptidase IV and prolyl oligopeptidase show good homology in the upper part of their catalytic cavities orientating the molecule. In contrast, significant differences are present in the bottom part of these molecules, like the Glu-Glu motif of dipeptidyl peptidase IV, explaining their different substrate specificities. The most interesting discovery from the structure of dipeptidyl peptidase IV is the extent, in comparison to prolyl oligopeptidase, with which the propeller domain regulates its peptidase activity.

### 1.3.7. Specificity

Dipeptidyl peptidase IV exhibits relatively restricted substrate specificity (Figure 1.12.). In the P<sub>1</sub> position almost exclusively proline and alanine are accepted. In a study with growth hormone-releasing factor (GRF) analogues, other P<sub>1</sub> residues such as serine, leucine and glycine were also cleaved but with lower rates (Bongers *et al.* 1992; Martin *et al.* 1993). The P<sub>2</sub> position can contain any proteinogenic amino acid including the proline residue. Substrates with hydrophobic or basic residues in this position are better hydrolysed than those with acidic ones. S configuration of the amino acids in both P<sub>1</sub> and P<sub>2</sub> positions in the case of proline substrates (Heins *et al.* 1988) and in the P<sub>1</sub> position in the case of alanine substrates (Heins *et al.* 1988), a free N-terminus as well as *trans* conformation of the peptide bond to be cleaved (Fischer *et al.* 1983) are important for enzymatic hydrolysis. The P<sub>1</sub>' position also accepts all amino acid residues but hydrolysis will not take place with proline or hydroxyproline in this position (Kenny *et al.* 1976). Extensive studies into the specificity of dipeptidyl peptidase IV using growth hormone-releasing factor of different peptide lengths have shown that the specificity extends beyond the P<sub>1</sub>' position. The requirement for an L residue in position P<sub>4</sub>' indicates that the enzyme-binding site extends possibly to the S<sub>4</sub>' subsite (Bongers *et al.* 1992). The chain length of the peptides cleaved has not been systematically investigated. Peptides up to 80 residues appear to be good substrates (Mentlein, 1999).

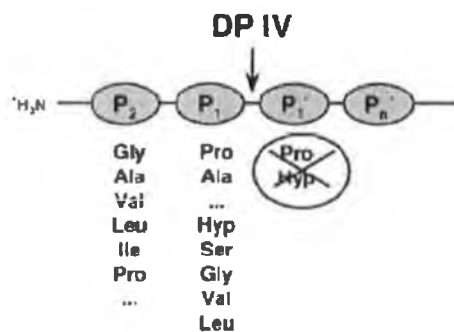


**Figure 1.12. Substrate Selectivity of Dipeptidyl Peptidase IV (Reinhold *et al.* 2002)**

### 1.3.8. Inhibitors

Many dipeptidyl peptidase IV inhibitors have been synthesised and their effect measured both enzymatically and physiologically. Demuth *et al.* (1988) investigated the inhibitory effect of *N*-peptidyl-*O*-aroylhydroxylamines on dipeptidyl peptidase IV. They were reported as mechanism based inhibitors of dipeptidyl peptidase IV with only modest potency. A comparison by this group of the turnover values for different Xaa residues in the P<sub>2</sub> position demonstrated that the more hydrophobic or longer the side chain of the amino acid, the more potent the inhibitor towards dipeptidyl peptidase IV.

The simple tripeptides diprotein A (Ile-Pro-Ile) and diprotein B (Val-Pro-Leu) are competitive inhibitors of dipeptidyl peptidase IV. Even though they are substrates for dipeptidyl peptidase IV, an apparent competitive inhibition of dipeptidyl peptidase IV by these compounds is an interesting kinetic artifact, which originates from the substrate-like nature of these tripeptides with a penultimate proline residue (Rahfeld *et al.* 1991). These compounds have been used widely for dipeptidyl peptidase IV characterisation studies (De Meester *et al.* 1992; Ohkubo *et al.* 1994).

Flentke *et al.* (1991) used Xaa-boroPro (boroPro is an analog of proline in which the carboxylate group is replaced by a boronyl group) as potent and specific inhibitors of dipeptidyl peptidase IV. They belong to a class of serine protease inhibitors known as peptide boronic acids with their potency being attributed to the ability of the boronyl group to form a tetrahedral adduct with the active serine, which closely mimics the transition state of the enzyme catalysed reaction. Ala-boroPro gave a K<sub>i</sub> of 2nM, while Pro-boroPro gave a K<sub>i</sub> of 3nM against porcine kidney dipeptidyl peptidase IV activity. N-terminus blocking of Ala-boroPro abolished affinity of the inhibitor, while removal of the N-terminus leaving boroPro reduced affinity of inhibitory for dipeptidyl peptidase IV by five orders of magnitude. The dipeptide boronic acids exhibit slow-binding kinetics, while boroPro does not. Unfortunately, these compounds are highly unstable with t<sub>1/2</sub> of Ala-boroPro between 2-30 minutes and that of Pro-boroPro is 1.5 hours in aqueous solution. Guitheil and Bachovchin (1993) fractionated L-Pro-DL-boroPro into its component L-L and L-D diastereomers, with the L-L compound giving a K<sub>i</sub> of 16pM but the L-D isomer bound 1000 fold less weakly.

A series of aminoacylpyrrolidine-2-nitriles in which a nitrile group replaces the carboxyl group of proline were synthesised as dipeptidyl peptidase IV inhibitors (Li *et al.* 1995). Four aminoacylpyrrolidine-2-nitriles were prepared. These compounds studied had varied N-terminal amino acids. Arg-Pyrr-2-CN inhibits dipeptidyl peptidase IV with a  $K_i$  of  $0.37\mu\text{M}$  but when the bulky PMC (2,2,5,7,8-pentamethyl chroman-6-sulfonyl) guanidine blocking group was introduced, Arg(PMC)-Pyrr-2-CN gave a  $K_i$  of  $0.19\mu\text{M}$ . This is more than likely due to the bulky group present in the  $P_2$  position. All compounds tested were competitive inhibitors. Aminoacylpyrrolidine-2-nitriles are easily synthesised, relatively potent, specific and stable inhibitors of dipeptidyl peptidase IV.

Many chemical classes of dipeptidyl peptidase IV inhibitors have been synthesised and evaluated but most suffer from significant toxicity and instability *in vivo* which prohibits their introduction into biological systems. De Meester *et al.* (1997) prepared and characterised a number of peptide-derived diphenylphosphonates. One of these slow-binding and irreversible inhibitors of dipeptidyl peptidase IV, Pro-Pro-diphenylphosphonate or prodipine was investigated for its *in vivo* applicability. Treatment with prodipine led to inhibition of plasma and tissue dipeptidyl peptidase IV activity in animals. The *in vivo* use of this non-toxic, chemically stable, irreversible inhibitor of dipeptidyl peptidase IV would help in unravelling the biological function of this ectopeptidase.

Amino acid pyrrolidides (Pyr) and thiazolidides (Thia) are another set of dipeptidyl peptidase IV inhibitors. Such compounds are known to be effective competitive dipeptidyl peptidase IV inhibitors with  $K_i$  values in the low micromolar to nanomolar range (Hoffman and Demuth, 2002). They represent a minimal recognition structure necessary for inhibition of dipeptidyl peptidase IV characterized by a free N-terminus, the  $\alpha$ -carboxyl function of the peptide bond and a C-terminal proline analog. They also harbour no chemical reactive group and are stable for weeks in aqueous solution. These inhibitors are recently gaining recognition as potential new treatments for type 2 diabetes. Glucagon and glucagon-like peptide (GLP-1), which are directly involved in type 2 diabetes, are known biological substrates of dipeptidyl peptidase IV *in vitro* and *in vivo*. Pospisilik *et al.* (2001) reported the prevention of glucagon degradation

by dipeptidyl peptidase IV using isoleucyl thiazolidine. More recently, one of the two 2-cyanopyrrolidide compounds which are potent dipeptidyl peptidase IV inhibitors, NVP-DPP728 has been reported to increase plasma GLP-1 concentrations and improve oral glucose tolerance in obese Zucker rats (Willand *et al.* 2002). In other physiological processes, degradation of neuropeptide Y and peptide YY was prevented in human serum by administration of lys-pyrrolidide (Mentlein *et al.* 1993).

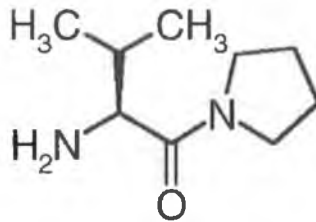


**Figure 1.13. The Chemical Structure of Inhibitor Val-Pyrrolidine**

### 1.3.9. Physiological Relevance

Dipeptidyl peptidase IV is involved in a number of different physiological regulation processes. On one hand the enzyme is a peptidase, which can change the activity of a number of peptide hormones, neuropeptides and chemokines in a very specific manner (Mentlein, 1999), while also this enzyme exerts protein-protein interactions, so mediating the regulation of intracellular signalling cascades independent of its peptidase activity (De Meester *et al.* 1999)

Dipeptidyl peptidase IV is involved in peptide degradation and amino acid scavenging at the intestinal and renal brush border membranes. Using gliadin, a proline rich protein, in feeding rats that were normal and genetically deficient in dipeptidyl peptidase IV, the control group maintained their weight, whereas the deficient group experienced a significant weight loss. The expression of dipeptidyl peptidase IV in the intestinal brush border was also seen to increase dramatically by feeding with a high proline containing diet (Tirupathi *et al.* 1990).

This enzyme is also well known to modulate the biological activity of several peptide hormones, chemokines and neuropeptides by specifically cleaving N-terminal dipeptides. Various genetic and pharmacological studies have revealed a prominent

physiological role for this regulatory enzyme. Marguet *et al.* (2000) showed that mice lacking the gene for dipeptidyl peptidase IV show enhanced insulin secretion and improved clearance of blood glucose partly due to increased levels of active glucagon-like peptide-1 (GLP-1) and glucose-dependent insulinotropic polypeptide (GIP). These two peptide hormones are known as incretins and both are involved in potent stimulation of insulin release. It is well established that dipeptidyl peptidase IV rapidly cleaves the N-terminal dipeptide from these incretins, yielding truncated, biologically inactive GIP<sub>3-42</sub> and GLP-1<sub>9-36</sub>. Type II diabetes is a disease characterised by elevated blood glucose levels and an insufficiency of insulin. Inhibition of dipeptidyl peptidase IV activity increases insulin secretion and improves glucose control in diabetic animals and humans. Therefore, modulation of dipeptidyl peptidase IV activity using specific inhibitors could be a feasible approach to managing Type II diabetes (Hoffman and Demuth, 2002).

Dipeptidyl peptidase IV (CD 26) is considered to be an activation factor on the surface of human T lymphocytes, where it is considered to participate in regulation of proliferation and differentiation of the lymphocytes and in production of cytokines (Reinhold *et al.* 1994).

Adenosine deaminase, an enzyme that metabolises extracellular adenosine is a known ligand of cell surface and soluble dipeptidyl peptidase IV. As extracellular adenosine inhibits T-cell proliferation in a dose dependent manner, it is likely that this inhibition is relieved by localization of adenosine deaminase to the cell surface by binding to dipeptidyl peptidase IV, so therefore association of ADA with DPIV/CD26 is possibly importantly involved in the ability of DPIV/CD26 to promote proliferation and cytokine production. (Gorrell *et al.* 2001).

Dipeptidyl peptidase IV is also reported to bind to the extracellular matrix components collagen and fibronectin, potentially modifying cell adhesion, migration and metastatic behaviour (Drucker, 2003).

<b>Peptide</b>	<b>N-terminus</b>	<b>Amino acids</b>
Neuropeptide Y	Try-Pro-Ser-Lys	36
Peptide YY	Try-Pro-Ile-Lys	36
RANTES	Ser-Pro-Tyr-Ser	68
IP-10	Val-Pro-Leu-Ser	77
Eotaxin	Gly-Pro-Ala-Ser	74
Substance P	Arg-Pro-Lys-Pro	11
Endomorphin 2	Tyr-Pro-Phe-Phe-NH <sub>2</sub>	4
Enterostatin	Val-Pro-Leu-Ser	5
$\beta$ -Casomorphin	Tyr-Pro-Phe-Pro-Gly-Pro-Ile	7
GRF (1-44) amide	Tyr-Ala-Asp-Ala	44
GIP	Tyr-Ala-Glu-Gly	42
GLP-1 (7-36) amide	His-Ala-Glu-Gly	30
GLP-2	His Ala-Asp-Gly	33

**Table 1.7. Some Peptides Cleaved By Dipeptidyl Peptidase IV**

Abbreviations: IP-10, interferon-inducible protein; GRF, growth hormone-releasing factor; GIP, glucose-dependent insulintropic polypeptide; GLP-1, glucagons-like peptide 1; RANTES, regulated on activation normal T-cell expressed and secreted.



## 1.4. Seprase

**Seprase** (surface expressed protease) is an N-glycosylated, type II transmembrane protein belonging to the small family of serine integral membrane peptidases (SIMP). These peptidases are inducible, specific for proline-containing peptides and macromolecules and active on the cell surface (Chen *et al.* 2003). Seprase shows up to 52% homology to dipeptidyl peptidase IV and its essentially identical to fibroblast activation protein  $\alpha$  (FAP $\alpha$ ) (Goldstein *et al.* 1997). Seprase/FAP $\alpha$  is therefore a member of the DPIV-like gene family (Abbott and Gorrell, 2002) grouped in subfamily S9B of the peptidase family S9 (prolyl oligopeptidase family), clan SC (Barrett *et al.* 1998). Even though all SIMP members are known to cleave prolyl peptide (Pro-Xaa) bonds, there are conflicting reports on possible dipeptidyl peptidase activity by seprase but its main distinguishing feature is its gelatinase activity (Pineiro-Sanchez *et al.* 1997).

### 1.4.1. Distribution and Purification

Seprase is not expressed in most normal adult tissues but is expressed and localised on cell surface invadopodia of human melanoma and carcinoma cells (Monsky *et al.* 1984; Pineiro-Sanchez *et al.* 1997). Seprase has been purified mainly from cell membranes and shed vesicles of LOX human melanoma cells. Size exclusion chromatography (S-200) and affinity chromatography using wheat germ agglutinin (WGA)-agarose are two of the most widely used resins for seprase purification (Aoyama and Chen, 1990; Pineiro-Sanchez *et al.* 1997). Soluble forms and isoforms of these membrane proteases are beginning to be found in biological fluids, but their roles are poorly understood (Chen *et al.* 2003).

### 1.4.2. Activity Detection and Specificity

The most sensitive assay available to date for seprase detection involves gelatin zymography due to the established gelatinase activity associated with seprase, though this is not a quantitative assay. Kelly (1999) developed an assay based on the degradation of radiolabelled gelatin substrate and subsequent qualitative measurement of the released fragments.

Substrate specificity studies using zymography have shown that seprase degrades gelatin (Aoyama and Chen, 1990). Pineiro-Sanchez *et al.* (1997) examined possible

extracellular matrix substrates, such as type I collagen, type IV collagen, laminin and fibronectin. Native collagens were not degraded by seprase, whereas thermally denatured collagens were digested into smaller polypeptides. Seprase did not degrade fibronectin or laminin. Also, based possibly on such homology in the catalytic domains of seprase and DP IV, seprase is reported (Chen *et al.* 2003) to possess prolyl dipeptidyl peptidase activity. In this case Ala-Pro-AFC was seen as a sensitive fluorogenic substrate. Interestingly, conflicting reports still exist with Pineiro-Sanchez *et al.* (1997) and Ghersi *et al.* (2002) reporting no such prolyl dipeptidyl peptidase cleavage. Therefore, seprase is classified as a gelatinolytic endopeptidase due to its specific cleavage of gelatin.

#### **1.4.3. Structural and Biochemical Aspects**

Goldstein *et al.* (1997) reported the molecular cloning of a cDNA that encodes the 97kDa subunit of seprase. As with dipeptidyl peptidase IV, seprase is a homodimer containing N-glycosylated subunits. Its deduced amino acid sequence predicts a type II integral membrane protein consisting of a cytoplasmic tail of six amino acids, followed by a twenty amino acid transmembrane domain at the N-terminus, an N-glycosylation and cysteine rich domain and a 200 amino acid region at the C-terminus that contains the catalytic region (Goldstein *et al.* 1997; Pineiro-Sanchez *et al.* 1997). Its catalytic triad residues Ser<sup>624</sup>, Asp<sup>702</sup> and His<sup>734</sup> are contained within this catalytic region at the carboxyl end of each subunit (Goldstein and Chen, 2000). This order of the catalytic triad members, similar to dipeptidyl peptidase IV and prolyl oligopeptidase is characteristic of the  $\alpha/\beta$  hydrolase fold secondary structure. Dimerisation of its inactive subunits is an essential structural requirement for seprase activity (Goldstein *et al.* 1997; Pineiro-Sanchez *et al.* 1997).

Seprase is an active homodimeric 170kDa membrane protease composed of proteolytically inactive 97kDa subunits. An isoelectric point (pI) of 5 is reported for this enzyme with optimum assay temperature being 37°C (Pineiro-Sanchez *et al.* 1997).

#### 1.4.4. Catalytic Classification

Seprase is a gelatinolytic endopeptidase due to its ability to degrade gelatin, giving this enzyme its distinct gelatinase activity. As mentioned, many reports claim seprase to have exopeptidase (prolyl dipeptidase) activity due to its ability to cleave dipeptidyl peptidase IV substrates such as Gly-Pro-AMC and Ala-Pro-AFC and its similar sequence homology in the catalytic region with this enzyme, but these reports are still to be clarified for this enzyme (Chen *et al.* 2003).

Initial classification studies showed that seprase was a serine protease sensitive to PMSF and the sulfhydryl-modifying agent NEM (Aoyama and Chen, 1990). Pineiro-Sanchez *et al.* (1997) showed that seprase is a serine protease by virtue of its inhibition by the serine protease inhibitors DFP, PMSF, APSF, AEBSF and by affinity-labelling with [<sup>3</sup>H] DFP. Molecular cloning of seprase revealed Ser<sup>624</sup> as its catalytic serine residue (Goldstein *et al.* 1997).

Analysis of the deduced amino acid sequence of the seprase monomer revealed 52% homology to dipeptidyl peptidase IV (68% in the catalytic domain) and also that seprase is actually identical to fibroblast activation protein  $\alpha$  (FAP $\alpha$ ). The conserved serine protease motif G-X-S-X-G is present as G-W-S-Y-G. Since the orientation of the residues of the catalytic triad of seprase is similar to members of the prolyl oligopeptidase family, along with its structural organization similarity to dipeptidyl peptidase IV this enzyme is classified as a nonclassical serine protease and grouped along with other serine integral membrane peptidases in the subfamily S9B, known as the DPIV gene family (Abbott and Gorrell, 2002).

#### 1.4.5. Catalytic and Structural Mechanism

The catalytic triad members of seprase play an important role in its possible dipeptidyl peptidase activity and more importantly its gelatinase activity. This suggests a single active site for various proteolytic activities (Park *et al.* 1999). Also, seprase requires dimerisation to exhibit its gelatinase activity thereby showing a structural regulation of its protease activity, already seen previously with dipeptidyl peptidase IV.

Apart from the proteolytic or gelatinolytic activity of seprase, these serine integral membrane proteases have glycosylation and cysteine rich domains present in their structures. These structural features may function in recognition and binding to their

substrates, such as peptides, macromolecules, other enzymes or themselves (Chen *et al.*, 2003).

#### **1.4.6. Inhibitors and Physiological Relevance**

There is no specific inhibitor for seprase yet reported, but Chen *et al.* (2003) describe inhibitor profiling of seprase to be identical with that of dipeptidyl peptidase IV. Therefore, most work on seprase activity to date report the use of active site directed inhibitors such as DFP and PMSF for inactivation of its proteolytic activity (Aoyama and Chen, 1990; Pineiro-Sanchez *et al.* 1997).

The main function of serine integral membrane peptidases such as seprase resides in their proteolytic and adhesive abilities, thus influencing cellular activities, migration and invasion. Accumulation of these proteases and their complexes at cell surface protrusions, called invadopodia may play a prominent role in processing soluble factors (such as chemokines, hormones, bioactive peptides) in addition to the well-established role of invadopodia degrading components of the extracellular matrix (ECM) (Chen *et al.* 2003).

Due to the ability of seprase to degrade extracellular matrix components, which is essential to the cellular migration and matrix invasion that occurs during tumour invasion and metastasis (Gherzi *et al.* 2002), it is thought to have a role in facilitating tumour cell progression (Aoyama and Chen, 1990). This role of seprase is further enhanced by reports of its over expression by invasive tumour cells (Monksy *et al.* 1994) a feature also observed in pathologic specimens of human breast cancer tissue by immunohistochemistry (Kelly *et al.* 1998). Non-toxic inhibitors of seprase could be valuable for clarifying the role of this membrane protease in tumour cell invasion.

## 1.5. Oligopeptidase B

The oligopeptidase B (OpdB; EC 3.4.21.83) subfamily of serine peptidases represents one of two branches of the prolyl oligopeptidase family of serine peptidases. Previously called protease II, it is homologous to prolyl oligopeptidase, indicating that the tertiary structures of the enzymes are similar (Kanatani *et al.* 1991; Barrett and Rawlings, 1992). Oligopeptidase B was first isolated with trypsin-like substrate specificity from *Escherichia coli* cells, cleaving peptides at lysine and arginine residues (Pacaud and Richaud, 1975). Due to the ability of oligopeptidase B to cleave seemingly only low molecular weight peptides with a preferential specificity for **B**asic amino acid residues led to the name oligopeptidase **B**. Initial examples of this enzyme was restricted to prokaryotes which led to them receiving little attention, but more recently oligopeptidase B has been isolated, cloned and studied in trypanosomatids (Burleigh *et al.* 1997).

### 1.5.1. Distribution and Purification

Oligopeptidase B is a cytosolic enzyme (Pacaud and Richaud, 1975) only found in unicellular eukaryotes (kinetoplastid protozoan parasites), gram-negative bacteria, spirochetes and plants. To date, no oligopeptidase B enzymes has been isolated or cloned from mammalian cells. All life stages of the parasite *Trypanosoma cruzi* express oligopeptidase B (Burleigh *et al.* 1997), with *T.cruzi* oligopeptidase B often isolated from epimastigotes, which are a good source of the parasite (Burleigh and Andrews, 1995). The enzyme has been purified from a number of sources such as *E.coli*, *T.brucei*, *T.cruzi* and soybean seed (Pacaud and Richaud, 1975; Troeberg *et al.* 1996; Ashall, 1990; Nishikata, 1984). Utilizing expression of the recombinant enzyme in *E.coli* systems is the most convenient method for preparation of the enzyme. This procedure was used for isolation of oligopeptidase B from the following sources, *E.coli*, *T.brucei*, *T.cruzi*, *Moraxella lacunata* and *Salmonella enterica* (Juhasz *et al.* 2002; Morty *et al.* 1999; Burleigh *et al.* 1997; Yoshimoto *et al.* 1995; Morty *et al.* 2002). Despite the wide distribution of oligopeptidase B in nature, the physiochemical properties of the enzyme differ between sources (Tsuru and Yoshimoto, 1994).

### 1.5.2. Biochemical and Structural Aspects

Pachaud and Richaud (1975) first estimated a molecular weight of about 58-110kDa for *E.coli* oligopeptidase B. Subsequent reports (Kanatani *et al.* 1991; Kornblatt *et al.* 1992; Morty *et al.* 2002) have deduced oligopeptidase B to be a monomeric protein of about 80kDa, except for soybean seed oligopeptidase B which has a molecular weight of 59kDa (Nishikata, 1984). Studies on the *T.cruzi* oligopeptidase B enzyme that was formerly known as alkaline peptidase (Ashall *et al.* 1990; Burleigh *et al.* 1995) revealed a molecular mass of 120kDa when active enzyme was applied under non-reducing conditions to an SDS PAGE gel (Burleigh *et al.* 1995). When this enzyme was fully denatured, SDS PAGE analysis revealed a molecular mass of 80kDa; this along with gel filtration results on native and recombinant enzyme possibly reveals dimerization (Burleigh *et al.* 1997).

The idea that the catalytic site of oligopeptidase B may be accessible only to unstructured oligopeptides similar to prolyl oligopeptidase, led to the construction of a three-dimensional homology model for *Escherichia.coli* oligopeptidase B based on the structure of prolyl oligopeptidase (Gerczei *et al.* 2000). This model showed that the S<sub>2</sub> binding site-contained residues Asp<sup>460</sup> and Asp<sup>462</sup> thus implicating them in directing P<sub>2</sub> specificity. Recent site-specific mutagenesis studies (Morty *et al.* 2002) identified a pair of glutamic acid residues, Glu<sup>576</sup> and Glu<sup>578</sup> which define P<sub>1</sub> specificity and also a second pair of residues Asp<sup>460</sup> and Asp<sup>462</sup> as proposed by the 3D model, involved in directing P<sub>2</sub> specificity. It is noteworthy that residue Glu<sup>576</sup> occupies the same steric position as Trp<sup>595</sup> in prolyl oligopeptidase, which is known to interact with the P<sub>1</sub> proline ring (Polgar, 2002a).

The order of the catalytic serine and histidine of oligopeptidase B is reversed with respect to that in trypsin and subtilisin but similar to prolyl oligopeptidase, thus indicating an unrelated three-dimensional structure (Polgar, 1992a).

Source	MW kDa	pI	pH optima	Temp. optima (°C)	Reference
<i>Escherichia.coli</i>	81.858	5.2	8.0	45	Kanatani <i>et al.</i> 1991
<i>Moraxella.lacunata</i>	80	4.3	6.5	35	Yoshimoto <i>et al.</i> 1995
<i>Trypanosoma.cruzi</i>	120	4.8-5.0	ND	ND	Burleigh and Andrews, 1995
<i>Trypanosoma.brucei</i>	80	ND	8-9.5	25	Troeberg <i>et al.</i> 1996
Soyabean seed	59	ND	8.5	ND	Nishikata, 1984

**Table. 1.8. Biochemical Properties of Oligopeptidase B from Various Sources**

### 1.5.3. Activity Detection

Spectrophotometric assays using N-benzoyl-DL-arginine-p-nitroanilide (Bz-Arg-pNA) were the first described by Pachaud and Richaud (1975) for the identification of oligopeptidase B (Protease II) hydrolysing activity from *E.coli*. Other chromogenic substrates for the *E.coli* enzyme were N-benzoyl-arginine- $\beta$ -naphthylamide (Bz-Arg- $\beta$ NA), releasing  $\beta$ NA, which can be measured at 550nm (Tsuru and Yoshimoto, 1994; Kanatani *et al.* 1991). In these substrates mentioned above, arginine can be replaced with lysine but these enzymes prefer arginine to lysine in the P<sub>1</sub> position (Ashall, 1990). The more sensitive fluorimetric assays where AMC replaces pNA or  $\beta$ NA have also been employed (Shannon *et al.* 1982; Tsuru and Yoshimoto, 1994). The discovery that oligopeptidase B cleaves much faster peptides with two adjacent basic residues (Ashall *et al.* 1990; Polgar, 1997) has led to the widespread use of the substrate Z-Arg-Arg-AMC for the detection of oligopeptidase B from *T.brucei* (Morty *et al.* 1999).

### 1.5.4. Catalytic Classification

Oligopeptidase B is a serine endopeptidase which catalyses the hydrolysis of oligopeptides at the carboxyl side of basic amino acids, but is only slightly active towards high molecular mass peptides (Tsuru and Yoshimoto, 1994). The enzyme is classified as a serine protease due to its inhibition by diisopropyl fluorophosphate (DFP), leupeptin, antipain and N-tosyl-L-lysyl-chloromethylketone (TLCK). Even though oligopeptidase B resembles trypsin in that it's classified as a serine protease, which cleaves peptide bonds on the carboxyl side of basic amino acids, it is distinctly different with regards to its specificity for oligopeptides and insensitivity to protein inhibitors of trypsin. Interestingly, oligopeptidase B is not a member of the S1 family of trypsin proteases but shares a high degree of homology with prolyl oligopeptidase and hence have been classified as a member of the S9 family of serine proteases (Rawlings and Barrett, 1994). Oligopeptidase B from *E.coli* shows about 25% homology with prolyl oligopeptidase from porcine brain (Kanatani *et al.* 1991), while *T.cruzi* oligopeptidase B shows only 18% homology with porcine brain prolyl oligopeptidase (Burleigh *et al.* 1997). It is also shown that the sequence homology is greater in the peptidase domain, especially around the catalytic groups, than in the propeller domain (Barrett and Rawlings, 1992).



Barrett and Rawlings (1992) postulated that the S9 prolyl oligopeptidase family contain a consensus sequence GxSxGGzz (where x is any residue and z is a hydrophobic residue) that includes the active site serine residue. Oligopeptidase B contains this consensus sequence, where the active site serine (Ser<sup>532</sup>) was identified using radiolabelled DFP for *E.coli* (Kanatani *et al.* 1991). The catalytic triad of oligopeptidase B from *E.coli* was deduced to be ser<sup>532</sup>, Asp<sup>617</sup> and His<sup>652</sup> (Tsuru, 1998).

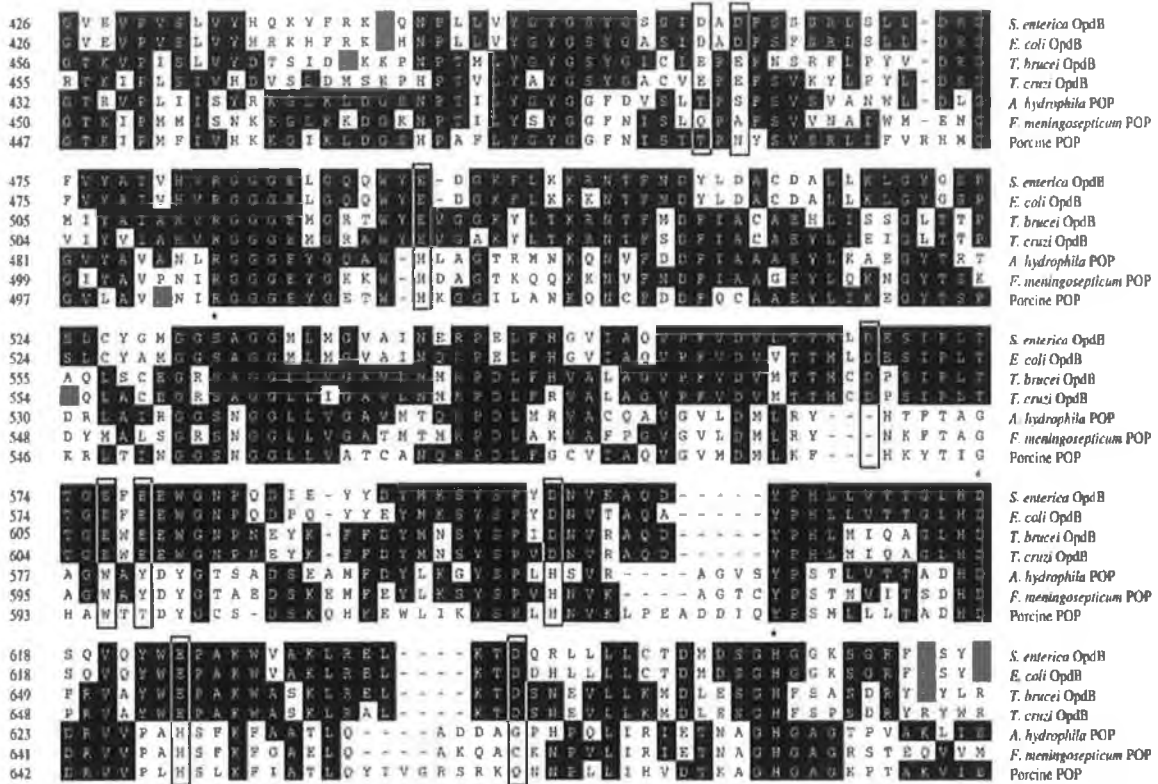


**Figure 1.14. Catalytic Domain Homology of Oligopeptidase B and Prolyl Oligopeptidase**

Multiple sequence alignment of the amino acid sequences of the catalytic domains from representatives of the OpdB and POP branches of the prolyl oligopeptidase family of serine peptidases. Sources of sequences are given in the legend to Fig.1.14. Asterisks indicate the active-site serine, histidine and aspartic acid residues that constitute the catalytic triad.

### 1.5.5. Catalytic and Structural Mechanism

#### Active site and substrate binding

The catalytic triad amino acids play a significant role in the catalysis of oligopeptidase B. This serine protease catalysis is similar to that explained in sections 1.2.6. In order to understand substrate binding and specificity of the active site of oligopeptidase B Morty *et al.* (2002) performed site directed mutagenesis on acidic residues conserved in oligopeptidase B but absent from prolyl oligopeptidase. This study identified Glu<sup>576</sup> and Glu<sup>578</sup> being critically involved in the interaction of oligopeptidase B with the P<sub>1</sub> substrate residue and direct its cleavage C terminal to basic residues. They proposed that the carboxyl groups of Glu<sup>576</sup> and Glu<sup>578</sup> direct P<sub>1</sub> substrate specificity by electrostatic interaction with the charged side chains of P<sub>1</sub> arginine or lysine in substrates. Given their close proximity (Figure.1.14.) separated by a single tryptophan in the sequence they speculated the formation of a carboxyl dyad by these two glutamic acid residues that binds the basic substrate side chains. As mentioned in section 1.3.2., this idea is reinforced by the fact that Glu<sup>576</sup> corresponds to Trp<sup>595</sup> (Figure.1.14.) of porcine prolyl oligopeptidase, which directs P<sub>1</sub> specificity of prolyl oligopeptidase for proline residues (Fulop *et al.* 1998). Morty *et al.* (2002) also identified Asp<sup>460</sup> and Asp<sup>462</sup> as possibly being involved in defining P<sub>2</sub> specificity and so direct preferential cleavage by oligopeptidase B after a pair of basic residues. This proposing the presence of a second carboxyl dyad formed by the side chains of Asp<sup>460</sup> and Asp<sup>462</sup>. These results correspond exactly with the report by Gerczei *et al.* (2000) explained in section 1.3.2. on their three-dimensional structure of oligopeptidase B.

It is also reported (Juhász *et al.* 2002) that Tyr<sup>452</sup> of oligopeptidase B, which corresponds to Tyr<sup>473</sup> of prolyl oligopeptidase is a member of the oligopeptidase B oxyanion binding site (Figure.1.14.).

The observations that oligopeptidase B is unable to hydrolyse proteins (Polgar, 1997) could suggest a similar catalytic mechanism as shown in prolyl oligopeptidase (Fulop *et al.* 1998) where the catalytic triad is located in a tunnel like cavity, thus impeding the access of proteins to its catalytic site.

### Kinetic properties of catalysis

The reactions of oligopeptidase B are sensitive to ionic strength especially substrates containing arginines in positions P<sub>1</sub> and P<sub>2</sub>. The rate is often seen to decrease by one order of magnitude by addition of 1M NaCl. The reactions are very sensitive in regions of low ionic strength and more reproducible rate constants can be measured at high ionic strength. The rate constant for Z-Arg-Arg-AMC one of the best substrates is 63 $\mu\text{M}^{-1}\text{S}^{-1}$  at low ionic strength. It is now known that the inhibition of hydrolysis at high ionic strength (decrease in rate constant) is caused by disruption of the electrostatic interactions between substrate arginines and enzyme carboxyl groups. This is caused by an elevation in K<sub>m</sub> due to reduced binding of substrate, which in turn decreases the specificity rate constant K<sub>cat</sub>/K<sub>m</sub> (Polgar, 1997).

The importance of the positive charge of arginine was studied by using a neutral, structurally similar citrulline derivative. The very low rate constant observed while using this substrate indicated that the positive charge of arginine is essential for catalysis (Polgar, 1999).

In serine protease reactions the catalytic serine OH group attacks the substrate carbonyl carbon atom, with this process being assisted by general base catalysis afforded by the catalytic histidine side chain. The resulting tetrahedral intermediate then decomposes by general acid catalysis by the protonated histidine. These general acid/base catalysed reactions are commonly rate limiting in the classic serine proteases. General acid-base catalysed reactions proceed faster by a factor of 2-3 in water than in heavy water. The kinetic deuterium isotope effect indicated that general acid/base catalysis is not rate limiting in oligopeptidase B reactions. Therefore a rate-limiting conformational change induced by substrate binding as reported for prolyl oligopeptidase is also the rate-limiting step in oligopeptidase B catalysis (Polgar, 1997).

#### **1.5.6. Substrate Specificity and Inhibitors**

Oligopeptidase B of trypanosoma and prokaryotic organisms show both similar and strict specificity. Oligopeptidase B will only hydrolyse peptide substrates at the carboxyl end of basic amino acid residues (Arginine or Lysine) in the P<sub>1</sub> position. No

cleavage will occur with substrates of the general sequence H-Arg-Xaa or H-Lys-Xaa unless a blocking group (Cbz, Z) is placed at the N-terminus. Arginine appears to be the preferred P<sub>1</sub> residue. Many different residues can be accommodated in the P<sub>2</sub> position such as aromatic (Phe), hydrophobic (Val), hydrophilic (Thr), small uncharged (Gly) and proline. Ultimately though there is a preference for cleavage of substrates with basic amino acids at the P<sub>2</sub> position as well as the P<sub>1</sub>. It has actually been shown that oligopeptidase B hydrolyzes peptides with dibasic sites much faster than monobasic substrates with both arginine and lysine equally acceptable in the P<sub>2</sub> position (Polgar, 1997). An influence of the P<sub>3</sub> residue on substrate hydrolysis is also reported (Ashall *et al.* 1990), while the P<sub>1</sub>' position can accommodate all amino acid residues including proline (Tsuru, 1998).

The substrate size limitation of oligopeptidase B restricts its action to low-molecular mass (< 3kDa) peptides (Kanatani *et al.* 1991; Polgar, 1997; Troeberg *et al.* 1996; Yoshimoto *et al.* 1995). In addition to these oligopeptide substrates, restricted proteolysis of histone proteins was discovered, though no cleavage was detected at or near residues that had been posttranslationally modified or at defined secondary structures (Morty *et al.* 2002).

There are little reports available of specific and potent inhibitors of oligopeptidase B. Commonly used trypanocidal drugs inhibit oligopeptidase B from the African trypanosome, *Trypanosoma brucei* (Morty *et al.* 1998). These serine protease inhibitors namely pentamidine, diminazene and suramin reversibly inhibited oligopeptidase B *in vitro*. In the case of pentamidine and suramin the inhibition of oligopeptidase B *in vivo* may be of significant importance. Structurally, the pentamidine molecule represents two benzamidine molecules joined together, resembling a pair of basic amino acids (arginine residues) in a dipeptide, thus possibly mimicking potential oligopeptidase B substrates. Pentamidine resulted in competitive inhibition with a K<sub>i</sub> of 3.4µM for oligopeptidase B.

### 1.5.7. Physiological Importance

Oligopeptidase B is well known to be actively present in protozoan parasites, such as *Trypanosoma cruzi*, the causative agent of chagas disease in humans (Burleigh and Andrews, 1998) and in the African trypanosomes that produce the diseases nagana and sleeping sickness in cattle and human respectively (Troberg *et al.* 1996; Lonsdale *et al.* 2002).

It has been demonstrated that oligopeptidase B from *Trypanosoma brucei* is capable of cleaving biologically active peptides *in vitro* (Troberg *et al.* 1996). Oligopeptidase B activity correlates with blood parasitemia levels and it was reported that live trypanosomes do not release oligopeptidase B *in vitro* but that it is released by dying parasites into the host bloodstream, where it remains stable and catalytically active. It may therefore contribute to the pathogenesis of nagana and sleeping sickness through degradation of biologically active peptides in the bloodstream of infected hosts (Morty *et al.* 2001). Also administration of irreversible oligopeptidase B inhibitors to trypanosome infected mice significantly impaired disease progression (Morty *et al.* 1998).

Mammalian cell invasion by the intracellular protozoan parasite *Trypanosoma cruzi* is mediated by recruitment and fusion of host cell lysosomes, an unusual process that has been proposed to be dependent on the ability of parasites to trigger intracellular free calcium concentration ( $[Ca^{2+}]$ ) transients in host cells (Caler *et al.* 1998; Burleigh and Woolsey, 2002). Oligopeptidase B has been proposed as the enzyme possibly responsible for the generation of a  $Ca^{2+}$  signalling agonist from a cytosolic precursor molecule for mammalian cells (Burleigh and Andrews, 1995; Burleigh *et al.* 1997; Caler *et al.* 1998). Inhibition of oligopeptidase B activity using protease inhibitors (Burleigh and Andrews, 1995) or by specific antibodies to recombinant oligopeptidase B (Burleigh *et al.* 1997) results in loss of  $Ca^{2+}$  signalling.

The role of oligopeptidase B in *E.coli* and other prokaryotic cells is still not known. It has been suggested by Polgar (1997) that oligopeptidase B in prokaryotic cells may be a specialized processing enzyme due to its extremely efficient cleavage of peptides at paired basic sites, but to date its natural substrate remain unknown.

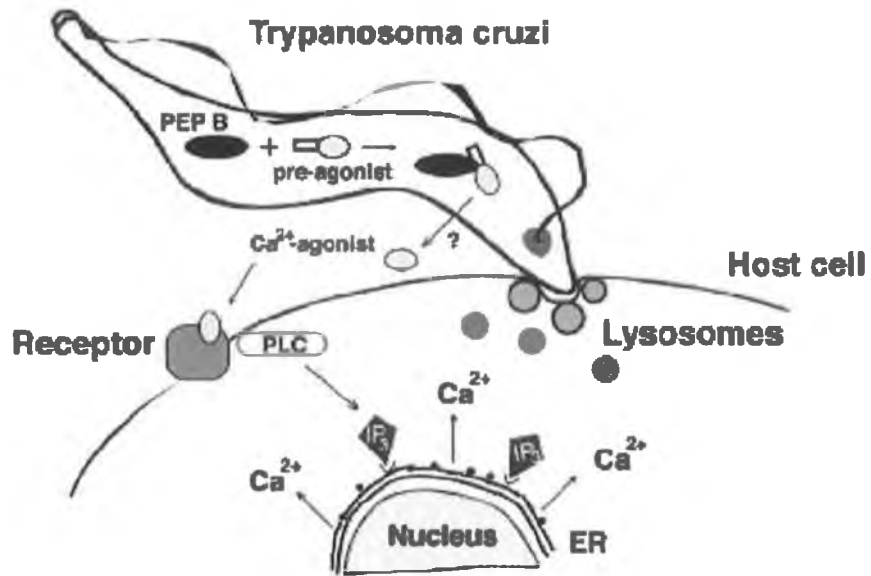


**Figure 1.15. A Model for *T.cruzi* Oligopeptidase B-Mediated Signalling in Mammalian Cells**

## 1.6. Acylaminoacyl Peptidase

Acylaminoacyl peptidase (EC 3.4.19.1) is an omega-peptidase that catalyses the removal of an N-acylated amino acid from blocked peptides (Jones *et al.* 1994). It has also been referred to by the names acylpeptide hydrolase (Gade and Brown, 1978), acylaminoacid-releasing enzyme (Mitta *et al.* 1989) and as of now usually acylaminoacyl peptidase (Radhakrishna and Wold, 1989).

### 1.6.1. Distribution and Purification

Acylaminoacyl peptidase is a cytosolic enzyme that is present in all tissues but is absent from small cell lung carcinoma. Due to its wide distribution in tissues it has been isolated and subsequently purified to homogeneity from a number of sources. The enzyme has been purified from bovine liver (Gade and Brown, 1978), Rabbit muscle (Radhakrishna and Wold, 1989), human erythrocytes (Jones *et al.* 1994) and porcine intestine mucosa (Raphel *et al.* 1999).

Ammonium sulphate precipitation is widely used as the initial step in the isolation of acylaminoacyl peptidase from tissue source. It proved to be very effective in removing bulk-contaminating protein from the soluble extract with up to 85% recovery of applied peptidase activity (Gade and Brown, 1978; Radhakrishna and Wold, 1989). Conventional chromatographic techniques such as anion exchange and gel filtration chromatography are the two most widely used techniques reportedly employed for the purification of acylaminoacyl peptidase. Radhakrishna and Wold, (1989) obtained a 7000-fold purification using anion exchange and the gel filtration resin S-300 twice. Whereas Jones *et al.* (1994) employed a double anion exchange step along with S-300 gel filtration for the purification of acylaminoacyl peptidase from human erythrocytes. This use of a second anion exchange step during purification was also reported by Gade and Brown (1978).

Apart from isolation of acylaminoacyl peptidase from mammalian tissue, Ishikawa *et al.* (1998) purified the enzyme from the Archaeon *Pyrococcus horikoshii* and cloned and expressed it in *Escherichia coli*.

### 1.6.2. Biochemical and Structural Aspects

The enzyme is a homotetramer composed of four identical subunits giving a total molecular mass of about 300kDa. The pI is reported to be acidic with a value of 4.0 (Scaloni *et al.* 1994). The enzyme is active over a wide pH of ~ 4.5-9.0. Rabbit muscle acylaminoacyl peptidase was reported to have a pH optimum of 6.9 whereas the enzyme from bovine liver resulted in a pH optimum of 8.2.

The complete primary amino acid sequence of rat, porcine and human acylaminoacyl peptidase has been reported (Kobayashi *et al.* 1989; Mitta *et al.* 1989; Scaloni *et al.* 1999). They are all 732 amino acids in length and having over 90% homology with each other. The primary structure revealed that the N-terminus methionine is acetylated and that all cysteine residues are present in a reduced form (Miyagi *et al.* 1995). The crystal structure of this protein and preliminary x-ray studies has been reported (Feese *et al.* 1993) but to date no three-dimensional structure is available. The linear arrangement of the catalytic triad amino acids as nucleophile-acid-base in the secondary structural organization of the protease domain of this enzyme is consistent with  $\alpha/\beta$  hydrolase fold (Scaloni *et al.* 1999). Durand *et al.* (2003) reported a three-dimensional model of porcine intestine acylaminoacyl peptidase consisting of a  $\beta$ -propeller in the N-terminus as well as a C-terminal catalytic domain with an  $\alpha/\beta$  hydrolase fold.

As well as isolation from eukaryotic cells, acylaminoacyl peptidase has been purified and cloned from the archaeon *Pyrococcus horikoshii*. This enzyme is only 632 amino acid residues in length and appears to be a dimer rather than a tetramer. A modification in the protein structure was seen to occur when incubated at 95°C for a few hours (Ishikawa *et al.* 1998).



### 1.6.3. Substrate Specificity and Activity Detection

Acylaminoacyl peptidase catalyses the hydrolysis of N-terminus acylated peptide substrates of various sizes and containing different types of acyl groups (acetyl, chloroacetyl, formyl and carbamyl) to generate an acylamino acid and a peptide with a free NH<sub>2</sub> terminus that is shortened by one amino acid as below (Radharishka and Wold, 1989).



The rates of hydrolysis of different blocked peptides vary considerably, depending on the nature of the first (P<sub>1</sub>) and second (P<sub>1</sub>') amino acids. Thus acylaminoacyl peptidase cleaves primarily Ac-Ala, Ac-Met, Ac-Ser in peptides with neutral side chains. If the side chain of the P<sub>1</sub>' or the P<sub>2</sub>' amino acid residues is charged the rate of cleavage is reduced. A proline residue at either side of the scissile bond abolishes activity (Jones and Manning, 1988; Radhakrishna and Wold, 1989; Sokolik *et al.* 1994). It is well known that acylaminoacyl peptidase has a preference for hydrolysis of oligopeptides due to its inability to cleave N-blocked proteins. The optimum length of the blocked peptide substrate is 2-3 amino acids with a decrease in activity apparent with increasing chain length (Manning, 1998).

Acetylalanine-pnitroanilide is the most commonly used substrate for activity detection (Jones *et al.* 1994).

### 1.6.4. Catalytic Classification

Due to the ability of acylaminoacyl peptidase to remove N-acetylated N-terminal residues from oligopeptides, classifies it as an exopeptidase. This enzyme is a serine protease due to inactivation by modification of Ser<sup>587</sup> by DFP (Scaloni *et al.* 1992). Further active site studies identified His<sup>707</sup> using a radiolabelled chloromethyl ketone as a second active site residue. The third member of the triad was identified as Asp<sup>675</sup> by Mitta *et al.* (1998) using site directed mutagenesis. When the complete primary sequence of acylaminoacyl peptidase was discovered no resemblance to the known classic serine peptidase was noted. A similarity in the sequences around the active site serine residue and the order of the catalytic triad of this enzyme was evident with

other oligopeptidases. It was classified as a member of the prolyl oligopeptidase family of oligopeptidases (Rawlings *et al.* 1991; Barrett and Rawlings, 1992). It is highly likely there is an overall similarity in the three-dimensional structure of this enzyme to other known members of this family.

#### **1.6.5. Catalytic Mechanism**

The catalytic triad residues will govern catalysis of acylaminoacyl peptidase. The sensitivity of the catalytic activity of this peptidase to various thiol reagents is very similar to the role played by Cys<sup>255</sup> in possibly regulating the activity of prolyl oligopeptidase (see section 1.2.6.). As with prolyl oligopeptidase this sensitivity to thiol reagents can be explained by their size. The larger p-hydroxymercuribenzoate (pHMB) or N-ethylmaleimide (NEM) can inhibit activity completely but the smaller iodoacetamide only partially under the same conditions. As with prolyl oligopeptidase it is postulated that the larger pHMB or NEM will react with a cysteine residue near the active site and block substrate entry, whereas the smaller iodoacetamide only partially blocks entry (Scaloni *et al.* 1994).

#### Kinetic properties

As mentioned the activity of acylaminoacyl peptidase can be assayed with acetylalanine-pnitroanilide as substrate (Jones *et al.* 1994). The enzyme exhibits different pH optima depending on the substrate used. For acetylglutamate-pnitroanilide the pH optima is 6.0, whereas for acetylalanine-pnitroanilide its 8.4. Also, Ac-Ala-Ala-OH and Ac-Ala-Ala-Ala-OH are better substrates than Ac-Ala-pNa, though pNa is a better leaving group than an amino acid. Ac-Ala-OH was reported to be a product like inhibitor ( $K_i$  of 0.4mM) being higher than Ac-D-Ala-OH ( $K_i$  of 17mM) (Raphael *et al.* 1999).

#### **1.6.6. Inhibitors and Physiological Relevance**

Apart from active site directed inhibitors such as DFP and some chloromethyl ketones, very few specific acylaminoacyl peptidase inhibitors are reported. Scaloni *et al.* (1992) have used blocked amino acids to great effect for peptidase inhibition. They report one of their most efficient inhibitors was acetyl-L-valine giving an  $IC_{50}$  of 100 $\mu$ M. Transition state analog inhibitors are also very good competitive inhibitors of

acylaminoacyl peptidase. Phenyl-n-butylborinic acid gave a  $K_i$  of 22 $\mu$ M for this enzyme (Scaloni *et al.* 1994).

The exact physiological role of this enzyme is still largely unknown. It possibly plays a role in the catabolism of N-acetylated proteins, which are abundant in living cells, after action of possible endopeptidases in the release of N-acetylated peptides (Richards *et al.* 2000). The blocked 13-residue peptide  $\alpha$ -melanocyte stimulating hormone ( $\alpha$ MSH) is a substrate of acylaminoacyl peptidase. It may play a role in the regulation of this peptide hormone (Manning, 1998).

Deficiency in expression of acylaminoacyl peptidase is reported in small-cell lung carcinomas and renal carcinomas. It is still unknown the potential role, if any, the peptidase plays in the malignant state of these cell lines (Jones *et al.* 1991; Polgar, 2002a).

## **MATERIALS and METHODS**

## 2.1. Materials

### **Sigma Chemical Company (Poole, Dorset, England):**

2-Mercaptoethanol	Formic Acid
7-Amino-4-Methylcoumarin	Glacial Acetic Acid
Acetic Acid (HPLC grade)	Glycine
Acetonitrile (HPLC grade)	High Range MW Markers
Acetonitrile (Spectranal grade)	Hydrochloric Acid
Acrylamide/bis-Acrylamide solution	Methanol (HPLC grade)
Ala-AMC	Phenyl Sepharose CL-4B
Ammonium Acetate (HPLC grade)	Potassium Phosphate (dibasic)
Ammonium Persulphate	Potassium Phosphate (monobasic)
Ammonium Sulphate	Protein G agarose
Arg-AMC	Pro-AMC
Biuret Reagent	Sample Buffer, Laemmli
Blotting Paper	SDS
Bovine Serum Albumin	Silver Nitrate
CAPS	Sodium Carbonate
Cellulose Dialysis Tubing	Sodium Chloride
Cellulose Type 50	Sodium Phosphate (Dibasic)
Cibacron Blue 3GA	Sodium Phosphate (Monobasic)
Colorburst Electrophoresis Markers	Sodium Thiosulfate
DFP	TEMED
Dithiothreitol	Thioglycolic Acid
EDTA	Trifluoroacetic Acid
Formaldehyde	Trizma Base

### **BDH Chemicals Ltd. (Poole, Dorset, England):**

Bromophenol Blue	Glycerol
Calcium Chloride	



**The Royal College of Surgeons (Dublin, Ireland):**

Z-Gly-Pro-Phe

Z-Gly-Pro-Met

Z-Gly-Pro-Ser

Z-Gly-Pro-Tyr

Z-Gly-Pro-Leu

Z-Gly-Pro-Glu

Z-Gly-Pro-His

Z-Gly-Pro-Phe-His

Z-Gly-Pro-Phe-His-Arg

Z-Gly-Pro-Phe-His-Arg-Ser

Z-Gly-Pro-Met-His

Z-Gly-Pro-Met-His-Arg

Z-Gly-Pro-Met-His-Arg-Ser

Z-Gly-Leu-Phe-His

**Probiodrug AG (Halle, Germany):**

Anti-human PEP antibody (S449)

Anti-actin antibody

Human glioma cell line U343

Neuroblastoma cell line SH-SY5Y

Rat Cortex

Fmoc-Ala-PyrrCN

Z-Phe-Pro-BT

SR 063298

SR 063125

## **2.2. Protein Standard Curves**

### **2.2.1. Biuret Assay**

The Biuret assay was used to monitor protein in post column chromatography fractions and also to quantify protein in crude serum and post chromatography active enzyme pooled sample containing greater than 2mg/ml protein. For protein quantification, all samples were dialysed into ultra-pure water and diluted appropriately to achieve a concentration suitably determinable by the assay. Bovine serum albumin (BSA) standards (2-10mg/ml) were prepared and assayed in triplicate along with the pooled active enzyme samples as above. Absorbances were determined at 540nm using a Techan Spectra Plate Reader.

### **2.2.2. Standard BCA Assay**

The standard bicinchoninic acid (BCA) assay was used for protein monitoring and quantification in post column chromatography fractions and pooled samples containing less than 2mg/ml of protein. Samples were prepared as outlined in section 2.2.1 and BSA standards in the range 0-2mg/ml were included. 25 $\mu$ l of standard or sample was added in triplicate with 200 $\mu$ l of BCA reagent at 37°C for 30 minutes. Absorbances were read at 570nm.

### **2.2.3. Coomassie Plus Assay**

The coomassie plus protein assay was used to monitor and quantify protein concentration in post column chromatography fractions and pooled samples containing between 2.5 and 25 $\mu$ g/ml. Samples were prepared as outlined in section 2.2.1 and BSA standards in the range 2.5-25 $\mu$ g/ml were included. 150 $\mu$ l of standard or sample was added in triplicate to 150 $\mu$ l of coomassie plus reagent, allowed stand at room temperature for 5 minutes and finally read at 595nm.

## **2.3. Fluorescence Spectrometry using 7-Amino-4-Methyl-Coumarin (AMC)**

### **2.3.1. AMC Standard Curves**

100 $\mu$ M stock AMC solution containing 4%v/v methanol was prepared in 100mM potassium phosphate, pH 7.4. All lower AMC concentrations were obtained using



100mM potassium phosphate, pH 7.4 containing 4%v/v methanol as diluent. Stock solution and standards were stored in the dark at 4°C for up to one month. Standard curves in the range 0-5µM and 0-20µM AMC were prepared in triplicate by combining 100µl of 100mM potassium phosphate pH 7.4, 400µl of appropriate AMC concentration and 1ml of 1.5M acetic acid. Fluorimetric analysis of these samples was achieved using a Perkin Elmer LS50 Fluorescence Spectrophotometer at excitation and emission wavelengths of 370nm and 440nm respectively. Excitation slit widths were maintained at 10nm while emission slit widths were adjusted accordingly for the range being analysed.

### **2.3.2. Inner Filter Effect**

The inner filter or quenching effect of enzyme samples was determined by combining 100µl of enzyme sample, 400µl appropriate AMC dilution and finally 1.5M acetic acid. The filtering effect of crude serum samples was assessed in the presence and absence of  $2.5 \times 10^{-4}$ M JTP-4819\* in 10%v/v MeOH. The samples were all assayed in triplicate as described in section 2.3.1.

\* Note: Even though the peptidase under study is named ZIP (Z-Pro-prolinal Insensitive Peptidase), JTP-4819, which is also a potent and specific inhibitor of prolyl oligopeptidase, is used throughout this work for distinguishing between these peptidases. This is due to the unavailability of Z-Pro-prolinal.

## **2.4. Enzyme Assays**

### **2.4.1. Substrate Preparation**

Both Prolyl Oligopeptidase (PO) and Z-Pro-prolinal Insensitive Peptidase (ZIP) activities were determined using the fluorimetric substrate Z-Gly-Pro-AMC, with modification of the original protocol of Yoshimoto *et al.* (1979). 10mM Z-Gly-Pro-AMC stock was prepared in 100% methanol, aliquoted and stored at -20°C. 100µM substrate containing 4%v/v MeOH was prepared by adding slowly 300µl MeOH and 100µl Z-Gly-Pro-AMC stock to 9.6mls of 100mM potassium phosphate, pH 7.4 at 37°C. Prolyl Oligopeptidase activity was determined with 10mM DTT in the above substrate, while for determination of ZIP activity 500mM NaCl was included.

#### **2.4.2. Quantitative Z-Gly-Pro-AMC Degrading Activity Measurements.**

400µl of the 100µM substrate was added to 100µl enzyme sample in triplicate and incubated at 37°C for 60mins. Both samples and substrate were preincubated at 37°C to allow them reach thermal equilibrium. Reactions were terminated by the addition of 1ml of 1.5M acetic acid. Blanks or negative controls were prepared by adding 1ml of 1.5M acetic acid to 100µl of enzyme sample prior to substrate addition and incubation at 37°C for 60mins. Formation of AMC was measured as described in section 2.3.1. End point measurements were allowed, as the enzyme assay was linear with respect to time and enzyme concentration up to 60mins. Fluorimetric intensities observed were converted to nanomoles AMC released per minute per ml using the appropriate standard curve as outlined in section 2.3.2. Enzyme units were defined as nanomoles of AMC released per minute at 37°C.

#### **2.4.3. Quantitative Z-Pro-prolinal Insensitive Z-Gly-Pro-AMC Degrading Activity Measurement.**

Section 2.4.2 describes the determination of ZIP activity in situations where it was most certainly separated from prolyl oligopeptidase activity. In crude bovine serum, ZIP activity had to be distinguished from PO activity so the following assay modifications were necessary. 100µl of enzyme sample was pre-incubated for 15 minutes at 37°C with 20µl of  $2.5 \times 10^{-4}$ M JTP-4819 in 10%v/v MeOH prior to substrate addition. Negative controls were also included as in section 2.4.2 incorporating JTP-4819 and determinations were carried out in triplicate. AMC released was determined fluorimetrically as in section 2.3.1. with end point measurements taken as in section 2.4.2. Fluorimetric intensities obtained for each sample were converted to nanomoles of AMC released per minute per ml using the standard curves incorporating JTP-4819, prepared as outlined in section 2.3.2. Enzyme units were defined as nanomoles of AMC released per minute at 37°C.

#### **2.4.4. Non-Quantitative Z-Gly-Pro-AMC Degrading Activity Measurements.**

A non-quantitative fluorimetric microtitre plate assay was developed to assist in the rapid identification of Z-Gly-Pro-AMC degrading activities in post-column chromatography fractions. 200µl of 100µM Z-Gly-Pro-AMC in 4% MeOH containing 500mM NaCl or 10mM DTT, at 37°C was added to 100µl of sample in each well.

Post phenyl sepharose fractions were assayed in the presence and absence of 20 $\mu$ l 2.5 $\times$ 10<sup>-4</sup>M JTP 4819 in 10% MeOH. The microtitre plate was incubated at 37°C for 30 minutes. AMC released was determined fluorimetrically as outlined in section 2.3.1. using the Perkin Elmer LS-50B plate reader attachment.

## **2.5. An Optimised Purification Procedure for Bovine Serum ZIP.**

Purification steps were all carried out at 4°C apart from the final size exclusion column, which was performed using FPLC at room temperature.

### **2.5.1. Bovine Serum Preparation.**

Bovine whole blood was collected from a freshly slaughtered animal and stored at 4°C over 24 hours to allow clot formation. The remaining un-clotted whole blood was decanted and centrifuged at 6000rpm for 1 hour at 4°C using a Beckman J2-MC centrifuge fitted with JL-10.5 rotor. The supernatant and loose cellular debris was decanted and re-centrifuged at 20,000rpm for 15mins using a JL-20 rotor. The final serum was collected and stored at -17°C in 20ml aliquots.

### **2.5.2. Phenyl Sepharose Hydrophobic Interaction Chromatography.**

A 20ml Phenyl Sepharose CL-4B hydrophobic interaction column (2.5cm x 7cm) was equilibrated with 100ml of 100mM potassium phosphate containing 200mM ammonium sulphate, pH 7.4. Solid ammonium sulphate was dissolved in 20ml of bovine serum to give a final concentration of 200mM. This sample was then applied to the equilibrated column followed by a 100ml wash with 100mM potassium phosphate containing 200mM ammonium sulphate, pH 7.4. The column was then washed with 100ml of 100mM potassium phosphate containing 50mM ammonium sulphate, pH 7.4. Bound protein was eluted isocratically with a 100ml ultra-pure water wash. Equilibration of the column was carried out at a flow rate of 1ml/min, while all other steps were performed at 2ml/min. 5ml fractions were collected throughout the procedure and were assayed for ZIP activity according to section 2.4.4. Protein content in each fraction was determined using the biuret assay according to section 2.2.1. Fractions containing ZIP activity were pooled to yield post phenyl sepharose ZIP and enzyme activity and protein content was quantified using the

fluorimetric assay as outlined in section 2.4.2 and the biuret assay as in section 2.2.1. The phenyl sepharose resin was regenerated with a 100ml wash of pure ethanol at 0.5ml/min, followed by 150ml of equilibration buffer.

### **2.5.3 Calcium Phosphate Cellulose Chromatography.**

#### **2.5.3.1. Resin Preparation**

1l of 500mM sodium hydrogen phosphate was added (at 6.4ml/min) to 1.5l of constantly stirred 500mM calcium chloride at room temperature. Following a 15min agitation, 1.5ml of concentrated ammonia solution was added and stirred for a further 10min. The precipitated gel was allowed to settle and the supernatant decanted and discarded. 1l of ultra-pure water was added and the stirring continued for 5min. Settling and decanting was performed and this procedure was repeated until the gel was washed with 10l of ultra-pure water. The washed calcium phosphate gel was stored in 1l of ultra-pure water at 4°C. 10g Sigma cellulose type 50 was soaked overnight in 200ml 500mM potassium phosphate containing 150mM potassium chloride, pH 6.8. The cellulose was washed eight times with ultra-pure water and dried overnight at 70°C. 2g washed and dried cellulose was dissolved in 20ml 20mM potassium phosphate, pH 7.5 and added to 24ml of evenly suspended calcium phosphate gel. The calcium phosphate cellulose was poured into a column (2.5 x 7.0cm) and allowed to settle yielding 15ml of packed resin.

#### **2.5.3.2. Column Chromatography**

The column was equilibrated at 1ml/min with 10mM potassium phosphate, pH 7.4. The post phenyl sepharose ZIP was concentrated to 10ml and applied to the column followed by a 100ml wash with 10mM potassium phosphate, pH 7.4. The column was then washed with 100ml of 170mM potassium phosphate, pH 7.4. Bound protein was eluted with 100ml of 500mM potassium phosphate, pH 7.4. Loading and washing steps were performed at 1ml/min, while elution was performed at 2ml/min. 5ml fractions were collected throughout the procedure, and again were assayed for ZIP activity according to section 2.4.4. Protein content in each fraction was determined using the standard BCA assay as outlined in section 2.2.2. Fractions containing ZIP

activity were pooled to yield post calcium phosphate cellulose ZIP. Enzyme activity and protein content were then quantified as outlined in section 2.4.2. and 2.2.2.

#### **2.5.4. Cibacron Blue 3GA Chromatography.**

100ml of 20mM potassium phosphate, pH 7.4 was used to equilibrate a 20ml Cibacron blue 3GA resin. The post calcium phosphate cellulose ZIP was concentrated and then dialysed overnight against 2l of 20mM potassium phosphate, pH 7.4. After sample application the column was washed with 100ml of 20mM potassium phosphate, pH 7.4 to remove any unbound protein. Elution was performed using a 100ml linear 0-2M NaCl gradient in 20mM potassium phosphate, pH 7.4. Loading, washing and elution were all performed at 1ml/min. 5ml fractions were collected and assayed for ZIP activity according to section 2.4.4. Protein content in each fraction was determined using coomassie plus protein reagent as in section 2.2.3. Fractions containing ZIP activity were pooled and enzyme activity and protein content were quantified as outlined in section 2.4.2. and 2.2.3.

#### **2.5.5. Sephacryl S-300 Size Exclusion Chromatography.**

A 16/60 S-300 size exclusion chromatography column was attached to a fast protein liquid chromatography system. The column was equilibrated at 0.8ml/min with 250ml of 100mM potassium phosphate containing 150mM NaCl, pH 7.4. The post cibacron blue 3GA ZIP pool was concentrated to 2ml and applied to the column followed by a 150ml wash with equilibration buffer at 0.8ml/min. 5ml fractions were collected and assayed for ZIP activity as outlined in section 2.4.4. Protein content in each fraction was monitored online at 280nm and also using coomassie plus protein reagent as outlined in section 2.2.3. Fractions containing ZIP activity were pooled and enzyme activity and protein content were quantified as in section 2.4.2 and 2.2.3.

### **2.6. Assessment of Purity of Purified Bovine Serum ZIP.**

#### **2.6.1. Fluorimetric Assays**

Purified ZIP activity was assayed in the presence of various fluorimetric substrates to assess the enzymatic purity of the sample. The substrates used and the peptidase activity they are most commonly used to detect are outlined in Table 2.1. 1ml of each

substrate was prepared as a 10mM stock in 100% MeOH. 50µl of each substrate and 150µl MeOH was added to 100mM potassium phosphate, pH 7.4 at 37°C to a final volume of 5ml. This yielded a final substrate concentration of 100µM in 4%v/v MeOH. As a positive control, ZIP activity was assayed in the presence of 100µM Z-Gly-Pro-AMC in 4%v/v MeOH containing no NaCl. Assays were performed according to section 2.4.2.

<b>Fluorimetric Substrate</b>	<b>Cleavage Detected by</b>
Z-Phe-Arg-AMC	Plasma Kallikrein, Cathepsin B Cathepsin L, Papain Oligopeptidase B
Z-Arg-AMC	Trypsin, Papain
Z-Gly-Pro-AMC	Prolyl oligopeptidase, ZIP
Ala-AMC	Alanine aminopeptidase
Arg-AMC	Arginine aminopeptidase
Leu-AMC	Leucine aminopeptidase
Lys-AMC	Aminopeptidase B
Pro-AMC	Proline aminopeptidase
Gly-Pro-AMC	Dipeptidyl Peptidase IV
Glu-Phe-AMC	Chymotrypsin
Pyr-AMC	Pyroglutamyl aminopeptidase I
Pyr-His-Pro-AMC	Prolyl oligopeptidase Pyroglutamyl aminopeptidase II
Lys-Ala-AMC	Dipeptidyl Peptidase II
Z-Arg-Arg-AMC	Cathepsin B

**Table 2.1. Fluorimetric Substrates Tested for the Presence or Absence of Contaminating Peptidase Activity.**

## 2.6.2. Polyacrylamide Gel Electrophoresis

SDS polyacrylamide gel electrophoresis based on the method of Laemmli (1970) was employed to determine the effectiveness of the purification procedure.

### 2.6.2.1. Preparation of SDS Gels

10% resolving and 4.5% stacking gels were prepared as in Table 2.2. from the following stock solutions which were all prepared using ultra-pure water.

<u>Solution</u>	<u>Composition</u>
Resolving Gel Buffer	1.5M Tris/HCl, pH 8.8
Stacking Gel Buffer	0.5M Tris/HCl, pH 6.8
Acryl/Bisacryl Stock	30% w/v Acrylamide, 0.8% Bisacryl
SDS	10% w/v SDS
Ammonium Persulphate	1.5% Ammonium Persulphate
Running Buffer	25mM Tris/HCl, 192mM glycine, 0.1% SDS

Gels were cast using an ATTO vertical mini electrophoresis system. The resolving gel solution (Table 2.2.) was degassed and filtered, TEMED added, mixed and the gel poured immediately. An overlay of ethanol/water was placed over the resolving gel. After polymerisation, the overlay was removed. The stacking gel solution (Table 2.2.) was degassed and filtered, TEMED added, mixed and the gel poured immediately. A comb was placed into the top of the gel liquid and the gel was allowed polymerise.

<u>Solution</u>	<u>10%v/v Resolving Gel</u>	<u>4.5%v/v Stacking Gel</u>
Acrylamide/Bisacryl soln.	5ml	1.5ml
Ultra-pure water	7.225ml	5.4ml
Ammonium Persulphate	750µl	500µl
SDS	150µl	100µl
Resolving Gel Buffer	1.875ml	-
Stacking Gel Buffer	-	2.5ml
TEMED	7.5µl	7.5µl

**Table 2.2. SDS PAGE Gel Preparation**

#### **2.6.2.2. Sample Preparation**

Samples generated over the purification of bovine serum ZIP (Post phenyl sepharose, post calcium phosphate cellulose, post cibacron blue 3GA and post S-300 gel filtration) were extensively dialysed overnight into ultra-pure water. Each dialysed sample was added to an equal volume of 2x solubilisation buffer which consisted of 20% v/v glycerol, 4% w/v SDS, 10% v/v 2-mercaptoethanol, 0.004% w/v bromophenol blue and 125mM Tris/HCl, pH 6.8. Samples were boiled for 2 minutes and stored on ice until application.

#### **2.6.2.3. Sample Application**

20 $\mu$ l of each prepared sample from section 2.6.2.2. was applied to the 10% SDS PAGE gel. The high molecular weight standards used consisted of Myosin (205kDa),  $\beta$ -Galactosidase (116kDa), Phosphorylase B (97kDa), Fructose-6-phosphate kinase (84kDa), BSA (66kDa), Glutamic dehydrogenase (55kDa), Ovalbumin (45kDa) and Glyceraldehyde-3-phosphate dehydrogenase (36kDa). 20 $\mu$ l of the standards solution was also applied to the gel, which was then run at 20mA for 2hrs at room temperature.

#### **2.6.2.4. SDS PAGE Gel Staining**

Polyacrylamide gels were stained using gelcode blue (a coomassie based product) and silver stained based on the method by Blum *et al.*, (1987). Gels stained using gelcode blue were removed from the electrophoresis chamber, washed 3 x 5mins in ultra-pure water and then placed in gelcode blue stain for at least an hour. After the hour, washing in ultra-pure water enhances band visibility. Table 2.3. outlines the stages for silver staining. An image of each stained gel was scanned or captured using a Kodak digital camera coupled to Kodak software.



<b>Step</b>	<b>Reagent</b>	<b>Time</b>
Fix	50% ethanol, 12% acetic acid, 0.05% formaldehyde (37% stock)	1 hour at least
Wash	50% ethanol	3 x 20 min
Pretreat	200µl of a 5% Na <sub>2</sub> S <sub>2</sub> O <sub>3</sub> x H <sub>2</sub> O stock soln. in 100ml H <sub>2</sub> O	1 min
Rinse	H <sub>2</sub> O	2 x 20 sec
Impregnate	0.1g AgNO <sub>3</sub> , 70µl formaldehyde in 100ml H <sub>2</sub> O	20 min
Rinse	H <sub>2</sub> O	2 x 20sec
Development	3g Na <sub>2</sub> CO <sub>3</sub> , 50µl formaldehyde, 4µl Na <sub>2</sub> S <sub>2</sub> O <sub>3</sub> x H <sub>2</sub> O stock soln. in 100ml H <sub>2</sub> O	Max. 10min
Stop	0.1M EDTA	5 min at least

**Table 2.3. Silver Staining Procedure**

## **2.7. Substrate Specificity Studies**

### **2.7.1. Kinetic Analysis**

Substrate specificity studies on bovine serum ZIP, based on kinetic analysis were performed.

#### **2.7.1.1. K<sub>m</sub> Determination For Z-Gly-Pro-AMC**

A 300µM stock solution of Z-Gly-Pro-AMC in 5%v/v MeOH containing 500mM NaCl was prepared. A range of concentrations (0-300µM) was prepared from this stock using 100mM potassium phosphate, pH 7.4, containing 5%v/v MeOH and 500mM NaCl as diluant. Purified ZIP was assayed with each concentration in triplicate as outlined in section 2.4.2. The K<sub>m</sub> of ZIP for the substrate Z-Gly-Pro-AMC was estimated when the data obtained was applied to various kinetic models (section 6.4.1.).

### 2.7.1.2. $K_{i(\text{app})}$ Determination Using Selected Synthetic Peptides

The effect of a variety of selected synthetic peptides on the kinetic interaction between ZIP and the substrate Z-Gly-Pro-AMC was determined. Substrate concentrations in the range 100-300 $\mu$ M Z-Gly-Pro-AMC in 5%v/v MeOH containing 500mM NaCl was prepared in the presence of 200 $\mu$ M peptide, each in a final volume of 2ml. The assay MeOH concentration was maintained at 5%. The peptides studied and their preparation is outlined in Table 2.3. ZIP activity was assayed in triplicate using these substrate mixtures as outlined in section 2.4.2. The data obtained was applied to the Lineweaver-Burk analysis model, where the inhibition constant ( $K_{i(\text{app})}$ ) and the type of inhibition observed were determined as outlined in sections 6.4.2. and 6.4.3. respectively.

Peptide	Stock Conc. (Mm)	Solubility	Assay Conc. ( $\mu$ M)
Z-Gly-Pro-Phe	5	10%v/v MeOH *	200
Z-Gly-Pro-Met	5	10%v/v MeOH *	200
Z-Gly-Pro-Ser	5	Ultra-pure water	200
Z-Gly-Pro-Tyr	5	10%v/v MeOH	200
Z-Gly-Pro-Leu	5	10%v/v MeOH *	200
Z-Gly-Pro-Ala	5	Ultra-pure water	200
Z-Gly-Pro-Glu	5	Ultra-pure water	200
Z-Gly-Pro-His	5	10%v/v MeOH *	200
Z-Gly-Pro-Phe-His	5	Ultra-pure water	200
Z-Gly-Pro-Phe-His-Arg	5	Ultra-pure water	200
Z-Gly-Pro-Phe-His-Arg-Ser	5	Ultra-pure water	200
Z-Gly-Pro-Met-His	5	10%v/v MeOH *	200
Z-Gly-Pro-Met-His-Arg	5	Ultra-pure water	200
Z-Gly-Pro-Met-His-Arg-Ser	5	Ultra-pure water	200
Z-Gly-Leu-Phe-His	5	Ultra-pure water	200

**Table 2.4. Peptide Preparation for  $K_{i(\text{app})}$  Determinations**

\* Sonication using an ultrasonic water bath was required for complete dissolution.

### **2.7.2. Reverse Phase High Performance Liquid Chromatography**

The formation of products upon digestion of the NH<sub>2</sub>-terminal protected peptides by ZIP were analysed on a Beckman Chromatographic system incorporating a dual pump, a 526 Photo-Diode array detector and a 507 autosampler served by Beckman 32 Karat HPLC software. A Waters Spherisorb ODS-2 C-18 analytical column (250mm × 4.6mm) and a Supelguard LC-18 guard column were used for all analysis. All solvents and buffers used in sample preparation and chromatography were prepared from ultra-pure water and then filtered and degassed.

#### **2.7.2.1. Preparation of Substrates and Standards**

1ml of 1mM substrate/standard was prepared as outlined in Table 2.4. Stock substrate concentrations as outlined in Table 2.3 were diluted using 50mM ammonium acetate, pH 7.2. The 1mM standard Z-Gly-Pro was diluted using 50mM ammonium acetate, pH 7.2 giving concentrations from 0.1-1mM for the construction of a standard curve.

#### **2.7.2.2. Hydrolysis of the Peptide Substrates by ZIP**

Purified ZIP (post S-300 gel filtration) was concentrated 10-fold and dialysed extensively overnight against 50mM ammonium acetate, pH 7.2. 50µl of ZIP in 50mM ammonium acetate, pH 7.2, was added to 200µl of each peptide substrate (1mM) in 50mM ammonium acetate, pH 7.2 containing 2%v/v methanol. Hydrolysis of the peptides was performed at 37°C over a 24hr period. Enzyme control was 50µl ZIP added to 200µl 50mM ammonium acetate, pH 7.2 containing 2%v/v methanol. Peptide control was 200µl of each peptide solution added to 50µl ammonium acetate, pH 7.2. All controls were incubated under the same conditions. Reactions were terminated with 25µl of 50mM ammonium acetate containing 50%v/v acetonitrile and 5%v/v acetic acid.

#### **2.7.2.3. Reverse Phase HPLC of Incubates and Standards**

Mobile phases for the HPLC system consisted of solvent A; 80% (v/v) Acetonitrile, 0.2% (v/v) TFA and solvent B; 5% (v/v) Acetonitrile, 0.2% (v/v) TFA. The reverse phase C-18 column was equilibrated for ten minutes with 100% solvent B. 20µl of sample and controls were injected onto the column followed by a four-minute wash with 100% solvent B. A linear gradient from 100% solvent B to 100% solvent A over

a twenty-one minute period was then applied. Finally, a five-minute wash with 100% solvent A was applied. A flow rate of 0.7ml/min was used throughout. The absorbance of the eluent was monitored at 214nm.

<b>Peptide</b>	<b>Concentration</b>	<b>Preparation</b>
Z-Pro-Phe	1mM	2%v/v MeOH
Gly-Gly-Pro-Ala	1mM	2%v/v MeOH
Z-Gly-Pro-Phe	1mM	2%v/v MeOH
Z-Gly-Pro-Met	1mM	2%v/v MeOH
Z-Gly-Pro-Ser	1mM	2%v/v MeOH
Z-Gly-Pro-Tyr	1mM	2%v/v MeOH
Z-Gly-Pro-Leu	1mM	2%v/v MeOH
Z-Gly-Pro-Ala	1mM	2%v/v MeOH
Z-Gly-Pro-Glu	1mM	2%v/v MeOH
Z-Gly-Pro-His	1mM	2%v/v MeOH
Z-Gly-Pro-Phe-His	1mM	2%v/v MeOH
Z-Gly-Pro-Phe-His-Arg	1mM	2%v/v MeOH
Z-Gly-Pro-Phe-His-Arg-Ser	1mM	2%v/v MeOH
Z-Gly-Pro-Met-His	1mM	2%v/v MeOH
Z-Gly-Pro-Met-His-Arg	1mM	2%v/v MeOH
Z-Gly-Pro-Met-His-Arg-Ser	1mM	2%v/v MeOH
Z-Gly-Leu-Phe-His	1mM	2%v/v MeOH
Z-Gly-Leu	1mM	2%v/v MeOH
Z-Gly-Pro	0.1-1mM	2%v/v MeOH

**Table 2.5. Preparation of the Peptide Substrates and Standards for Substrate Specificity studies using HPLC and Mass Spectrometry.**

### **2.7.3. Identification of Hydrolysis Products Using Mass Spectrometry**

Mass Spectrometry data was acquired to identify the digest products been formed. Sample preparation and hydrolysis of the peptide substrates were as according to Table 2.4. and section 2.7.2.2. respectively.

### **2.7.3.1. Direct Infusion MS Analysis**

Initially, incubate samples were directly infused into the MS source but some components of the mixtures were preferentially ionised over others which led to ambiguous results. Thus, it was decided to use LC-MS but the direct infusion analysis did aid in the development of the MS experimental conditions.

### **2.7.3.2. LC-MS Analysis of Incubates**

The instrument used was the Bruker/Hewlett-Packard Esquire LC - a Bruker mass spectrometer linked to a HP liquid chromatograph. The LC module of the instrument was a HP1100 with a variable wavelength detector, a low-volume pump, an in-line degasser and an autosampler. This LC system generally uses low flow rates, narrow bore columns and a micro flow cell in the UV detector. The MS module of the instrument comprised the ionisation chamber, the ion-trap to collect the ions and then to release them according to mass, and the ion detector to generate the spectrum. The Esquire-LC is capable of two types of ionisation - electrospray ionisation (ESI) and atmospheric pressure chemical ionisation, although in this work, we used only ESI. With ESI, samples are subjected to 'gentle' ionisation such that in-source fragmentation generally does not occur to any great extent. The LC isocratic method used a Zorbax RX-C18, 150 x 2.1mm, 5 $\mu$ M column with a mobile phase of 78/22/0.1 v/v/v water/ACN/formic acid at a flowrate of 0.15ml/min. The monitoring wavelength was 205nm and an injection volume of 4 $\mu$ l was used. After passing through the UV detector, the samples were introduced directly into the mass spectrometer, with the ESI source in the positive mode, enabling simultaneous UV and TIC (Total Ion Current) traces to be obtained. The nebulisation gas and drying gas (both nitrogen) were set to 30psi and 8l/min respectively. The temperature of the source was maintained at 340°C. Depending on the chosen target mass, the octopole voltage, skimmer 1 voltage and the trap drive voltage changed, but for mass 329 (sodiated Z-gly-pro) for example, these values were 2.48V, 34.4V and 32.5V respectively. Mass spectral data was generally collected in the scan range 50-1000 m/z.

## **2.8. Partial Purification Procedure for Bovine Serum Prolyl Oligopeptidase**

### **2.8.1. Phenyl Sepharose Hydrophobic Interaction Chromatography I**

A 20ml Phenyl Sepharose CL-4B hydrophobic interaction column (2.5 x 7cm) was equilibrated with 100ml of 100mM potassium phosphate containing 20mM ammonium sulphate, pH 7.4. Solid ammonium sulphate was dissolved in 20ml of bovine serum to give a final concentration of 200mM. This sample was then applied to the equilibrated column followed by a 100ml wash with 100mM potassium phosphate containing 200mM ammonium sulphate, pH 7.4. The column was then washed with 100ml of 100mM potassium phosphate containing 50mM ammonium sulphate, pH 7.4. Bound protein was eluted with a distilled water wash. Equilibration of the column was carried out at a flow rate of 1ml/min, while all other steps were performed at 2ml/min. 5ml fractions were collected throughout the procedure and were assayed for PO activity according to section 2.4.4. Protein content in each fraction was determined using the biuret assay according to section 2.2.1. Fractions containing PO were pooled to yield post phenyl sepharose I PO and enzyme activity and protein content were quantified using the fluorimetric assay as outlined in section 2.4.2. and the biuret assay as in section 2.2.1.

### **2.8.2. Phenyl Sepharose Hydrophobic Interaction Chromatography II**

The 20ml resin used in section 2.8.1. was regenerated with a 100ml wash of pure ethanol at 0.5ml/min. The column was then equilibrated with 100ml of 100mM potassium phosphate containing 1M ammonium sulphate, pH 7.4. Solid ammonium sulphate was dissolved in the concentrated post phenyl sepharose I pool (pH was maintained at 7.4 using 1M NaOH), to give a final concentration of 1M. The sample was then applied to the column followed by a 100ml wash of equilibration buffer. Bound protein was eluted with a 100ml linear gradient of 1-0M ammonium sulphate, 100-0mM potassium phosphate, pH 7.4. The column was then washed with 25ml of ultra-pure water. All steps were performed at a flow rate of 2ml/min. 5ml fractions were collected throughout the procedure, and again were assayed for PO activity according to section 2.4.4. Protein content in each fraction was determined using the standard BCA assay as outlined in section 2.2.2. Fractions containing PO activity were pooled to yield post phenyl sepharose II PO. Enzyme activity and protein content were then quantified as outlined in section 2.4.2. and 2.2.2.

### **2.8.3 Cibacron Blue 3GA Chromatography**

The post phenyl sepharose II pool was concentrated and dialysed overnight against 2l of 20mM potassium phosphate. 100 ml of 20mM potassium phosphate, pH 7.4. was used to equilibrate a 20ml cibacron blue 3GA resin. After sample application the column was washed with 100ml of 20mM potassium phosphate, pH 7.4. to remove any unbound protein. Elution was performed using a 100ml linear 0-2M NaCl gradient in 20mM potassium phosphate, pH 7.4. Loading, washing and elution were all performed at 1ml/min. 5ml fractions were collected and assayed for PO activity according to section 2.4.4. Protein content in each fraction was determined using coomassie plus protein reagent as in section 2.2.3. Fractions containing PO activity were pooled and enzyme activity and protein content were quantified as outlined in section 2.4.2. and 2.2.3.

## **2.9. Inhibitor Studies**

### **2.9.1. Catalytic Classification Using Diisopropylfluorophosphate**

A range of concentrations of DFP was prepared from a stock concentration of 20mM using 100mM potassium phosphate containing 500mM NaCl as diluant. A stock substrate of 200 $\mu$ M Z-Gly-Pro-AMC in 8% v/v MeOH and containing 500mM NaCl was prepared using 100mM potassium phosphate, pH 7.4. This stock was preincubated at 37°C until completely dissolved and thermal equilibrium was reached. 1ml of substrate stock was added to 1ml of appropriate DFP concentration to give a final substrate concentration of 100 $\mu$ M Z-Gly-Pro-AMC in 4%v/v MeOH containing 500mM NaCl. ZIP activity using these substrate: inhibitor mixtures was assayed in triplicate as outlined in section 2.4.2. Suitable negative and positive controls were prepared. The IC<sub>50</sub> value of DFP for ZIP was determined as explained in section 6.4.4.

### **2.9.2. Effect of Specific Prolyl Oligopeptidase Inhibitors**

The potency of some specific Prolyl Oligopeptidase inhibitors towards purified ZIP and partially purified PO from bovine serum was assessed. IC<sub>50</sub> values were evaluated using steady-state enzyme-substrate reaction. Reactions were initiated by the addition of 100 $\mu$ l enzyme to 1.9ml 20 $\mu$ M Z-Gly-Pro-AMC containing 1%v/v MeOH, giving a

final volume of 2ml. The reaction was constantly monitored for 15 minutes until a constant rate was observed. 2 $\mu$ l of each inhibitor concentration was then added and the reaction allowed to proceed for 45 minutes at 37°C. Reaction buffer for purified ZIP was 100mM potassium phosphate containing 500mM NaCl, pH 7.4 and for PO was 100mM potassium phosphate containing 10mM DTT, pH 7.4. Suitable positive and negative controls were also prepared. Enzyme activity was continuously monitored on a Kontron spectrofluorimeter SFM 25 (excitation wavelength 370nm, emission wavelength 440nm) equipped with a thermostated four-cell changer and controlled by an IBM-compatible computer.

<b>Inhibitor</b>	<b>Stock Conc. (M)</b>	<b>Preparation</b>	<b>Assay Conc. (M)</b>
Fmoc-Ala-PyrrCN	1x10 <sup>-6</sup> -1x10 <sup>-3</sup>	10% DMSO	1x10 <sup>-9</sup> -1x10 <sup>-6</sup>
Z-Phe-Pro-BT	1x10 <sup>-5</sup> -2x10 <sup>-3</sup>	10% DMSO	1x10 <sup>-8</sup> -2x10 <sup>-6</sup>
SR 063298	1x10 <sup>-7</sup> -2x10 <sup>-2</sup>	Ultra-pure water	1x10 <sup>-10</sup> -2x10 <sup>-5</sup>
SR 063125	1x10 <sup>-7</sup> -2x10 <sup>-2</sup>	10% DMSO	1x10 <sup>-10</sup> -2x10 <sup>-5</sup>
JTP-4819	5x10 <sup>-5</sup> -1x10 <sup>-8</sup>	10% MeOH	1x10 <sup>-11</sup> -5x10 <sup>-8</sup>

**Table 2.6. Preparation of Specific Inhibitors**

## **2.10. Immunological Studies**

Using a polyclonal antibody against human prolyl oligopeptidase, studies were performed to check for any cross reactivity with bovine serum PO and ZIP. The polyclonal antibody (S449) against human PO/PEP was generated when rabbits were immunized with a peptide containing the N-terminal PO/PEP sequence of amino acids 10-25.

### **2.10.1. SDS PAGE and Immunoblotting**

Separating gels containing 10% acrylamide were prepared according to Table 2.2. and section 2.6.2.1. except the system used was a mini Biorad vertical electrophoresis unit. Two cell lines expressing PEP activity were used as positive controls. They were the human glioma cell line U343 and the neuroblastoma cell line SH-SY5Y. Also Rat



cortex was used as a positive control. 15µg of the prepared positive controls were loaded per lane along with 140ng purified ZIP and 2.9µg partially purified PO from bovine serum. Coloured makers were also loaded, to aid visualising electrophoresis and electrotransfer.

After SDS-gel electrophoresis for 45 minutes at 200V the following procedure was performed. A blotting sandwich was constructed as follows, 5 layers of filter paper (What. Nr.3) Soaked in anode buffer 1, 3 layers filter paper (What. Nr.3) Soaked in anode buffer 2, nitrocellulose soaked in water, gel and finally 5 layers filter paper (What. Nr.3) Soaked in cathode buffer 3. Electroblotting transfer time was 1-1.5hr at a constant current of 0.8mA/cm<sup>2</sup>. The blot was carefully removed and blocked for 1hr with 30ml of 3% dry milk in PBS-Tween. Primary anti-PEP antibody (1:400 dilution) and monoclonal antibody anti-actin (1:1000 dilution) in PBS-Tween with 5% dry milk were prepared and placed on the blot overnight in cold room. The blot was then washed 3 x 10 min with PBS. It was then placed shaking for 1hr in HRP conjugated secondary antibody (1:10,000 dilution) in PBS-Tween with 5% dry milk. The blot was then washed again 3 x 10min with PBS.

The chemiluminescence substrate was prepared by mixing 2.5ml of each Biorad solution, added to the blot and shook by hand for 5 mins. The substrate solution was decanted off and clingfilm bound carefully around the blot. Air bubbles were removed, excess clingfilm removed from the edges and the blot dried. It was then placed in the x-ray chamber. In the dark room, an x-ray film was removed and placed firmly on the blot in the x-ray chamber, closed and exposure allowed for up to 60 seconds. The film was then placed in developer solution for 5 mins, briefly washed in water and fixed for up to 2 mins. The developed film was then washed with water and allowed air dry.

## **2.11. Identification of this Z-Pro-prolinal Insensitive Peptidase**

### **2.11.1. Determination of N-Terminal Protein Sequence**

Bryan Dunbar performed N-terminal sequencing of ZIP commercially at the University of Aberdeen, Scotland. The enzyme sample had to be firstly separated by SDS PAGE, then electroblotted onto polyvinylidene difluoride (PVDF) membrane and stained.

#### **2.11.1.1. SDS Polyacrylamide Gel Electrophoresis**

An SDS PAGE gel was precast according to Table 2.2. and section 2.6.2.1. and stored overnight at 4°C to prevent N-terminal blocking by free amines. 50ml of bovine serum was purified as in section 2.5. and the final purified ZIP sample was dialysed extensively overnight against ultra-pure water and concentrated to 500µl using a speedvac. An equal volume of sample was added to an equal volume of solubilisation buffer (see section 2.6.2.2.) and boiled for 2 minutes. Coloured markers were employed as in section 2.10.1. The gel was pre-run at 50V for 30min with 200µM thioglycolic acid in the upper reservoir in order to provide a scavenger for free radicals. The chamber was emptied, rinsed with reservoir buffer and further electrophoresis was performed at a constant current of 20mA for 2hr.

#### **2.11.1.2. PVDF Electroblotting**

1l of 10x CAPS buffer was prepared and adjusted to pH 11 using sodium hydroxide. 1x electroblotting buffer in 10% MeOH was prepared and stored at 4°C. On removal of the gel it was placed in electroblotting buffer for 1hr, while the PVDF membrane was dipped in MeOH for 10sec and also equilibrated in electroblotting buffer for 1hr. A transblotting sandwich was made using 8 layers of pre-soaked filter paper, cut to the exact size of the gel. The PVDF membrane was placed on top of the filter paper followed by the gel. Eight more layers of equilibrated filter paper were added to complete the sandwich. Electroblotting was performed at 0.8mA/cm<sup>2</sup> for 1hr 10min. Removal of the membrane was followed by a rapid membrane wash in ultra-pure water. It was then saturated in 100% MeOH for 10sec and stained with coomassie blue for 3min. Destaining in 1% acetic acid was repeated twice, then the blot was

extensively washed with ultra-pure water and finally allowed to air dry. The blot was wrapped in clingfilm and transported for sequencing.

## **2.11.2. UV Zymogram Development**

### **2.11.2.1. Native Polyacrylamide Gel Electrophoresis**

A 10% native polyacrylamide gel was prepared as in section 2.6.2.1. except that no SDS was present in the gel and the gels in this case were cast in the large ATTO electrophoresis system. The cast gels were stored overnight at 4°C. Purified ZIP sample was dialysed extensively overnight into ultra-pure water and concentrated to 500µl using a speedvac.

10x (non-denaturing) solubilisation buffer was prepared as follows: 3.2ml 10% SDS, 2ml 0.5M Tris/HCl pH 6.8, 1.6ml glycerol, 0.05%(w/v) bromophenol blue and 1.2ml of ultra-pure water, in a final volume of 8ml. This solution was stable for 4-6 weeks at 4°C, or for months if stored at -20°C.

Running buffer was prepared as in section 2.6.2.1. without SDS present. 54µl of concentrated ZIP sample was added to 6µl 10x (non-denaturing) solubilisation buffer and applied directly to the gel. The gel was run at a constant voltage of 125V at 4°C for up to 2.5hrs.

### **2.11.2.2. U.V. Zymogram Assessment**

After native page electrophoresis, the gel was rapidly removed and placed in 50ml of 100µM Z-Gly-Pro-AMC in 100mM potassium phosphate pH 7.4 containing 4%v/v MeOH and 500mM NaCl. It was incubated with shaking for 10-15mins at 37°C, after this excess substrate was removed and the gel placed under ultraviolet light in an image analyser for visualisation.

### **2.11.2.3. Protein G Affinity Chromatography**

2.5ml of protein G resin was equilibrated with 10ml of 100mM potassium phosphate containing 200mM NaCl, pH 7.4. 1-2ml of concentrated purified ZIP sample was applied to the affinity resin and allowed to shake slowly for 30mins at 4°C (Batch bind). The resin was allowed to settle and the supernatant removed. The resin was

then washed with 10ml of equilibration buffer, allowed settle and the supernatant removed. A second 10ml wash of 100mM potassium phosphate containing 500mM NaCl, pH 7.4. was then performed, with the resin again allowed to settle and the supernatant removed. Each supernatant was pooled and assayed for ZIP activity according to section 2.4.2. Bound protein was eluted using a 10ml wash with 0.1M glycine/HCl, pH 2.2.

#### **2.11.2.4. Gelatin Sepharose Chromatography**

5ml of gelatin sepharose was equilibrated with 15ml 100mM potassium phosphate containing 200mM NaCl, pH 7.4. The post protein G ZIP sample was concentrated, applied to the resin and allowed to batch bind slowly at 4°C. The resin was allowed to settle and the supernatant removed. This was followed by a wash with 15ml of equilibration buffer, resin allowed to settle and the supernatant removed. A second 15ml wash of 100mM potassium phosphate containing 1M NaCl, pH 7.4 was performed, with the resin again allowed to settle and the supernatant removed. Each supernatant was pooled and assayed for ZIP activity according to section 2.4.2. Bound protein was eluted with a 15ml wash of 4M urea, pH 7.0.

## **RESULTS**

### 3.0 Results

#### 3.1. Protein Determination

Protein standard curves incorporating BSA were prepared as outlined in sections 2.2.1. , 2.2.2. and 2.2.3. Plots of protein absorbance versus BSA concentration are presented in Figures 3.1.1. , 3.1.2. and 3.1.3. for the Biuret, standard BCA and coomassie plus assays respectively.

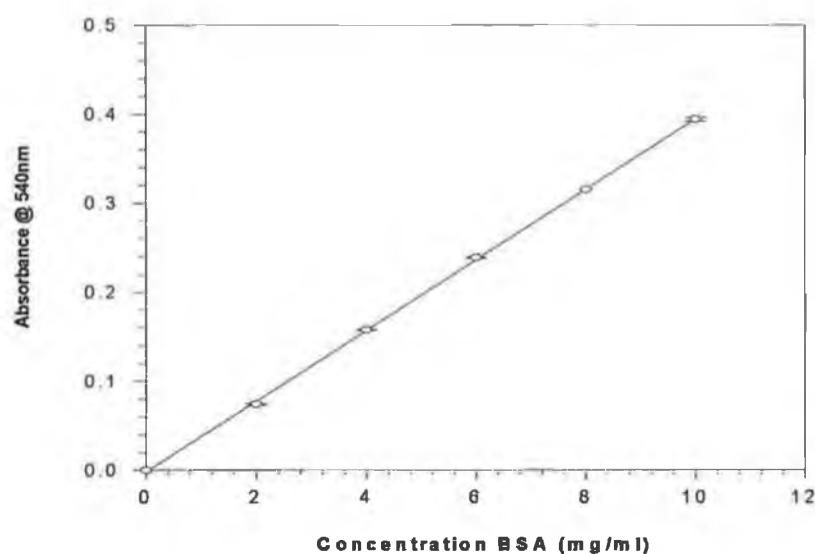


**Figure 3.1.1. BSA Standard Curve**

Plot of absorbance at 540nm versus BSA concentration obtained using the Biuret assay procedure as outlined in section 2.2.1. Error bars represent the SEM of triplicate readings.

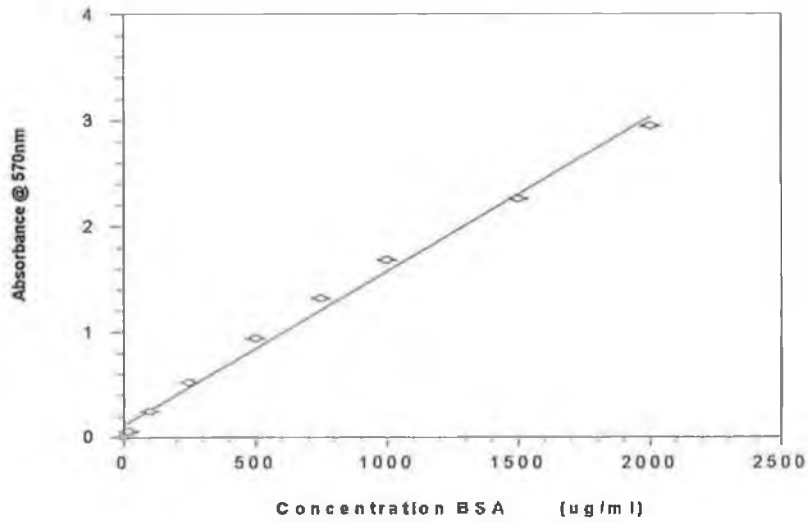


**Figure 3.1.2. BSA Standard Curve**

Plot of Absorbance at 570nm versus BSA concentration obtained using the standard BCA assay procedure as outlined in section 2.2.2. Error bars represent the SEM of triplicate readings.

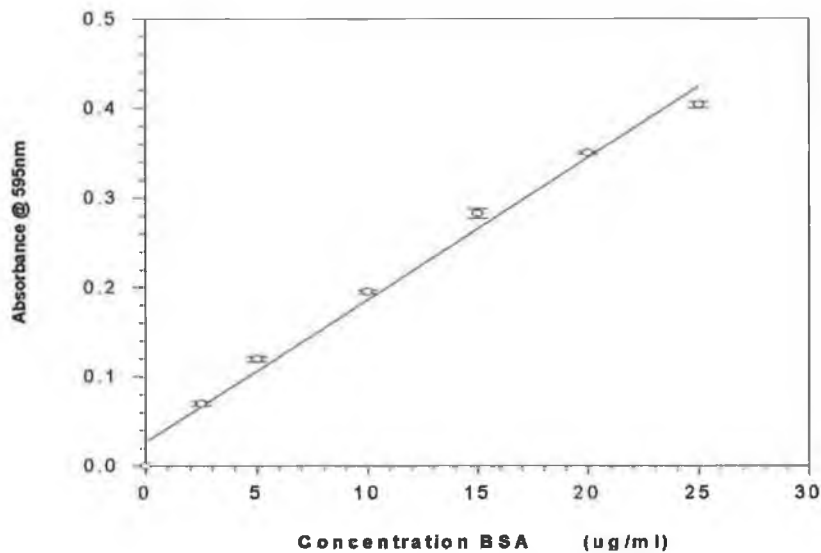
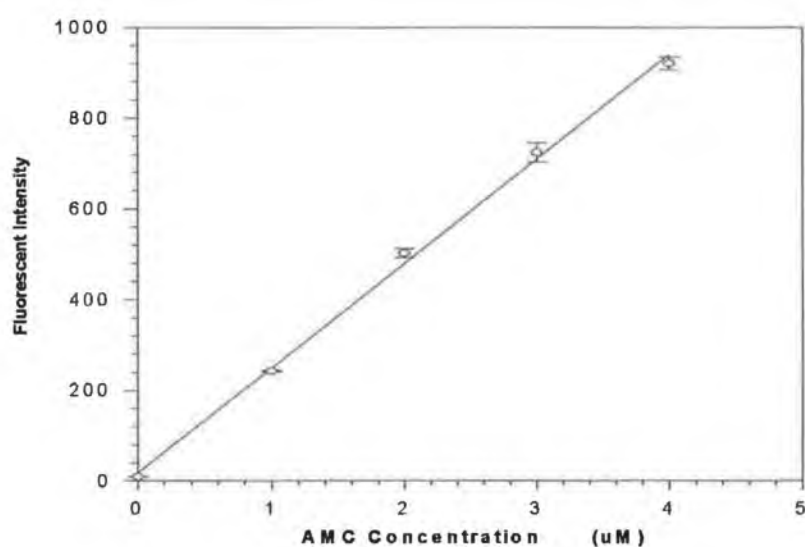


**Figure 3.1.3. BSA Standard Curve**

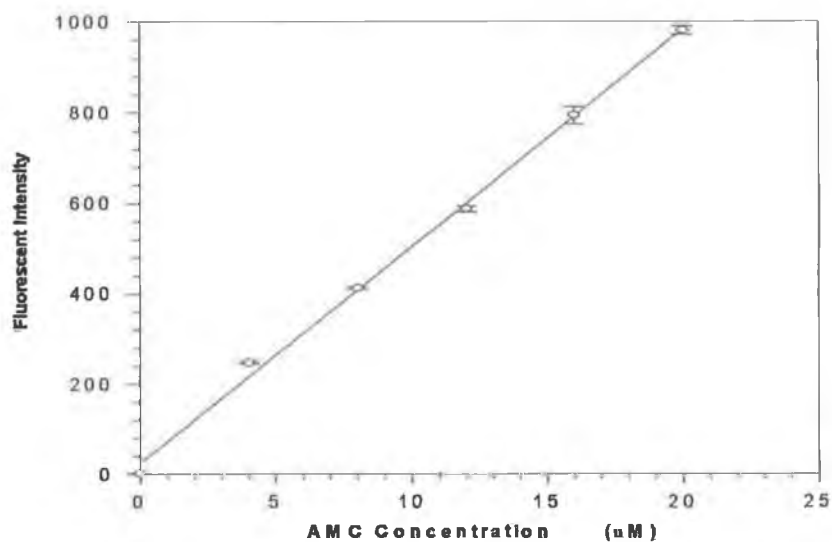
Plot of Absorbance at 595nm versus BSA concentration obtained using the coomassie plus assay procedure as outlined in section 2.2.3. Error bars represent the SEM of triplicate readings.

### 3.2. AMC Standard Curves and the Inner Filter Effect

AMC standard curves were prepared as outlined in section 2.3.1. Plots of fluorescent intensity versus AMC concentration are presented in Figures 3.2.1. and 3.2.2. The inner filter effect (quenching) was also performed according to section 2.3.2. This was performed to see the effect on fluorescence of including crude serum or post column pooled fractions in the assay mixture. Figures 3.2.3. and 3.2.4. are plots of fluorescent intensity versus AMC concentration for crude serum and post phenyl sepharose pool. Plots for the remaining post column pools are not included, as the inner filter effect was not observed for these samples. Table 3.1. shows the degree of filtering observed and the slopes obtained for each sample.

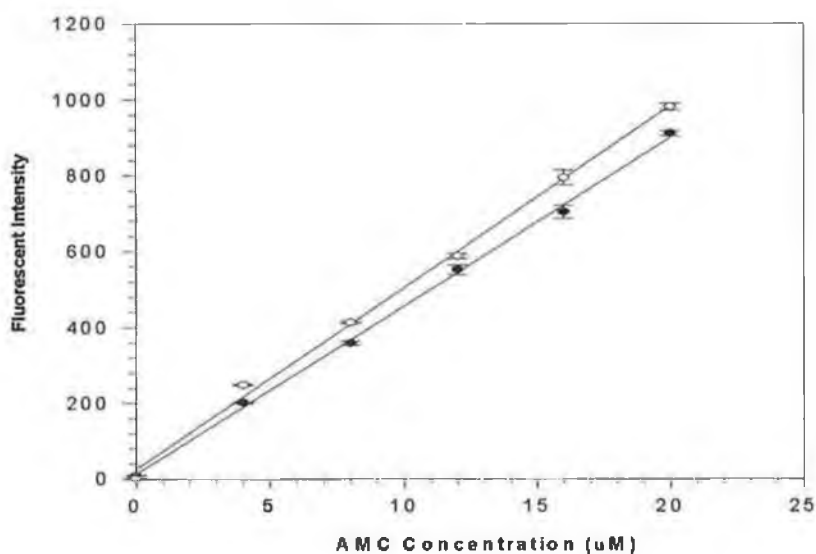


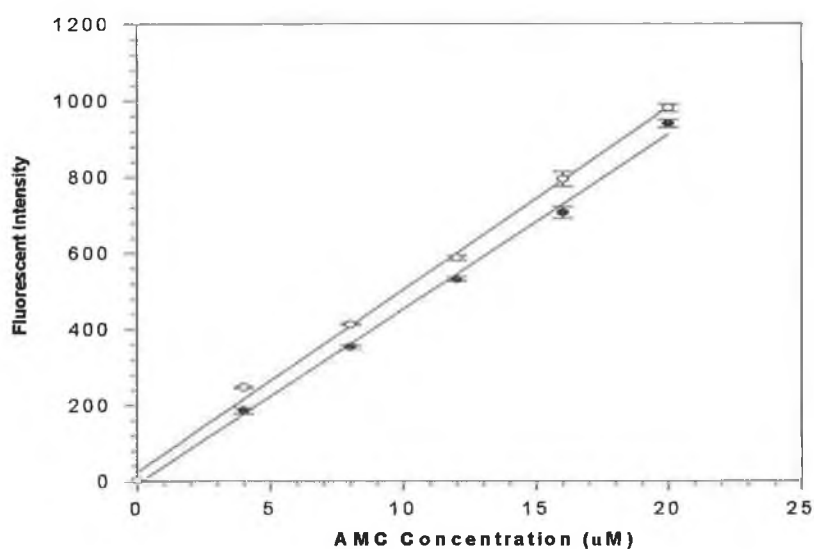




**Figures 3.2.1. and 3.2.2. AMC Standard Curves**

Plots of fluorescent intensity versus AMC concentration. Excitation slit width was maintained at 10nm, while emission slit widths were 10nm and 5nm for Figures 3.2.1. and 3.2.2. respectively.





**Figures 3.2.3. and 3.2.4. Quenched AMC Standard Curves**

Plots of fluorescent intensity versus AMC concentration. Figure 3.2.3. illustrates the filter effect for serum (●) in comparison to unfiltered for buffer (o). Figure 3.2.4. shows the filter effect for post phenyl sepharose ZIP (●) in comparison to buffer (o).

Sample	R <sup>2</sup>	Slope	% Filtering
<b>10nm, 5nm</b>			
Buffer	0.997	47.93	0.0
Serum	0.999	44.38	7.41
Post-phenyl sepharose	0.997	45.91	4.21
<b>10nm, 10nm</b>			
Buffer	0.998	230.42	0.0

**Table 3.1. Slopes and the Percentage Filtering of Quenched Standard Curves**

### **3.3. Purification of ZIP Activity From Bovine Serum**

#### **3.3.1. Serum Preparation**

5l of fresh bovine whole blood was collected, which resulted in 1l of serum post clotting and centrifugation at 4°C.

#### **3.3.2. Phenyl Sepharose Hydrophobic Interaction Chromatography**

Figure 3.3.2.1. illustrates the elution profile of ZIP activity from a phenyl sepharose column, which was prepared and run according to section 2.5.2. The profile shows the presence of two Z-Gly-Pro-AMC degrading activity peaks, measured as in section 2.4.4. The first activity peak is present in the run through wash, while the second major activity peak elutes with the ultra-pure water wash. These activities are distinguished according to their sensitivity to JTP-4819 (a potent and specific inhibitor of prolyl oligopeptidase), which is seen in Figure 3.3.2.2. Fractions 53-57 were combined yielding 25ml post phenyl sepharose ZIP sample. 1.5ml of this pooled sample was retained for quantitative ZIP activity (section 2.4.2.) and quantitative protein (section 2.2.1.) determinations.

#### **3.3.3. Calcium Phosphate Cellulose Chromatography**

After concentration of the post phenyl sepharose pool to 10ml, the sample was further purified using calcium phosphate cellulose as outlined in section 2.5.3. Figure 3.3.3. shows the elution profile of ZIP activity and protein, measured according to sections 2.4.4. and 2.2.2. ZIP bound to the column at a low phosphate concentration and eluted on application of 500mM phosphate. Fractions 46-47 were pooled yielding 10ml post calcium phosphate cellulose ZIP sample. 1.5ml of this pool was retained for quantitative ZIP activity (section 2.4.2.) and quantitative protein (section 2.2.2.) determinations.

#### **3.3.4. Cibacron Blue 3GA Chromatography**

Concentrated and dialysed post calcium phosphate cellulose ZIP was applied to a Cibacron blue 3GA column and further purified as outlined in section 2.5.4. ZIP bound to the resin and was eluted using an increasing linear gradient of sodium chloride. Figure 3.3.4. illustrates the elution profile from the column. Fractions 28-31

were combined yielding 20ml post Cibacron blue 3GA ZIP sample. 1.5ml of this pool was retained for quantitative ZIP activity (section 2.4.2.) and quantitative protein (section 2.2.3.) measurements.

### **3.3.5. Sephacryl S-300 Size Exclusion Chromatography**

2ml of concentrated post cibacron blue 3GA ZIP was applied to the S-300 column as outlined in section 2.5.4. Figure 3.3.5. shows the purification of ZIP on the gel filtration resin. Fractions 12-14, which contained activity, were combined to form 15ml post S-300 ZIP sample. 1.5ml of this pool was again retained for quantitative ZIP activity (section 2.4.2.) and quantitative protein (section 2.2.3.) determinations.

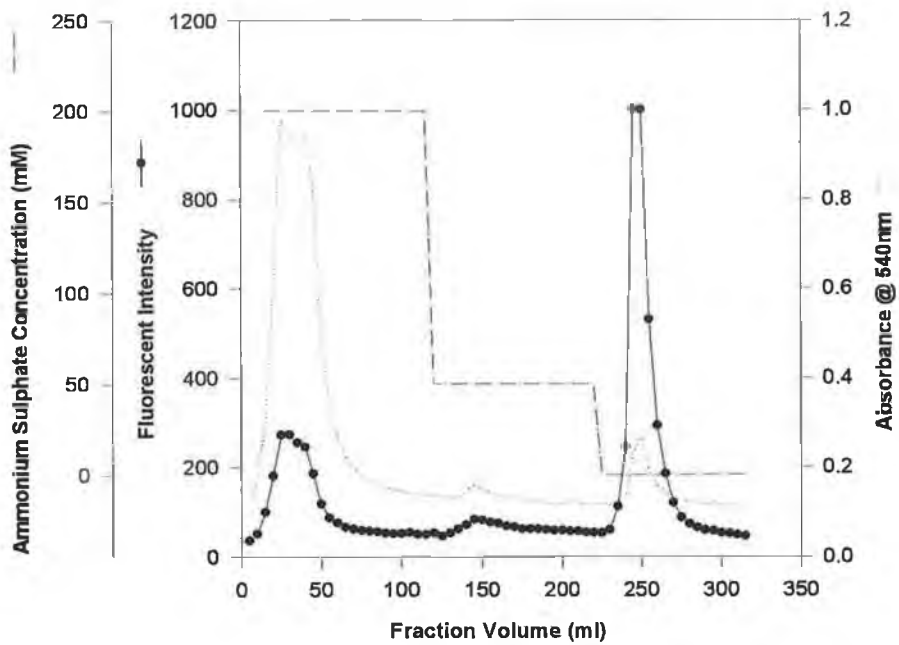


**Figure 3.3.2.1. Fractionation of the Two Z-Gly-Pro-AMC Hydrolysing Activities in Bovine Serum by Phenyl Sepharose Hydrophobic Interaction Chromatography.**

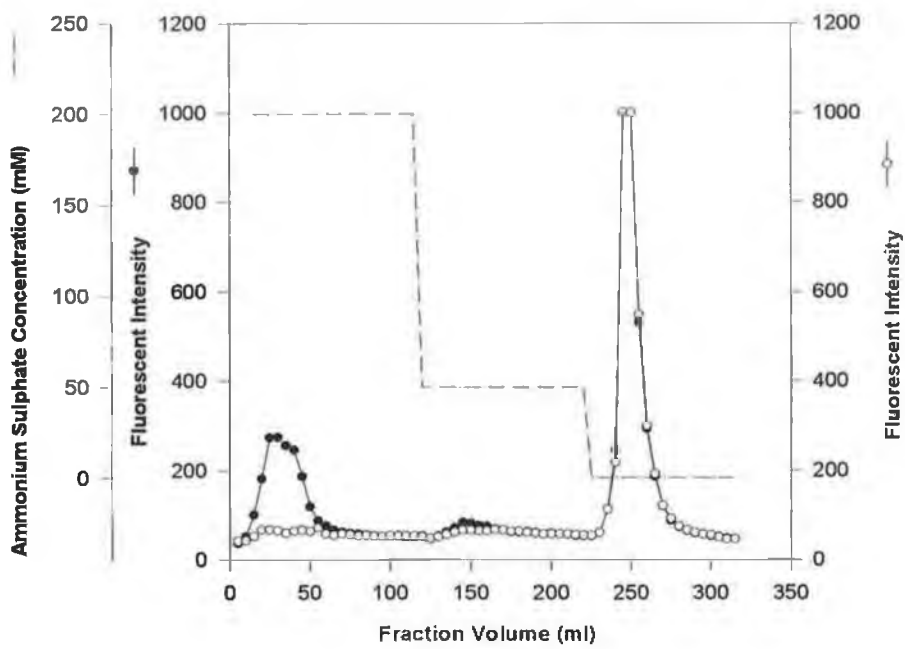


**Figure 3.3.2.2. Differentiation of the Two Distinct Z-Gly-Pro-AMC Degrading Activities (●) in Bovine Serum by the Inclusion of JTP-4819 (○).**

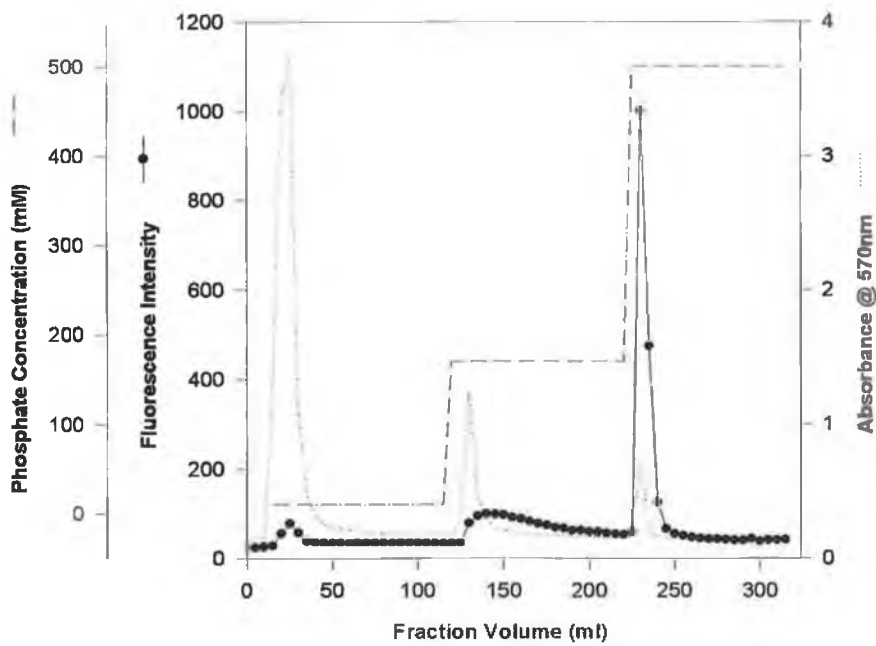


**Figure 3.3.3. Elution Profile of ZIP During Calcium Phosphate Cellulose Chromatography.**

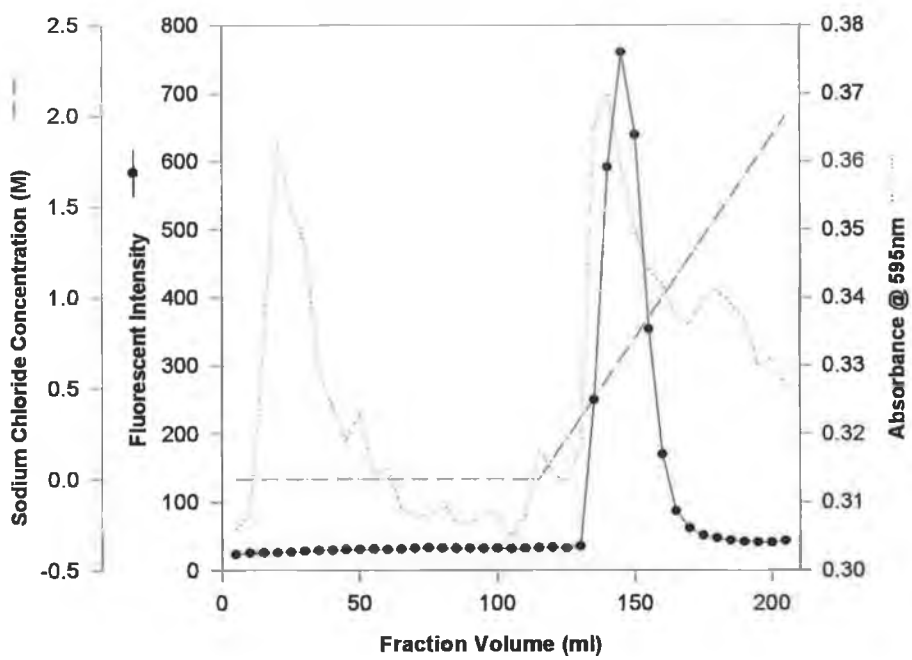


**Figure 3.3.4. Cibacron Blue 3GA Chromatography of ZIP**



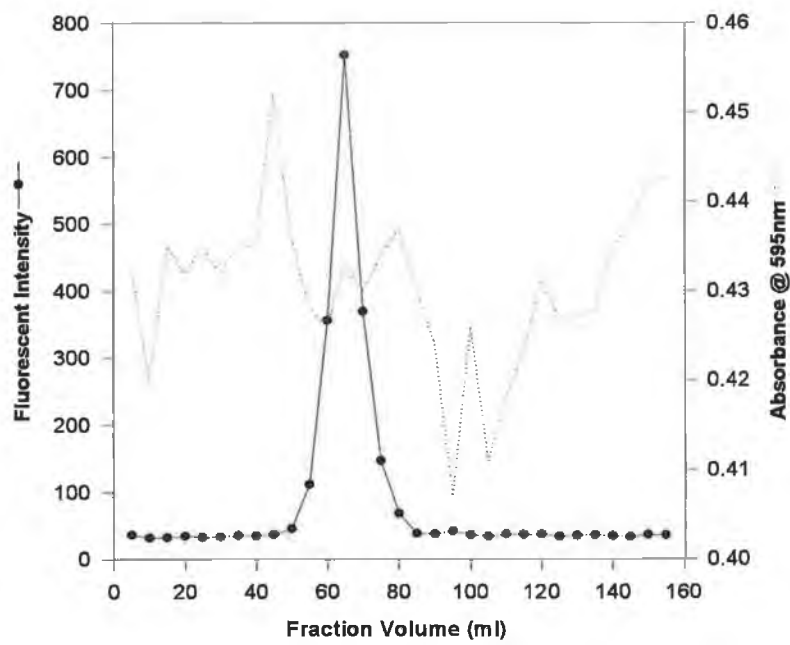


**Figure 3.3.5. Elution Profile of ZIP Activity During S-300 Gel Filtration Chromatography.**

<b>Purification Step</b>	<b>Volume</b>	<b>Total Activity <sup>a</sup></b>	<b>Total Protein</b>	<b>Specific Activity</b>	<b>Purification Factor</b>	<b>Recovery</b>
	<i>ml</i>	<i>Units</i>	<i>mg</i>	<i>Units/mg</i>		<i>%</i>
<b>Crude Serum</b>	20	16.12	1766	0.00913	1	100
<b>Phenyl Sepharose</b>	25	15.02	37.15	0.404	44.3	93.18
<b>CPC</b>	10	8.62	1.52	5.67	621	53.47
<b>Cibacron Blue</b>	20	3.25	0.019	171.05	18,735	20.16
<b>S-300</b>	15	1.93	0.007	275.7	30,197	11.97

**Table 3.2. Representative Purification of ZIP from Bovine Serum**

The representative purification table was constructed to assess the overall effectiveness of the purification procedure.

<sup>a</sup> Based on the enzymatic activity using 100 $\mu$ M Z-Gly-Pro-AMC, where Units = nmoles.min<sup>-1</sup> i.e. Units are expressed as nanomoles of AMC released per minute at 37°C.

### 3.4. Purity Assessment of ZIP

#### 3.4.1. The Activity of Purified ZIP Sample Against Fluorimetric Substrates

The presence of contaminating peptidase activities in purified ZIP sample was assessed by monitoring for hydrolysis a number of fluorimetric substrates. These substrates were prepared and assayed as outlined in section 2.6.1. Table 3.4. illustrates that no cleavage of these substrates was detected in the presence of purified ZIP sample.

Substrate	Hydrolysis	Substrate	Hydrolysis
Z-Phe-Arg-AMC	No	Pro-AMC	No
Z-Arg-Arg-AMC	No	Gly-AMC	No
Z-Gly-Pro-AMC	Yes	Pyr-AMC	No
Pyr-His-Pro-AMC	No	Arg-AMC	No
Glu-Phe-AMC	No	Ala-AMC	No
Gly-Pro-AMC	No	Leu-AMC	No
Lys-Ala-AMC	No	Lys-AMC	No

**Table 3.3. Cleavage of Fluorimetric Substrates by Contaminating Peptidases.**

#### 3.4.2. SDS Polyacrylamide Gel Electrophoresis

SDS polyacrylamide gel electrophoresis was performed as outlined in section 2.6.2. Figure 3.4.2.1. illustrates a gelcode blue stained gel image of the purification procedure, including post column ZIP samples and molecular weight markers. Figure 3.4.2.2. shows a silver stained image of lanes 4,5,6 & 7 of the gelcode stained gel.

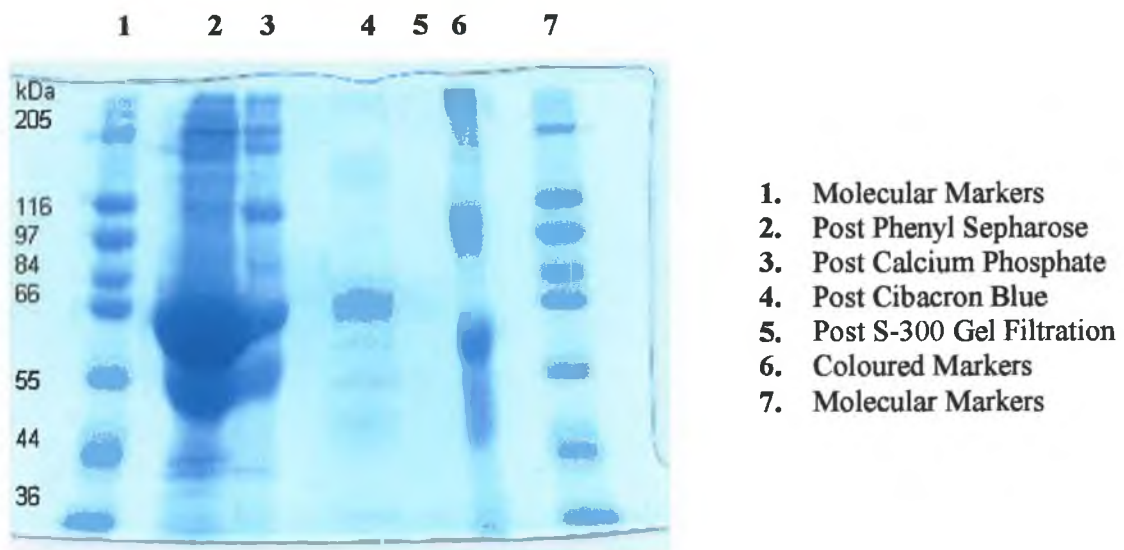


**Figure 3.4.2.1. 10% SDS PAGE for Bovine Serum ZIP Purification**

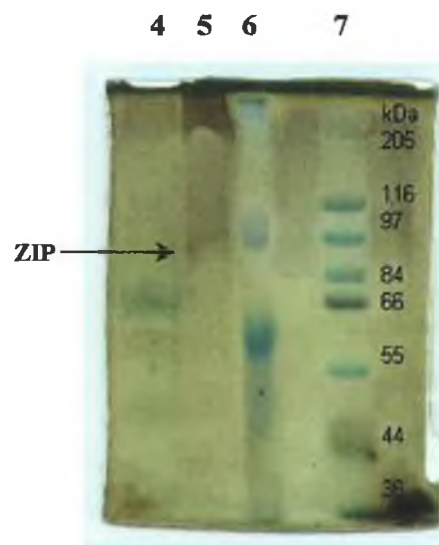


**Figure 3.4.2.2. Silver Stained Image-Showing Part of the Gel in Fig. 3.4.2.1.**

### 3.5. Substrate Specificity Studies

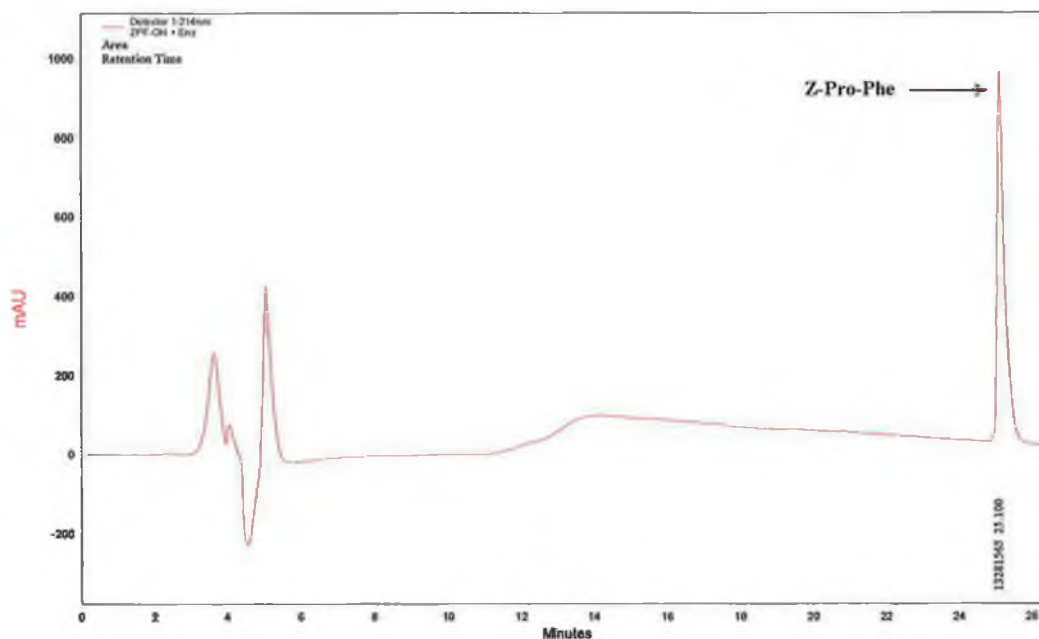
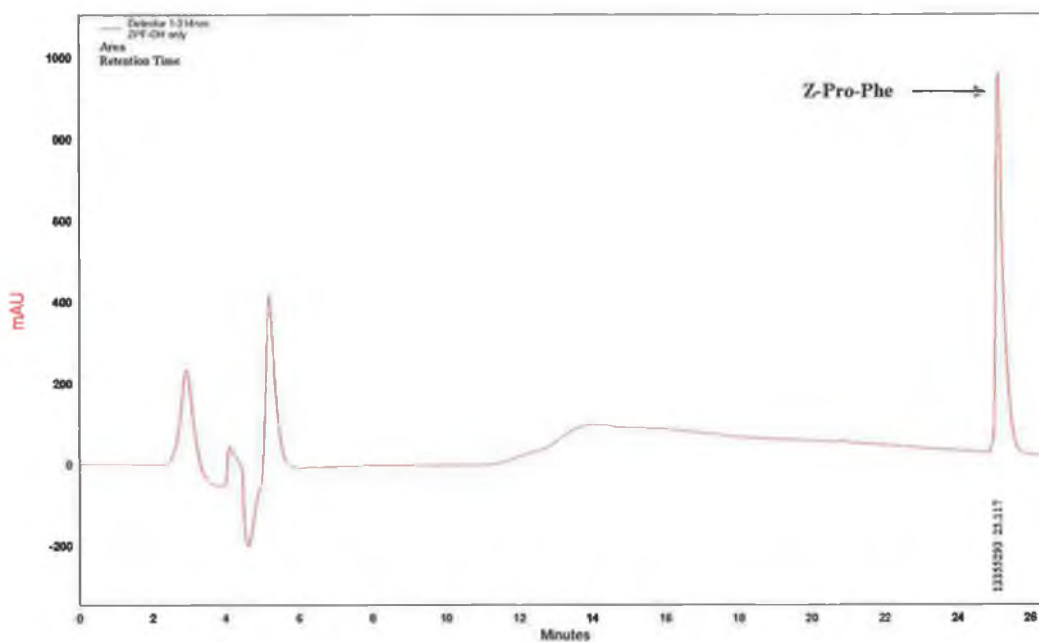
Substrate specificity studies on purified ZIP were performed as outlined in section 2.7. Kinetic analysis of residues located NH<sub>2</sub>-terminally and at the COOH- terminal site of the scissile bond of proline-containing peptides was investigated. Reverse Phase (RP) HPLC was used to separate and quantify peptide digest products of some of the proline-containing peptides. LC-MS was then performed on these complex digest products for identification.

#### 3.5.1. Effect of Residues Located NH<sub>2</sub>-Terminally from the Scissile Bond of Proline-Containing Peptides

The effect of increasing the peptide chain length from the Pro-X (P<sub>1</sub>-P<sub>1</sub>') bond to include P<sub>2</sub> and P<sub>3</sub> is shown in Table 3.4. Figure 3.5.1.1. and 3.5.1.2. show the chromatograms for the peptide Z-Pro-Phe-OH before and after incubation with ZIP as outlined in section 2.7.2.

Peptide	[Peptide]	Hydrolysis
P <sub>3</sub> P <sub>2</sub> P <sub>1</sub> ↓ P <sub>1</sub> '	(mM)	
Pro-AMC	0.1	No
Gly-Pro-AMC	0.1	No
Z-Gly-Pro-AMC	0.1	Yes
pGlu-His-Pro-AMC	0.1	No
Z-Gly-Pro-Ala	1	Yes
Gly-Gly-Pro-Ala	1	No
Z-Pro-Phe	1	No

**Table 3.4. The Effect on Hydrolysis of Proline-Containing Peptides Extended NH<sub>2</sub>-Terminally from the Scissile Bond.**



**Figures 3.5.1.1. and 3.5.1.2. HPLC chromatograms for Z-Pro-Phe incubation with ZIP.** Plots of absorbance at 214nm versus time for peptide only (Fig. 3.5.1.1.) and for peptide and ZIP incubate (Fig. 3.5.1.2.). Figure 3.5.1.2. illustrates the failure of ZIP to cleave the peptide Z-Pro-Phe-OH.

### 3.5.2. $K_m$ Determination for Z-Gly-Pro-AMC

The kinetic behaviour of purified ZIP was investigated using Z-Gly-Pro-AMC.  $K_m$  values for the hydrolysis of the substrate Z-Gly-Pro-AMC were determined according to section 2.7.1.1. Data obtained was applied to the Lineweaver-Burk, Eadie-Hofstee and Hanes-Woolf kinetic models for analysis (section 6.4.1.). Table 3.5. represents the  $K_m$  values deduced using these models. Figures 3.5.2.1. through to 3.5.2.3. illustrate Lineweaver-Burk, Eadie-Hofstee and Hanes-Woolf plots for ZIP assayed with Z-Gly-Pro-AMC.

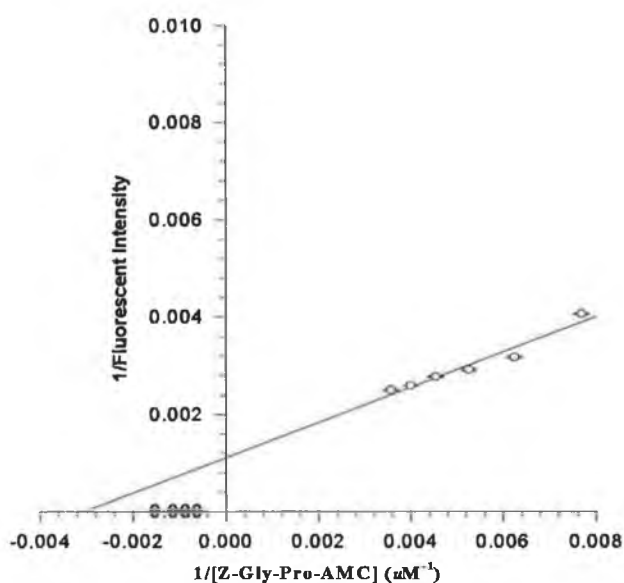


**Figure 3.5.2.1.  $K_m$  determination using the Lineweaver-Burk kinetic model**

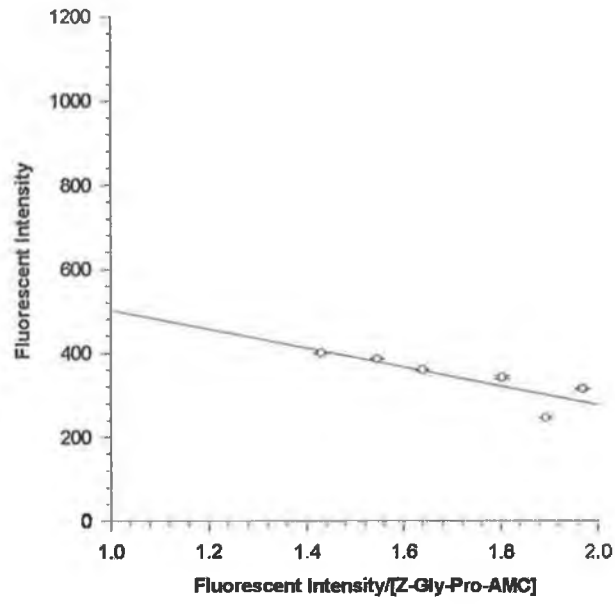


**Figure 3.5.2.2.  $K_m$  determination using the Eadie-Hofstee kinetic model**

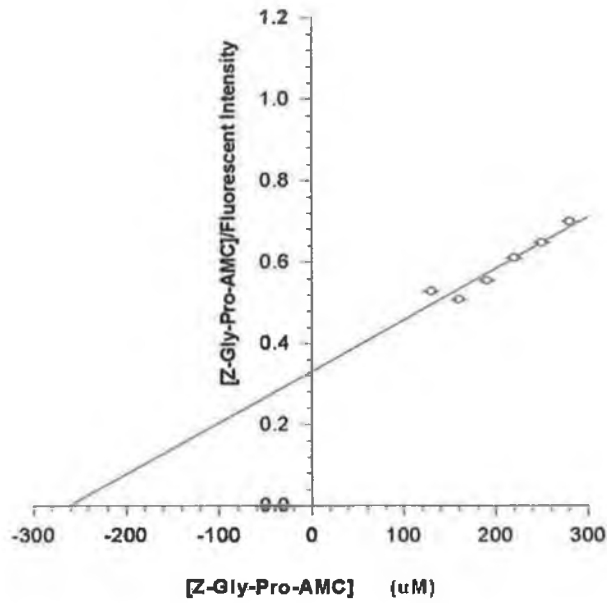


**Figure 3.5.2.3.  $K_m$  determination using the Hanes-Woolf kinetic model**



<b>Kinetic Model</b>	<b>K<sub>m</sub> (μM)</b>
Lineweaver-Burk	323.47
Eadie-Hofstee	225.20
Hanes-Woolf	261.67
<i>Average</i>	<b>270</b>

**Table 3.5. K<sub>m</sub> Value (μM) Obtained for the Substrate Z-Gly-Pro-AMC**

### **3.5.3. Effect of Residues Located at the COOH-Terminal Site of the Scissile Bond of Proline-Containing Peptides**

#### **3.5.3.1. Amino Acid Preference at the C-Terminal End of the Scissile Bond (P<sub>1</sub>' Position)**

While keeping the Z-Gly-Pro (P<sub>3</sub>, P<sub>2</sub>, P<sub>1</sub>) sequence constant, a range of N-blocked tripeptides with variable amino acids in the P<sub>1</sub>' position were synthesised and then prepared according to Table 2.3.

##### **3.5.3.1.1. Determination of K<sub>i (app)</sub> Values for Proline-Containing Peptides**

Determination of K<sub>i (app)</sub> values in the ZIP-catalysed hydrolysis of Z-Gly-Pro-AMC using proline-containing peptides was performed according to section 2.7.1.2. K<sub>m</sub> and V<sub>max</sub> values were determined for ZIP using the Lineweaver-Burk kinetic model described in section 3.5.2. K<sub>m</sub><sup>app</sup> and V<sub>max</sub><sup>app</sup> values were determined graphically for each of the peptides using the Lineweaver-Burk kinetic plot. K<sub>i (app)</sub> values and the nature of inhibition were estimated for each peptide (sections 6.4.2. & 6.4.3.). Figures 3.5.3.1.1.1. to 3.5.3.1.1.8. represent Lineweaver-Burk plots for each peptide studied. Table 3.6. lists the K<sub>i (app)</sub> values and the type of inhibition obtained.

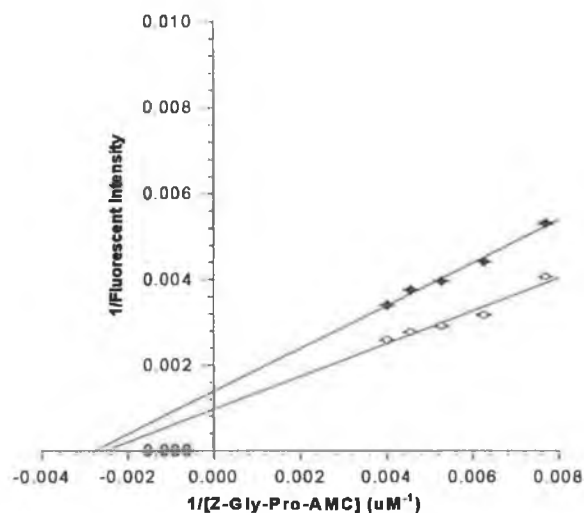


**Figure 3.5.3.1.1.1.** Kinetic analysis of the effect of Z-Gly-Pro-Phe (♦) on ZIP catalysed hydrolysis of Z-Gly-Pro-AMC (o). Lineweaver-Burk reciprocal plot of fluorescent intensity versus  $[Z-Gly-Pro-AMC]$ . Plot illustrates the mixed inhibition of ZIP by Z-Gly-Pro-Phe.

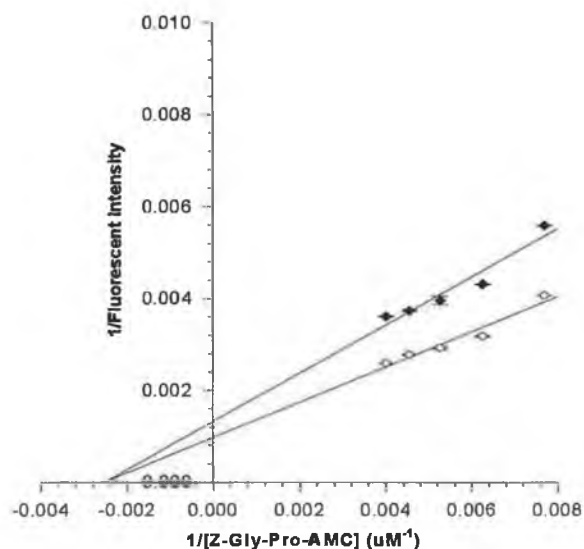


**Figure 3.5.3.1.1.2.** Kinetic analysis of the effect of Z-Gly-Pro-Met (♦) on ZIP catalysed hydrolysis of Z-Gly-Pro-AMC (o). Lineweaver-Burk reciprocal plot of fluorescent intensity versus  $[Z-Gly-Pro-AMC]$ . Plot illustrates the non-competitive inhibition of ZIP by Z-Gly-Pro-Met.

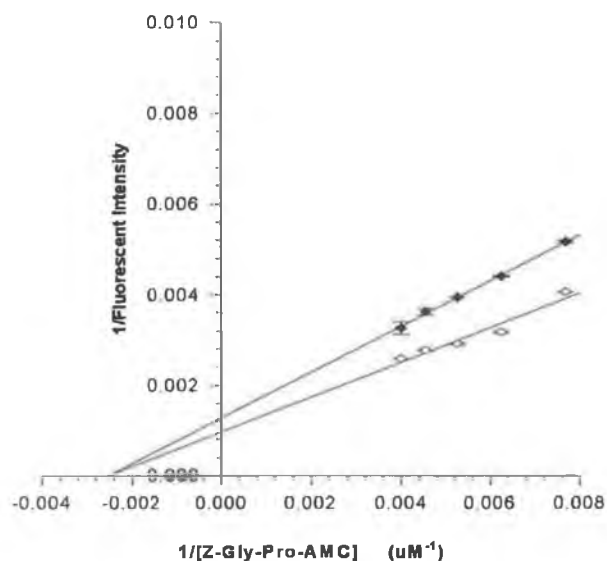


**Figure 3.5.3.1.1.3. Kinetic analysis of the effect of Z-Gly-Pro-Tyr (♦) on ZIP catalysed hydrolysis of Z-Gly-Pro-AMC (o). Lineweaver-Burk reciprocal plot of fluorescent intensity versus [Z-Gly-Pro-AMC]. Plot illustrates the non-competitive inhibition of ZIP by Z-Gly-Pro-Tyr.**

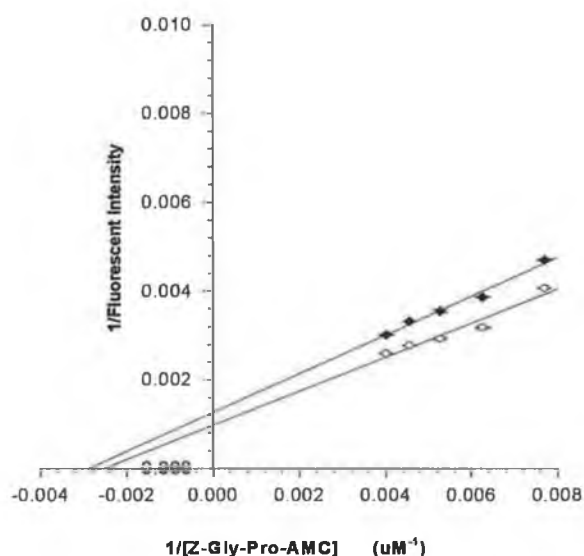


**Figure 3.5.3.1.1.4. Kinetic analysis of the effect of Z-Gly-Pro-Ser (♦) on ZIP catalysed hydrolysis of Z-Gly-Pro-AMC (o). Lineweaver-Burk reciprocal plot of fluorescent intensity versus [Z-Gly-Pro-AMC]. Plot illustrates the mixed inhibition of ZIP by Z-Gly-Pro-Ser.**

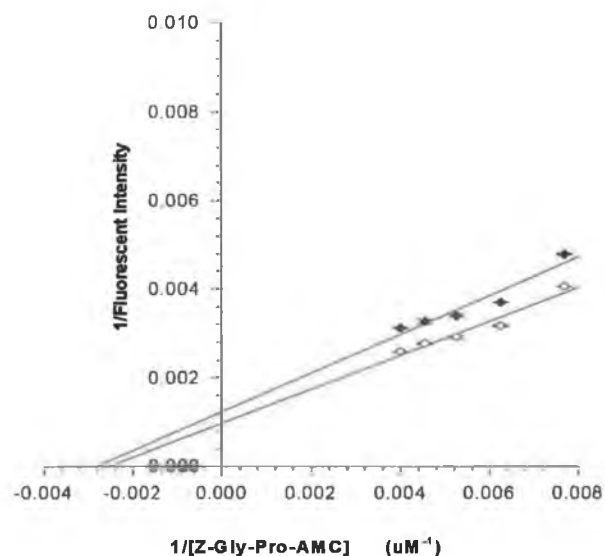


**Figure 3.5.3.1.1.5.** Kinetic analysis of the effect of Z-Gly-Pro-Glu (◆) on ZIP catalysed hydrolysis of Z-Gly-Pro-AMC (o). Lineweaver-Burk reciprocal plot of fluorescent intensity versus [Z-Gly-Pro-AMC]. Plot illustrates the mixed inhibition of ZIP by Z-Gly-Pro-Glu.

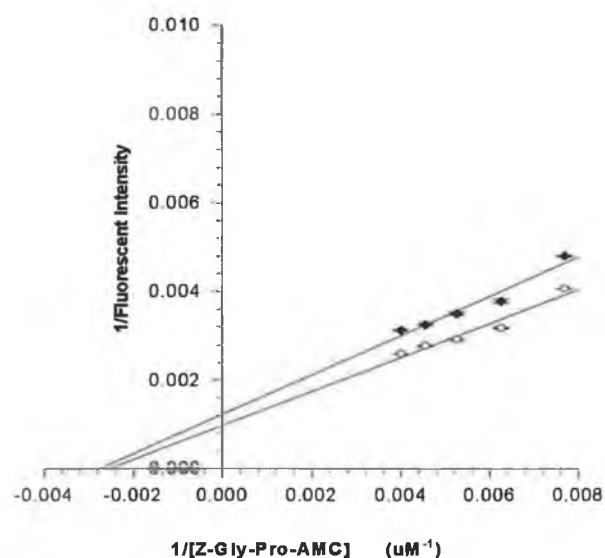


**Figure 3.5.3.1.1.6.** Kinetic analysis of the effect of Z-Gly-Pro-His (◆) on ZIP catalysed hydrolysis of Z-Gly-Pro-AMC (o). Lineweaver-Burk reciprocal plot of fluorescent intensity versus [Z-Gly-Pro-AMC]. Plot illustrates the mixed inhibition of ZIP by Z-Gly-Pro-His.

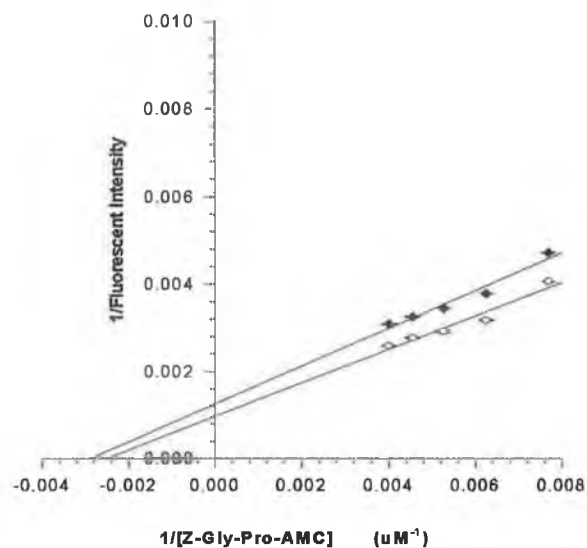


**Figure 3.5.3.1.1.7.** Kinetic analysis of the effect of Z-Gly-Pro-Leu (◆) on ZIP catalysed hydrolysis of Z-Gly-Pro-AMC (o). Lineweaver-Burk reciprocal plot of fluorescent intensity versus [Z-Gly-Pro-AMC]. Plot illustrates the mixed inhibition of ZIP by Z-Gly-Pro-Leu.

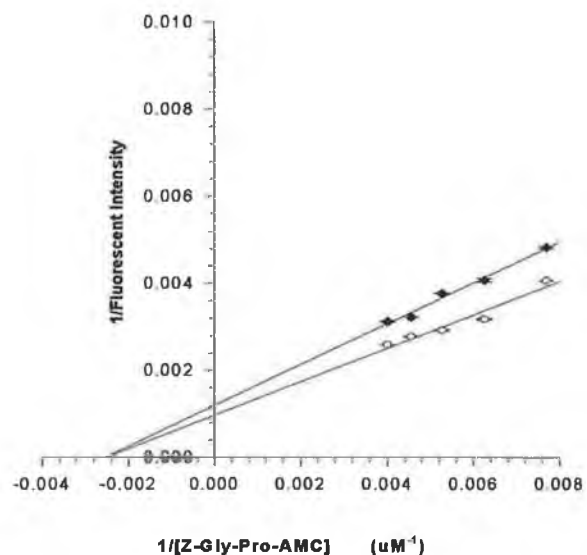


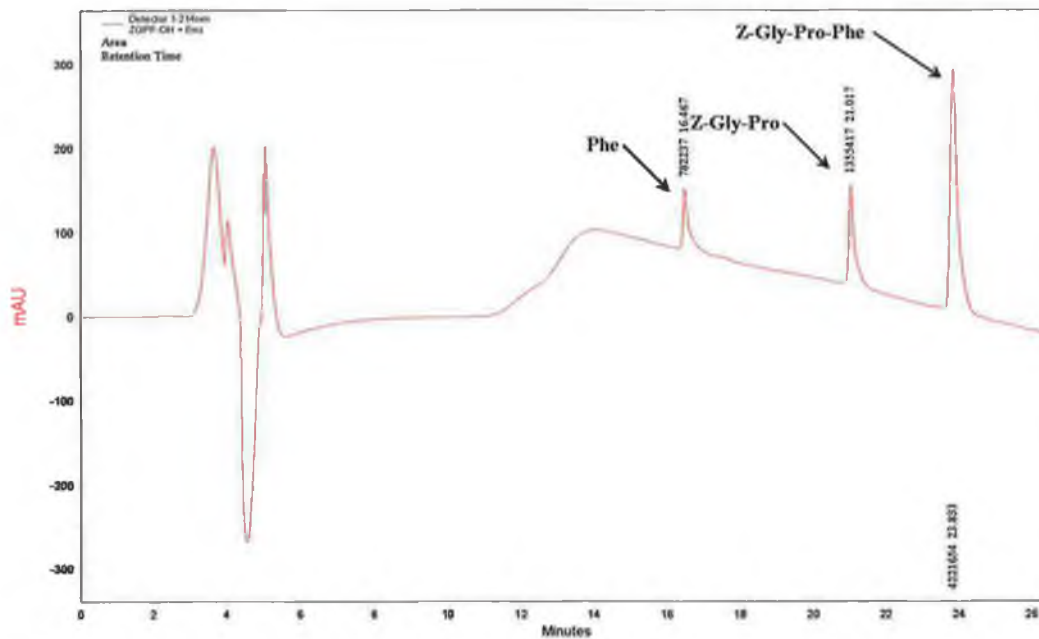
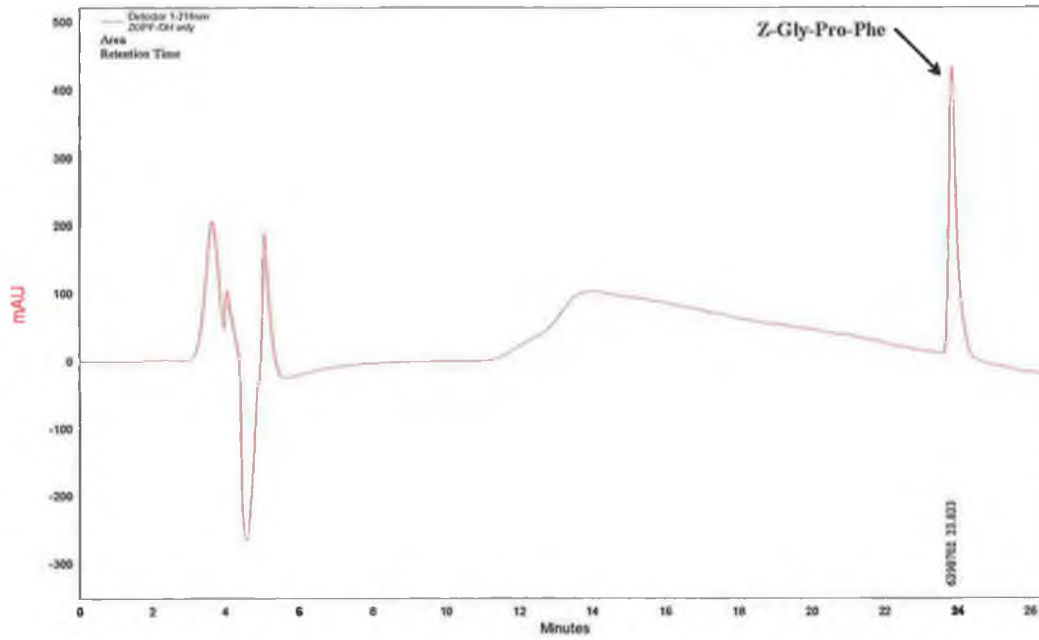
**Figure 3.5.3.1.1.8.** Kinetic analysis of the effect of Z-Gly-Pro-Ala (◆) on ZIP catalysed hydrolysis of Z-Gly-Pro-AMC (o). Lineweaver-Burk reciprocal plot of fluorescent intensity versus [Z-Gly-Pro-AMC]. Plot illustrates the non-competitive inhibition of ZIP by Z-Gly-Pro-Ala.

Peptide	Assay Conc.	$K_{i (app)}$ ( $\mu\text{M}$ )	Inhibition Type
$\text{P}_3 \text{ P}_2 \text{ P}_1 \downarrow \text{P}'_1$	( $\mu\text{M}$ )		
Z-Gly-Pro-Phe	200	461.53	Mixed
Z-Gly-Pro-Met	200	554.72	Non-competitive
Z-Gly-Pro-Tyr	200	632.76	Non-competitive
Z-Gly-Pro-Ser	200	672.80	Mixed
Z-Gly-Pro-Leu	200	687.97	Mixed
Z-Gly-Pro-Glu	200	748.90	Mixed
Z-Gly-Pro-His	200	769.07	Mixed
Z-Gly-Pro-Ala	200	862.65	Non-competitive

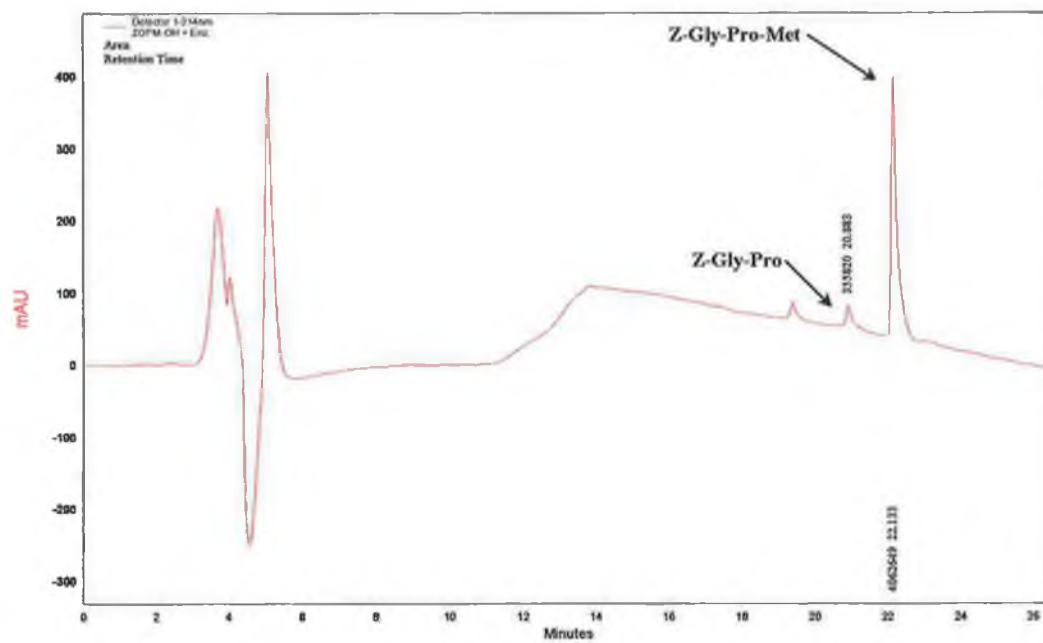
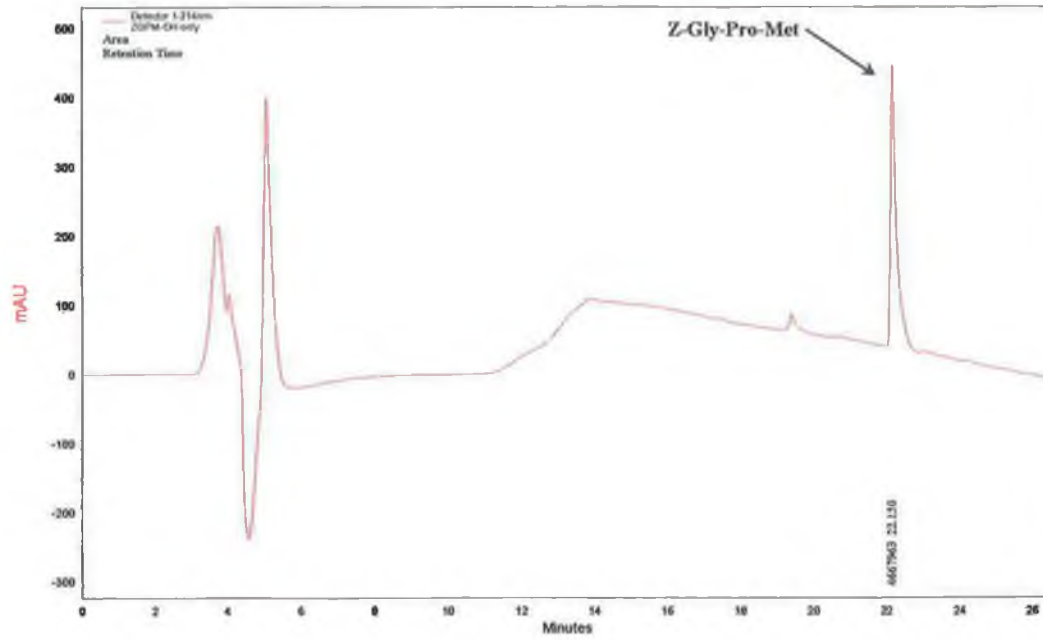
**Table 3.6.  $K_{i (app)}$  Values Obtained for Proline-Containing N-blocked Tripeptides**

#### **3.5.3.1.2. Reverse Phase HPLC of Proline-Containing N-blocked Tripeptides**

To determine the ability of ZIP to hydrolyse a variety of N-blocked tripeptides, the products of hydrolysis were separated by reverse phase HPLC. Reaction of peptides with ZIP and reverse phase HPLC were performed according to sections 2.7.2.2. and 2.7.2.3. respectively. Figures 3.5.3.1.2.1 to 3.5.3.1.2.16 represent chromatograms of each of the peptides tested. Figure 3.5.3.1.2.18 shows a standard curve of the peptide standard Z-Gly-Pro, prepared according to section 2.7.2.1. Table 3.7. gives a summary of the peptides studied, whether hydrolysis was detected and if so, a quantified product value. The optimum wavelength for detection of peptides was found to be at 214nm.

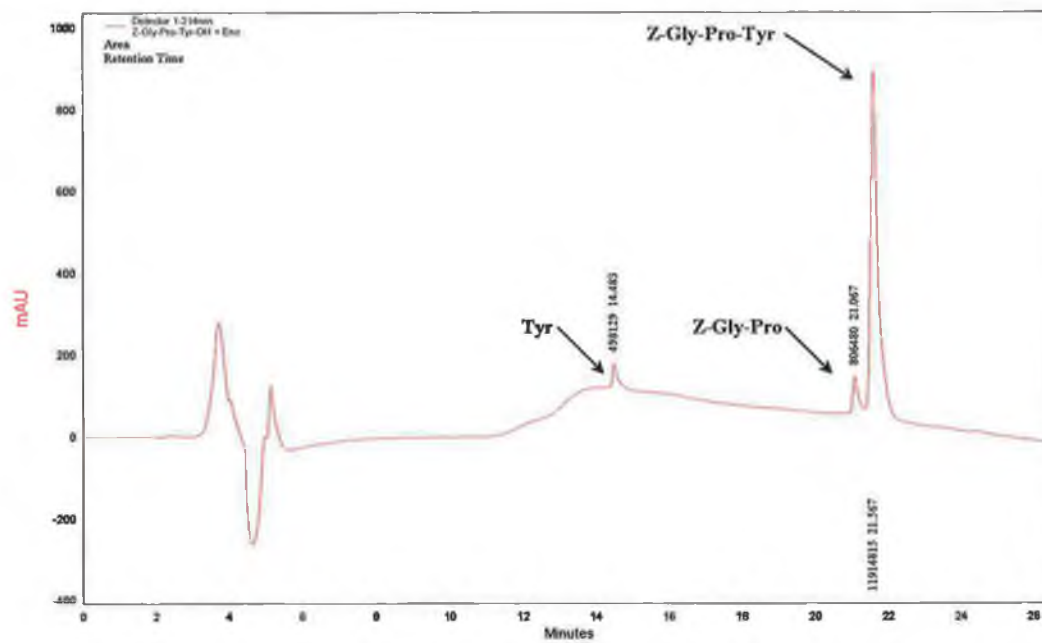
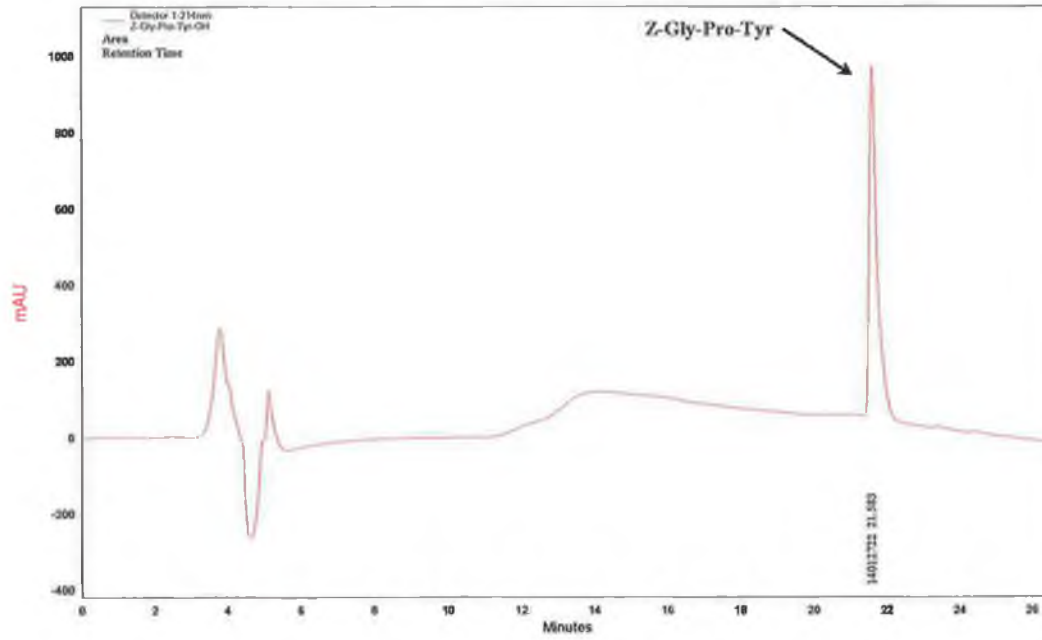


**Figures 3.5.3.1.2.1. and 3.5.3.1.2.2. HPLC chromatogram of Z-Gly-Pro-Phe hydrolysis by ZIP.** Plots of absorbance at 214nm versus time for peptide only (Fig. 3.5.3.1.2.1.) and for peptide and ZIP incubate (Fig. 3.5.3.1.2.2.). Figure 3.5.3.1.2.2. clearly shows the cleavage of Z-Gly-Pro-Phe by ZIP.

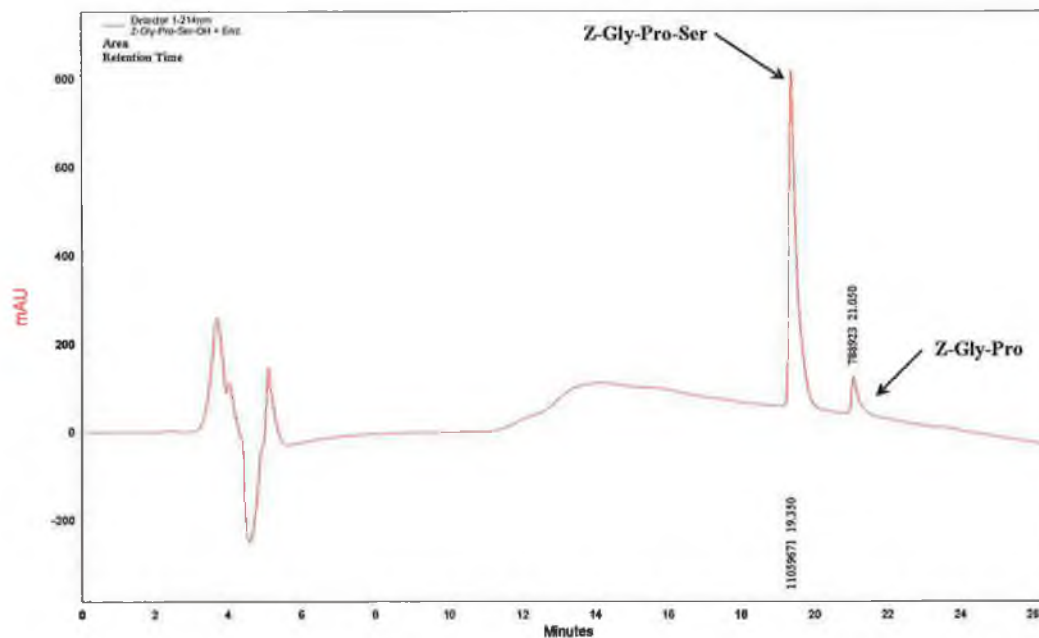
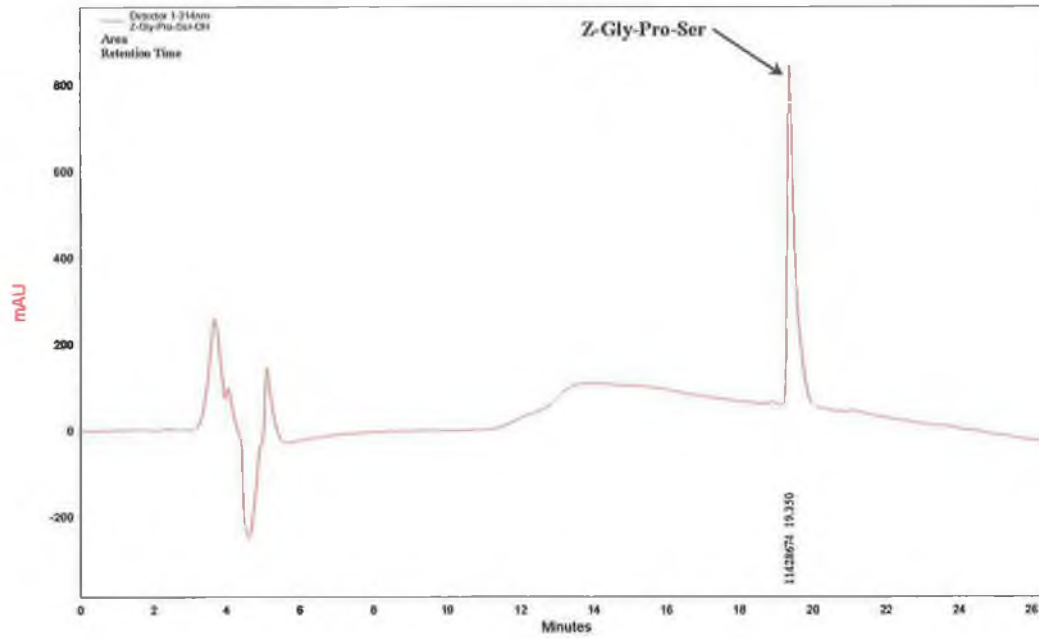


**Figures 3.5.3.1.2.3. and 3.5.3.1.2.4. HPLC chromatogram of Z-Gly-Pro-Met hydrolysis by ZIP.** Plots of absorbance at 214nm versus time for peptide only (Fig. 3.5.3.1.2.3.) and for peptide and ZIP incubate (Fig. 3.5.3.1.2.4.). Figure 3.5.3.1.2.4. shows the slight cleavage of Z-Gly-Pro-Met by ZIP.

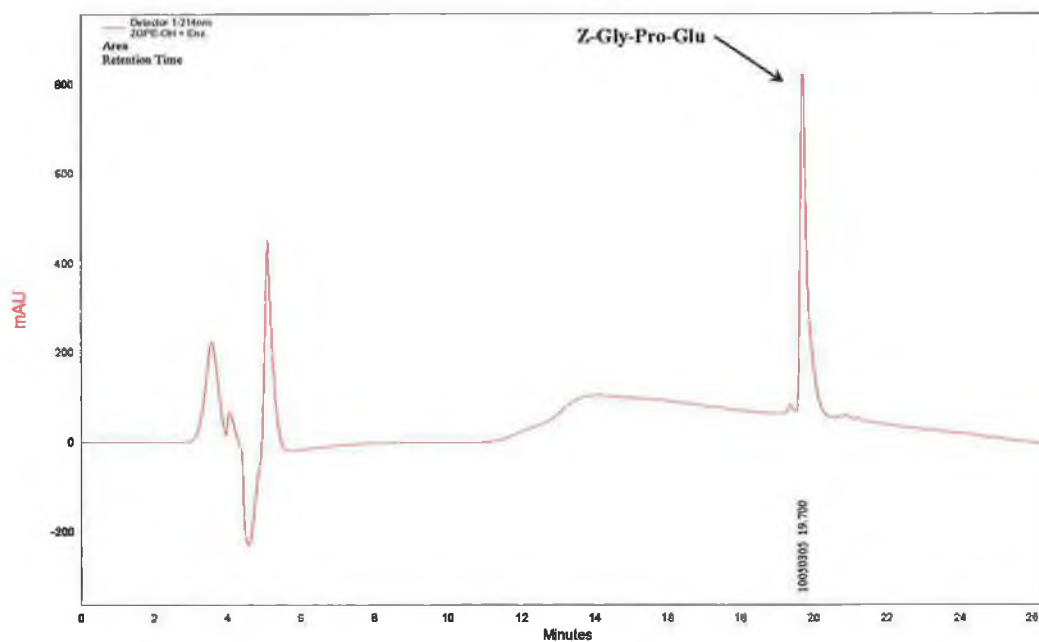
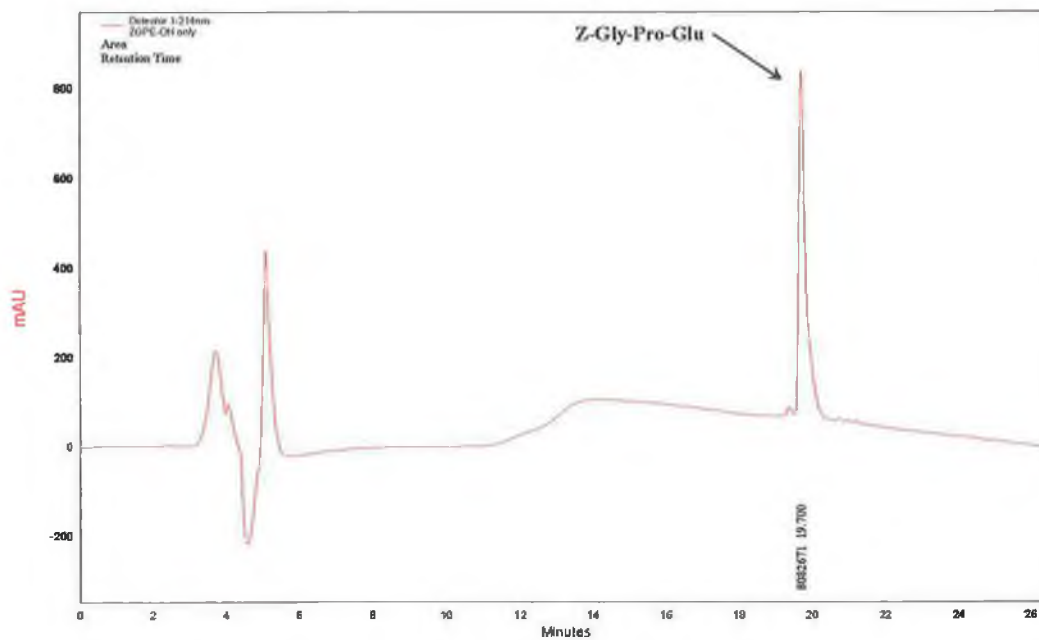




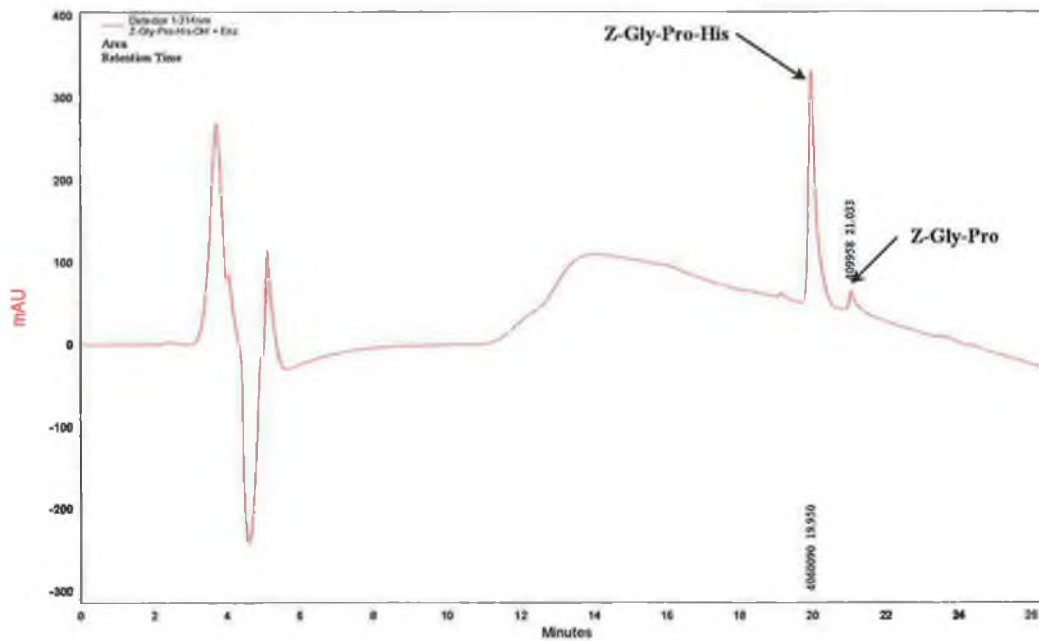
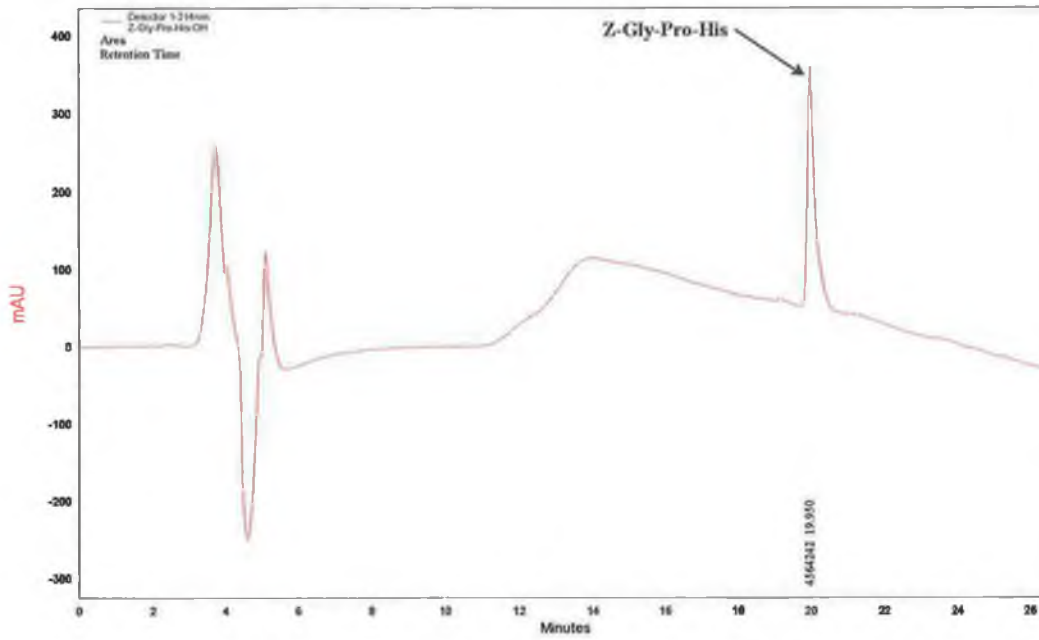
**Figures 3.5.3.1.2.5. and 3.5.3.1.2.6. HPLC chromatogram of Z-Gly-Pro-Tyr hydrolysis by ZIP.** Plots of absorbance at 214nm versus time for peptide only (Fig. 3.5.3.2.1.5.) and for peptide and ZIP incubate (Fig. 3.5.3.2.1.6.). Figure 3.5.3.2.1.6. shows the cleavage of Z-Gly-Pro-Tyr by ZIP.



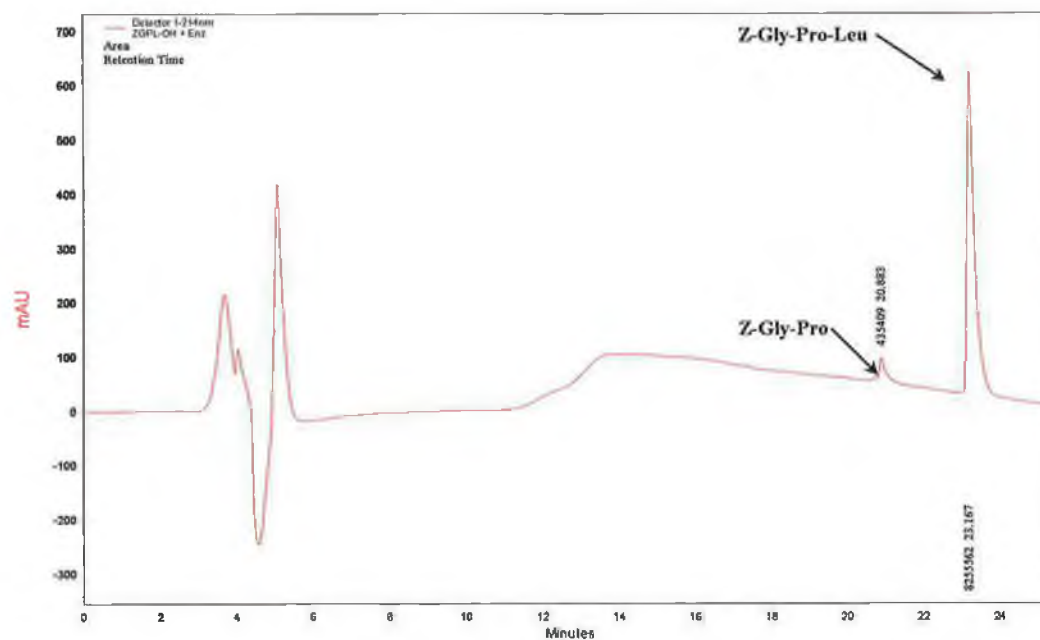
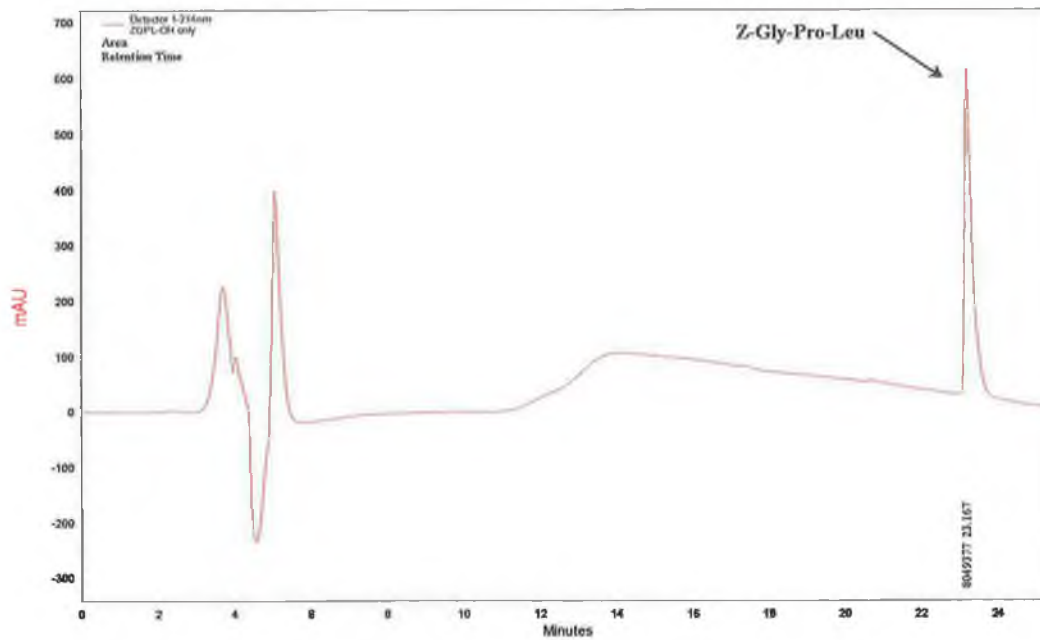
**Figures 3.5.3.1.2.7. and 3.5.3.1.2.8. HPLC chromatogram of Z-Gly-Pro-Ser hydrolysis by ZIP.** Plot of absorbance at 214nm versus time for peptide only (Fig. 3.5.3.1.2.7.) and for peptide and ZIP incubate (Fig. 3.5.3.1.2.8.). Figure 3.5.3.1.2.8. illustrates the hydrolysis of Z-Gly-Pro-Ser by ZIP.



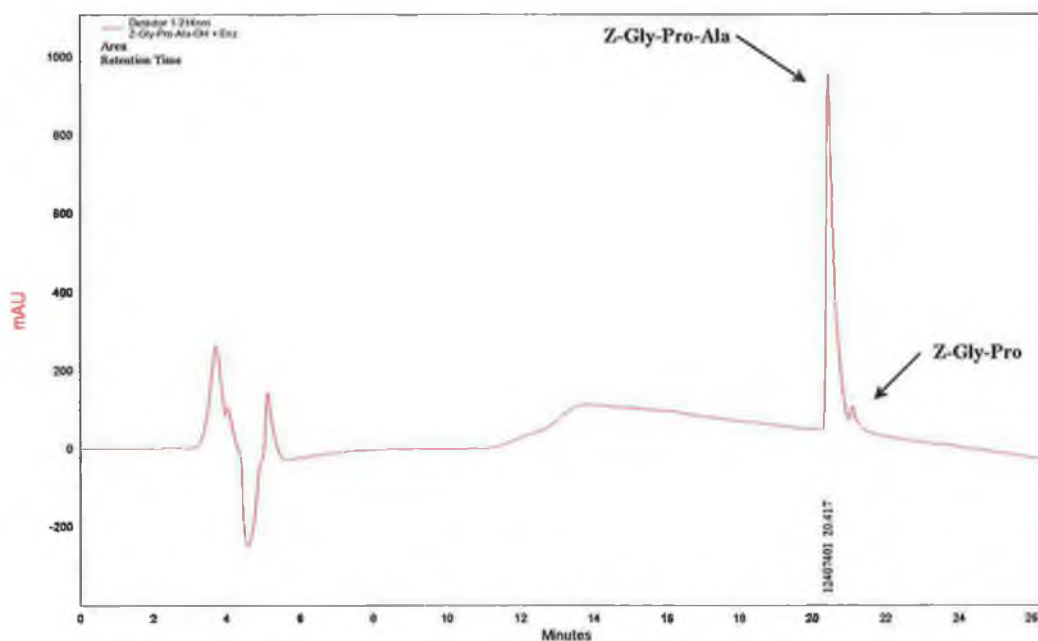
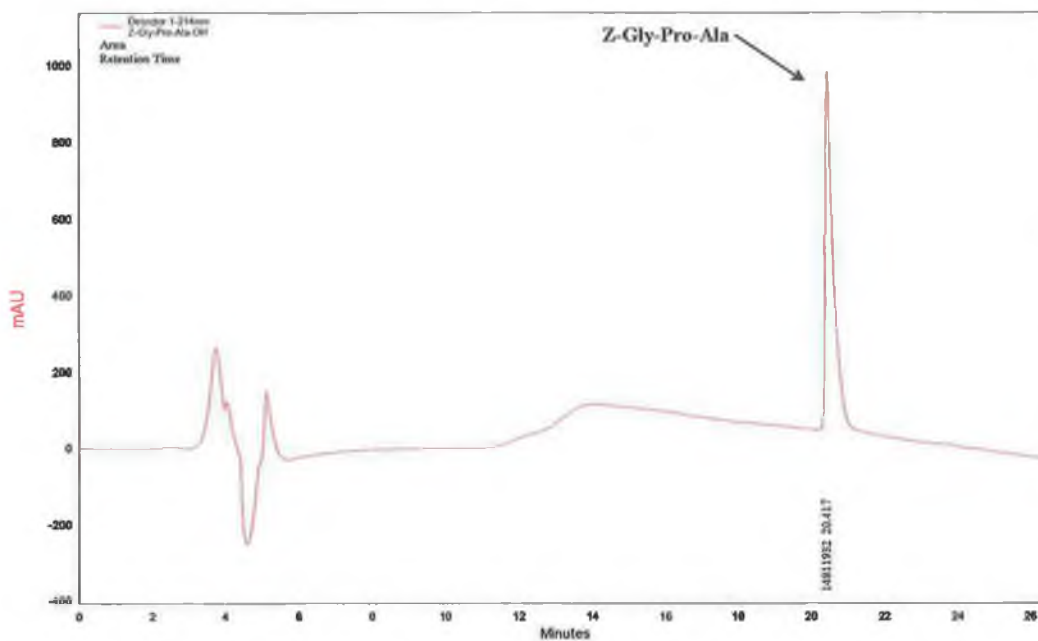
**Figures 3.5.3.1.2.9. and 3.5.3.1.2.10 HPLC chromatogram of Z-Gly-Pro-Glu hydrolysis by ZIP.** Plots of absorbance at 214nm versus time for peptide only (Fig. 3.5.3.1.2.9.) and for peptide and ZIP incubate (Fig. 3.5.3.1.2.10). Figure 3.5.3.1.2.10 illustrates the negligible hydrolysis of Z-Gly-Pro-Glu by ZIP.



**Figures 3.5.3.1.2.11. and 3.5.3.1.2.12. HPLC chromatograms of Z-Gly-Pro-His hydrolysis by ZIP. Plots of absorbance at 214nm versus time for peptide only (Fig. 3.5.3.1.2.11.) and for peptide and ZIP incubate (Fig. 3.5.3.1.2.12.). Figure 3.5.3.1.2.12. illustrates the cleavage of Z-Gly-Pro-His by ZIP.**



**Figures 3.5.3.1.2.13. and 3.5.3.1.2.14. HPLC chromatograms of Z-Gly-Pro-Leu hydrolysis by ZIP. Plot of absorbance at 214nm versus time for peptide only (Fig. 3.5.3.1.2.13.) and for peptide and ZIP incubate (Fig. 3.5.3.1.2.14.). Figure 3.5.3.1.2.14. illustrates the cleavage of Z-Gly-Pro-Leu by ZIP.**



**Figures 3.5.3.1.2.15. and 3.5.3.1.2.16. HPLC chromatograms of Z-Gly-Pro-Ala hydrolysis by ZIP, Plots of absorbance at 214nm versus time for peptide only (Fig. 3.5.3.1.2.15.) and for peptide and ZIP incubate (Fig. 3.5.3.1.2.16.). Figure 3.5.3.1.2.16. shows the hydrolysis of Z-Gly-Pro-Ala by ZIP.**

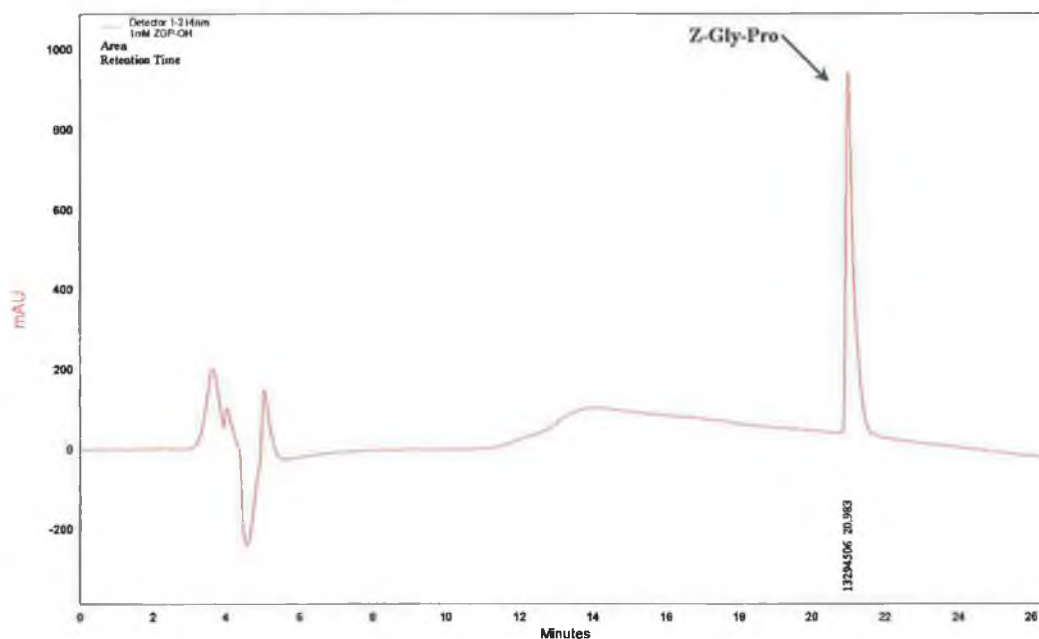


**Figure 3.5.3.1.2.17. HPLC chromatogram of the standard Z-Gly-Pro**

Plot of absorbance at 214nm versus time for the peptide standard Z-Gly-Pro. The plot illustrates a retention time of 20.983 minutes for 1mM Z-Gly-Pro standard. This correlates well with the major product formed in figures 3.5.3.1.2.1. to 3.5.3.1.2.16.

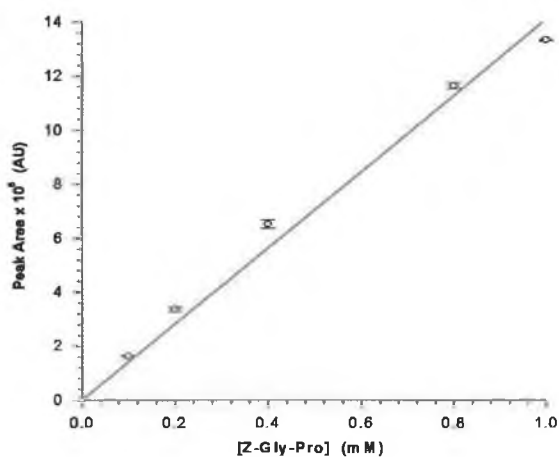


**Figure 3.5.3.1.2.18. Z-Gly-Pro standard curve**

Plot of peak area (absorbance) at 214nm versus Z-Gly-Pro concentration obtained using reverse phase HPLC as outlined in section 2.7.2.3. Errors bars represent the SEM of duplicate readings.

Peptide	Hydrolysis	[Z-Gly-Pro] (mM)
Z-Gly-Pro-Phe	Yes	0.096
Z-Gly-Pro-Tyr	Yes	0.057
Z-Gly-Pro-Ser	Yes	0.056
Z-Gly-Pro-Met	Yes	0.025
Z-Gly-Pro-His	Yes	0.029
Z-Gly-Pro-Glu	Negligible	-
Z-Gly-Pro-Leu	Yes	0.031
Z-Gly-Pro-Ala	Yes	0.037

**Table 3.7. Quantification of Z-Gly-Pro after hydrolysis by ZIP**

### **3.5.3.1.3. Identification of the Hydrolysis Products Separated by Reverse Phase HPLC using LC-MS.**

As outlined in section 2.7.3.1. direct infusion MS analysis was initially used to identify the hydrolysis products. This led to some components of the reaction been preferentially ionised over others, thus leading to inaccurate results. LC-MS analysis was then employed to first separate the products of hydrolysis and then identify them individually using ion spray mass spectrometry according to section 2.7.3.2. This also enabled the confirmation of cleavage post proline in each of the peptides analysed. Figures 3.5.3.1.3.1. to 3.5.3.1.3.7. represent the LC-MS spectra obtained for some of the peptides analysed for P<sub>1</sub>' specificity.



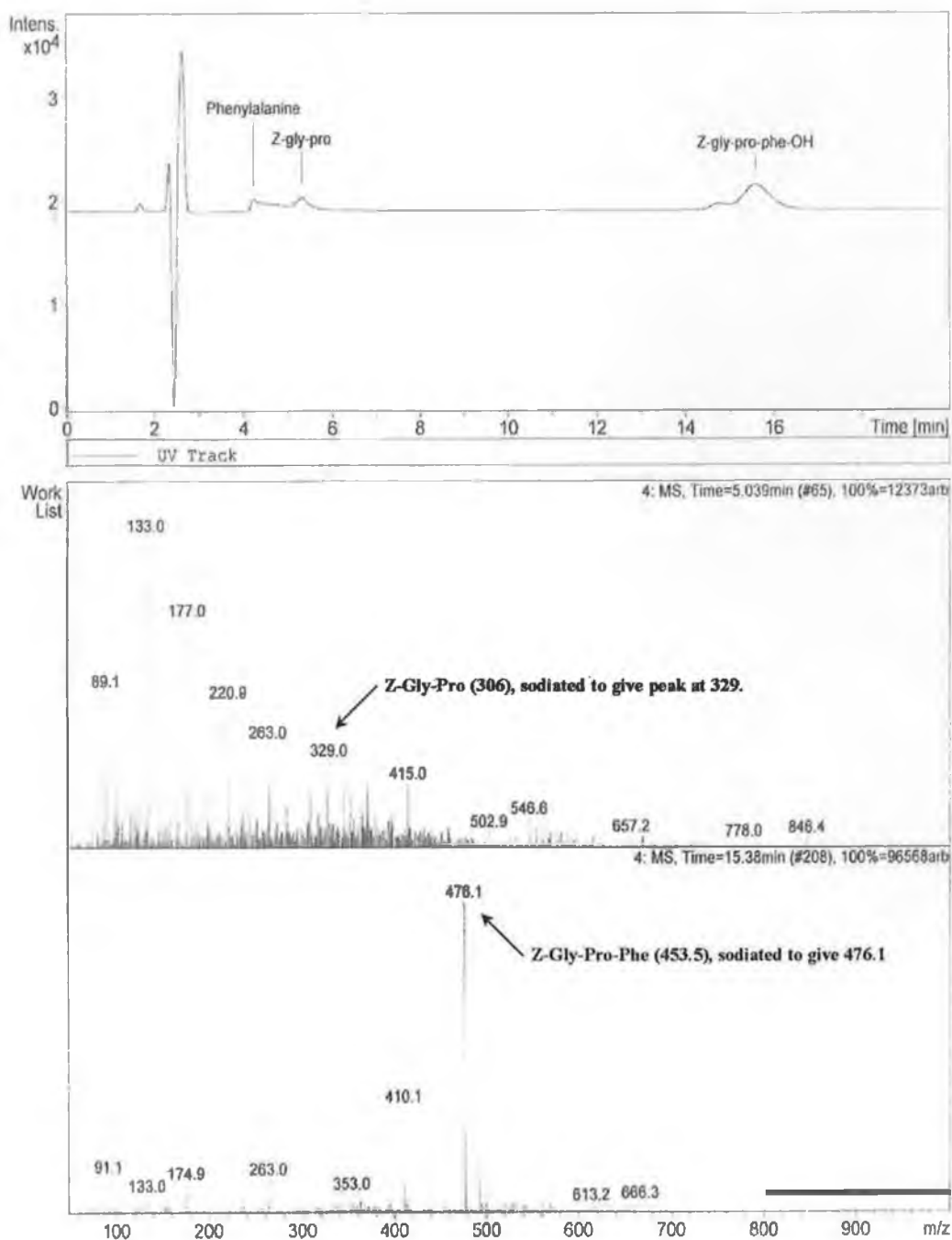


**Figure 3.5.3.1.3.1. LC-MS spectra of Z-Gly-Pro-Phe digestion**

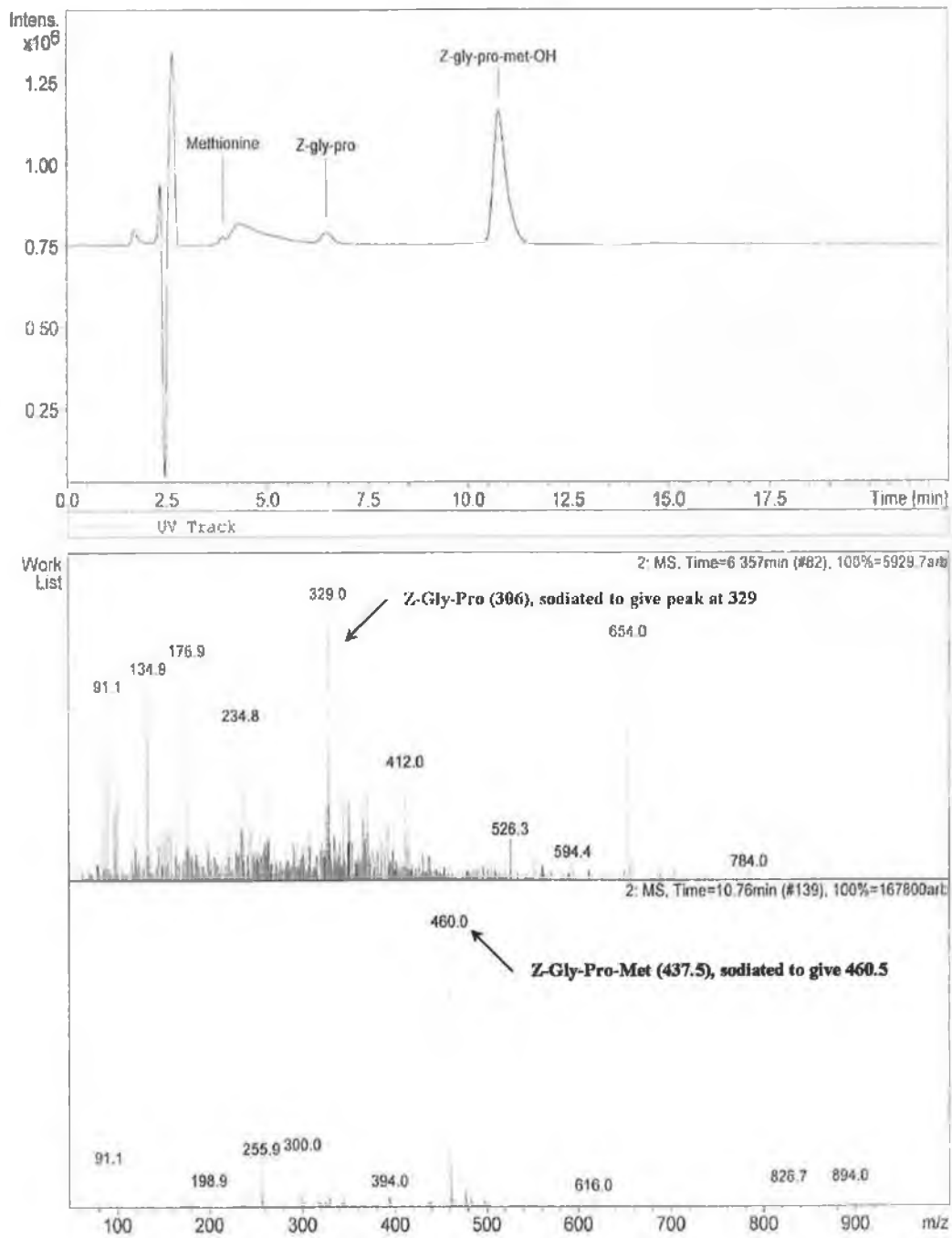


**Figure 3.5.3.1.3.2. LC-MS spectra of Z-Gly-Pro-Met digestion**

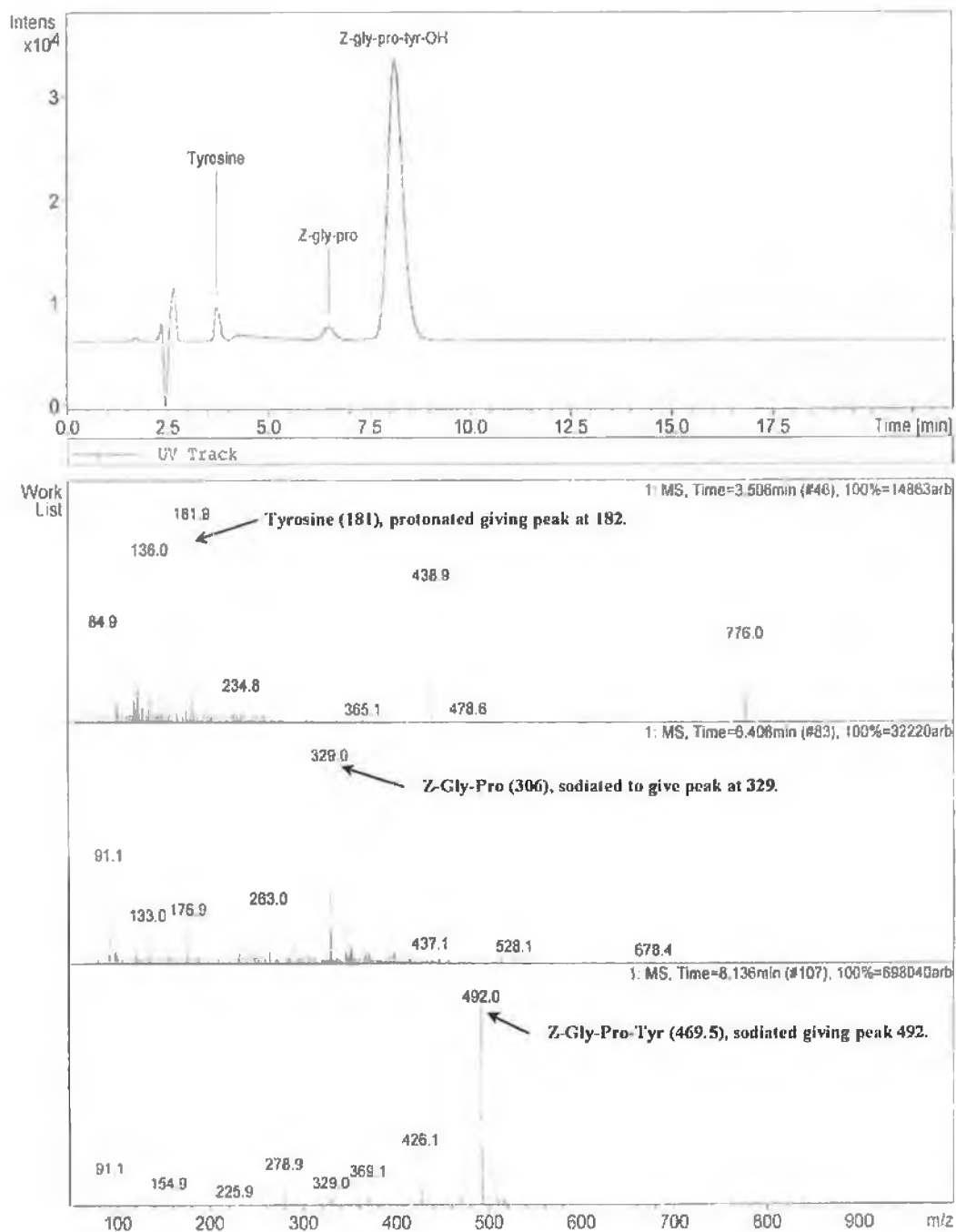


**Figure 3.5.3.1.3.3. LC-MS spectra of Z-Gly-Pro-Tyr digestion**

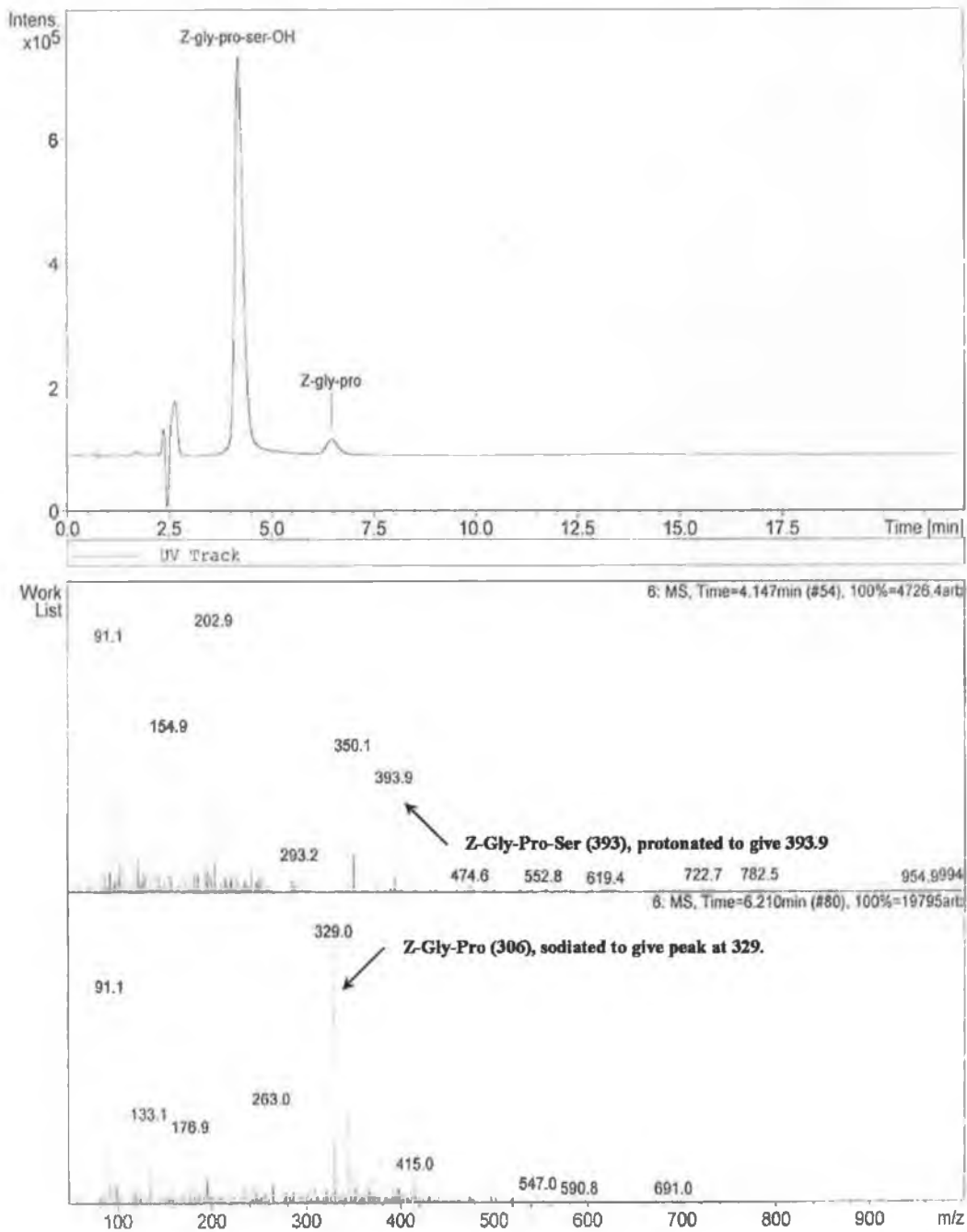


**Figure 3.5.3.1.3.4. LC-MS spectra of Z-Gly-Pro-Ser digestion**

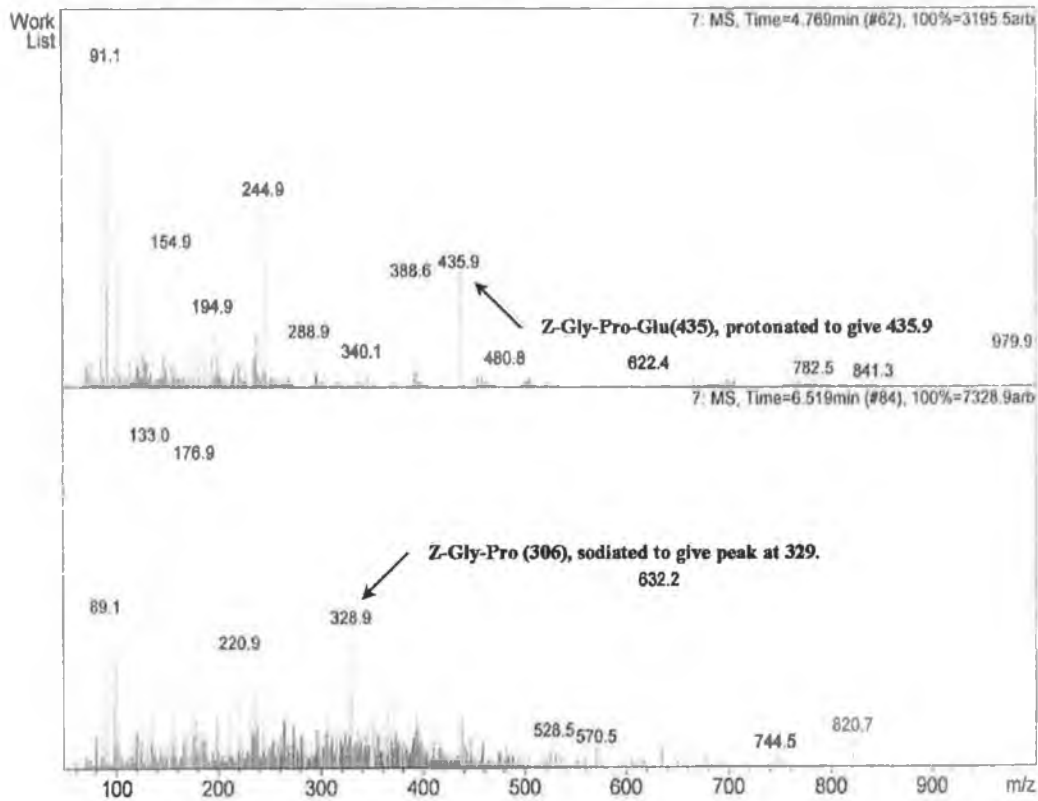
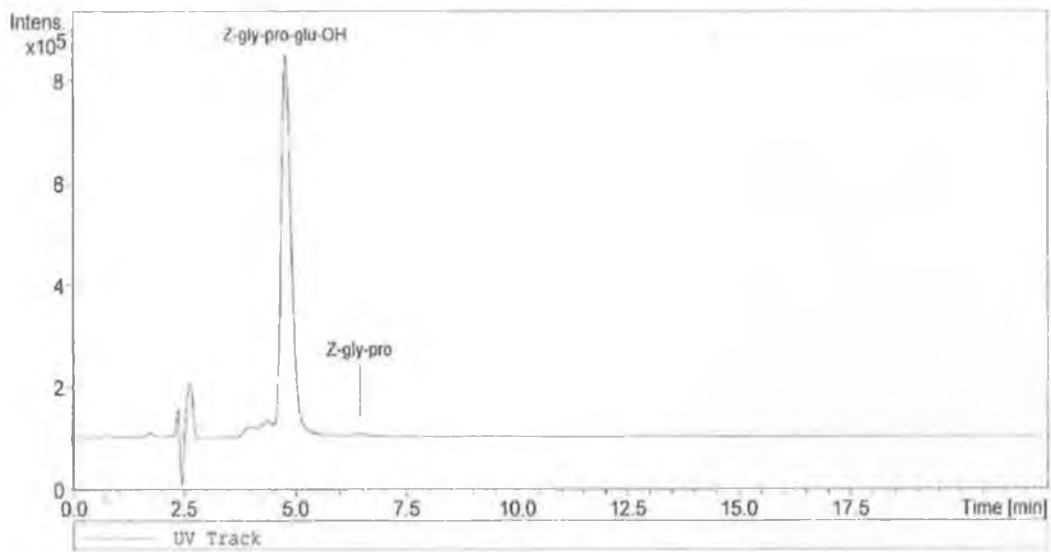


**Figure 3.5.3.1.3.5. LC-MS spectra of Z-Gly-Pro-Glu digestion**

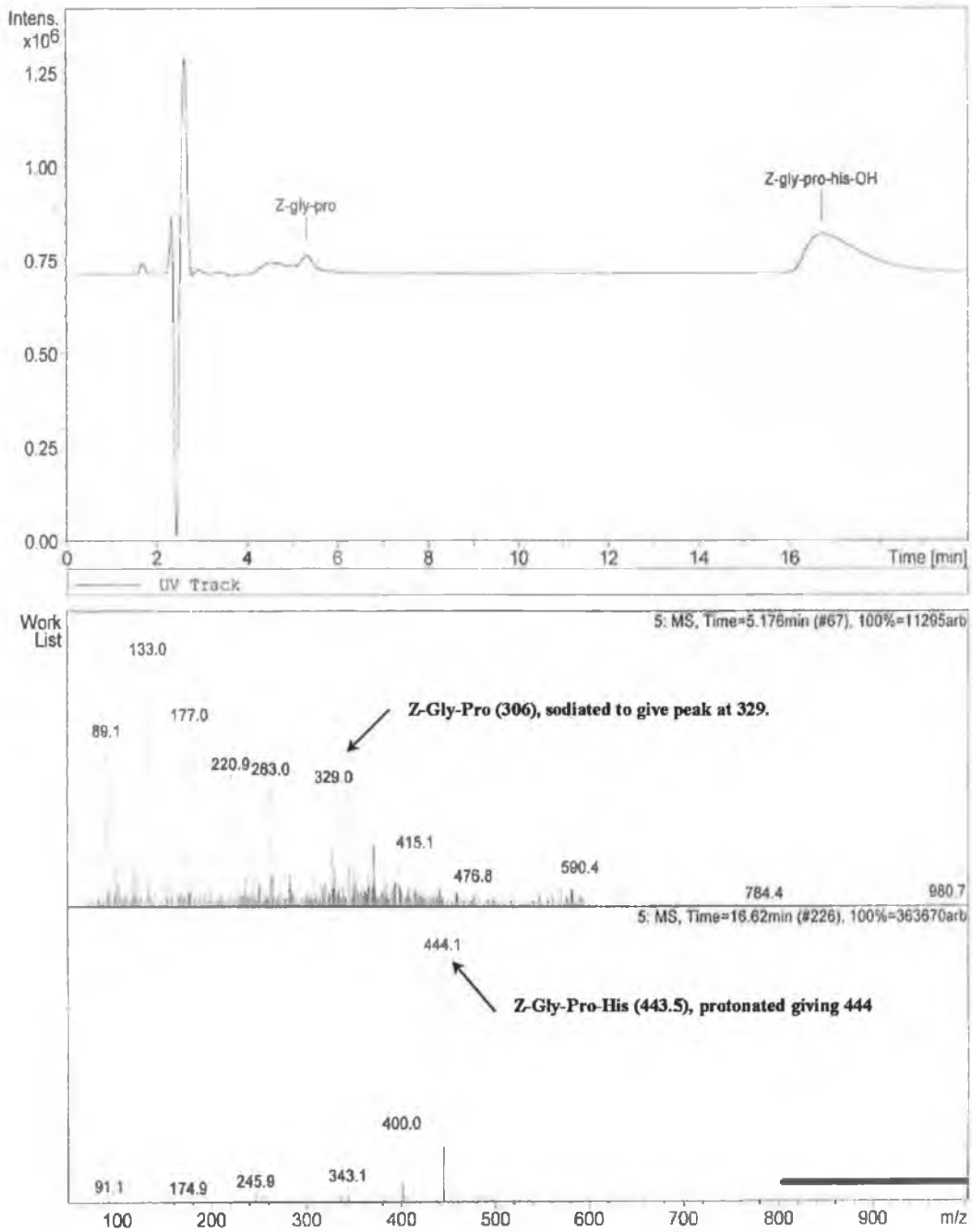


**Figure 3.5.3.1.3.6. LC-MS spectra of Z-Gly-Pro-His digestion**

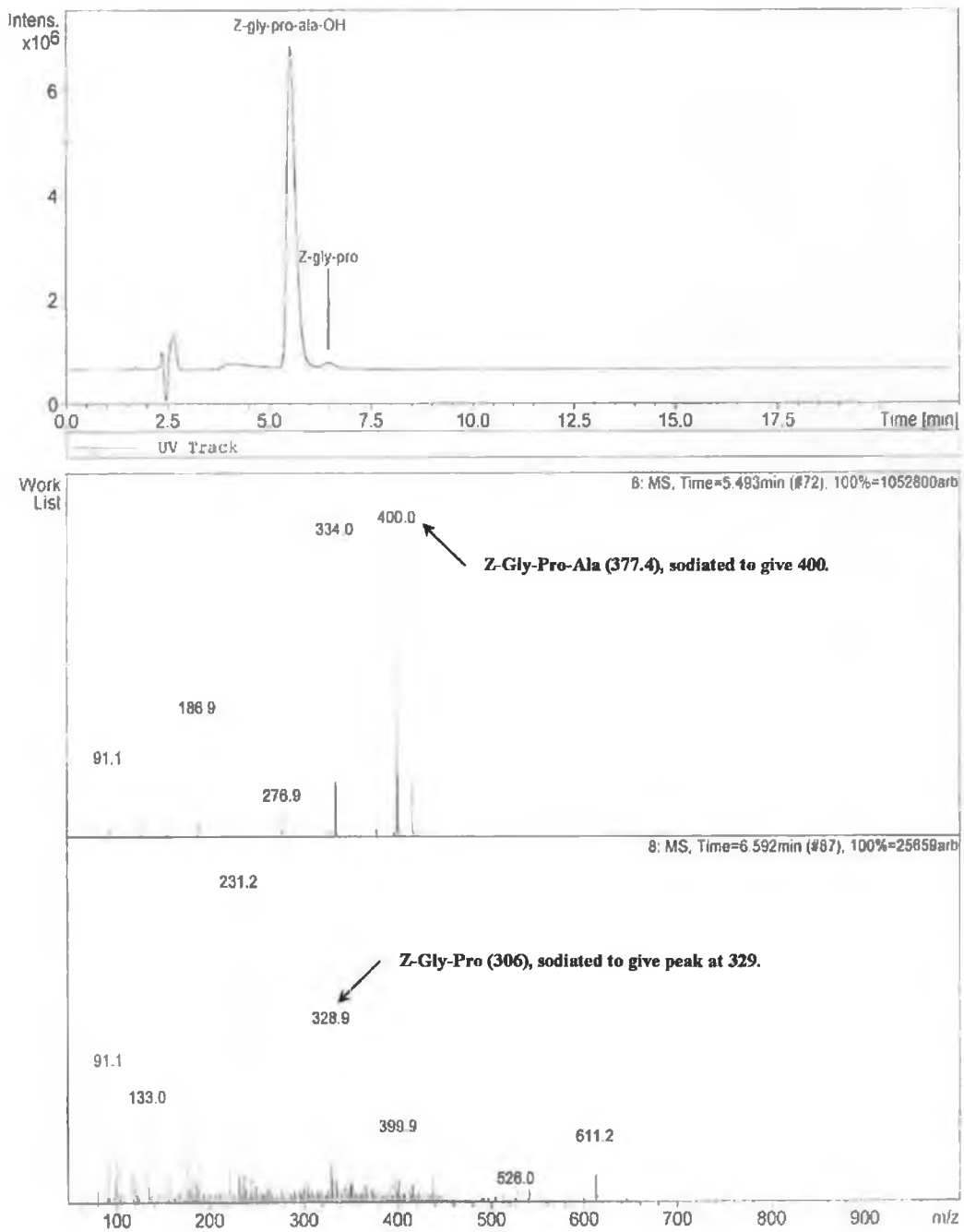


**Figure 3.5.3.1.3.7. LC-MS spectra of Z-Gly-Pro-Ala digestion**

### 3.5.3.2. Chain Length Elongation at the Carboxyl Terminal Site

The chain length of substrates was increased at the carboxyl terminal site while again keeping the Z-Gly-Pro sequence constant. With the lowest  $K_{i (app)}$  values (Table 3.6.) obtained with Methionine and Phenylalanine in the  $P_1'$  position, peptides were elongated to include  $P_2'$ ,  $P_3'$  and  $P_4'$ . The peptides sequence and preparation is as according to Table 2.3.

#### 3.5.3.2.1. Determination of $K_{i (app)}$ Values for Proline-Containing Peptides Elongated in the COOH-Terminal Direction.

Determination of  $K_{i (app)}$  values in the ZIP catalysed hydrolysis of Z-Gly-Pro-AMC using proline-containing peptides of increasing chain length was performed as in section 2.7.1.2. Kinetic parameters were determined as according to section 3.5.3.1.1. Figures 3.5.3.2.1.1. to 3.5.3.2.1.6. represent Lineweaver-Burk reciprocal plots of each of the peptides tested. Table 3.8. lists the  $K_{i (app)}$  values obtained and the type of inhibition observed.

Peptide	Assay Conc.	$K_{i (app)}$ ( $\mu$ M)	Inhibition Type
$P_3$ $P_2$ $P_1 \downarrow$ $P_1'$ $P_2'$ $P_3'$ $P_4'$	( $\mu$ M)		
Z-Gly-Pro-Phe *	200	461.53	Mixed
Z-Gly-Pro-Phe-His	200	206.88	Mixed
Z-Gly-Pro-Phe-His-Arg	200	309.40	Competitive
Z-Gly-Pro-Phe-His-Arg-Ser	200	401.72	Mixed
Z-Gly-Pro-Met *	200	554.72	Non-competitive
Z-Gly-Pro-Met-His	200	270.28	Mixed
Z-Gly-Pro-Met-His-Arg	200	333.90	Mixed
Z-Gly-Pro-Met-His-Arg-Ser	200	474.07	Mixed

**Table 3.8. Kinetic parameters for the inhibition of ZIP catalysed hydrolysis of Z-Gly-Pro-AMC by peptides extended COOH-terminally from the scissile bond.**

\* See Table 3.6.



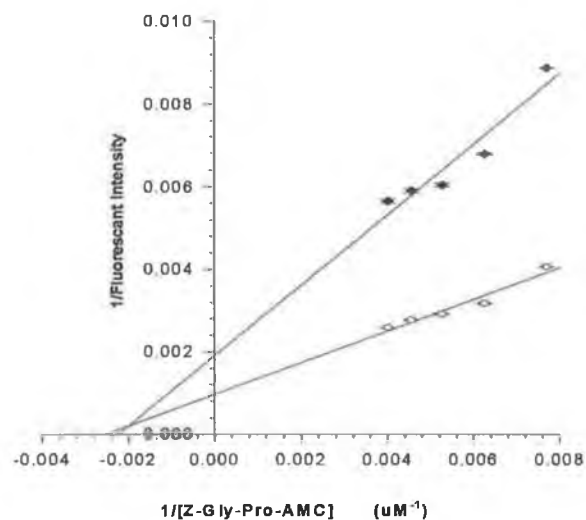


**Figure 3.5.3.2.1.1. Kinetic analysis of the effect of Z-Gly-Pro-Phe-His (♦) on ZIP catalysed hydrolysis of Z-Gly-Pro-AMC (o).** Lineweaver-Burk reciprocal plot of fluorescent intensity versus [Z-Gly-Pro-AMC]. Plot illustrates the mixed inhibition of ZIP by Z-Gly-Pro-Phe-His.

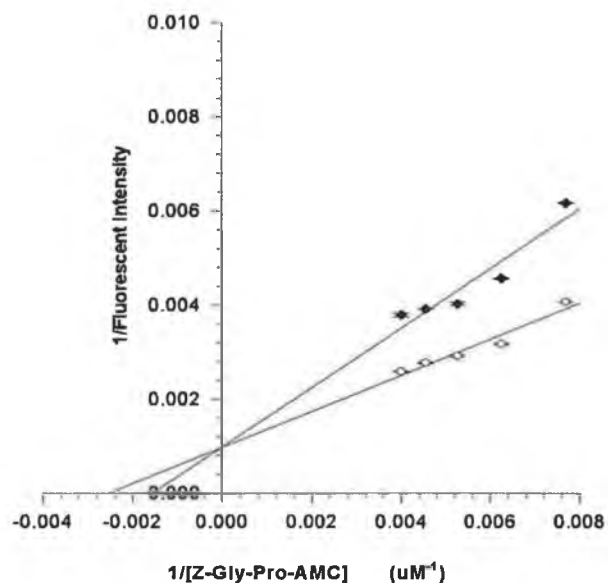


**Figure 3.5.3.2.1.2. Kinetic analysis of the effect of Z-Gly-Pro-Phe-His-Arg (♦) on ZIP catalysed hydrolysis of Z-Gly-Pro-AMC (o).** Lineweaver-Burk reciprocal plot of fluorescent intensity versus [Z-Gly-Pro-AMC]. Plot illustrates the competitive inhibition of ZIP by Z-Gly-Pro-Phe-His-Arg.

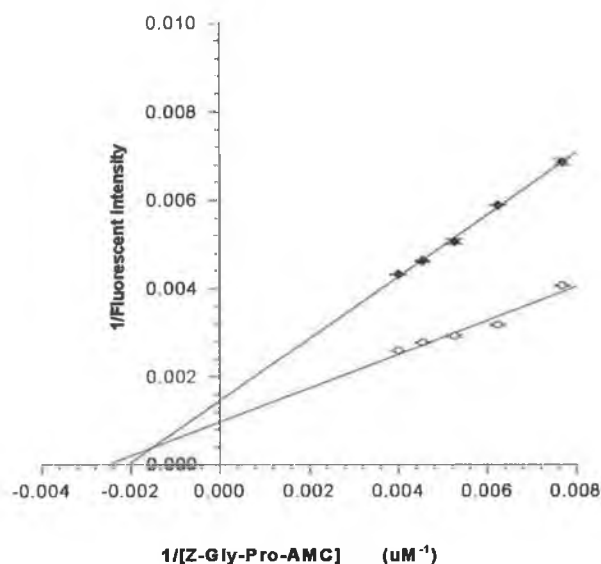


**Figure 3.5.3.2.1.3. Kinetic analysis of the effect of Z-Gly-Pro-Phe-His-Arg-Ser (◆) on ZIP catalyzed hydrolysis of Z-Gly-Pro-AMC (○). Lineweaver-Burk reciprocal plot of fluorescent intensity versus [Z-Gly-Pro-AMC]. Plot illustrates the mixed inhibition of ZIP by Z-Gly-Pro-Phe-His-Arg-Ser.**

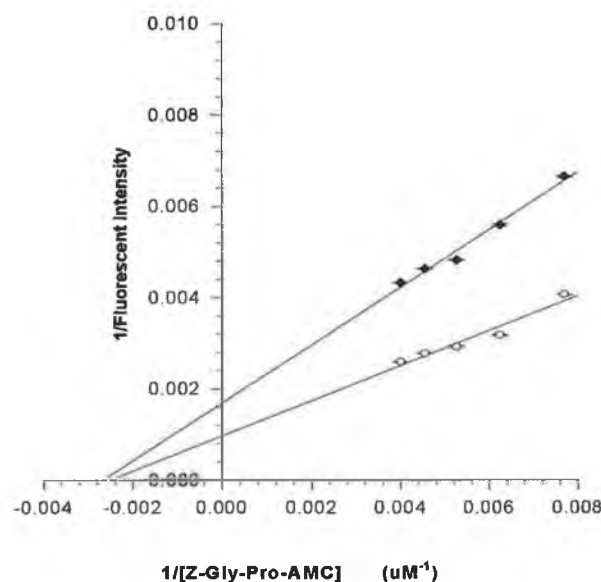


**Figure 3.5.3.2.1.4. Kinetic analysis of the effect of Z-Gly-Pro-Met-His (◆) on the ZIP catalyzed hydrolysis of Z-Gly-Pro-AMC (○). Lineweaver-Burk reciprocal plot of fluorescent intensity versus [Z-Gly-Pro-AMC]. Plot shows the mixed inhibition of ZIP by Z-Gly-Pro-Met-His.**

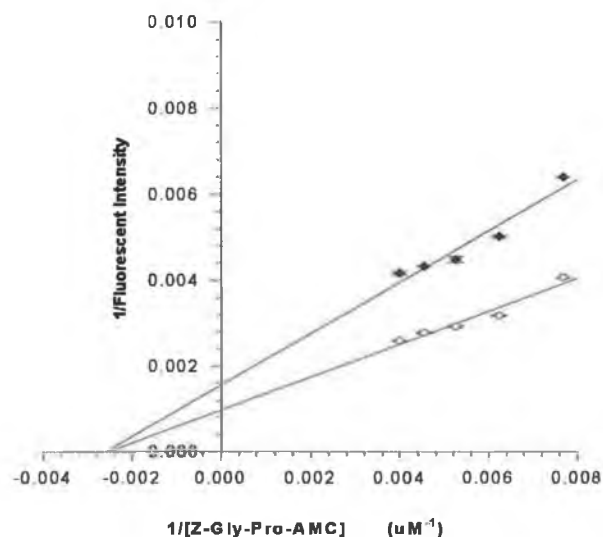


**Figure 3.5.3.2.1.5. Kinetic analysis of the effect of Z-Gly-Pro-Met-His-Arg (♦) on ZIP catalyzed hydrolysis of Z-Gly-Pro-AMC (o).** Lineweaver-Burk reciprocal plot of fluorescent intensity versus [Z-Gly-Pro-AMC]. Plot illustrates the mixed inhibition of ZIP by Z-Gly-Pro-Met-His-Arg.

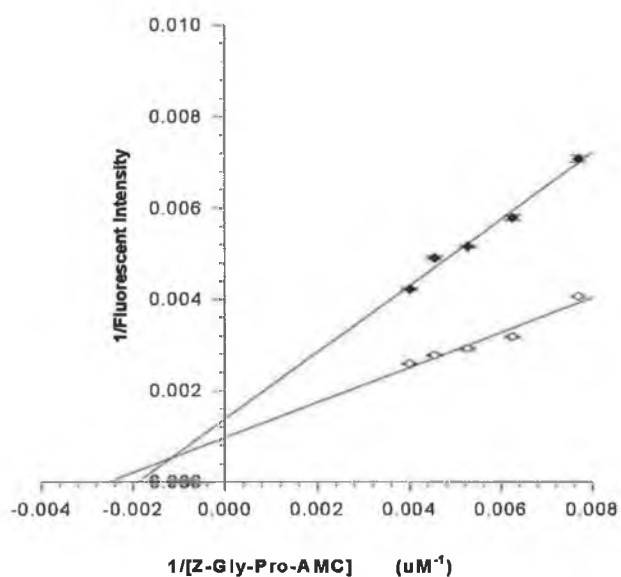


**Figure 3.5.3.2.1.6. Kinetic analysis of the effect of Z-Gly-Pro-Met-His-Arg-Ser (♦) on ZIP catalyzed hydrolysis of Z-Gly-Pro-AMC (o).** Lineweaver-Burk reciprocal plot of fluorescent intensity versus [Z-Gly-Pro-AMC]. Plot shows the mixed inhibition of ZIP by Z-Gly-Pro-Met-His-Arg-Ser.

### 3.5.3.2.2. Reverse Phase HPLC of COOH-Terminally Elongated Proline-Containing Peptides.

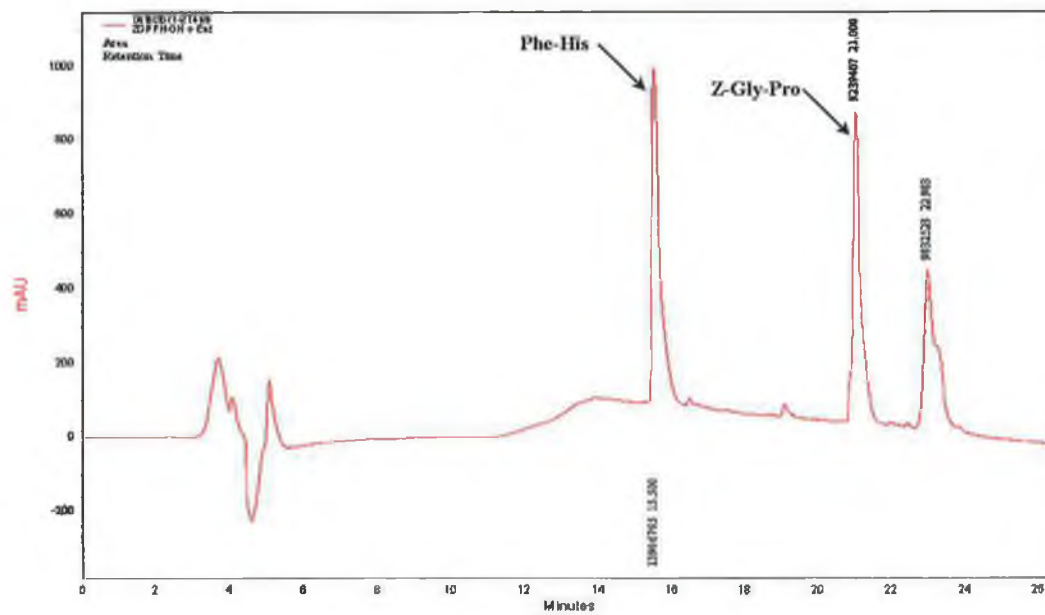
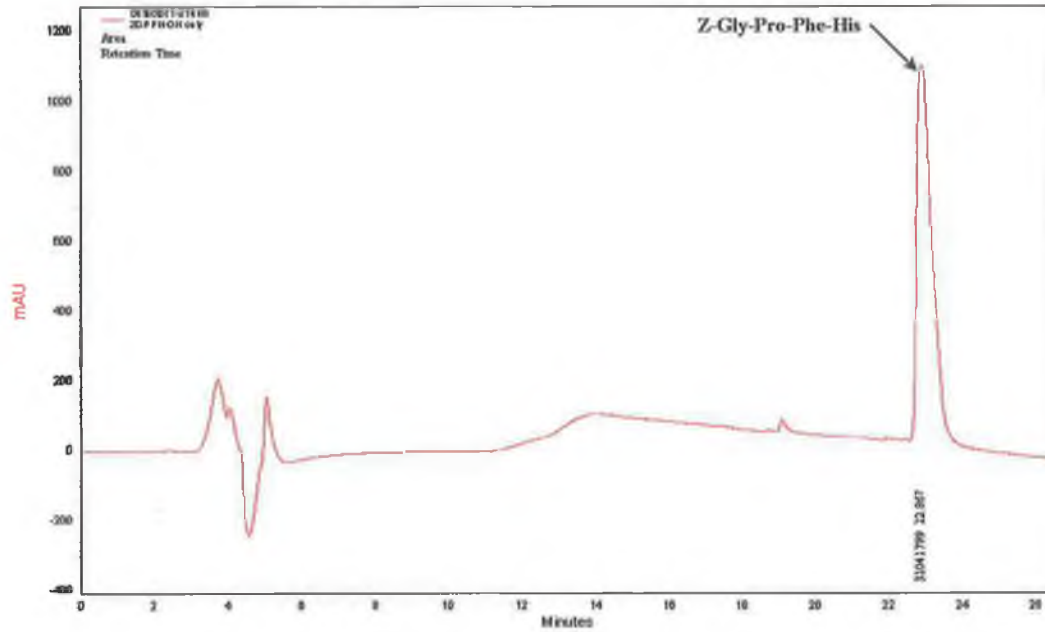
Reverse phase HPLC was performed to determine effect of chain length on ZIP hydrolysis of proline-containing peptides. Reaction of peptides with ZIP and reverse phase HPLC of the resulting digests was performed as outlined in sections 2.7.2.2. and 2.7.2.3. respectively. Figures 3.5.3.2.2.1. to 3.5.3.2.2.6. represent chromatograms of the peptides studied. Table 3.9. illustrates the peptides tested, detection of cleavage and a quantified Z-Gly-Pro value. Only peptides with phenylalanine in the P<sub>1</sub>' position were quantified in this study. This was basically due to the enhanced hydrolysis of the peptides with a phenylalanine in the P<sub>1</sub>' position compared with methionine for quantification purposes and ease of separation of these peptides digest products post hydrolysis using the method outlined in section 2.7.2.3. Digest products of peptides with a P<sub>1</sub>' methionine residue were separated and analysed using LC-MS only.

Peptide	Hydrolysis	[Z-Gly-Pro] (mM)
Z-Gly-Pro-Phe	Yes	0.096
Z-Gly-Pro-Phe-His	Yes	0.655
Z-Gly-Pro-Phe-His-Arg	Yes	0.579
Z-Gly-Pro-Phe-His-Arg-Ser	Yes	0.548

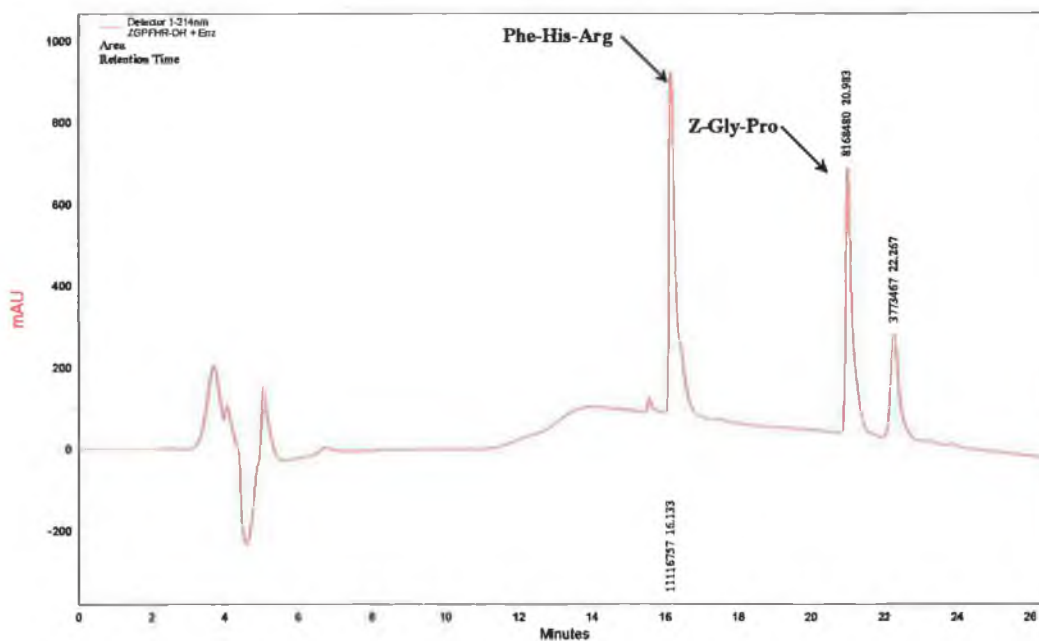
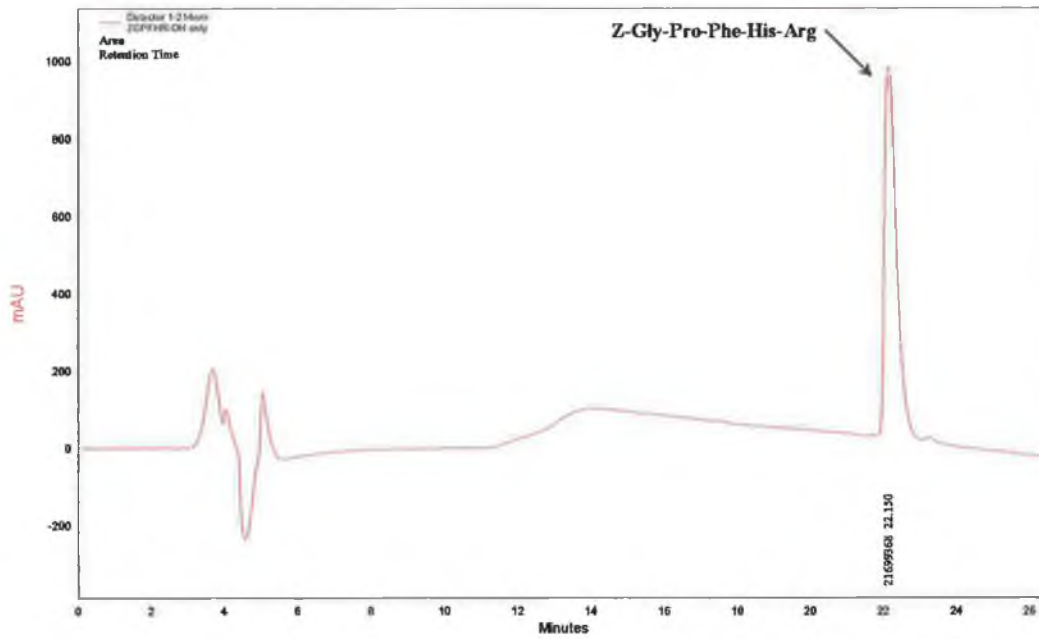
**Table 3.9. Reverse phase HPLC of proline-containing peptides elongated at the carboxyl terminal site.**

### 3.5.3.2.3. Identification of Hydrolysis Products Using Mass Spectrometry

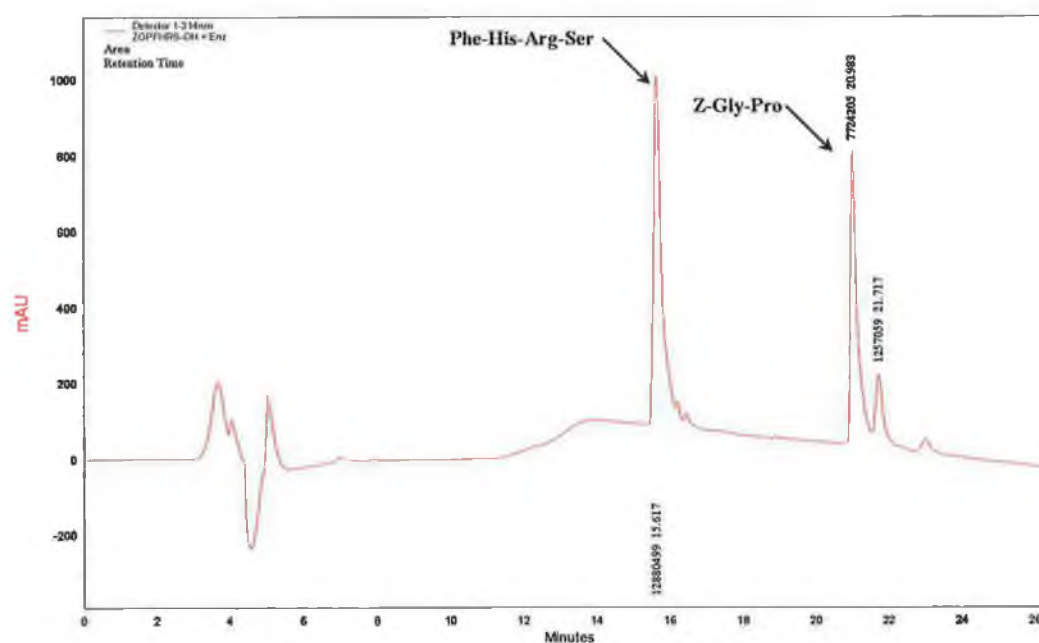
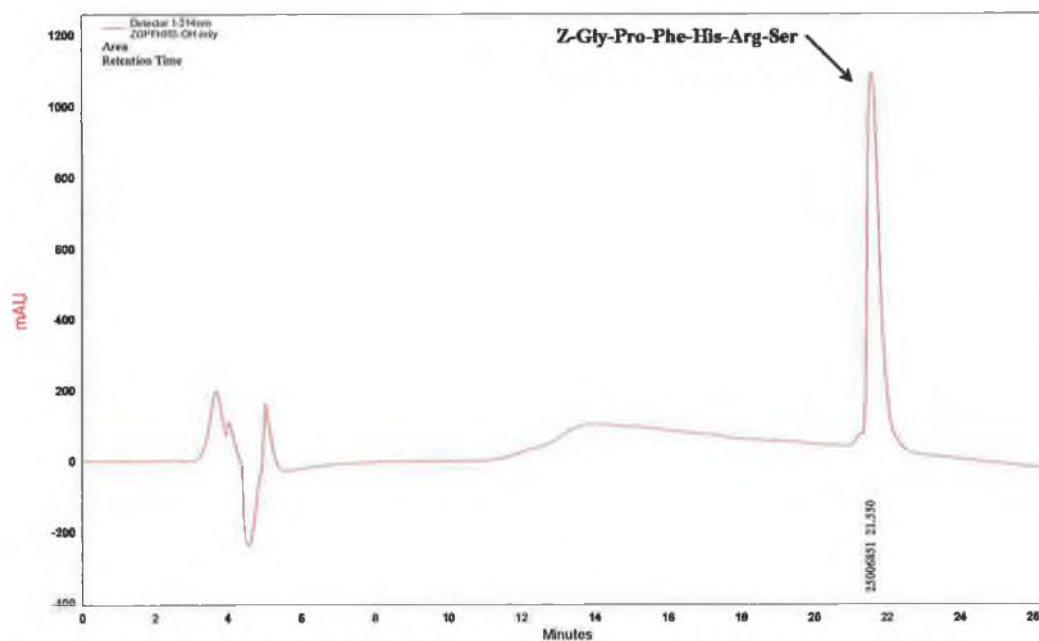
LC-MS was again employed to identify the products of hydrolysis of peptides elongated COOH-terminally from the scissile bond. Reaction of peptides with ZIP and LC-MS analysis of the resulting digests were performed as outlined in sections 2.7.2.2. and 2.7.3.2. respectively. Figures 3.5.3.2.3.1. to 3.5.3.2.3.6. represent the LC-MS spectra of the peptides analysed.



**Figures 3.5.3.2.2.1. and 3.5.3.2.2.2. HPLC chromatogram of Z-Gly-Pro-Phe-His hydrolysis by ZIP. Plots of absorbance at 214nm versus time for peptide only (Fig. 3.5.3.2.2.1.) and for peptide and ZIP incubate (Fig. 3.5.3.2.2.2.). Figure 3.5.3.2.2.2. illustrates the hydrolysis of Z-Gly-Pro-Phe-His by ZIP.**



**Figures 3.5.3.2.2.3. and 3.5.3.2.2.4. HPLC chromatogram of Z-Gly-Pro-Phe-His-Arg hydrolysis by ZIP.** Plots of absorbance at 214nm versus time for peptide only (Fig. 3.5.3.2.2.3.) and for peptide and ZIP incubate (Fig. 3.5.3.2.2.4.). Figure 3.5.3.2.2.4. illustrates the cleavage of Z-Gly-Pro-Phe-His-Arg by ZIP.



**Figures 3.5.3.2.2.5. and 3.5.3.2.2.6. HPLC chromatogram for Z-Gly-Pro-Phe-His-Arg-Ser hydrolysis by ZIP.** Plots of absorbance at 214nm versus time for peptide only (Fig. 3.5.3.2.2.5.) and for peptide and ZIP incubate (Fig. 3.5.3.2.2.6.). Figure 3.5.3.2.2.6. illustrates the hydrolysis of Z-Gly-Pro-Phe-His-Arg-Ser by ZIP.

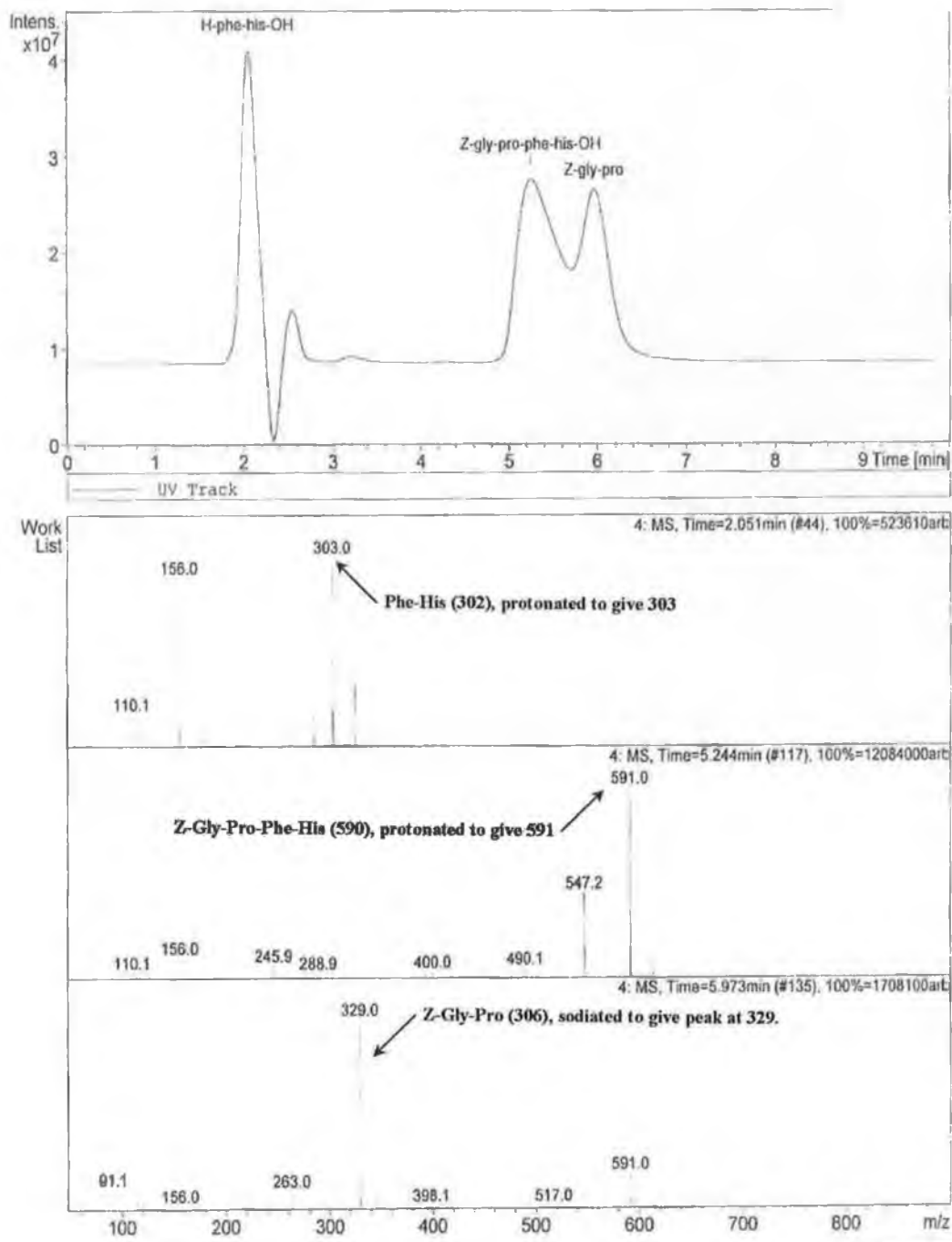


**Figure 3.5.3.2.3.1. LC-MS spectra for Z-Gly-Pro-Phe-His digestion**



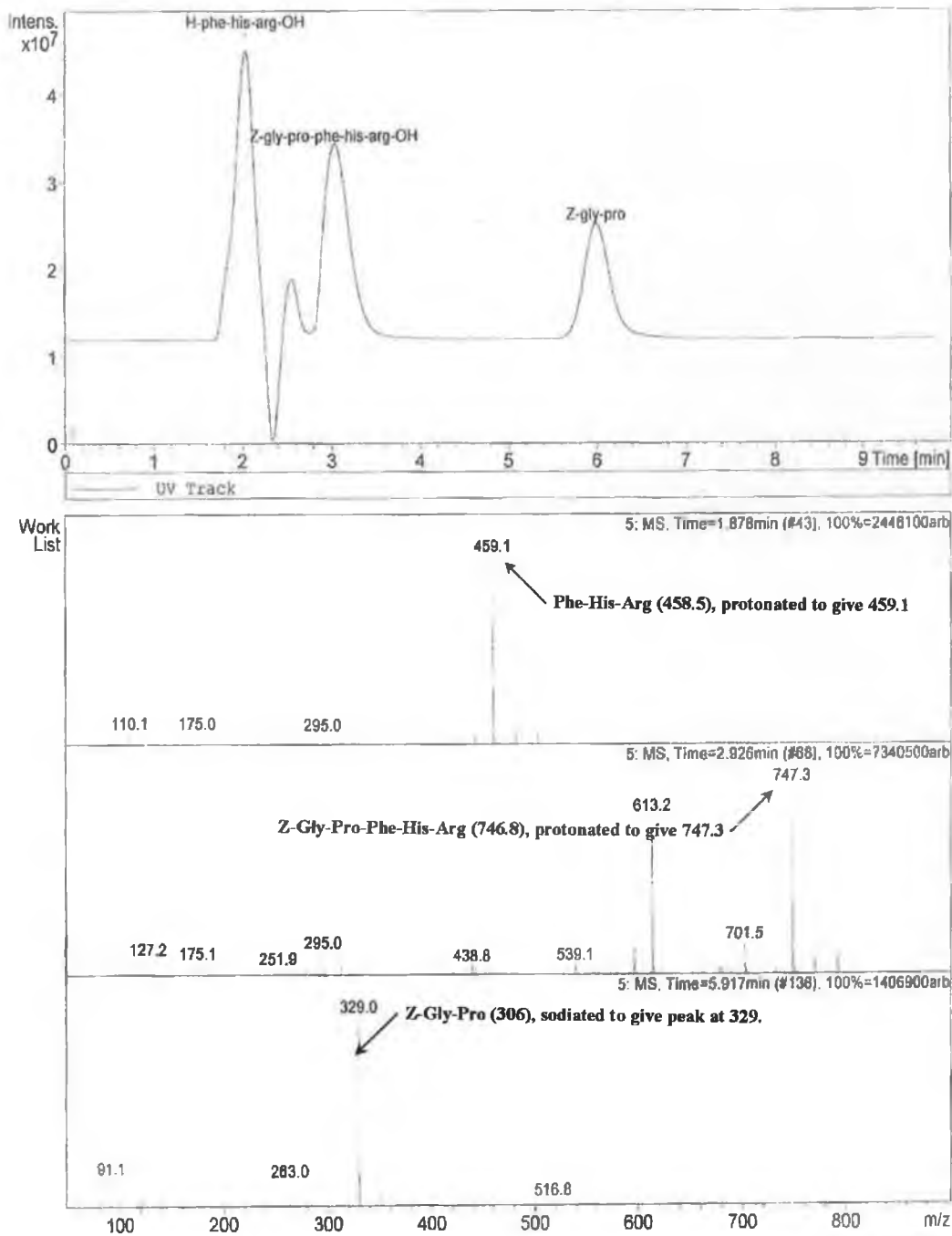


**Figure 3.5.3.2.3.2. LC-MS spectra for Z-Gly-Pro-Phe-His-Arg digestion**

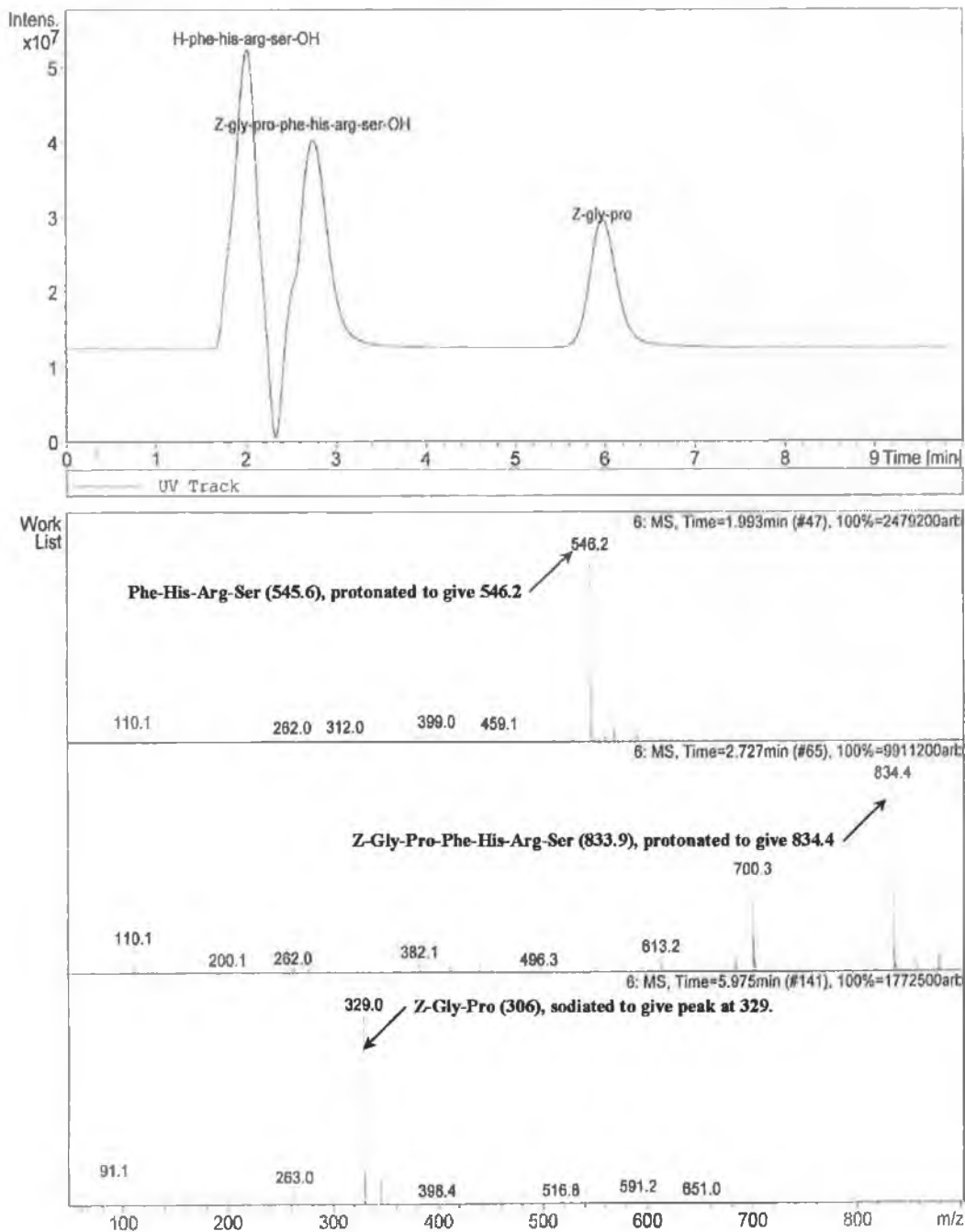


**Figure 3.5.3.2.3.3. LC-MS spectra for Z-Gly-Pro-Phe-His-Arg-Ser digestion**

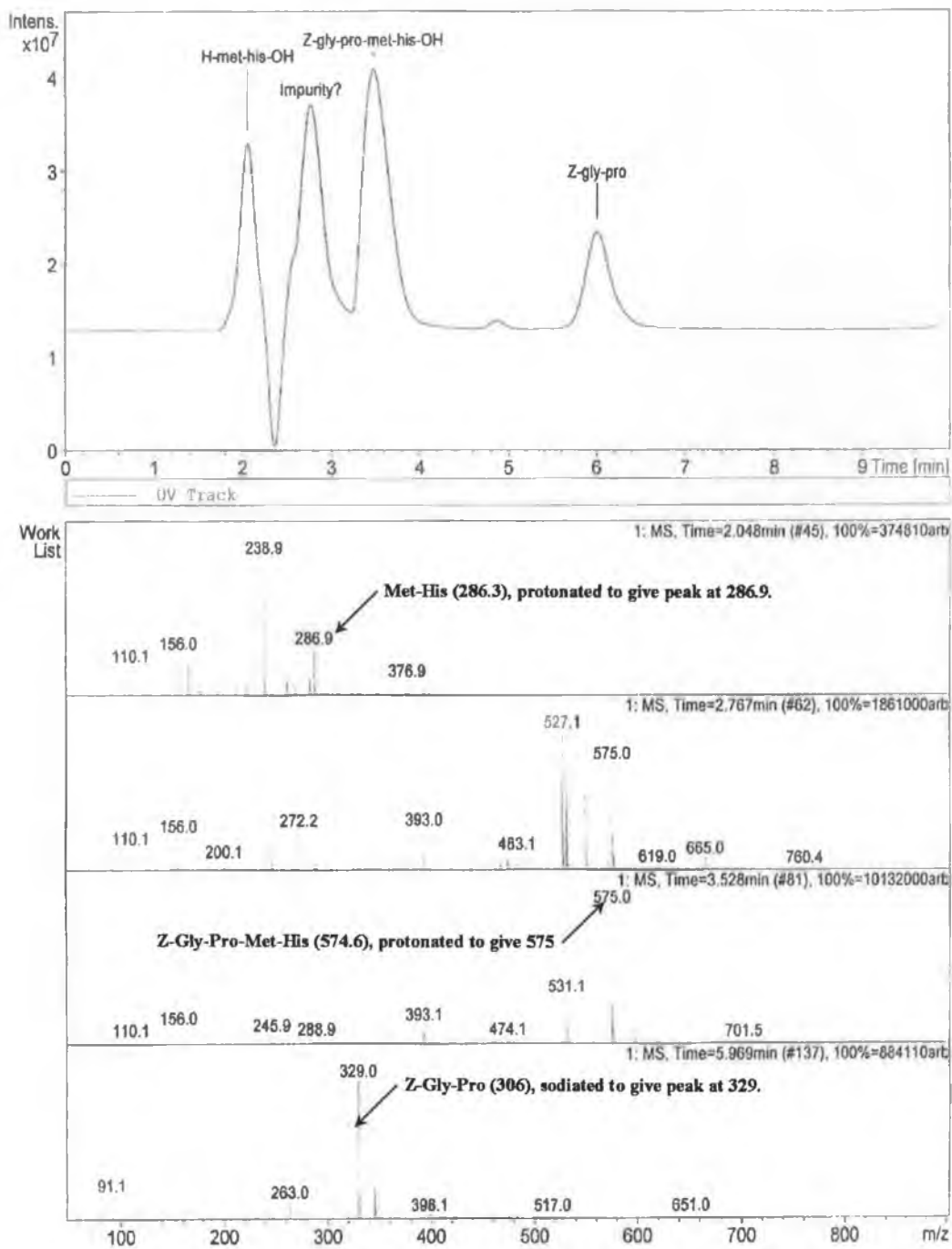


**Figure 3.5.3.2.3.4. LC-MS spectra for Z-Gly-Pro-Met-His digestion**

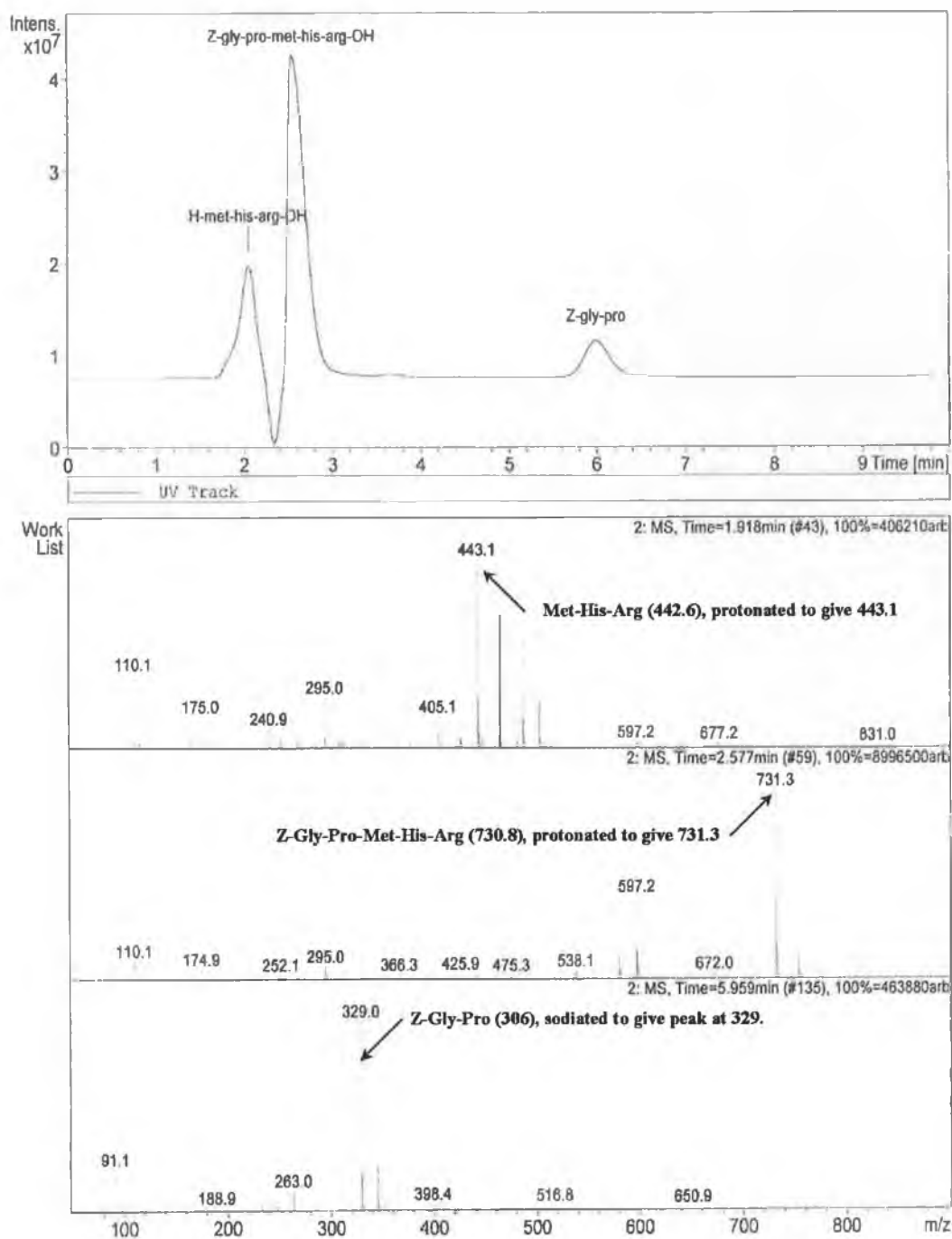


**Figure 3.5.3.2.3.5. LC-MS spectra for Z-Gly-Pro-Met-His-Arg digestion**

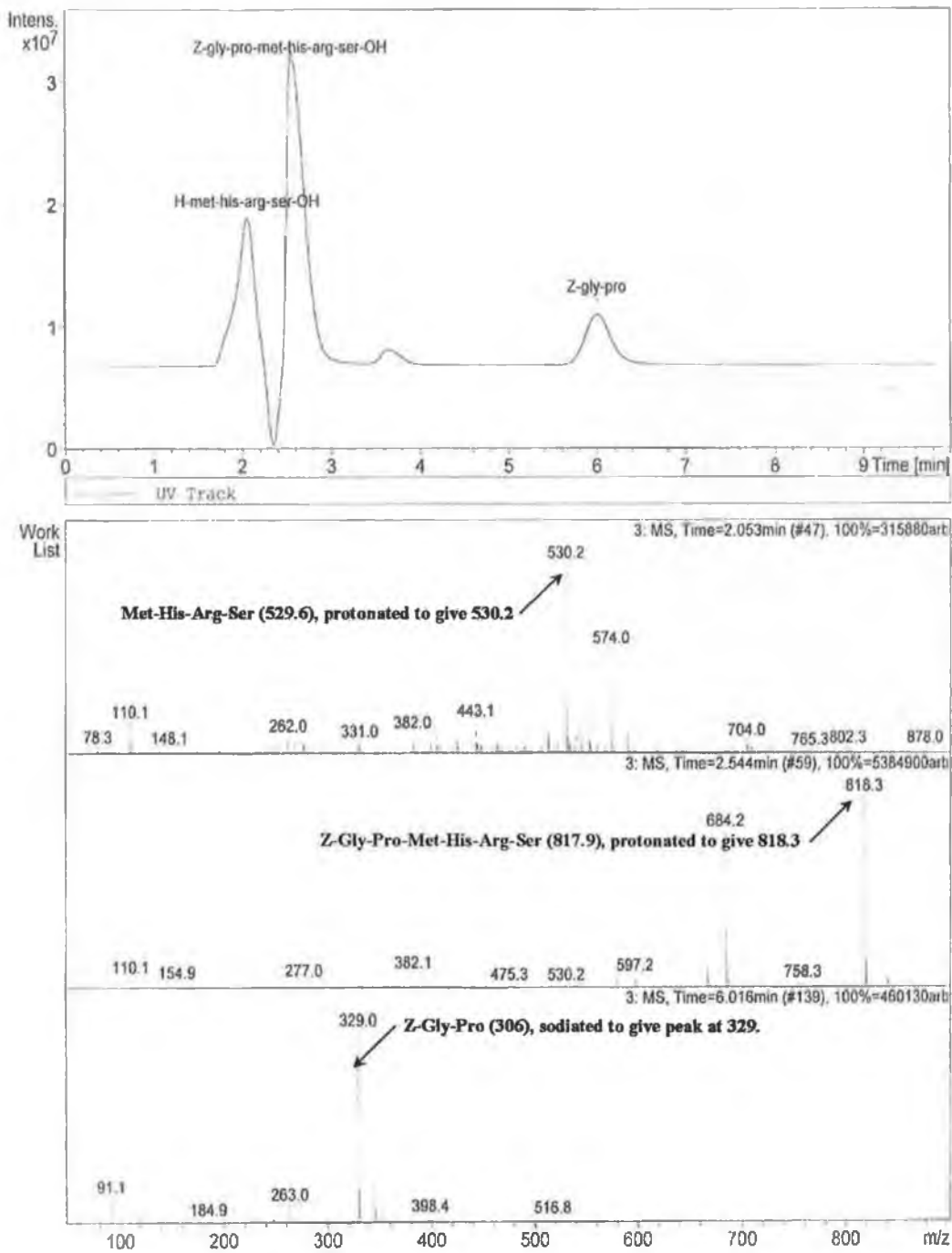


**Figure 3.5.3.2.3.6. LC-MS spectra for Z-Gly-Pro-Met-His-Arg-Ser digestion**

### 3.5.4. Specificity Studies Involving the P<sub>1</sub> Proline Position

The importance of a proline residue in the P<sub>1</sub> position was investigated using Z-Gly-Leu-Phe-His as substrate. Kinetic analysis and reverse phase HPLC was performed to determine the effect of replacing proline in the primary specificity position (P<sub>1</sub>) with a leucine residue.

#### 3.5.4.1. Kinetic Effect of Introducing Leucine in the P<sub>1</sub> Position

The kinetic effect of the peptide Z-Gly-Leu-Phe-His in the ZIP catalysed hydrolysis of Z-Gly-Pro-AMC was determined as outlined in section 2.7.1.2. Kinetic parameters were determined as explained in section 3.5.3.1.1. Figure 3.5.4.1 represents a Lineweaver-Burk reciprocal plot for the peptide using purified ZIP activity. Table 4.0 lists the K<sub>i (app)</sub> value and type of inhibition obtained compared to the values determined for the peptide Z-Gly-Pro-Phe-His.

Peptide P <sub>3</sub> P <sub>2</sub> P <sub>1</sub> ↓ P <sub>1</sub> ' P <sub>2</sub> '	Assay Conc. (μM)	K <sub>i (app)</sub> (μM)	Inhibition Type
Z-Gly-Leu-Phe-His	200	1473.74	Mixed
Z-Gly-Pro-Phe-His *	200	206.88	Mixed

**Table 3.10. Importance of a Proline Residue in the P<sub>1</sub> Position**

\* See Table 3.8.

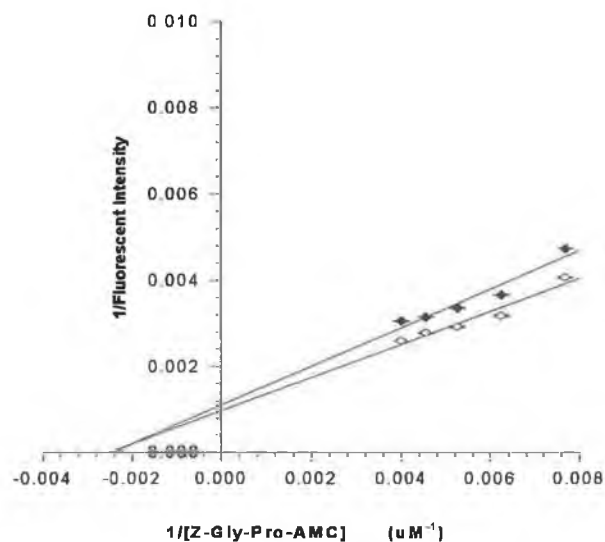
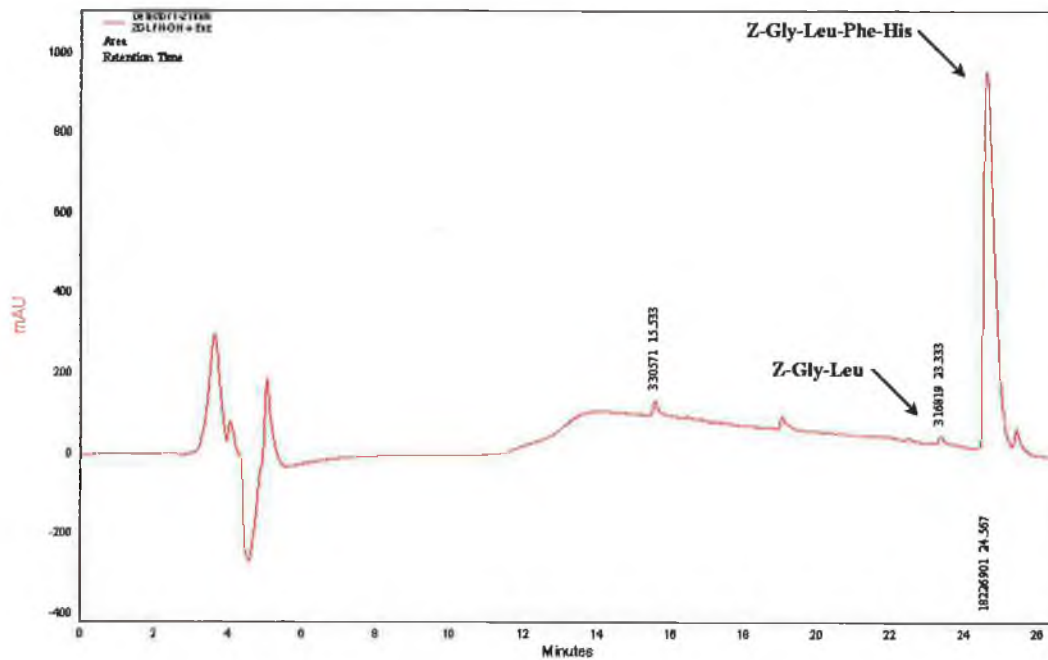
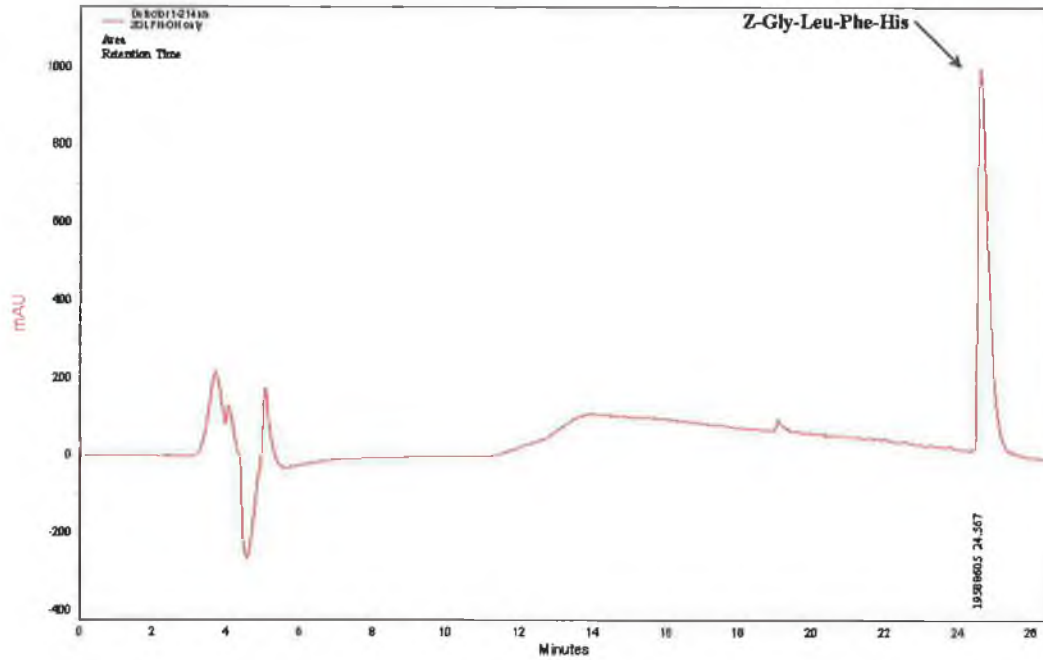


**Figure 3.5.4.1. Kinetic analysis of the effect of Z-Gly-Leu-Phe-His (◆) on the ZIP catalysed hydrolysis of Z-Gly-Pro-AMC (○). Lineweaver-Burk reciprocal plot of fluorescent intensity versus [Z-Gly-Pro-AMC]. Plot illustrates the mixed inhibition of ZIP by Z-Gly-Leu-Phe-His.**

### **3.5.4.2. Analysis of Hydrolysis by ZIP of Z-Gly-Leu-Phe-His using Reverse Phase HPLC**

Reverse phase HPLC was performed to determine if replacing the P<sub>1</sub> proline residue with leucine would have an effect on the peptides hydrolysis by ZIP. Reaction of the peptide with ZIP and reverse phase HPLC was performed as outlined in sections 2.7.2.2. and 2.7.2.3. respectively. Figures 3.5.4.2.1. and 3.5.4.2.2. represent chromatograms of the resulting digests post hydrolysis. Figure 3.5.4.2.3. shows the retention time of the standard Z-Gly-Leu.



**Figures 3.5.4.2.1. and 3.5.4.2.2. HPLC chromatogram post hydrolysis of Z-Gly-Leu-Phe-His by ZIP.** Plots of absorbance at 214nm versus time for peptide only (Fig. 3.5.4.2.1.) and for peptide and ZIP incubate (Fig. 3.5.4.2.2.). Figure 3.5.4.2.2. illustrates the possible negligible amount of Z-Gly-Leu formed.



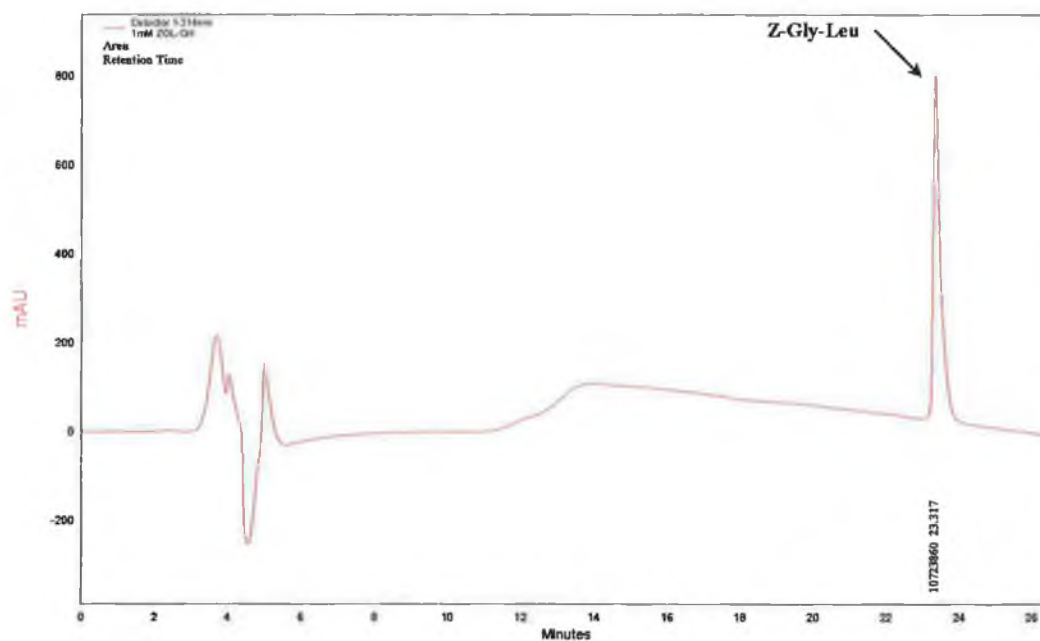


**Figure 3.5.4.2.3. HPLC chromatogram of the standard Z-Gly-Leu.**

Plot of absorbance at 214nm versus time for the peptide standard Z-Gly-Leu. The chromatogram shows a retention time of 23.317 minutes for the standard, which correlates well with the appearance (Fig. 3.5.4.2.2.) of a slight digest product at 23.333 after the reaction of Z-Gly-Leu-Phe-His with ZIP.

### 3.5.4.3. LC-MS Analysis of Peptide Digest

LC-MS was employed to determine if cleavage of the peptide Z-Gly-Leu-Phe-His had occurred as shown by reverse phase HPLC and to identify the digest products as before. Figure 3.5.4.3. illustrates the LC-MS spectra obtained.

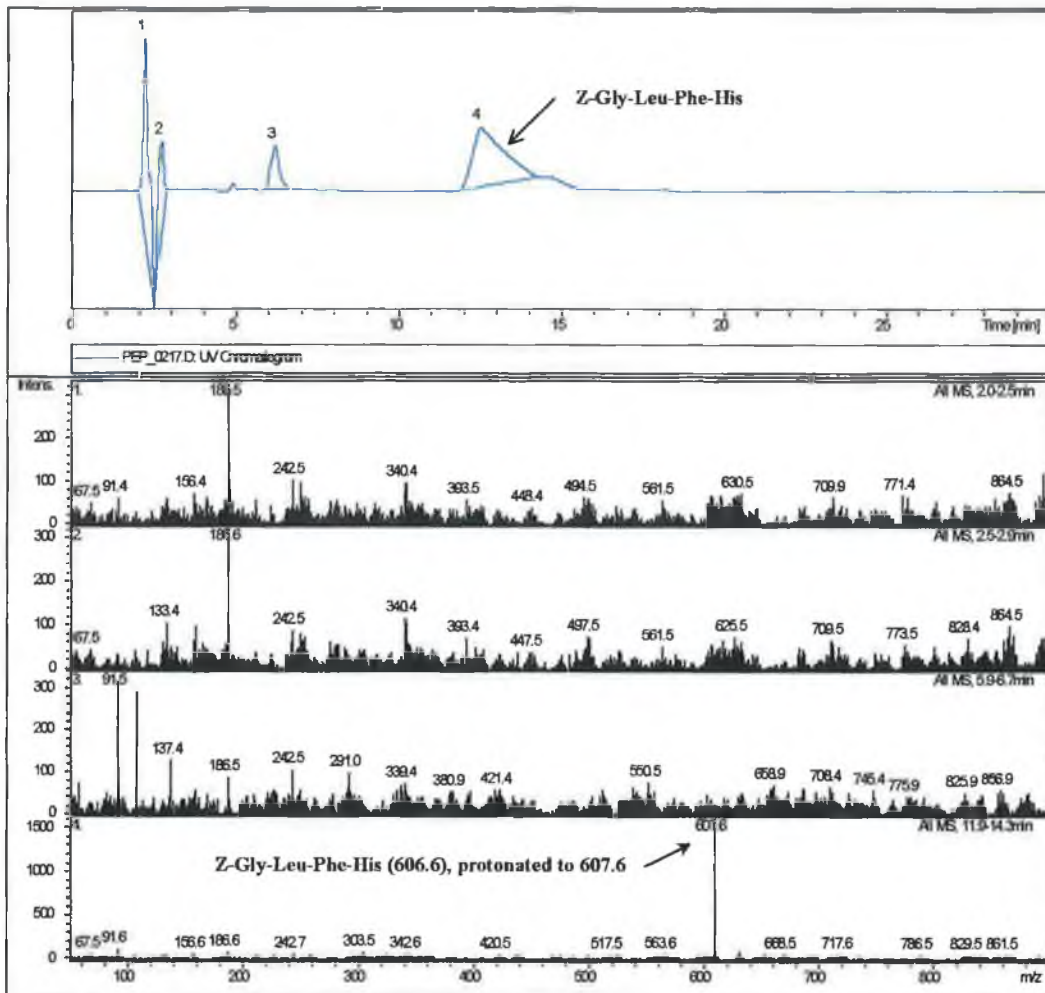


Figure 3.5.4.3. LC-MS spectra of Z-Gly-Leu-Phe-His digestion

Substrate/Peptide	Hydrolysis +	$K_{i(\text{app})}$ ( $\mu\text{M}$ )	$K_m$ ( $\mu\text{M}$ )
$P_3$ $P_2$ $P_1\downarrow$ $P_1'$ $P_2'$ $P_3'$ $P_4'$			
Pro-AMC	-	ND	
Gly-Pro-AMC	-	ND	
Z-Gly-Pro-AMC	+		270
pGlu-His-Pro-AMC	-	ND	
Z-Pro-Phe	-	ND	
Gly-Gly-Pro-Ala	-	ND	
Z-Gly-Pro-Ala	+	862.65	
Z-Gly-Pro-Met	+	554.72	
Z-Gly-Pro-Tyr	+	632.76	
Z-Gly-Pro-Ser	+	672.80	
Z-Gly-Pro-Leu	+	687.97	
Z-Gly-Pro-Glu	+ (Negligible)	748.90	
Z-Gly-Pro-His	+	769.07	
Z-Gly-Pro-Phe	+	461.53	
Z-Gly-Pro-Phe-His	+	206.88	
Z-Gly-Pro-Phe-His-Arg	+	309.40	
Z-Gly-Pro-Phe-His-Arg-Ser	+	401.72	
Z-Gly-Pro-Met-His	+	270.28	
Z-Gly-Pro-Met-His-Arg	+	333.90	
Z-Gly-Pro-Met-His-Arg-Ser	+	474.07	
Z-Gly-Leu-Phe-His	+ (Negligible)	1473.74	

**Table 3.11. Overall Substrate Specificity Studies on ZIP from Bovine Serum**

### **3.6. Partial Purification of Prolyl Oligopeptidase From Bovine Serum**

#### **3.6.1. Phenyl Sepharose Hydrophobic Interaction Chromatography I**

Figure 3.6.1. shows the elution profile of PO activity from a phenyl sepharose column, prepared and run according to section 2.8.1. This purification column is the exact same as that used for the isolation of ZIP activity (see section 3.3.2.). The first activity peak, which is present in the run through and inhibited by JTP-4819, is prolyl oligopeptidase activity (see Figure 3.3.2.2). Fractions 5-9 were pooled yielding 25ml post phenyl sepharose I PO sample. 1.5ml was retained for quantitative PO (section 2.4.2.) and quantitative protein (section 2.2.1.) determinations.

#### **3.6.2. Phenyl Sepharose Hydrophobic Interaction Chromatography II**

After concentration and salting of the post phenyl sepharose I PO pool, the sample was further purified by application to a second phenyl sepharose column as outlined in section 2.8.2. Figure 3.6.2. illustrates the elution profile of PO activity and protein, measured according to sections 2.4.4. and 2.2.2. Fractions 35-38 were combined to give 20ml post phenyl sepharose chromatography II PO pool. 1.5ml of this pool was retained for quantitative PO activity (section 2.4.2.) and quantitative protein (section 2.2.2) measurements.

#### **3.6.3. Cibacron Blue 3GA Chromatography**

Concentrated and dialysed post phenyl sepharose II PO was applied to a cibacron blue 3GA column and further purified as outlined in section 2.8.3. PO activity failed to bind to the resin and was collected in the run through. Figure 3.6.3. illustrates the elution profile of PO activity and protein, measured according to sections 2.4.4. and 2.2.3. Fractions 4-6 were combined to yield 15ml post cibacron blue PO sample. 1.5ml of this pool was retained for quantitative PO activity (section 2.4.2.) and quantitative (section 2.2.2.) determinations.

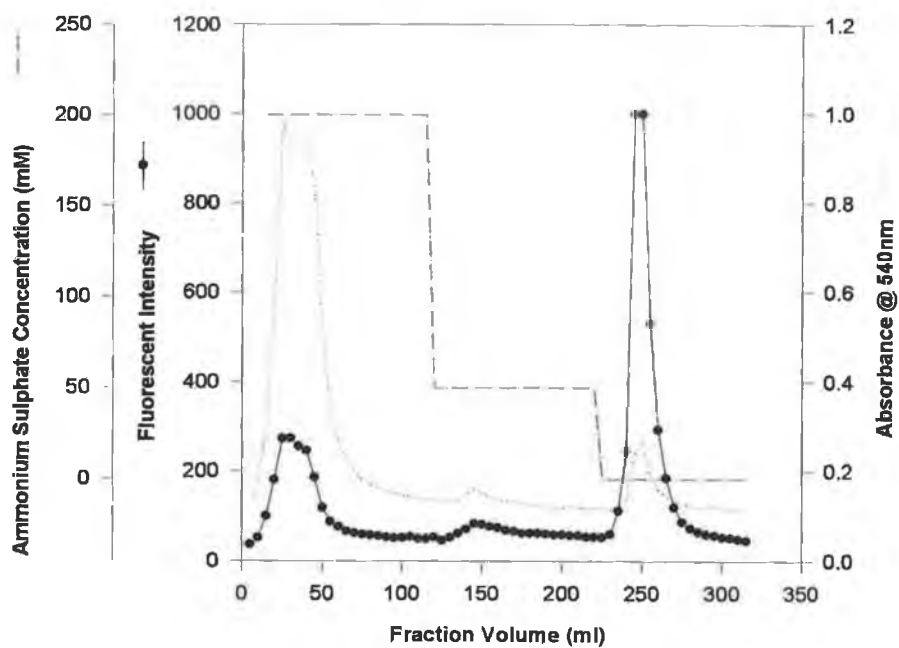


**Figure 3.6.1. Elution Profile of PO Activity During Phenyl Sepharose Hydrophobic Interaction Chromatography I.**

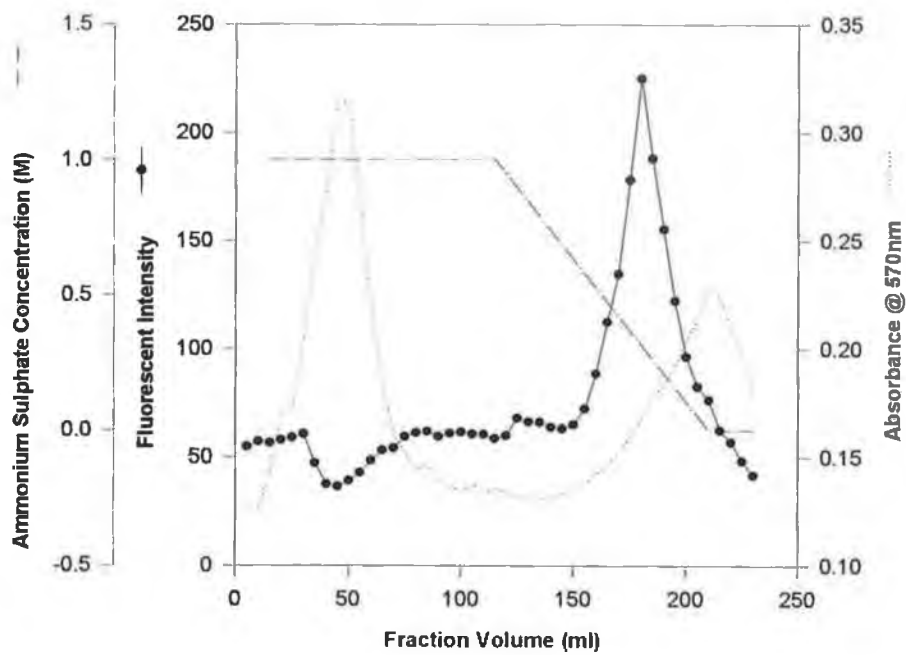
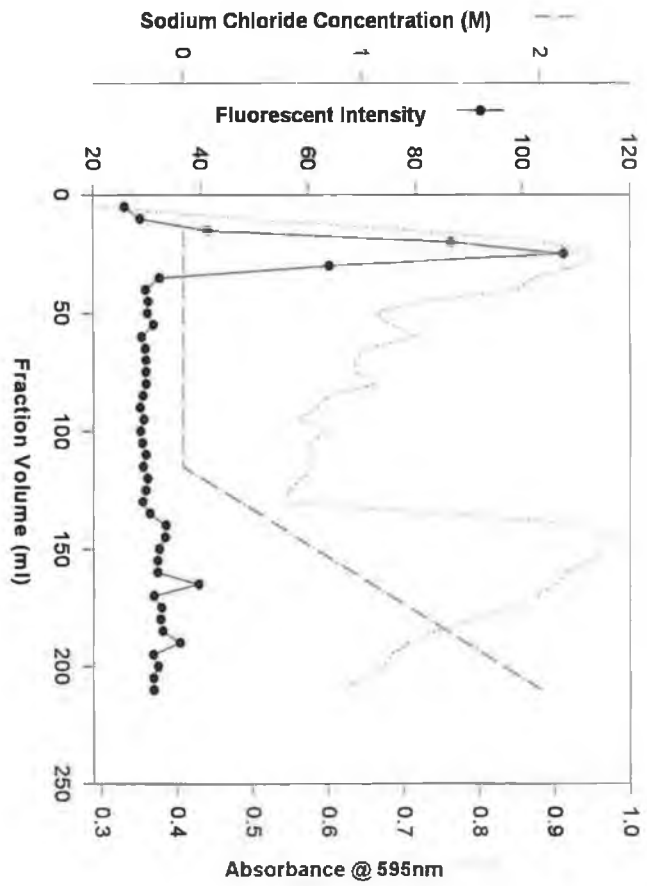


**Figure 3.6.2. Elution Profile of PO Activity During Purification using Phenyl Sepharose Hydrophobic Interaction Chromatography II.**



**Figure 3.6.3. Cibacron Blue 3GA Chromatography of PO Activity**





<b>Purification Step</b>	<b>Volume</b> <i>ml</i>	<b>Total Activity</b> <i>Units</i>	<b>Total Protein</b> <i>mg</i>
<b>Crude Serum</b>	20	12.64	1766
<b>Phenyl Sepharose I</b>	25	12.42	534.44
<b>Phenyl Sepharose II</b>	20	2.55	24.82
<b>Cibacron Blue</b>	15	1.13	4.33

**Table 3.12. Purification of PO from Bovine Serum**

<b>Specific Activity</b>	<b>Purification Factor</b>	<b>Recovery</b>
<i>Units/mg</i>		<i>%</i>
0.00716	1	100
0.023	3.2	98.26
0.103	14.39	20.17
0.261	36.45	8.94

### 3.7. Inhibitor Studies

#### 3.7.1. Effect of Diisopropylfluorophosphate (DFP) on Purified ZIP Activity

Previous studies on the catalytic classification of ZIP from bovine serum only possibly confirmed it as a serine protease (Birney and O'Connor, 2001). This was due to 58% inhibition by AEBSF at 22.5mM concentration. To finally catalytically classify ZIP as a serine protease, the irreversible and classic serine protease inactivator DFP (Barrett, 1994) was used. The effect of DFP on purified ZIP activity was investigated as outlined in section 2.9.1. Figure 3.7.1. illustrates the inactivation of purified ZIP activity from bovine serum by DFP.

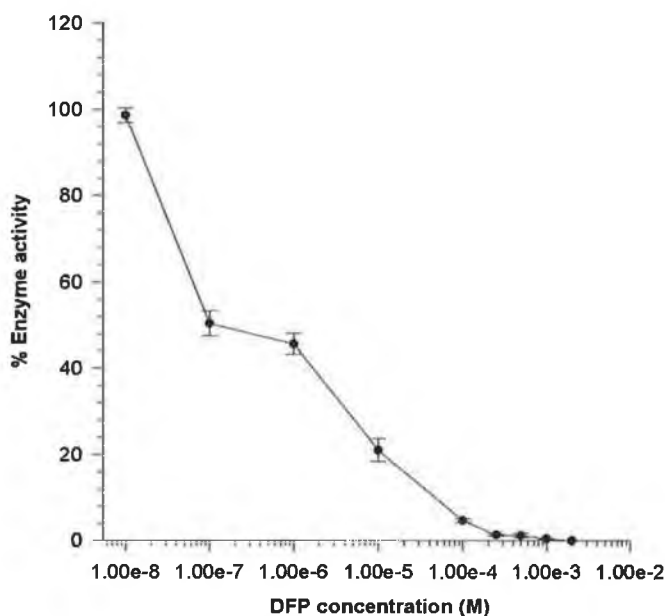


**Figure 3.7.1. Inhibitor Profile Effect of DFP**

Log plot of enzyme activity versus DFP concentration. Plot shows the concentration of DFP required to reduce the activity by 50%. The  $IC_{50}$  value of DFP for purified bovine serum ZIP was deduced to be  $0.1\mu\text{M}$ . Enzyme activities are expressed as a percentage of uninhibited enzyme.

### 3.7.2. Effect of Specific Prolyl Oligopeptidase Inhibitors

The potency of specific Prolyl oligopeptidase inhibitors towards purified ZIP and partially purified PO activities from bovine serum was assessed.

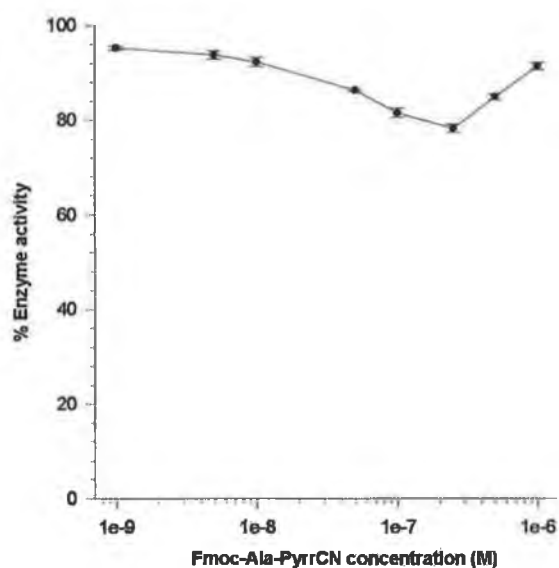
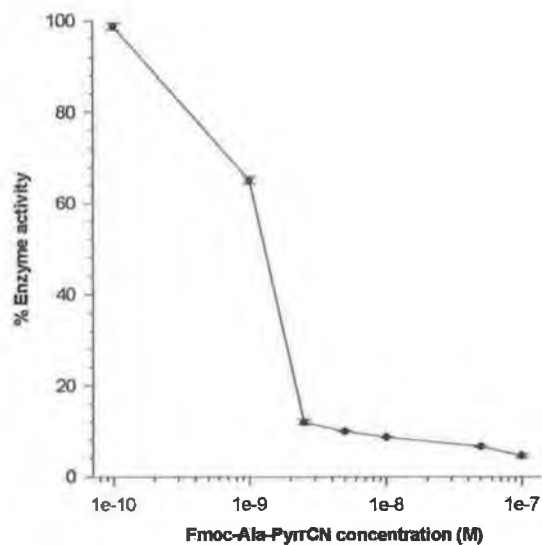
#### 3.7.2.1. Determination of IC<sub>50</sub> Values

The effect of four potent and specific inhibitors on bovine serum ZIP and PO activities was investigated as outlined in section 2.9.2. Figures 3.7.2.1. to 3.7.2.10. illustrate the effect each inhibitor has on both serum activities. Interestingly, all five inhibitors had little or no effect on ZIP activity even at high concentrations of inhibitor. JTP-4819 and Fmoc-Ala-PyrrCN with IC<sub>50</sub> values of 0.8nM and 1.5nM respectively, were the most potent towards PO activity. Table 4.2. summarises the IC<sub>50</sub> values determined for ZIP and PO activities.

Inhibitor	IC <sub>50</sub> for ZIP (M)	IC <sub>50</sub> for PO (M)
Fmoc-Ala-PyrrCN	ND	1.5x10 <sup>-9</sup>
Z-Phe-Pro-Benzothiazol	ND	4.5x10 <sup>-8</sup>
SR 063298	ND	1x10 <sup>-7</sup>
SR 063125	ND	9x10 <sup>-8</sup>
JTP-4819	ND	8x10 <sup>-10</sup>

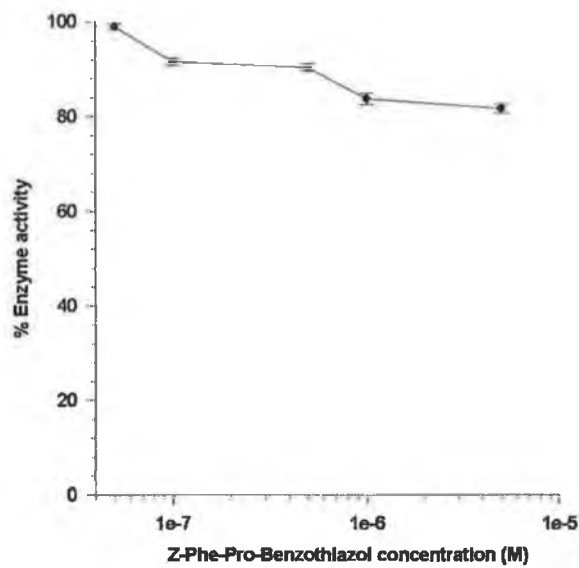
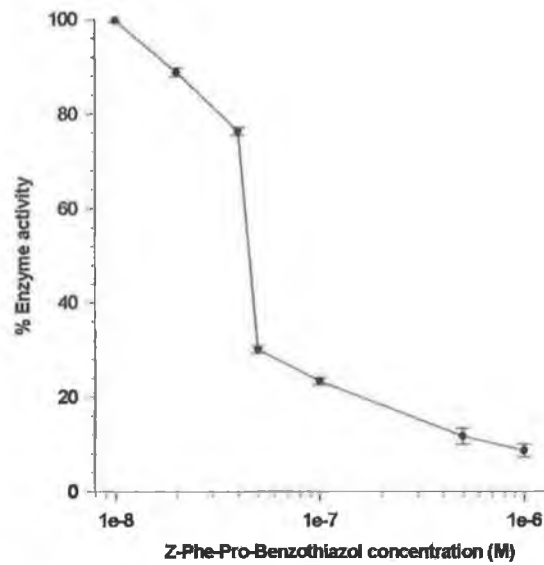
**Table 3.13. IC<sub>50</sub> Values Determined for Prolyl Oligopeptidase Inhibitors**

Results are expressed as IC<sub>50</sub> (M), which were taken as the concentration of inhibitor required to inhibit enzyme activity by 50% (section 6.4.4.).



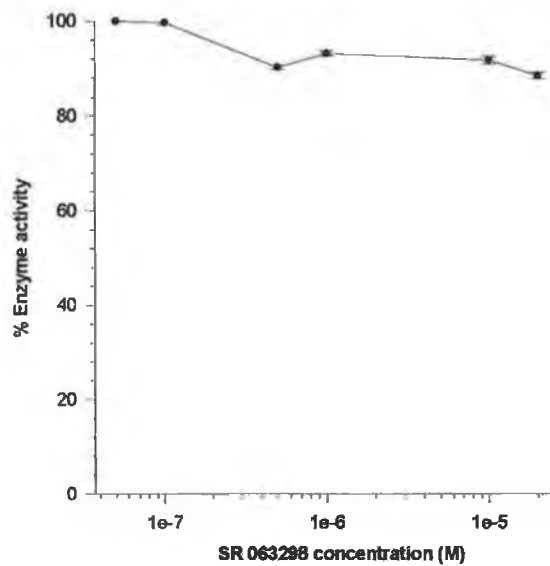
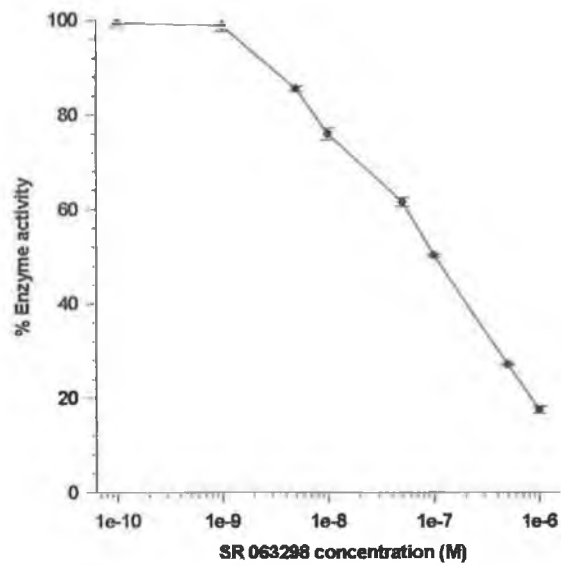
**Figures 3.7.2.1. and 3.7.2.2. Inhibitor Profile Effects of Fmoc-Ala-PyrrCN**

Log plots of enzyme activity versus specific inhibitor concentrations. Figure 3.7.2.1. shows the effect of Fmoc-Ala-PyrrCN on PO activity, whereas Figure 3.7.2.2. illustrates the failure of Fmoc-Ala-PyrrCN to have any effect on ZIP activity. Enzyme activities are expressed as a percentage of uninhibited enzyme.



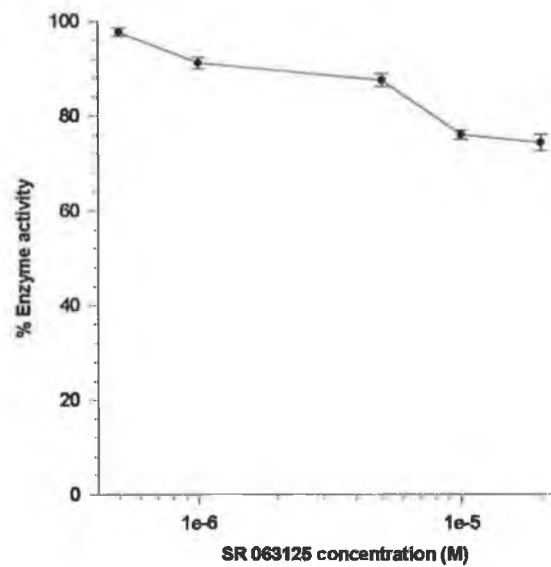
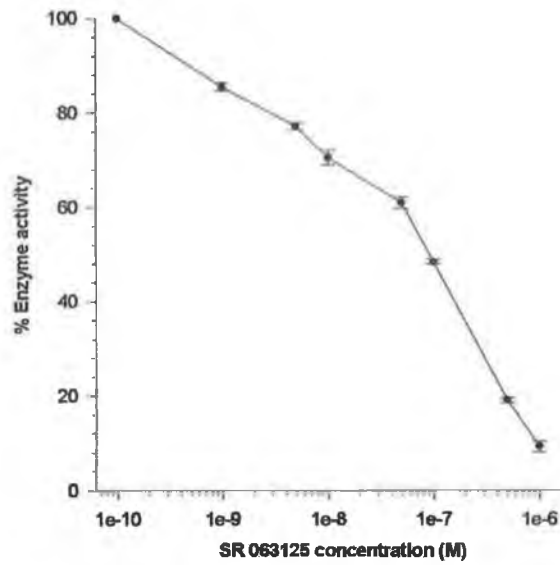
**Figures 3.7.2.3. and 3.7.2.4. Inhibitor Profile Effects of Z-Phe-Pro-BT**

Log plots of enzyme activity versus specific inhibitor concentrations. Figure 3.7.2.3. illustrates the inhibition of PO activity with Z-Phe-Pro-BT, whereas Figure 3.7.2.4. shows the failure of Z-Phe-Pro-BT to inhibit ZIP activity. Enzyme activity expressed as a percentage of uninhibited enzyme.



**Figures 3.7.2.5. and 3.7.2.6. Inhibitor Profile Effects of SR 063298**

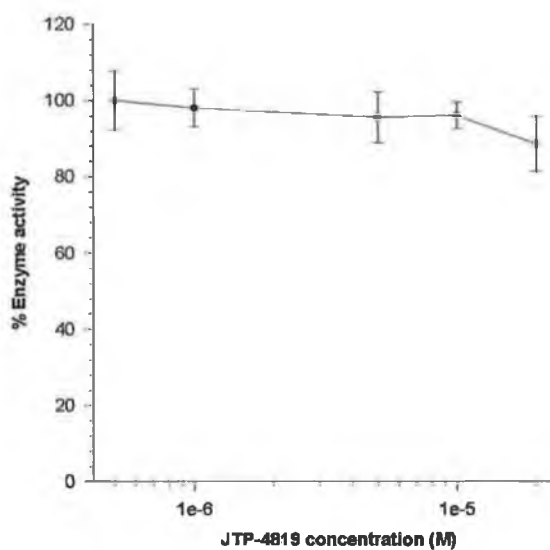
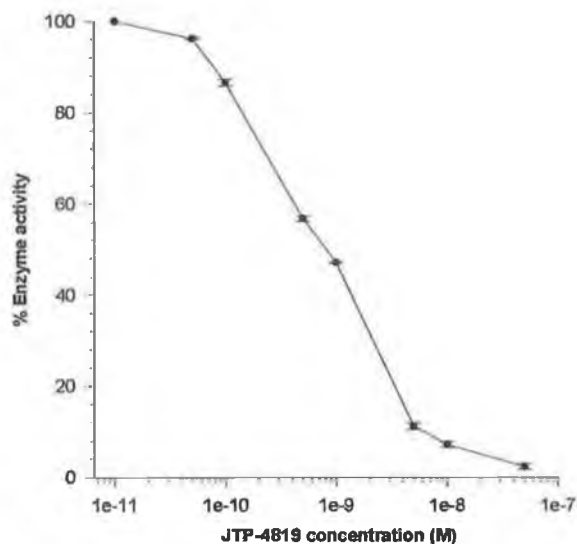
Log plots of enzyme activity versus specific inhibitor concentrations. Figure 3.7.2.5. illustrates the inhibition of PO activity with SR 063298. Figure 3.7.2.6. shows the failure of SR 063298 to inhibit ZIP even at high concentrations.



**Figures 3.7.2.7. and 3.7.2.8. Inhibitor Profile Effects of SR 063125**

Log plots of enzyme activity versus specific inhibitor concentrations. Figure 3.7.2.7. illustrates the inhibition of PO activity by SR 063125. Figure 3.7.2.8. shows almost 30% inhibition but at an inhibitor concentration of 20µM.





**Figures 3.7.2.9. and 3.7.2.10. Inhibitor Profile Effects of JTP-4819**

Log plots of enzyme activity versus specific inhibitor concentrations. Figure 3.7.2.9. illustrates the inhibition of PO activity by JTP-4819. Figure 3.7.2.10. shows the failure of JTP-4819 to inhibit ZIP activity.

### 3.8. Immunological Studies

Western blot analysis was performed as outlined in section 2.10.1. to determine if a polyclonal antibody (anti-human prolyl oligopeptidase) would show any immunological cross reactivity with purified ZIP protein and partial purified PO from bovine serum. Figures 3.8.1.1. and 3.8.1.2. represent western-blot analysis of the proteins.

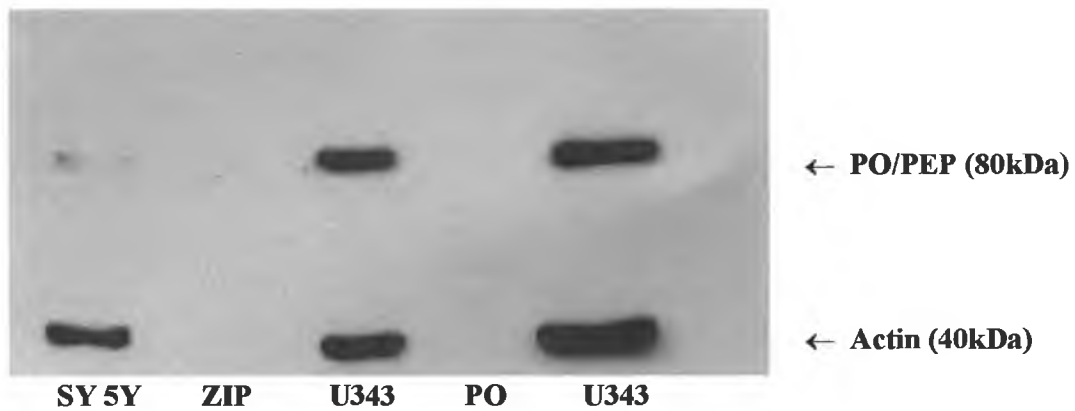


**Figure 3.8.1.1. Western-Blot Analysis of Bovine ZIP and PO**

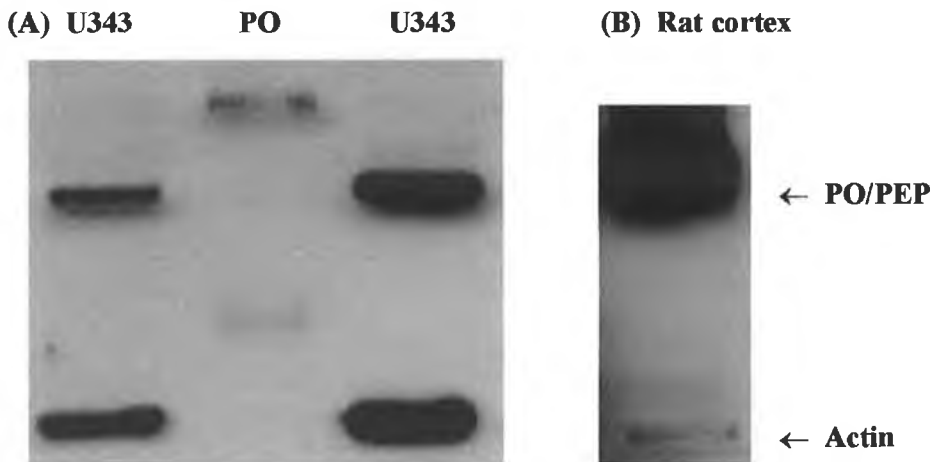


**Figure 3.8.1.2. Western-Blot Analysis**

(A) A more concentrated PO sample applied with possible cross reactivity. (B) The ability of the anti-human PO/PEP antibody to immunoreact with rat cortex PO.

### 3.9. Identification of this Z-Pro-prolinal Insensitive Peptidase

#### 3.9.1. N-Terminal and Internal Sequencing

50ml of bovine serum was purified to obtain sufficient ZIP sample for sequence analysis. SDS PAGE was performed as outlined in section 2.11.1.1. and followed by electroblotting to a PVDF membrane (section 2.11.1.2.). Figure 3.9.1. is an image of the coomassie-stained blot. This blot was sent to Dr. Bryan Dunbar, Protein Sequencing Department, University of Dundee, Scotland for N-terminal sequencing. The molecular weight reported previously for ZIP was 95kDa (Birney, 2000). The blot showed a possible faint band close to this location but also a number of other bands possibly due to purifying up to 50ml starting material.

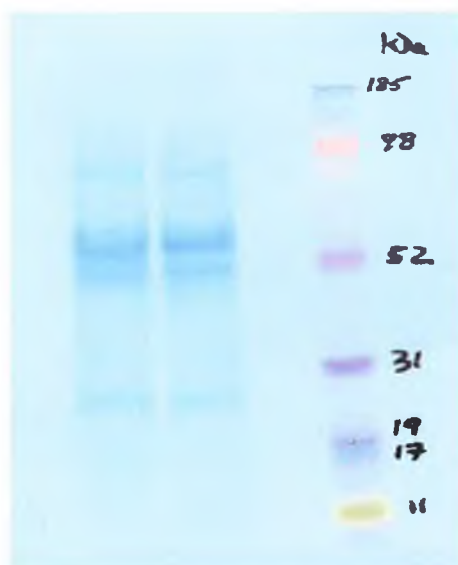


**Figure 3.9.1.1. Coomassie-Stained PVDF Membrane Blot**

The N-terminal sequence of the faint band visible just below the 98kDa marker in Figure 3.9.1.1. failed to be successfully determined after many attempts. This was reported to be due to an inadequate amount of protein present in this band. The strong band above the 52kDa was determined to be BSA from sequencing, while the band just below was N-terminally blocked, resulting in no sequence data. Due to failing to obtain any sequence data that may be of interest with regards to our activity, another larger sample was prepared. 60ml of bovine serum was purified over the first three columns in the purification procedure and this partial purified concentrated ZIP

sample was sent to the Proteomics Department, University of Dundee for internal sequencing.

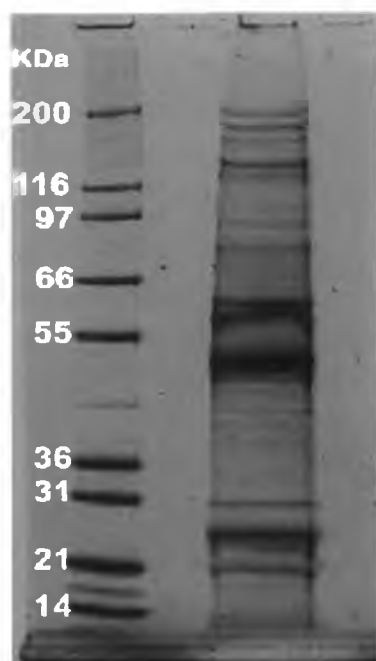


**Figure 3.9.1.2. SDS PAGE Gel of Partial Purified ZIP Sample**

It is obvious from Figure 3.9.1.2. that using such a large volume of starting material and only performing partial purification of the sample caused many more contaminant bands to be present. The reason for removing a step in the purification procedure was the hope that there would be more of our target protein present to obtain sequence data from. Internal sequencing of the major band below the 55kDa marker, which corresponds to the N-blocked protein in Figure 3.9.1.1. resulted in identification of up to seven proteins with the major protein identified being bovine heavy chain IgG. No other protein identified was of any interest to our protease activity.

It was obvious from these results that without knowledge of the exact location of the ZIP band under denaturing conditions it was impossible to sequence and identify the protein of interest. This was made more difficult when trying to purify up to 60ml of serum using the optimised protocol in order to obtain enough target protein and the unavailability of an antibody towards ZIP.

### 3.9.2. In Gel (Zymogram) Assay

The only alternative remaining, in order to be sure that the correct protein of interest was being sequenced was an in gel (zymogram) assay for ZIP. There was no reports of this technique been performed previously using this enzyme. A 10% native polyacrylamide gel was prepared and run according to section 2.11.2.1. Figure 3.9.2.1. illustrates a zymogram showing the presence of native ZIP hydrolysing the substrate Z-Gly-Pro-AMC, viewed under ultraviolet light.

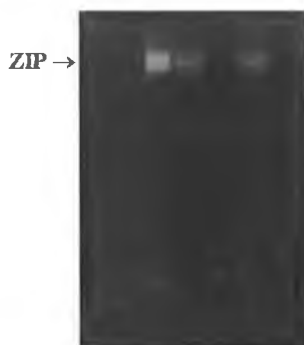


**Figure 3.9.2.1. Native PAGE Analysis of ZIP Proteolytic Activity.**

The zymogram clearly shows fluorescent bands (→), which appear in the region of substrate hydrolysis after visualisation under ultraviolet light.

The fluorescent bands above were excised and placed in ultra-pure water overnight at 4°C. This was performed so that the protein present in the bands would diffuse out of the bands into solution. Due to the small amount of protein present in each band this technique didn't seem to work to any great extent. A fluorescent band, which was also excised from the same gel, was then sent to the University of Dundee for internal sequence analysis. Again, due to such a low level of protein present within this gel piece it was rather difficult to identify the protein/s present. The two proteins that were identified by internal sequence analysis were IgG and fibronectin. Fibronectin was interesting at first, as its plasma form is known to have potential proteolytic activity. Therefore, it was important to remove these two proteins from the sample if they are contaminants, but if the activity is being caused by fibronectin to try and remove this activity by gelatin chromatography.

80ml of bovine serum was purified, but this time in 20ml batches as described as always in section 2.5. The pooled activity from each purification was concentrated

and chromatography performed using protein G affinity resin as outlined in section 2.11.2.3. This resin failed to bind ZIP and any IgG present in the sample was successfully removed. The next step as outlined in section 2.11.2.4. involved running this post protein G ZIP sample on a gelatin sepharose resin. The ZIP activity failed to bind to this resin also, thus eliminating any involvement of fibronectin in our protease activity. The final sample was prepared and run on a native page gel and finally analysed using ultraviolet zymography and silver staining as outlined in sections 2.11.2. and 2.6.2.4.

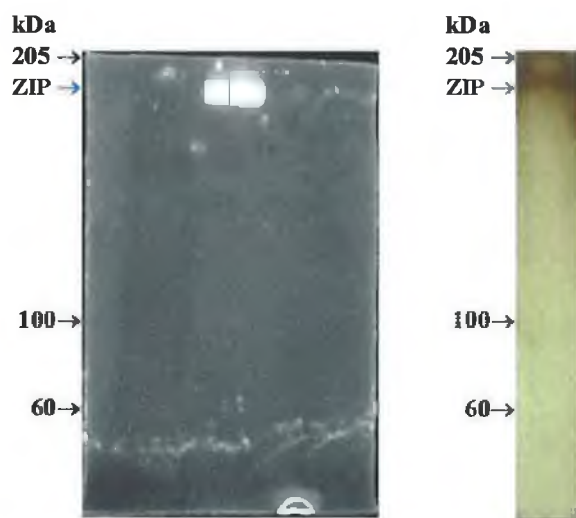


**Figure 3.9.2.2. In Gel Assay (Zymogram) and Silver Staining of Native ZIP**

The fluorescent band in Figure 3.9.2.2. was excised and sent to the Harvard Microchemistry Facility where sequence analysis was performed by microcapillary reverse-phase HPLC nano-electrospray tandem mass spectrometry ( $\mu$ LC/MS/MS) on a Finnigan LCQ DECA XP Plus quadrupole ion trap mass spectrometer.

The procedure used as mentioned identified the ZIP protein as Seprase, which is a known serine protease, associated with the small group of serine integral membrane peptidases. The peptides sequenced and identified are shown below.

gi 16933540		MS/MS Spectra: 12	Sum TIC: 4.1e8	Avg TIC: 3.4e7	
fibroblast activation protein, alpha subunit; integral membrane serine protease; seprase [Homo sapiens] gi 1924982 gb AAC51668.1  integral membrane serine protease Seprase [Homo sapiens] gi 20072811 gb AAH26250.1  fibroblast activation protein, alpha [Homo sapiens]					
Sequence	Reference	TIC	Ions	Scan	
(-) KLGVEVEDQITAVR	gi 16933540 +3	5.4e7	22/28	899	
(-) KLGVEVEDQITAVR	gi 16933540 +3	1.1e8	35/56	897	
(-) LAYVYQNNIYLK	gi 16933540 +5	3.1e7	17/22	858	
(-) IFNGIPDWVYEEEM*LATK	gi 16933540 +3	1.7e7	20/34	1243	
(-) FIEM*GFIDEKR	gi 16933540 +3	6.6e6	16/20	734	
(-) NVDYLLIHGTADDNVHFQNSAQIAK	gi 16933540 +6	1.2e6	25/96	1260	
(-) YALWVSPNGK	gi 16933540 +2	3.2e6	14/18	1019	
(-) LLYAVYR	gi 16933540 +3	7.5e7	11/12	713	
(-) FIEM*GFIDEK	gi 16933540 +3	2.7e6	13/18	789	
(-) WEAINIFR	gi 16933540 +2	1.0e8	13/14	1052	
(-) TINIPYPK	gi 16933540 +5	3.3e6	10/14	733	

**Figure 3.9.2.3. The Peptides Sequenced and Identification of the Serine Protease Seprase.**

## **DISCUSSION**



## 4.0. Discussion

### 4.1. Fluorescence Spectrometry using 7-Amino-4-Methyl-Coumarin

This work presented focused mainly on the study of ZIP (Z-Pro-proline Inensitive Peptidase), a possibly novel proline specific peptidase activity from bovine serum. The uniqueness of this peptidase was its ability to cleave the supposedly specific prolyl oligopeptidase substrate Z-Gly-Pro-AMC, but being completely distinct to this serine peptidase (Cunningham and O'Connor, 1997a).

A method capable of detecting low-levels of these peptidase in biological systems is essential. The selection of substrates for the enzyme of interest has evolved over the years when when the properties and functionality become clearer like, Walter *et al.* (1971) identifying prolyl oligopeptidase using radiolabelled oxytocin. In recent years synthetic substrates have been specifically designed for enzyme detection. The main parameters ruling substrate selection are enzyme specificity and the fluorophore or chromophore employed. Generally, fluorescence spectroscopy offers increased safety, sensitivity and specificity over colorimetric, spectrometric and radiometric assays. The high sensitivity results from the wavelength difference between the exciting and fluorescence radiation, resulting in minimal background, while the high specificity is due to the dependence on both an excitation and emission spectra (Willard *et al.* 1988).

The substrate used for ZIP detection was Z-Gly-Pro-AMC. This substrate was first synthesised and applied in the detection of prolyl oligopeptidase by Yoshimoto *et al.* (1979) who determined a  $K_m$  value of 20 $\mu$ M and noticed increased sensitivity over other substrates. This externally quenched fluorimetric substrate is suitable for endopeptidase mediated peptide bond cleavage on the carboxyl side of the proline residue leading to the liberation of the fluorophore, AMC. Excitation to a higher energy state occurs at 370nm due to the absorption of electromagnetic radiation by AMC, followed by the return of the molecule to a lower state and re-emission of radiation at 440nm. The sensitivity of fluorimetric assays may be improved by expansion of the emission slit width, which consequently broadens the bandwidth over which light is integrated. Therefore, for samples with low enzyme activity

resulting in low fluorescence, adaptation of the emission slit width ensures improved sensitivity.

The major disadvantage of fluorimetric assays is the occurrence of quenching and the inner filter effect. With regard to fluorescence a variety of forms of quenching can affect sensitivity resulting in misleadingly low fluorescence. Quenching mostly involves the removal of energy from a molecule in the excited state by another molecule. The most common form is collisional impurity quenching caused by molecular collisions. It is the form of quenching that is a result of the presence of impurities that absorb either the exciting or emitted radiation, leading to the reduction in fluorescence that is particularly problematic when using crude biological samples such as serum. This form of quenching is better known as the inner filter effect.

#### **4.1.1. AMC Standard Curves and the Inner Filter Effect**

Enzyme activity was quantified (section 6.1.) from liberated AMC, as a result of peptide cleavage, by reference to standard curves. Free AMC standard were prepared according to section 2.2.1. and the linear relationship between AMC concentration and fluorescence intensity at excitation and emission wavelengths of 370nm and 440nm is clearly exhibited in Figures 3.2.1. and 3.2.2. The slope of each standard curve is reported in Table 3.1.

To compensate for the inner filter effect it was necessary to prepare AMC standard curves in the presence of serum. Section 2.3.2. described the preparation of these standard curves and from Figure 3.2.3. a notable reduction in fluorescence was obvious on incorporation of serum. This decrease is obvious from the reduced slope (Table 3.1.), which is indicative of a reduced sensitivity. Bovine serum accounted for up to 7.4% filtering at excitation and emission slit widths of 10nm and 5nm respectively. All post column chromatography samples were checked for possible inner filter interference. As shown in Figure 3.2.4. and reported in Table 3.1. post phenyl sepharose showed 4.2% filtering but further purification of the sample resulted in no apparent effect of filtering.

These results are very important when assessing a purification procedure. Starting material for such procedures usually constitute a crude sample, like serum, highly susceptible to inner filtering. When using such crude, highly coloured, high protein

samples failure to consider effect of filtering would reveal a lower activity than actually present. It is evident that filtered AMC standard curves are essential for accurate enzyme quantification using fluorimetric assays.

The inner filter effect was also investigated during characterisation studies using inhibitors, functional reagents and even buffers to be certain the compound is affecting the enzyme and not the liberated fluorescence.

#### **4.2. Protein Determinations**

As described earlier the fluorimetric enzyme assay was essential for activity determination in a particular sample. It is also equally essential to determine total protein content, which in relation to the purification of ZIP was evident when calculation of specific activity relied heavily on accurate determination of the protein content. Determination of protein content is also essential for estimating the degree of purification obtained by a particular fractionation step.

Many protein assays have evolved each with their own advantages and disadvantages (Dunn, 1989). The most non-specific, rapid and inexpensive method utilises ultraviolet spectrometry commonly at a wavelength of 280nm for protein detection. This assay exploits the ability of the aromatic amino acids, tyrosine and tryptophan to absorb at 280nm. Unfortunately, it is well known that serum has a great variety of nonproteinaceous, uv-absorbing compounds (Schlabach, 1984).

The biuret assay (section 2.2.1.) was employed for protein detection in crude samples. It is not reliant on amino acid composition of the protein and less prone to interference than ultraviolet spectrometry at 280nm. Under alkaline conditions copper ions readily complex adjacent peptide bonds, producing a purple colour with an adsorption maximum at 540nm. The linear relationship observed between protein concentration and absorbance at 540nm up to 10mg/ml (Figure 3.1.1.) for this assay allowed for total protein estimation in enzyme samples. This assay was performed in a microtitre plate, using only 50 $\mu$ l of sample.

Samples containing less than 2mg/ml of protein were assayed using the bicinchoninic acid (BCA) assay, first developed by Smith *et al.* (1985). It combines the biuret reaction of the reduction of  $\text{Cu}^{2+}$  by protein to  $\text{Cu}^{1+}$ , with the highly sensitive and selective colorimetric detection of the cuprous cation ( $\text{Cu}^{1+}$ ) by BCA. The assay is generally linear up to 2mg/ml (Figure 3.1.2.) and only 25 $\mu\text{l}$  of sample is required for analysis.

The Coomassie Plus protein assay was used for detection of low levels of protein, typical values between 2.5 and 25 $\mu\text{g}/\text{ml}$ . The coomassie molecule binds to protein in an acidic medium causing a colour change from brown to blue, maximally absorbing at 595nm. This assay is linear up to 25 $\mu\text{g}/\text{ml}$  (Figure 3.1.3.). A disadvantage of this reagent is batch to batch variation and the need for up to 150 $\mu\text{l}$  of sample for analysis.

<b>Method and Detection Range</b>	<b>Interferants</b>	<b>Comments</b>
<b>A<sub>280</sub></b> (0.05-2mg/ml)	Nucleic acids, Haem containing compounds	Relatively insensitive, non-specific, Rapid
<b>Biuret</b> (1-10mg/ml)	Ammonia, Bile pigments	Low sensitivity, unaffected by amino acid composition
<b>BCA</b> (0.02-2mg/ml)	Reducing agents, Sugars	Little interferants, Extremely sensitive
<b>Coomassie Plus</b> (2.5-25 $\mu\text{g}/\text{ml}$ )	High concentrations of DTT	Batch to batch variation Very sensitive

**Table 4.1. Comparison of some protein determination assays**

### 4.3. Enzyme Assays

The activity of ZIP studied in this work was determined fluorimetrically using AMC release. The linear relationship between fluorescence and AMC concentration allows for the accurate quantification of enzyme activity (see appendix, section 6.1.).

Z-Gly-Pro-AMC was the synthetic substrate used for the detection of ZIP activity. Enzyme assays were performed as outlined in sections 2.4.2., 2.4.3. and 2.4.4. showing a slight modification of the assay system employed previously by Birney and O'Connor (2001). When designing the assays it had to be carefully considered that Yoshimoto *et al.* (1979) described Z-Gly-Pro-AMC as a specific prolyl oligopeptidase substrate. So as outlined in section 2.4.3. a specific prolyl oligopeptidase inhibitor, in this case JTP-4819 instead of Z-Pro-prolinal, was incorporated into the assay. This enabled the identification of ZIP activity alone in samples such as serum also containing prolyl oligopeptidase activity. The procedure described in section 2.4.2. was therefore employed for the detection of either ZIP or PO activity once they were separated. In this case the assay was used for ZIP activity detection in samples, which were known to be free of prolyl oligopeptidase activity (e.g. post column pools).

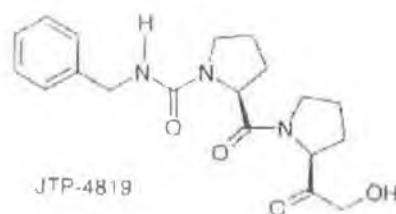


**Figure 4.1. Chemical Structure of Inhibitor JTP-4819**

The cuvette based assays were ideal in that they proved specific for ZIP or PO activity, were sensitive, quantifiable, rapid and simple so meeting the requirements of any enzyme assay. The third assay described in section 2.4.4. is a microtitre plate assay, developed to enable rapid identification of enzyme activity in post column chromatography fractions. The microtitre plate assay proved ideal for non-quantitative enzyme detection, using less sample, substrate and acid volumes than the cuvette and only half the incubation period before analysis.

In order to express the activity of an enzyme quantitatively it is necessary to ensure that the assay procedure used is measuring the true initial velocity and that this is proportional to the enzyme concentration. When the time-course of product formation, or substrate utilisation, is determined a curve such as that shown in Figure 4.2. is usually obtained. The time-course is initially linear but the rate of product formation starts to decline at longer times. There are several possible reasons for departure from linearity such as substrate depletion, product inhibition, enzyme or substrate instability, time-dependant inhibition or a change in assay conditions. Therefore, due to these potential problems it is desirable, if possible to adjust assay conditions such that a linear response is maintained for a sufficient time to allow direct measurement of initial rate/velocity.

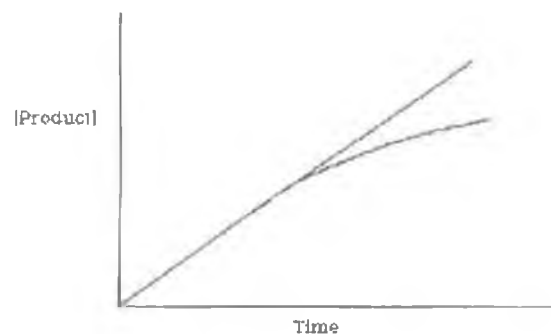


**Figure 4.2. A Typical Progress Curve of an Enzyme-Catalysed Reaction**

Due to using a discontinuous assay (section 2.4.2.), quantification of ZIP or PO activity could not be relied upon unless linearity of the assay had previously been assured using a continuous assay system. Purified ZIP and partial purified PO were linear using 100 $\mu$ M substrate with respect to time, over a 60-minute period, and with respect to enzyme concentration. These assay conditions for ZIP activity was also used previously by Birney and O'Connor (2001). Overall, the linearity of these assays with respect to time and enzyme concentration permitted quantitative expression of enzyme activity using a fluorescent reading (section 6.1.).

#### **4.4. Protein Purification**

The purification of a protein from a mixture that may only constitute 1% of the species of interest incorporates the exploitation of a number of physical, chemical and biological characteristics of the target protein. The purification of a protein is frequently not the end point itself, but the means of obtaining a pure protein for further studies. These studies may be on the activity of the protein, on its structure or on its structure-function relationships. Overall, these studies will dictate the necessary purity, activity and quantity of the protein required. It is these parameters that play a considerable role in the selection of the purification process for the target protein.

##### **4.4.1. Purification of ZIP from Bovine Serum**

The isolation of ZIP for characterisation studies required the production of relatively large quantities of highly purified active enzyme. The most important factor to be taken into consideration was the conservation of biological activity throughout the purification process. The purification of ZIP from bovine serum was performed according to section 2.5. showing significant modification of the original procedure reported by Birney and O'Connor (2001). These modifications were deemed necessary in order to obtain an increased level of purity. Overall, a highly effective purification procedure was established.

##### **4.4.1.1. Serum Preparation**

Due to the optimisation of the purification protocol for ZIP and subsequent characterisation studies, a relatively large volume of purified enzyme was necessary, which in turn necessitates a large amount of starting material. Therefore, a reliable commercially available, inexpensive source that was high in ZIP content was essential. Bovine serum fulfilled these criteria and was thus selected as the ideal source for the isolation of ZIP. Bovine serum was prepared as outlined in section 2.5.1. by centrifugation of the non-clotted portion of bovine whole blood thus generating a large volume of serum. Storage at -17°C had no effect on the stability of ZIP activity over a long period of time.

#### **4.4.1.2. Phenyl Sepharose Hydrophobic Interaction Chromatography**

Protein surface hydrophobicity occurs due to the presence at the surface, of the side chains of non-polar amino acids such as alanine, methionine, tryptophan and phenylalanine. These surface hydrophobic amino acids are usually arranged in patches. The number, size and distribution of these non-ionic regions is a characteristic of each individual protein, which can therefore be exploited as a basis for their separation. In solution a protein molecule holds a film of water in an ordered structure at its surface, which must be removed from non-ionic domains so hydrophobic interaction can occur. Salting-out ions decrease the availability of water molecules in solution, increase the surface tension and enhance hydrophobic interaction (Roe, 1989). Phenyl sepharose is classified as a high capacity resin (20mg protein/ml), therefore with serum as the enzyme source this resin was chosen as the initial column for the purification procedure.

Before application to the phenyl sepharose resin solid ammonium sulphate to a final concentration of 200mM was added to serum as outlined in section 2.5.2. This method of salting avoided dilution and dialysis, which were shown to substantially decrease biological activity. The most interesting observation from the elution profile in Figure 3.3.2.2. of the HIC column was the presence of the two distinct Z-Gly-Pro-AMC hydrolysing activities. Knowing of the existence of ZIP and from previous fractionation of these activities by HIC chromatography, it was assumed that the first peak was prolyl oligopeptidase activity, while the second showed the presence of ZIP in bovine serum. Figure 3.3.2.2. confirmed this when the run through peak was totally inhibited by JTP-4819, with the elution peak, hence deduced ZIP, showing no effect by the specific inhibitor.

On the purification of ZIP, this resin was very successful in separating ZIP from bulk contaminating protein. A large protein peak (Figure 3.3.2.1.) is evident in the column run through with a smaller peak observed during the second wash. ZIP activity co-eluted with the third peak in the final wash in the complete absence of salt. The substantial loss of protein, 1766mg to 37.15mg, along with only a 6.8% loss of ZIP activity resulted in a 44-fold purification using HIC.



#### **4.4.1.3. Calcium Phosphate Cellulose Chromatography**

The resin for this purification step was produced in the laboratory (section 2.5.3.1.) according to modifications of the methods described by Tiselius *et al.* (1956) and Donlon and Kaufman (1980). Bulk preparation of calcium phosphate cellulose resin in the laboratory eliminates any concerns of possible batch to batch variation. The difficulty in predicting the precise mechanism of action of this resin in column chromatography has limited its use as a purification tool. It is thought that the mechanism of protein adsorption onto calcium phosphate cellulose involves both  $\text{Ca}^{2+}$  and  $\text{PO}_4^{3-}$  groups on the crystal surface (Bernardi *et al.* 1972).

The elution profile of ZIP on this resin is presented in Figure 3.3.3. with resolution of ZIP activity from contaminating protein being observed. The inclusion of the 170mM wash (section 2.5.3.2.) was essential for removal of contaminating protein but more importantly was responsible for separating ZIP from Gly-Pro-AMC and Z-Phe-Arg-AMC degrading peptidases.

The effectiveness of this resin is seen by the 96% reduction in protein applied to the column but as shown in Table 3.2. this is coupled with only a 57% recovery of applied activity. There was still a 621-fold purification factor achieved using this resin. It was therefore apparent that the calcium phosphate cellulose resin proved successful for the further purification of ZIP.

#### **4.4.1.4. Cibacron Blue 3GA Chromatography**

The use of an anion exchange resin as employed by Birney and O'Connor (2001) failed in this case to further resolve ZIP activity from contaminating protein. Cibacron blue 3GA is a reactive dye, which is used in affinity chromatography protein purification. This resin is ideal for removing bovine serum albumin contamination from serum samples, so it was employed in this case for the removal of possible bovine serum contamination and hence further purify ZIP.

Figure 3.3.4. presents the elution profile, which clearly shows that ZIP activity actually bound to the resin and eluted during the increasing salt gradient applied. The initial reason for this resin was in the hope that ZIP would run through and thus be separated from any contaminating bovine serum albumin present in the sample. Even

though this failed to be the case, the chromatography step proved incredibly effective with a 80-fold decrease in total protein content. The recovery of applied activity was only 37% but it still enabled a 18,735-fold purification to be obtained along with 20% overall recovery of biological activity after three chromatographic steps (Table 3.2.). This 18,735-fold purification factor compares to the 4023-fold obtained previously for a three step purification of ZIP from bovine serum (Birney and O'Connor, 2001).

#### **4.4.1.5. S-300 HR Gel Filtration Chromatography**

Proteins have a characteristic molecular size and shape when dealing with gel filtration chromatography. This is based on their molecular weight due to the number and size of their amino acids and the folding of the protein. The separation mechanism of gel filtration chromatography involves both molecular shape and mass of the protein. It is a very popular non-binding technique employed for protein purification. When a mixture of differing molecular weights is applied to the resin, large molecules fail to enter the pore beads and move through the column rapidly, while small sized molecules become retarded as they become trapped in the pore beads. The rate of movement is directly proportional to the size of the molecule and on this basis protein separation occurs.

S-300 gel filtration chromatography was chosen as the final column in the purification procedure. It is ideal at this stage due to its relatively low capacity and ability to aid in assessing the purity of a preparation. The elution profile is presented in Figure 3.3.5. The resin was very effective in removing some large molecular weight contaminants as shown by the protein peak prior to the activity peak of ZIP. It also removed any of the remaining Z-Phe-Arg-AMC degrading peptidase activity present in the sample. Overall, it was an ideal clean up step for the preparation only losing about 40% of applied activity while still reducing protein from 19 $\mu$ g to 7 $\mu$ g.

During the purification of ZIP, appropriate precautions and considerations were taken throughout. Even though concentration steps were involved throughout the procedure extensive dialysis was only performed once, as this step is known to be detrimental to activity at times during protein purification. All steps were carried out at 4°C except the final column, which was at room temperature, but this change didn't affect

activity to any large extent. All steps were performed consecutively leading to the specific activity of purified ZIP being 30,197-fold higher compared to that in crude serum. A 12% conservation of biological activity after the reduction of protein from 1766mg to 0.007mg was considered very successful. Defining the purity of the protein for enzymic studies in terms of the percentage of total protein shows that the ZIP sample is possibly up to 99% pure.

#### **4.5. Purity Assessment**

Purity of the protein of interest after purification can simply be defined in terms of the percentage of total protein as mentioned in section 4.4.1.5. though other contaminants, which are important, must be considered. Typically for enzymic studies a purity of 80-90% is adequate, though the presence of active proteases or other enzymes that could interfere with activity are unacceptable. Therefore, it is unnecessary and almost unattainable to try and obtain a pure protein i.e. one population of molecules all with identical covalent and three-dimensional structures in solution. For the purpose of this study, purity was assumed if the sample was shown not to contain any contaminants that would interfere with intended experiments with ZIP. Assessment of a suitable purity level was achieved using fluorimetry-based analysis and SDS PAGE.

To detect for the presence of contaminating peptidases in the purified (post S-300) ZIP sample a number of fluorimetric assays were performed. The substrates employed are shown in Table 2.1. with the presence of the peptidase being determined by a measure of AMC release (section 2.6.1.). As highlighted in Table 3.3. no hydrolysis of any substrate other than Z-Gly-Pro-AMC was detected. The absence of contaminating peptidases such as prolyl oligopeptidase and dipeptidyl peptidase IV was essential since they would have interfered with subsequent physiochemical analysis such as substrate specificity studies further on.

Figures 3.4.2.1. and 3.4.2.2. represent images of gelcode blue and silver stained polyacrylamide gels respectively. Figure 3.4.2.1. illustrates that as the purification procedure progressed (lanes 2-4) there was a reduction of the bands present. The final step in the purification, post S-300 (lane 5) clearly shows no visible band present when stained with this coomassie based reagent. Silver staining (Figure 3.4.2.2.) of lanes 4-7 show the presence of a faint band with a molecular weight of about 95-

96kDa present in lane 5 i.e. purified sample. This band is relatively faint with no other bands apparently visible in this lane. Birney (2000) also reported a molecular weight of 95kDa for ZIP based on silver stained SDS PAGE analysis.

Based on fluorimetric and SDS PAGE analysis, post S-300 gel filtration ZIP sample was deemed acceptably pure for further studies.

#### **4.6. Substrate Specificity**

The substrate specificity of ZIP is potentially the most important study that can be undertaken to ultimately understand the possible function of this enzyme. Previous work on the specificity of ZIP studied proline containing bioactive peptides as potential substrates (Birney and O'Connor, 2001). It is known that the specificity of a protease is determined not only by the two amino acid residues at either side of the scissile bond of a peptide substrate, but also by amino acid residues more distant from the point of hydrolysis. Therefore, this work was performed in order to investigate the secondary specificity of ZIP using peptide substrates of various structural conformation and length (Table 3.11.). These studies involved, (i) chain elongation at the amino side of the primary specificity proline residue, (ii) amino acid preference at the carboxyl side of the scissile bond, (iii) chain elongation at the carboxyl side of the primary specificity proline residue and, (iv) a final study was undertaken to investigate the importance of the primary specificity proline residue in ZIP catalysed hydrolysis. These studies were performed using kinetic analysis, RP-HPLC and LC-MS. Prolyl oligopeptidase is the only other proline specific endopeptidase known and its substrate specificity is thoroughly documented. Thus all results discussed will be directly compared to the specificity of prolyl oligopeptidase.

The effect of a range of proline containing peptides on the ZIP catalysed hydrolysis of Z-Gly-Pro-AMC enabled  $K_i$  (app) values to be obtained for each peptide according to section 6.4.1. The complex situation arises when one questions whether a substrate can be classified as an actual inhibitor. Rahfeld *et al.* (1991) explained the situation where one enzyme hydrolyses two substrates simultaneously that one substrate (S2) formally acts as the inhibitor for the other substrate (S1) (e.g. S1 = Z-Gly-Pro-AMC; S2 = Z-Gly-Pro-Phe). The  $K_i$  value in this case is not the true thermodynamic dissociation constant of the E-S2-complex but the  $K_m$  value for the substrate S2.

Therefore  $K_i$  ( $_{app}$ ) values obtained in this study will be regarded as the affinity constants of the enzyme ZIP for that particular peptide.

The high resolving power, speed and efficiencies typically achieved using reverse phase high performance liquid chromatography (RP HPLC) makes it the predominant technique for peptide separation. In this study RP HPLC was performed (section 2.7.2.) to detect hydrolysis and the subsequent cleavage products following incubation of certain peptides with purified ZIP. A silica based analytical column containing octadecyl ligands ( $C_{18}$ ) was employed as the non-polar stationary phase. The polar mobile phase of acetonitrile and water contained the hydrophobic ion-pairing reagent trifluoroacetic acid (TFA). TFA is a weak hydrophobic ion-pairing reagent that also serves to maintain a low pH ( $\sim 2$ ), thereby minimizing ionic interactions between peptide and the stationary phase. Thus, RP HPLC was chosen as the optimum analytical tool for substrate specificity studies on ZIP.

Due to the formation of complex standards after hydrolysis of the peptides by ZIP, LC-MS analysis was used to give exact identification of each product formed. As mentioned in section 3.5.3.1.3. direct infusion MS analysis, which was initially used preferentially ionised some components over others that led to the failure to identify any product formation post incubation. LC-MS analysis was then chosen to identify each product of hydrolysis (section 2.7.3.2.). Mass spectrometry using electrospray ionisation was used. This enabled the compounds of interest to only become singly charged and so their molecular weight being readily obtained (McMahon *et al.* 2003).

(i) Effects resulting from an increase of the number of residues of the substrate in the  $NH_2$ -terminal direction from the scissile bond are shown in Table 3.4. The enzyme was completely inert towards Pro-AMC and Gly-Pro-AMC. Further elongation at the amino terminal by placing an N-benzyloxycarbonyl (Z) group in the  $P_3$  position resulted in hydrolysis. These results are the same for prolyl oligopeptidase where cleavage will not occur if a free  $\alpha$ -amine exists in the N-terminal sequence Yaa-Pro-Xaa or Pro-Xaa (Cunningham and O'Connor, 1997b). Figure 3.5.1.2. clearly shows that ZIP failed to cleave Z-Pro-Phe, a similar trait of prolyl oligopeptidase (Wilk, 1983). Therefore it seems a strong interaction in the substrate-ZIP complex at the level  $P_3$ - $S_3$  in addition to  $P_1$ - $S_1$  and  $P_2$ - $S_2$  occurs. Interestingly, replacement of the Z group in the peptide Z-Gly-Pro-Ala with a glycine residue seems to prevent

hydrolysis. A bulky hydrophobic residue (Z-group) may be a preference for ZIP in the P<sub>3</sub> position. This interaction at the P<sub>3</sub>-S<sub>3</sub> level may also be the reason for the failure of ZIP to cleave pGlu-His-Pro-AMC, a known substrate of prolyl oligopeptidase. Overall, analysis of substrates with increasing chain length in the NH<sub>2</sub>-terminal direction from residue P<sub>1</sub> reveals that binding of the peptides to ZIP involves interactions between P<sub>1</sub>-S<sub>1</sub>, P<sub>2</sub>-S<sub>2</sub> and P<sub>3</sub>-S<sub>3</sub> and that the minimum hydrolysable peptide size is an N-blocked tripeptide. Initial investigations seem to suggest that the P<sub>3</sub>-S<sub>3</sub> interaction may be a lot more specific in ZIP than prolyl oligopeptidase.

The affinity constant  $K_m$ , for the ZIP catalysed hydrolysis of Z-Gly-Pro-AMC was determined according to section 2.7.1.1. The hydrolysis followed the normal Michaelis-Menten kinetics allowing Lineweaver-Burk, Eadie-Hofstee and Hanes-Woolf kinetic models to be applied to the data. Figures 3.5.2.1. to 3.5.2.3. shows the results obtained when the kinetic data was applied to each model as detailed in section 6.4.1. Table 3.5. presents the calculated constants for ZIP. The  $K_m$  value obtained of 270 $\mu$ M shows the high affinity ZIP has for the substrate Z-Gly-Pro-AMC. This value is much higher though than the  $K_m$  value of 54 $\mu$ M reported previously for ZIP by Birney and O'Connor (2001). Though interestingly Cunningham (1996) reported a  $K_m$  of 267 $\mu$ M for bovine serum ZIP hydrolysis of Z-Gly-Pro-AMC, almost identical to the value obtained in this work.

(ii) It is well established that the specificity of a protease is determined by the nature of the amino acid residues at both sides of the peptide bond subject to hydrolysis. The effect on the ZIP catalysed hydrolysis of Z-Gly-Pro-AMC of proline-containing substrates (section 2.7.1.2.) with variations of amino acid residues located at the carboxyl-terminal site of the scissile bond (position P<sub>1</sub>'), but with a constant sequence of Z-Gly-Pro are shown in Figures 3.5.3.1.1.1. to 3.5.3.1.1.8. and their  $K_i$  (app) values presented in Table 3.6. All peptides inhibited ZIP either in a mixed or non-competitive mode. The lowest  $K_i$  (app) values were obtained for peptides Z-Gly-Pro-Phe and Z-Gly-Pro-Met. The highest  $K_i$  (app) values originated when the charged residues histidine and glutamic acid along with the small hydrophobic alanine residue were in the P<sub>1</sub>' position. Kinetic analysis would therefore seem to show that ZIP has greatest affinity for large hydrophobic residues in the P<sub>1</sub>' position with less affinity for

acidic, basic and small amino acids in this position. These results are rather similar to the preference of prolyl oligopeptidase for a hydrophobic residue in the P<sub>1</sub>' position with lower specificities for basic and acidic (Koida and Walter, 1976).

As outlined in section 2.7.2. RP HPLC was performed for peptide digest separations in order to evaluate the ability of ZIP to hydrolyse the peptides outlined in Table 3.7., determination of the cleavage point and the effect, as discussed for the kinetic analysis, of the amino acid variation in the P<sub>1</sub>' position on hydrolysis. Figures 3.5.3.1.2.1. to 3.5.3.1.2.16. are chromatograms showing the hydrolysis of each peptide by ZIP. A common product peak is obvious for each peptide except in the case of the hydrolysis of Z-Gly-Pro-Glu. This common product peak corresponds to the peak for the standard Z-Gly-Pro shown in Figure 3.5.3.1.2.17. The definite identification of this product peak as Z-Gly-Pro for each peptide hydrolysed is shown by LC-MS analysis in Figures 3.5.3.1.3.1. to 3.5.3.1.3.7. Quantification of the amount of Z-Gly-Pro formed in each case is evaluated in Table 3.7. The most hydrolysis seemed to take place with phenylalanine in the P<sub>1</sub>' position, whereas it is obvious as shown in Figure 3.5.3.1.2.10. that when glutamic acid occupied the P<sub>1</sub>' position, hydrolysis took place at a negligible rate making quantification impossible, though LC-MS analysis (Figure 3.5.3.1.3.5.) did show hydrolysis took place.

(iii) Taking peptides with phenylalanine and methionine in the P<sub>1</sub>' position as explained, the effect of further chain elongation on the carboxyl-terminal site to include P<sub>2</sub>', P<sub>3</sub>' and P<sub>4</sub>' on the ZIP catalysed hydrolysis of Z-Gly-Pro-AMC was evaluated as outlined in section 3.5.3.2.1. Table 3.8. presents the K<sub>i (app)</sub> values obtained and the mode of inhibition observed. A 2-fold increase in affinity was observed in going from Z-Gly-Pro-Phe to Z-Gly-Pro-Phe-His i.e. to include P<sub>2</sub>' position. An affinity constant of 206μM obtained for Z-Gly-Pro-Phe-His is even greater than the K<sub>m</sub> of 270μM obtained for ZIP using Z-Gly-Pro-AMC. Quantification of Z-Gly-Pro formed after hydrolysis of Z-Gly-Pro-Phe-His by ZIP (Figure 3.5.3.2.2.2.), identified according to Figure 3.5.3.2.3.1. is shown in Table 3.9. There is almost a 7-fold increase in the amount of Z-Gly-Pro formed when the P<sub>2</sub>' position is occupied. However, addition of residues in locations P<sub>3</sub>' and P<sub>4</sub>' caused an increase in K<sub>i (app)</sub> values (Table 3.6.), therefore showing a decrease in affinity of ZIP for elongated peptides beyond P<sub>2</sub>' position. Table 3.9. also shows a decrease in the

amount of Z-Gly-Pro formed with peptide elongation beyond the P<sub>2</sub>' position. An interesting feature showed that ZIP seemed to have a better affinity and hydrolysed peptides to a greater extent when multiple substrate-binding sites are occupied. So overall the important interactions in the substrate-ZIP complex at the carboxyl site of the substrate cleavage point seems to involve P<sub>1</sub>'-S<sub>1</sub>' and P<sub>2</sub>'-S<sub>2</sub>'.

(iv) Extensive studies on the importance of the P<sub>1</sub> proline residue in catalysis by prolyl oligopeptidase are well reported. These studies conclude that the S<sub>1</sub> subsite is designed specifically to fit proline but tolerates other residues carrying substituent groups provided they do not exceed the size of prolines pyrrolidine ring (Nomura, 1986; Makinen *et al.* 1994; Kreig and Wolfe, 1995). Therefore it was paramount to study the importance of the P<sub>1</sub>-S<sub>1</sub> interaction in ZIP catalysis. It was decided due to the high affinity of ZIP for Z-Gly-Pro-Phe-His, to replace the P<sub>1</sub> proline residue with leucine in this peptide. Replacement of the proline residue with leucine in the primary specificity position (P<sub>1</sub>) caused a 7-fold decrease in affinity of ZIP for this peptide as shown in Table 4.0. Analysis of hydrolysis of Z-Gly-Leu-Phe-His by RP HPLC described in section 3.5.4.2. is presented in Figure 3.5.4.2.2. There seems to be the slightest formation of a Z-Gly-Leu product peak after incubation but as shown in Figure 3.5.4.3., LC-MS analysis failed to detect any peak with mass corresponding to the formation of a Z-Gly-Leu product. Therefore, it is evident that the S<sub>1</sub> subsite of ZIP, like prolyl oligopeptidase, is more than likely also designed to specifically fit a proline residue.

In summary, these results suggest that ZIP has an extended substrate-binding region in addition to the primary specificity site, S<sub>1</sub>. Its possible it is comprised of three sites located at the amino-terminal site (S<sub>1</sub>, S<sub>2</sub>, S<sub>3</sub>) and two sites at the carboxyl site from the scissile bond (S<sub>1</sub>' and S<sub>2</sub>'). Regarding these subsites the S<sub>1</sub>' position has a preference for a bulky hydrophobic residue along with the S<sub>3</sub> subsite. An imino acid residue (proline) in the P<sub>1</sub> position is absolutely necessary and a tetrapeptide P<sub>3</sub>P<sub>2</sub>P<sub>1</sub>P<sub>1</sub>' is the minimum hydrolysable peptide size. Further increase in substrate chain length beyond the P<sub>2</sub>' position causes a continuous decrease in ZIP affinity and hydrolysis ability for substrates. The kinetic, RP HPLC and LC-MS data on the substrate specificity of ZIP suggests it's extremely similar to that of prolyl oligopeptidase.



#### **4.7. Partial Purification of Prolyl Oligopeptidase From Bovine Serum**

Prolyl oligopeptidase from bovine serum was partially purified as outlined in section 2.8. This enabled comparative work to be completed in inhibitor and immunological studies with ZIP. Enzyme assays for prolyl oligopeptidase were performed, as for the determination of ZIP activity, explained in section 2.4.2. The only difference was the addition of DTT in substrate preparation as outlined in section 2.4.1.

##### **4.7.1. Phenyl Sepharose Hydrophobic Interaction Chromatography I**

The first step in prolyl oligopeptidase purification from bovine serum is the exact step discussed in section 4.4.1. for the isolation of ZIP. Indeed this step is extremely important in the purification of both peptidases in that it separates both activities from each other in crude serum along with purifying each to some extent.

The elution profile of prolyl oligopeptidase during hydrophobic interaction chromatography I is shown in Figure 3.6.1. The first activity peak shown, which runs through the column is prolyl oligopeptidase, shown in Figure 3.3.2.2. It is likely that the retention of over 98% activity is due to the enzyme not binding to the column but running through, but only a 3.2-fold purification factor resulted due to up to 534mg of protein also running through with the prolyl oligopeptidase activity.

##### **4.7.2. Phenyl Sepharose Hydrophobic Interaction Chromatography II**

As the first chromatography step in the purification of prolyl oligopeptidase was basically applied to separate both ZIP and PO activities, a second hydrophobic interaction chromatography column was used for further purification. The higher ammonium sulphate concentration (1M) during the running of this second hydrophobic interaction chromatography column allowed for binding of prolyl oligopeptidase. Prolyl oligopeptidase activity eluted during a linear decreasing ammonium sulphate concentration gradient as shown in Figure 3.6.2. Compared to ZIP the instability of prolyl oligopeptidase was a huge factor during the purification.

As shown in Table 4.2. a loss of almost 80% applied activity occurred during this purification step alone. This was extremely significant considering the loss of only 2% for the first hydrophobic interaction chromatography step. The 95% decrease in protein was significant in obtaining a 14.4-fold purification factor for this step. The

concentration and addition of ammonium sulphate to the sample prior to chromatography and the removal of that amount of contaminating protein were possibly detrimental to activity leading to only 20.17% overall biological activity remaining after only two purification steps. It is interesting to note that serum prolyl oligopeptidase has been reported to be rather unstable during purification (Cunningham and O'Connor, 1998; Dowling, 1998).

#### **4.7.3. Cibacron Blue 3GA Chromatography**

Preliminary investigation of the post phenyl sepharose II sample on SDS PAGE gels showed the presence of a major band corresponding to BSA. The employment of this resin was hoped to remove any BSA present in the sample and purify prolyl oligopeptidase to a greater extent. Prolyl oligopeptidase failed to bind to the cibacron blue resin, which is the direct opposite to ZIP, as shown in Figure 3.6.3. Up to 44% applied activity was retained and even though the enzyme failed to bind it was removed from contaminating protein substantially with an 83% reduction in protein achieved.

An overall 36.45-fold purification factor along with almost 9% retention of biological activity was deemed rather effective for only a partial purification of prolyl oligopeptidase from bovine serum.

### **4.8. Inhibitor Studies**

#### **4.8.1. Catalytic Classification**

Sensitivity to specific active site directed inhibitors along with amino acid sequence analysis is frequently investigated to determine the catalytic class of an enzyme. ZIP has been previously classified as a serine protease due to inhibition by the classic serine protease inhibitors, 4-(2-aminoethyl)-benzenesulphonyl fluoride (AEBSF) and aprotinin. Interestingly, AEBSF even at a concentration of 22.5mM only gave 58% inhibition. It was also reported that 4-amidino-phenylmethanesulphonyl fluoride (APMSF), a reportedly specific, irreversible serine protease inhibitor and the reversible serine protease inhibitor phenylmethyl-sulphonyl fluoride (PMSF) failed to inhibit ZIP (Birney and O'Connor, 2001). It is known that enzymes are often classified as serine proteases despite not exhibiting sensitivity towards all of the

possible active site directed serine protease inhibitors. Many factors may contribute to this with one reason possibly due to active site serine being the target for these studies and inaccessibility by steric hindrance may prevent inhibition.

Prolyl oligopeptidase is classified as a serine protease based on its sensitivity towards inhibitors such as DFP and PMSF (Rennex *et al.* 1991). Goosens *et al.* (1995) reported inhibition of prolyl oligopeptidase by DFP and PMSF but resistance to aprotinin, whereas Yoshimoto *et al.* (1983) reported complete inhibition of prolyl oligopeptidase by DFP yet none by PMSF. To finally catalytically classify ZIP as a serine protease, the irreversible and classic serine protease inactivator DFP (Barrett, 1994) was employed as outlined in section 2.9.1. Figure 3.7.1. illustrates the inhibition of ZIP by DFP with an  $IC_{50}$  value of 100nM being obtained. This shows the high specificity of DFP for the catalytic serine of ZIP, thus catalytically classifying this enzyme as a possible serine protease.

#### **4.8.2. Effect of Specific Prolyl Oligopeptidase Inhibitors**

Prolyl oligopeptidase specific inhibitors are commonly used to investigate the enzymes physiological effect in the body. Several studies have pointed out the potential therapeutic relevance of prolyl oligopeptidase inhibitors as memory promoting drugs, which is possibly attributable to the protection of various neuropeptides against degradation by prolyl oligopeptidase (Shinoda *et al.* 1996 and 1999; Marighetto *et al.* 2000; Bellemere *et al.* 2003).

In general, specific inhibitors are synthesised to bind to the enzymes active site, so these inhibitors interact with the enzyme in a substrate-like manner and restrict changes to the active site. Therefore, prolyl oligopeptidase inhibitors are in general very specific because of the proline residue in the  $P_1$  position and the substrate-like peptide structure (e.g. Z-Pro-prolinal). Due to the near identical substrate specificity requirements of both enzymes, it is most intriguing that ZIP is totally insensitive to the prolyl oligopeptidase inhibitor Z-Pro-prolinal (Cunningham and O'Connor, 1997a).

A number of prolyl oligopeptidase specific inhibitors were incubated with purified ZIP to determine any possible inhibitory effect; partial purified prolyl oligopeptidase was also assayed for comparison (section 2.9.2.). As highlighted in Table 3.13. all inhibitors tested had little or no inhibitory effect on ZIP activity. On the other hand,

partial purified prolyl oligopeptidase was extremely sensitive to all inhibitors;  $IC_{50}$  values are listed in Table 3.13. JTP-4819 and Fmoc-Ala-PyrrCN were the most potent inhibitors tested towards prolyl oligopeptidase with  $IC_{50}$  values of 0.8nM and 1.5nM respectively.

Fmoc-Ala-PyrrCN interacts with prolyl oligopeptidase in a substrate-like manner and restricts changes to its active site. This inhibitor is cell permeable, has no inhibitory effect towards dipeptidyl peptidase IV and a  $K_i$  value of 5nM is reported for brain prolyl oligopeptidase (Li *et al.* 1996). This inhibitor was seen to potently inhibit serum prolyl oligopeptidase with an  $IC_{50}$  of 1.5nM (Figure 3.7.2.1.), which is greater than the 10nM obtained by Dowling (1998). As illustrated in Figure 3.7.2.2. this inhibitor had no effect whatsoever on ZIP activity.

Z-Phe-Pro-Benzothiazol, SR 063125 and SR 063298 are all Z-Pro-prolinal derivatives. The structures of the latter two are shown in Figure 4.3. They were all found to be relatively potent inhibitors of prolyl oligopeptidase with Z-Phe-Pro-Benzothiazol giving an  $IC_{50}$  of 45nM. Figures 3.7.2.5. and 3.7.2.7. show the inhibition of prolyl oligopeptidase with SR 063298 and SR 063125, resulting in similar  $IC_{50}$  values of 90nM and 100nM respectively. Again no significant inhibition was observed by each of these three inhibitors towards ZIP activity.

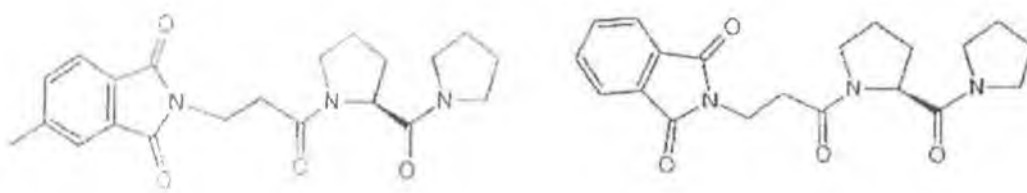


**Figure 4.3. Chemical Structures of SR 063125 and 063298**

Toide *et al.* (1995a) reported JTP-4819 as a potent and highly specific inhibitor of prolyl oligopeptidase, with no effect on other related proline specific enzymes. The therapeutic potential of JTP-4819 has been investigated due to its known pharmacological actions. One of these main actions is its inhibition of prolyl oligopeptidase mediated degradation of neuropeptides in rat brain thus linking it

possibly to ameliorating memory impairment in rats (Toide *et al.* 1995b and 1997b; Shinoda *et al.* 1996 and 1999). An  $IC_{50}$  value of 0.8nM was achieved towards partial purified prolyl oligopeptidase as outlined in Table 3.13 and shown in Figure 3.7.2.9. This shows the potency of this inhibitor towards prolyl oligopeptidase from bovine serum, the 0.8nM obtained being remarkably similar to the  $IC_{50}$  value of 0.83nM reported by Toide *et al.* (1995a) towards rat brain supernatant prolyl oligopeptidase. More importantly, as shown in Figure 3.7.2.10. ZIP remained completely resistant to inhibition by JTP-4819. This shows the advantage of using JTP-4819 as the optimum inhibitor for detection of ZIP alone in crude samples, like serum as explained in section 2.4.3. Also, as discussed (section 4.6.) ZIP and prolyl oligopeptidase seem to share very similar substrate specificity, so the total prevention of neuropeptide degradation using JTP-4819 may be futile due to the total resistance of ZIP towards this specific prolyl oligopeptidase inhibitor.

#### **4.9. Immunological Studies**

An anti-human prolyl oligopeptidase antibody was used as described in section 2.10. to check for immunological cross reactivity with purified ZIP and partial purified prolyl oligopeptidase. The antibody was raised when rabbits were immunized with a peptide containing the N-terminal prolyl oligopeptidase sequence of residues 10-25. Figure 3.8.1.1. shows no cross reactivity whatsoever with purified ZIP, once more showing a complete difference to prolyl oligopeptidase this time with respect to immunological characteristics.

Interestingly, also in Figure 3.8.1.1. partial purified prolyl oligopeptidase from bovine serum showed no cross-reactivity with anti-human brain prolyl oligopeptidase. A more concentrated prolyl oligopeptidase sample was used as shown in Figure 3.8.1.2A, which showed some cross reactivity, albeit at a higher molecular weight location than expected as bovine serum prolyl oligopeptidase is reported to be ~ 70kDa (Cunningham and O'Connor, 1998). Therefore it is more than likely just non-specific reactivity. This is rather interesting when one considers the N-terminal residues 10-25 of prolyl oligopeptidase from a host of mammals as below.

Human	<sup>10</sup> YRDETAVQDYHGHKIC <sup>25</sup>
Bovine	YRDETAVQDYHGHKIC
Rat	YRDETSVQDYHGHKIC
Mouse	YRDETSVQEYHGHKIC

Careful examination of the sequence 10-25 shows no difference whatsoever between human and bovine sequence. The rat sequence shows one slight change in position 15 but as shown in Figure 3.8.1.2.B, it is recognised by the anti-human prolyl oligopeptidase antibody. This is unusual when the human and bovine sequences are identical but as shown no cross reactivity occurs between the antibody and the prepared prolyl oligopeptidase from bovine serum. Even though Cunningham and O'Connor (1998) describe the biochemical characteristics of bovine serum prolyl oligopeptidase as identical to its cytosolic counterpart, no sequence data is available for this serum prolyl oligopeptidase to date. So either there wasn't enough sample present to cross-react with the antibody or more interestingly this serum prolyl oligopeptidase displays distinct immunological characteristics to its cytosolic counterpart.

#### **4.10. Identification of Z-Pro-prolinal Insensitive Peptidase (ZIP)**

The linear order of amino acids in a protein chain (primary structure) ultimately determines the three-dimensional structure required for active biological function. It was therefore very important to obtain sequence data by N-terminal or internal sequencing and so ultimately identify the protein/protease responsible for this second Z-Gly-Pro-AMC hydrolysing activity in bovine serum.

Initial analysis of ZIP using N-terminal sequencing as outlined in section 3.9.1. failed to identify this protease. As shown in Figure 3.4.2.2. purification using a starting volume of 20ml of serum resulted in extremely low levels of protein present just possibly visible using silver staining. It was deemed necessary, for successful sequence analysis, to provide a coomassie-stained band on a PVDF blot. To obtain this band a larger scale purification was necessary. This resulted (Figure 3.9.1.1.) in multiple bands present on the stained blot but also the possible band of interest located near the 98kDa marker was very faint, with protein detection level too low for sequencing. Due to only one reference available on the molecular weight of this

protein and its subsequent location on denaturing PAGE, the two major bands on the blot were sequenced just for clarification. Sequence analysis of the major bands present identified BSA just above the 52kDa but the band located below this marker was N-terminally blocked so no sequence data was obtained.

A partial purification over three columns was performed in the hope of obtaining more target protein for sequencing as outlined in section 3.9.1. Internal sequencing by digestion of target protein band with trypsin, purification of the resulting peptides and subsequent sequencing and identification, of the N-blocked protein mentioned earlier and shown in Figure 3.9.1.2. resulted in the identification of bovine heavy chain IgG along with six other proteins. All other sequence data obtained had no link to the protease activity of ZIP. Attempts at internal sequencing of the two faint bands located below the 97kDa marker (Figure 3.9.2.1.) resulted in too low a protein level for peptide detection after digestion and subsequent sequence analysis.

The main difficulties presented in trying to obtain sequence data via these methods were a) making sure adequate target protein was present on gel/blot, b) unsure exact location of this protein on denaturing PAGE and c) large volume of starting material for purification, especially in this case with serum, resulting in multiple contaminants present. Therefore it was impossible, especially without a specific antibody to recognise ZIP, to locate, sequence and finally identify this protein using samples from SDS PAGE gels under denaturing conditions.

An in gel (zymogram) assay was developed and optimised using highly concentrated active ZIP sample as outlined in section 2.11.2. and shown in Figure 3.9.2.1. This activity assayed allowed the correct protein of interest be located precisely in its native form and subsequent sequencing performed. As explained (section 3.9.2.), initial analysis of an excised fluorescent band revealed the presence of both IgG and fibronectin in the sample. IgG was just co-migrating with ZIP on the native gel, whereas fibronectin at first possibly could have been involved in the protease activity of ZIP. Planchenault *et al.* (1990) have reported potential proteolytic activity of human plasma fibronectin. Therefore gelatin sepharose was employed (section 2.11.2.4.) to remove this protein. ZIP activity failed to bind to the resin, thus showing that fibronectin was also a contaminant protein co-migrating with ZIP.

As outlined in section 3.9.2. four separate 20ml purifications were performed; with the resulting ZIP activity from each purification pooled, concentrated and further chromatography performed using the affinity resin protein G, to remove IgG and finally gelatin sepharose for the removal of fibronectin. The final sample was run on a large native PAGE gel, viewed under U.V. light (Figure 3.9.2.2.) and the resulting fluorescent band excised. This band was digested and the resultant peptides purified and individually sequenced at the Harvard University, Microchemistry Facility. Correlation of these sequenced peptides with known proteins identified ZIP protein as seprase (Figure 3.9.2.3.).

Seprase, a known serine protease is a member of the serine integral membrane peptidases. The most interesting feature of these serine integral peptidases is their specificity for cleavage of proline containing peptides and macromolecules (Chen *et al.* 2003). Seprase is a gelatinolytic endopeptidase due to its ability to cleave gelatin (Aoyama and Chen, 1990; Pineiro-Sanchez *et al.* 1997). A purified ZIP sample was run on a gelatin gel and an area of digestion was seen (results not shown). Even though it is not reported to date, it is possible that seprase hydrolyses gelatin at its many proline residues.

The detection assays for seprase activity available to date are gelatinase zymography or the detection of digested fragments of radiolabelled gelatin (Kelly, 1999). The use of Z-Gly-Pro-AMC as substrate in conjunction with a specific prolyl oligopeptidase inhibitor would provide a simple, rapid and sensitive assay for detection of this protease activity. As reported by Monsky *et al.* (1994) and Kelly *et al.* (1998) seprase is overexpressed by invasive tumour cells therefore, our specific assay may be highly valuable for early detection of elevated seprase activity levels in serum due to the onset of tumour progression. Also, there are no specific inhibitors available to date for seprase, so knowledge of this enzymes subsite specificity as detailed earlier (section 4.6.) may be very significant in the design of specific inhibitors for the enzyme and so possibly clarifying its role in tumour cell invasion.



	<b>ZIP</b>	<b>Seprase</b>
<b>MW (Native) kDa</b>	174*	170
<b>MW (Monomer) kDa</b>	95-96	97
<b>pI</b>	5.68*	~5
<b>pH (Optima)</b>	7.4-8.0*	7.8
<b>Assay Temp. (°C)</b>	37*	37
<b>Catalytic Type</b>	Serine protease*	Serine protease
<b>Reaction Catalysed</b>	Endopeptidase*, proline specific	Endopeptidase, proline specific ?
<b>Inhibitors</b>	DFP, AEBSF*	DFP, AEBSF
<b>Gelatinase activity</b>	Yes	Yes
<b>Reference</b>	*Birney and O'Connor, 2001	Pineiro-Sanchez <i>et al.</i> 1997

**Table 4.2. Comparison of Some Biochemical Properties of both Enzymes**

## **BIBLIOGRAPHY**

## 5.0. Bibliography

-A-

Abbott, C.A., Baker, E., Sutherland, G.R. and McCaughan, G.W. (1994) Genomic organization, exact localization, and tissue expression of the human CD26 (dipeptidyl peptidase IV) gene. *Immunogenetics* **40**, 331-338.

Abbott, C.A. and Gorrell, M.D. (2002) The Family of CD26/DPIV and Related Ectopeptidases. The DPIV Family. In: *Ectopeptidases: CD13/Aminopeptidase N and CD26/Dipeptidylpeptidase IV in Medicine and Biology*. (Langner, J. and Ansorge, S. eds.) Kluwer Academic/Plenum Publishers, New York. pp 171-195.

Abbott, C.A., McCaughan, G.W., Levy, M.T., Church, W.B. and Gorrell, M.D. (1999) Binding to human dipeptidyl peptidase IV by adenosine deaminase and antibodies that inhibit ligand binding involves overlapping, discontinuous sites on a predicted  $\beta$  propeller domain. *European Journal of Biochemistry* **266**, 798-810.

Ashall, F. (1990) Characterisation of an alkaline peptidase of *Trypanosoma cruzi* and other trypanosomatids. *Molecular and Biochemical Parasitology* **38**, 77-88.

Ashall, F., Harris, D., Roberts, H., Healy, N. and Shaw, E. (1990) Substrate specificity and inhibitor sensitivity of a trypanosomatid alkaline peptidase. *Biochimica et Biophysica Acta* **1035**, 293-299.

Aoyagi, T., Nagai, M., Ogawa, K., Kojima, F., Okada, M., Ikeda, T., Hamada, M. and Takeuchi, T. (1991) Postatin: A New Inhibitor of Prolyl Endopeptidase, Produced by *Streptomyces viridochromogenes* MH534-30F3, I: Taxonomy, Production, Isolation, Physico-Chemical Properties and Biological Activities. *Journal of Antibiotics* **44**(9), 949-955.

Aoyama, A. and Chen, W-T. (1990) A 170-kDa membrane-bound protease is associated with the expression of invasiveness by human malignant melanoma cells. *Proceedings of the National Academy of Science, USA* **87**, 8296-8300.

**-B-**

Bakker, A. V., Daffeh, J., Jung, S., Vincent, L.A., Nagel, A.A., Spencer, R.W., Vinick, F.J. and Faraci, W.S. (1991) Novel *in Vitro* and *in Vivo* Inhibitors of Prolyl Endopeptidase. *Bioorganic and Medicinal Chemistry Letters* **1**(11), 585-590.

Bakker, A. V., Jung, S., Spencer, R.W., Vinick, F.J. and Faraci, S. (1990) Slow Tight-Binding Inhibition of Prolyl Endopeptidase by Benzyloxycarbonyl-Prolyl-Proline. *Biochemical Journal* **271**, 559-562.

Barrelli, H., Petit, A., Hirsch, E., Wilk, S., De Nanteuil, G., Morain, P. and Checler, F. (1999) S-17092-1, a Highly Potent, Specific and Cell Permeable Inhibitor of Human Proline Endopeptidase. *Biochemical and Biophysical Research Communications* **257**(3), 657-661.

Barrett, A.J. (1994) Classification of Peptidases. *Methods in Enzymology* **244**, 1-15.

Barrett, A.J., Rawlings, N.D. & Woessner, J.F. (1998) Handbook of Proteolytic Enzymes. Academic Press, London.

Barrett, A.J. and Rawlings, N.D. (1992) Oligopeptidases, and the Emergence of the Prolyl Oligopeptidase Family. *Biological Chemistry Hoppe-Seyler* **373**, 353-360.

Bellemere, G., Morain, P., Vaudry, H. and Jegou, S. (2003) Effect of S 17092, a novel prolyl endopeptidase inhibitor on substance P and  $\alpha$ -melanocyte-stimulating hormone breakdown in the rat brain. *Journal of Neurochemistry* **84**, 919-929.

Bernardi, G., Giro, M-G. and Gaillard, C. (1972) Chromatography of Polypeptides and Proteins on Hydroxyapatite Columns: Some New Developments. *Biochimica et Biophysica Acta* **278**, 409-420.

Birney, Y. (2000) PhD Thesis, Dublin City University.

Birney, Y.A. and O'Connor, B.F. (2001) Purification and Characterisation of a Z-Pro-prolinal-Insensitive Z-Gly-Pro-7-amino-4-methyl Coumarin hydrolyzing Peptidase from Bovine Serum. A New Proline-Specific Peptidase. *Protein Expression and Purification* **22**, 286-298.

Blum, H., Beir, H. and Gross, H.J. (1987) Improved silver staining of plant proteins, RNA and DNA in polyacrylamide gels. *Electrophoresis* **8**, 93-99.

Bongers, J., Lambros T., Ahmad, M. and Heimer, E.P. (1992) Kinetics of dipeptidyl peptidase IV proteolysis of growth hormone-releasing factor and analogs. *Biochimica et Biophysica Acta* **1122**, 147-153.

Burleigh, B.A. and Andrews, N.W. (1998) Signalling and host cell invasion by *Trypanosoma cruzi*. *Current Opinion in Microbiology* **1**, 461-465.

Burleigh, B.A. and Andrews, N.W. (1995) A 120-kDa Alkaline Peptidase from *Trypanosoma cruzi* Is Involved in the Generation of a Novel  $Ca^{2+}$ -signaling Factor for Mammalian Cells. *The Journal of Biological Chemistry* **270**(10), 5172-5180.

Burleigh, B.A., Caler, E.V., Webster, P. and Andrews, N.W. (1997) A Cytosolic Serine Endopeptidase from *Trypanosoma cruzi* Is Required for the Generation of  $Ca^{2+}$  Signaling in Mammalian Cells. *The Journal of Cell Biology* **136**(3), 609-620.

Burleigh, B.A. and Woolsey, A.M. (2002) Cell Signalling and *Trypanosoma cruzi* invasion. *Cellular Microbiology* **4**(11), 701-711.

-C-

Caler, E.V., Morty, R.E., Burleigh, B.A. and Andrews, N.W. (2000) Dual Role of Signaling Pathways Leading to  $Ca^{2+}$  and Cyclic AMP Elevation in Host Cell Invasion by *Trypanosoma cruzi*. *Infection and Immunity* **68**(12), 6602-6610.

Caler, E.V., de Avalos, S.V., Haynes, P.A., Andrews, N.W. and Burleigh, B.A. (1998) Oligopeptidase B-dependent signalling mediates host cell invasion by *Trypanosoma cruzi*. *The EMBO Journal* **17**(17), 4975-4986.

Camargo, A.C., Caldo, H. and Reis, M.L. (1979) Susceptibility of a Peptide Derived from Bradykinin to Hydrolysis by Brain Endo-Oligopeptidases and Pancreatic Proteinases. *The Journal of Biological Chemistry* **254**(12), 5304-5307.

Camargo, A.C.M., Almeida, M.L.C. and Emson, P.C. (1984), Involvement of Endo-Oligopeptidases A and B in the Degradation of Neurotensin by Rabbit Brain, *Journal of Neurochemistry*, **42**(6), 1758-1761.

Checler, F., Vincent, J.P. and Kitabgi, P. (1986) Purification and Characterisation of a Novel Neurotensin-Degrading Peptidase from Rat Brain Synaptic Membranes. *The Journal of Biological Chemistry* **261**(24), 11274-11281.

Chen, W-T., Kelly, T. and Ghersi, G. (2003) DPPIV, Seprase, and Related Serine Peptidases in Multiple Cellular Functions. *Current Topics in Developmental Biology* **54**, 207-231.

Chevallier, S., Goeltz, P., Thibault, P., Banville, D. and Gagon, J. (1992) Characterization of a Prolyl Endopeptidase From *Flavobacterium meningosepticum*: Complete Sequence and Localization of the Active-Site Serine. *The Journal of Biological Chemistry* **267**(12), 8192-8199.

Cunningham, D. (1996) PhD Thesis, Dublin City University.

Cunningham, D.F. and O'Connor, B.F. (1997a) Identification and initial characterization of a N-benzyloxycarbonyl-prolyl-prolinal (Z-Pro-prolinal)-insensitive 7-(N-benzyloxycarbonyl-glycyl-prolyl-amido)-4-methylcoumarin (Z-Gly-Pro-NH-Mec)-hydrolysing peptidase in bovine serum. *European Journal of Biochemistry* **244**, 900-903.

Cunningham, D.F. and O'Connor, B.F., (1997b) Proline Specific Peptidases. *Biochimica et Biophysica ACTA* **1343**, 160-186.

Cunningham, D.F. and O'Connor, B.F., (1998) A study of prolyl endopeptidase in bovine serum and its relevance to the tissue enzyme. *Biochemistry and Cell Biology* **00**, 1-16.

**-D-**

Darmoul, D., Lacasa, M., Baricault, M., Marguet, D., Sapin, C., Trotot, P. (1992) Dipeptidyl peptidase IV (CD26) gene expression in enterocyte-like colon cancer cell lines HT-29 and Caco-2. Cloning of the complete human coding sequence and changes of dipeptidyl peptidase IV mRNA levels during cell differentiation. *The Journal of Biological Chemistry* **267**, 4824-4833.

David, F., Bernard, A.M., Pierres, M. and Marguet, D. (1993) Identification of Serine 624, Aspartic Acid 702, and Histidine 734 as the Catalytic Triad Residues of Mouse Dipeptidyl-peptidase IV (CD26). A member of a novel family of nonclassical serine hydrolases. *The Journal of Biological Chemistry* **268**(23), 17247-17252.

De Meester, I., Belyaev, A., Lambeir, A-M., De Meyer, G.R.Y., Van Osselaer, N., Haemer, A. and Scharpe, S. (1997) In Vivo Inhibition of Dipeptidyl peptidase IV Activity by Pro-Pro-diphenyl-phosphonate (Prodipine). *Biochemical Pharmacology* **54**, 173-179.

De Meester, I., Korom, S., Van Damme, J. and Scharpe, S. (1999) CD26, let it cut or cut it down. *Immunology Today* **20**(8), 367-375.

De Meester, I., Vanhoof, G., Hendriks, D., Demuth, H-U., Yaron, A. and Scharpe, S. (1992) Characterisation of dipeptidyl peptidase IV (CD26) from human lymphocytes. *Clinica Chimica Acta* **210**, 23-34.

De Meester, I., Vanhoof, G., Lambeir, A-M. and Scharpe, S. (1996) Use of immobilised adenosine deaminase (EC 3.5.4.4) for the rapid purification of native human CD26/dipeptidyl peptidase IV (EC 3.4.14.5). *Journal of Immunological Methods* **189**, 99-105.

Demuth, H-U., Baumgrass R., Schaper, C., Fischer, G. and Barth, A. (1988) Dipeptidyl peptidase IV-Inactivation with *N*-Peptidyl-*O*-Aroyl Hydroxlamines. *Journal of Enzyme Inhibition* **2**, 129-142.

De Wied, D., Gaffori, O., van Ree, J.M. and de Jong, W. (1984) Central target for the behavioural effects of vasopressin neuropeptides. *Nature* **308**, 276-277.

Diefenthal, T., Dargatz, H., Witte, V., Reipen, G. and Svendsen, I. (1993) Cloning of proline-specific endopeptidase gene from *Flavobacterium meningosepticum*: expression in *Escherichia coli* and purification of the heterologous protein. *Applied Microbiology and Biotechnology* **40**, 90-97.

Dobers, J., Grams, S., Reutter, W. and Fan, H. (2000) Roles of cysteines in rat dipeptidyl peptidase IV/CD26 in processing and proteolytic activity. *European Journal of Biochemistry* **267**, 5093-5100.

Dobers, J., Zimmermann-Kordmann, M., Leddermann, M., Schewe, T., Reutter, W. and Fan, H. (2002) Expression, purification, and characterization of human dipeptidyl peptidase IV/CD26 in Sf9 insect cells. *Protein Expression and Purification* **25**, 527-532.

Donlon, J. and Kaufman, S. (1980) Relationship Between the Multiple Forms of Rat Hepatic Phenylalanine Hydroxylase and Degree of Phosphorylation. *The Journal of Biological Chemistry* **255**(5), 2146-2152.

Dowling, O. (1998) PhD Thesis, Dublin City University.

Dunn, M.J. (1989), Initial Planning. In: *Protein Purification Methods-A Practical Approach*. (Harris, E.L.V. and Angal, S. eds.) IRL Press, Oxford. pp 10-15.

Durand, A., Villard, C., Giardina, T., Perrier, J., Juge, N. and Puigserver A. (2003) Structural Properties of Porcine Intestine Acylpeptide Hydrolase. *Journal of Protein Chemistry* **22**(2), 183-191.



Durinx, C., Lambeir, A.M., Bosmans, E., Falmagne, J-B., Berghmans, R., Haemers, A., Scharpe, S. and De Meester, I. (2000) Molecular characterization of dipeptidyl peptidase activity in serum. Soluble CD26/dipeptidyl peptidase IV is responsible for the release of X-Pro dipeptides. *European Journal of Biochemistry* **267**, 5608-5613.

Dresdner, K., Barker, L.A., Orlowski, M. and Wilk S. (1982) Subcellular Distribution of Prolyl Endopeptidase and Cation-Sensitive Neutral Endopeptidase in Rabbit Brain. *Journal of Neurochemistry* **38**(4), 1151-1154.

Drucker, D.J. (2003) Therapeutic potential of dipeptidyl peptidase IV inhibitors for the treatment of type 2 diabetes. *Expert Opin. Invest. Drugs* **12**(1), 87-100.

**-E-**

Engel, M., Hoffman, T., Wagner, L., Wermann, M., Heiser, U., Kiefersauer, R., Huber, R., Bode, W., Demuth, H-U. and Brandstetter, H. (2003) The crystal structure of dipeptidyl peptidase IV (CD26) reveals its functional regulation and enzymatic mechanism. *Biochemistry* **100**(9), 5063-5068.

**-F-**

Feese, M., Scaloni, A., Jones, W.M., Manning, J.M. and Remington, S.J. (1993) Crystallization and Preliminary X-ray Studies of Human Erythrocyte Acylpeptide Hydrolase. *Journal of Molecular Biology* **233**, 546-549.

Fink, A.L. (1987) Acyl Group Transfer-The Serine Proteinases, In: *Enzyme Mechanisms*. (Page, M.I. and Williams, A. ed.), Royal Society of Chemistry. pp. 159-177.

Fischer, G., Heins, J. and Barth, A. (1983) The Conformation Around the Peptide Bond Between the P<sub>1</sub>- and P<sub>2</sub>-Positions is Important for Catalytic Activity of Some Proline-Specific Proteases. *Biochimica et Biophysica Acta* **742**, 452-462.

Fleisher, B. (1994) CD26: a surface protease involved in T-cell activation. *Immunology Today* **15**(4), 180-184.

Flentke, G., Munoz, E., Huber, B., Plaut, A.G., Kettner, C.A. and Bachovchin, W.W. (1991) Inhibition of dipeptidyl aminopeptidase IV (DP-IV) by Xaa-boroPro dipeptides and use of these inhibitors to examine the role of DP-IV in T-cell function. *Proceedings of the National Academy of sciences, USA* **88**, 1556-1559.

Friedman, T.C., Orłowski, M. and Wilk, S. (1984) Prolyl Endopeptidase: Inhibition In Vivo by N-Benzylloxycarbonyl-Prolyl-Prolinal. *Journal of Neurochemistry* **42**(1), 237-241.

Fulop, V., Bocskei, Z., and Polgar, L. (1998) Prolyl oligopeptidase: an unusual  $\beta$ -propeller domain regulates proteolysis. *Cell* **94**, 161-170.

Fulop, V., Szeltner, Z., Renner, V. and Polgar, L. (2001) Structures of Prolyl Oligopeptidase Substrate/ Inhibitor Complexes: use of inhibitor binding for titration of the catalytic histidine residue. *The Journal of Biological Chemistry* **276**(2), 1262-1266.

Fulop, V., Szeltner, Z. and Polgar, L. (2000) Catalysis of serine oligopeptidases is controlled by a gating filter mechanism. *EMBO reports* **1**(3), 277-281.

**-G-**

Gade, W. and Brown, J.L. (1978) Purification and Partial Characterization of  $\alpha$ -N-Acylpeptide Hydrolase from Bovine Liver. *The Journal of Biological Chemistry* **253**(14), 5012-5018.

Gerczei, T., Keseru, G.M. and Naray-Szabo, G. (2000) Construction of a 3D model of oligopeptidase B, a potential processing enzyme in prokaryotes. *Journal of Molecular Graphics and Modelling* **18**, 7-17.

Gherzi, G., Dong, H., Goldstein, L.A., Yeh, Y., Hakkinen, L., Larjava, H.S. and Chen, W-T. (2002) Regulation of Fibroblast Migration on Collagenous Matrix by a Cell Surface Peptidase Complex. *The Journal of Biological Chemistry* **277**(32), 29231-29241.

Gilmartin, L. and O'Cuinn, G. (1999) Dipeptidyl peptidase IV and aminopeptidase P, two proline specific enzymes from the cytoplasm of guinea-pig brain: their role in metabolism of peptides containing consecutive prolines. *Neuroscience Research* **34**, 1-11.

Goldstein, L.A., Ghersi, G., Pineiro-Sanchez, M.L., Salamone, M., Yeh, Y., Flessate, D. and Chen, W-T. (1997) Molecular cloning of seprase: a serine integral membrane protease from human melanoma. *Biochimica et Biophysica Acta* **1361**, 11-19.

Goosens, F., De Meester, I., Vanhoof, G., Hendriks, D., Vriend, G. and Scharpe, S., (1995) The purification, characterisation and analysis of primary and secondary-structure of prolyl oligopeptidase from human lymphocytes. Evidence that the enzyme belongs to the  $\alpha/\beta$  hydrolase fold family. *European Journal of Biochemistry* **233**, 432-441.

Goosens, F., De Meester, I., Vanhoof, G. and Scharpe, S. (1996) Distribution of Prolyl Oligopeptidase in Human Peripheral Tissues and Body Fluids. *European Journal of Chemical and Clinical Biochemistry* **34**, 17-22.

Goosens, F., Vanhoof, G., De Meester, I., Augustyns, K., Borloo, M., Tourwe, D., Haemers, A. and Scharpe, S. (1997) Development and evaluation of peptide-based prolyl oligopeptidase inhibitors: introduction of N-benzyloxycarbonyl-prolyl-3-fluoropyrrolidine as a lead in inhibitor design. *European Journal of Biochemistry* **250**(1), 177-183.

Gorrell, M.D., Gysberg, V. and McCaughan, G.W. (2001) CD26: A Multifunctional Integral Membrane and Secreted Protein of Activated Lymphocytes. *Scandinavian Journal of Immunology* **54**, 249-264.

Gutheil, W. and Bachovchin, W.W. (1993) Separation of L-Pro-DL-boroPro into its Component Diastereomers and Kinetic Analysis of their Inhibition of Dipeptidyl Peptidase IV. A New Method for the Analysis of Slow, Tight-Binding Inhibition. *Biochemistry* **32**(34), 8723-8731.

Grellier, P., Vendeville, S., Joyeau, R., Bastos, I.M.D., Drobecq, H., Frappier, F., Teixeira, A.R.L., Schrevel, J., Davioud-Charvet, E., Sergheraert, C. and Santana, J.M. (2001) *Trypanosoma cruzi* Prolyl Oligopeptidase Tc80 Is Involved in Nonphagocytic Mammalian Cell Invasion by Trypomastigotes. *The Journal of Biological Chemistry* **276**(50), 47078-47086.

Griffiths, E. C. (1987) Clinical Applications of Thyrotropin-Releasing Hormone (Editorial Review). *Clinical Science* **73**, 449-457.

#### **-H-**

Harwood, V.J., Denson, J.D., Robinson-Bidle, K.A. and Schreier, H.J. (1997) Overexpression and Characterization of a Prolyl Endopeptidase from the Hyperthermophilic Archaeon *Pyrococcus furiosus*. *Journal of Bacteriology* **179**(11), 3613-3618.

Harwood, V.J. and Schreier, H.J. (2001) Prolyl Oligopeptidase from *Pyrococcus furiosus*. *Methods in Enzymology* **330**, 445-454.

Heins, J., Welker, P., Schonlein, C., Born, I., Hartrodt, B., Neubert, K., Tsuru, D. and Barth, A. (1988) Mechanism of proline-specific proteinases: (I) substrate specificity of dipeptidyl peptidase IV from pig kidney and proline-specific endopeptidase from *Flavobacterium meningosepticum*. *Biochimica et Biophysica Acta* **954**, 161-169.

Heinze, S., Ritzau, M., Ihn, W., Hulsmann, H., Schlegel, B., Dornberger, K., Fleck, W.F., Zerlin, M., Christner, C., Grafe, U., Kullertz, G. and Fischer, G. (1997) Lipohexin, a New Inhibitor of Prolyl Endopeptidase from *Moeszia lindtneri* (HKI-0054) and *Paecilomyces* sp. (HKI-0055; HKI-0096) I. Screening, Isolation and Structure Elucidation. *The Journal of Antibiotics* **50**(5), 379-383.

Hoffman, T. and Demuth, H-U. (2002) Therapeutic Strategies Exploiting DP IV inhibition. Target disease: Type 2 Diabetes. In: *Ectopeptidases: CD13/Aminopeptidase N and CD26/Dipeptidylpeptidase IV in Medicine and Biology*. (Langer, J. and Ansorge, S., eds.) Kluwer Academic/Plenum Publishers, New York. pp. 259-278.

Hopsu-Havu, V.K. and Glenner, G.G. (1966) A new dipeptide naphthylamidase hydrolysing glycyl-prolyl-beta-naphthylamide. *Histochemie* **7**, 197-201.

**-I-**

Irazusta, J., Larrinaga, G., Gonzalez-Maeso, J., Gil, J., Meana, J.J. and Casis, L. (2002) Distribution of prolyl endopeptidase activities in rat and human brain. *Neurochemistry International* **40**, 337-345.

Ikehera, Y., Ogata, S. and Misumi, Y. (1994) Dipeptidyl-peptidase IV from rat liver. *Methods in Enzymology* **244**, 215-227.

Ishikawa, K., Ishida, H., Koyama, Y., Kawarabayasi, Y., Kawahara, J., Matsui, E. and Matsui, I. (1998) Acylamino Acid-releasing Enzyme from the Thermophilic Archaeon *Pyrococcus horikoshii*. *The Journal of Biological Chemistry* **273**(28), 17726-17731.

Iwaki-Egawa, S., Watanabe, Y., Kikuya, Y. and Fujimoto, Y. (1998) Dipeptidyl peptidase IV from Human Serum: Purification, Characterization, and N-Terminal Amino Acid Sequence. *Journal of Biochemistry* **124**(2), 428-433.

**-J-**

Jones, W.M. and Manning, J.M. (1988) Substrate specificity of an acylaminopeptidase that catalyses the cleavage of the blocked amino termini of peptides. *Biochimica et Biophysica Acta* **953**, 357-360.

Jones, W.M., Scaloni, A., Bossa, F., Popowicz, A.M., Schneewind, O. and Manning, J.M. (1991) Genetic relationship between acylpeptide hydrolase and acylase, two hydrolytic enzymes with similar binding but different catalytic specificities. *Proceedings of the National Academy of Science USA* **88**, 2194-2198.

Jones, W.M., Scaloni, A. and Manning, J.M. (1994) Acylaminoacyl peptidase. *Methods in Enzymology* **244**, 227-231.

Juhasz, T., Szeltner, Z., Renner, V. and Polgar, L. (2002) Role of the Oxyanion Binding Site subsites S1 and S2 in the Catalysis of Oligopeptidase B, a Novel Target for Antimicrobial Chemotherapy. *Biochemistry* **41**, 4096-4106.

**-K-**

Kabashima T., Yoshida, T., Ito, K. and Yoshimoto, T. (1995) Cloning, sequencing and expression of the dipeptidyl peptidase IV gene from *Flavobacterium meningosepticum* in *Escherichia coli*. *Archives of Biochemistry and Biophysics* **320**, 123-128.

Kahyaoglu, A., Haghjoo, K., Kraicsovits, F., Jordan, F., and Polgar, L. (1997) Benzyloxycarbonylprolylprolinal, a transition-state analogue for prolyl oligopeptidase, forms a tetrahedral adduct with catalytic serine, not a reactive cysteine. *Biochemical Journal* **322**, 839-843.

Kalwant, S. and Porter, A. G. (1991) Purification and Characterisation of Human Brain Prolyl Endopeptidase. *Biochemical Journal* **276**, 237-244.

Kanatani, A., Masuda, T., Shimoda, T., Misoka, F., Sheng Lin, X., Yoshimoto, T., and Tsuru, D. (1991), Protease II from *Escherichia coli*: Sequencing and Expression of the Enzyme Gene, and Characterisation of the Expressed Enzyme. *Journal of Biochemistry* **110**(3), 315-320.

Kanatani, A., Yoshimoto, T., Kitazono, A., Kokubo, T. and Tsuru, D. (1993) Prolyl Endopeptidase from *Aeromonas hydrophilia*: Cloning, Sequencing, and Expression of the Enzyme Gene, and Characterisation of the Expressed Enzyme. *Journal of Biochemistry* **113**, 790-796.

Kato, T., Okada, M. and Nagatsu, T. (1980) Distribution of Post-Proline Cleaving Enzyme in Human Brain and the peripheral Tissues. *Molecular and Cellular Biochemistry* **32**, 117-121.

Katsube, N., Sunaga, K., Chuang, D. and Ishitani, R. (1996) ONO-1603, a potential antidementia drug, shows neuroprotective effects and increases m<sub>3</sub>-muscarinic receptor mRNA levels in differentiating rat cerebellar granule neurons. *Neuroscience Letters* **214**, 151-154.

Kelly, T. (1999) Evaluation of seprase activity. *Clinical & Experimental Metastasis* **17**, 57-62.

Kelly, T., Kechelava, S., Rozypal, T.L., West, K.W. and Korourian, S. (1998) Seprase, a Membrane-Bound Protease, Is Overpressed by Invasive Ductal Carcinoma Cells of Human Breast Cancers. *Modern Pathology* **11**(9), 855-863.

Kenny, A. J., Booth, A.G., George, S.G., Ingram, J., Kershaw, D., Wood, E.J. and Young, A.R. (1976) Dipeptidyl peptidase IV, a Kidney Brush-Border Serine Peptidase. *Biochemical Journal* **155**, 169-182.

Kimura, K-I, Kanou, F., Takahashi, H., Esumi, Y., Uramoto, M. and Yoshihama, M. (1997) Propeptin, a new inhibitor of prolyl endopeptidase produced by *Microbispora*. *Journal of Antibiotics* **50**, 373-378.

Kimura, A., Yoshida, I., Takagi, N. and Takahashi, T. (1999) Structure and Localization of the Mouse Prolyl Oligopeptidase Gene. *The Journal of Biological Science* **274**(34), 24047-24053.

Kobayashi, K., Lin, L-W., Yeadon, J.E., Klickstein, L.B. and Smith, J.A. (1989) Cloning and Sequence Analysis of a Rat Liver cDNA Encoding Acyl-peptide Hydrolase. *The Journal of Biological Chemistry* **264**(15), 8892-8899.

Koida, M. and Walter, R. (1976) Post-Proline Cleaving Enzyme: Purification of this Endopeptidase by Affinity Chromatography. *Journal of Biological Chemistry* **251**(23), 7593-7599.

Koreeda, Y., Hayakawa, M., Ikemi, T. and Abiko, Y. (2001) Isolation and characterization of dipeptidyl peptidase IV from *Prevotella loescheii* ATCC 15930. *Archives of Oral Biology* **46**, 759-766.

Kornblatt, M.J., Mpimbaza, G.W. and Lonsdale-Eccles, J.D. (1992) Characterisation of an endopeptidase of *Trypanosoma brucei brucei*. *Archives of Biochemistry and Biophysics* **293**(1), 25-31.

Kreig, F. and Wolf, N. (1995) Enzymatic peptide synthesis by the recombinant proline-specific endopeptidase from *Flavobacterium meningosepticum* and its mutationally altered Cys556 variant. *Applied Microbiology and Biotechnology* **42**, 844-852.

**-L-**

Laemmli, U.K. (1970) Cleavage of Structural proteins during assembly of the head of structural bacteriophage T4. *Nature* **227**, 680-685.

Laitinen, K.S.M., van Groen, T., Tanila, H., Venalainen, J., Mannisto, P.T. and Alafuzoff, I. (2001) Brain prolyl oligopeptidase activity is associated with neuronal damage rather than  $\beta$ -amyloid accumulation. *Clinical Neuroscience and Neuropathology* **12**(15), 3309-3312.

Li, J., Wilk, E. and Wilk, S. (1996) Inhibition of Prolyl Oligopeptidase by Fmoc-Aminoacylpyrrolidine-2-Nitriles. *Journal of Neurochemistry* **66**(5), 2105-2112.

Li, J., Wilk, E. and Wilk, S. (1995) Aminoacylpyrrolidine-2-nitriles: Potent and Stable Inhibitors of Dipeptidyl-Peptidase IV (CD26). *Archives of Biochemistry and Biophysics* **323**(1), 148-154.

Lojda, Z. (1977) Studies on glycyl-proline naphthylamidase. I. Lymphocytes. *Histochemistry* **54**, 299-309.



Lonsdale-Eccles, J.D. and Grab, D.J. (2002) Trypanosome hydrolases and the blood-brain barrier. *TRENDS in Parasitology* **18**(1), 17-19.

Lorey, S., Faust, J., Mrestani-Klaus, C., Kahne, T., Ansorge, S., Neubert, K. and Buhling, F. (2002) Transcellular Proteolysis Demonstrated by Novel Cell Surface-associated Substrates of Dipeptidyl Peptidase IV (CD26). *The Journal of Biological Chemistry* **277**(36), 33170-33177.

**-M-**

Maes, M., Goosens, F., Scharpe, S., Calabrese, J., Desnyder, R. and Meltzer, H.Y. (1995) Alterations in plasma prolyl endopeptidase activity in depression, mania and schizophrenia: effects of antidepressants, mood stabilisers and antipsychotic drugs. *Psychiatry Research* **58**, 217-225.

Maes, M., Goosens, F., Scharpe, S., Meltzer, H.Y., D'Hondt, P. and Cosyns, P. (1994) Lower Serum Prolyl Endopeptidase Enzyme Activity in Major Depression: Further Evidence that Peptidases Play a Role in the Pathophysiology of Depression. *Biological Psychiatry* **35**, 545-552.

Makinen, P-L., Makinen, K.K. and Syed, S.A. (1994) An Endo acting Proline-Specific oligopeptidase from *Treponema denticola* ATCC 35405: Evidence of Hydrolysis of Human Bioactive Peptides. *Infection and Immunity* **62**, 4938-4947.

Manning, J.M. (1998), Acylaminoacyl-peptidase. In: *Handbook of Proteolytic Enzymes*. (Barrett, A.J., Rawlings, N.D. and Woessner, J.F. eds.) Academic Press, London. pp. 384-385.

Marguet, D., Baggio, L., Kobayashi, T., Bernard, A.M., Pierres, M., Nielsen, P., Ribet, U., Watanabe, T., Drucker, D.J. and Wagtmann, N. (2000) Enhanced insulin secretion and improved glucose tolerance in mice lacking CD26. *Proceedings of the National Academy of Sciences, USA* **97**(12), 6874-6879.

Marguet, D., Bernard, A-M., Vivier, I., Darmoul, D., Naquet, P. and Pierres, M. (1992) cDNA Cloning for Mouse Thymocyte-activating Molecule. A multifunctional ecto-dipeptidyl peptidase IV (CD26) included in a subgroup of serine proteases. *The Journal of Biological Chemistry* **267**(4), 2200-2208.

Marighetto, A., Touzani, K., Etchamendy, N., Torrea, C.C., De Nanteuil, G., Guez, D., Jaffard, R. and Morain, P. (2000) Further Evidence for a Dissociation Between Different Forms of Mnemonic Expressions in a Mouse Model of Age Related Cognitive Decline: Effects of Tacrine and S 17092, a Novel Prolyl Endopeptidase Inhibitor. *Learning and Memory* **7**, 159-169.

Martin, R.A., Cleary., D.L., Guido, G.M. Zurcher-Neely, H.A., Kubiak., T.M. (1993) Dipeptidyl peptidase IV (DPIV) from pig kidney cleaves analogs of bovine growth hormone-releasing factor (bGRF) modified at position 2 with Ser, Thr or Val. Extended DPP IV substrate specificity?. *Biochimica et Biophysica Acta* **1164**, 252-260.

McDonald, J.K., Callahan, P.X., Ellis, S. and Smith, R.E. (1971) Polypeptide degradation by dipeptidyl peptidase II (cathepsin C) and related peptidases. In: *Tissue Proteinases*. (Barrett, A.J. and Dingle, J.T., eds.) pp. 69-107.

McMahon, G., Collins, P. and O'Connor, B. (2003) Characterisation of the active site of a newly discovered and potentially significant post-proline cleaving endopeptidase called ZIP using LC-UV-MS. *The Analyst* **128**(6), 670-675.

Mentlein, R. (1988) Proline residues in the maturation and degradation of peptide hormones and neuropeptides. *FEBS Letters* **234**(2), 251-256.

Mentlein, R. (1999) Dipeptidyl peptidase IV (CD26)-role in the inactivation of regulatory peptides. *Regulatory Peptides* **85**, 9-24.

Mentlein, R., Dahms, P., Grandt, D. and Kruger, R. (1993) Proteolytic processing of neuropeptide Y and peptide YY by dipeptidyl peptidase IV. *Regulatory peptides* **49**, 133-144.

Misumi, Y., Hayashi, Y., Arakawa, F. and Ikehara, Y. (1992) Molecular cloning and sequence analysis of human dipeptidyl-peptidase IV, a serine proteinase on the cell surface *Biochimica et Biophysica Acta* **1131**, 333-336.

Mitta, M., Asada, K., Uchimura, Y., Kimizuka, F., Kato, I., Sakiyama, F and Tsunasawa, (1989), The Primary Structure of Porcine Liver Acylamino Acid-Releasing Enzyme Deduced from cDNA Sequences, *Journal of Biochemistry*, **106**, 548-551.

Mitta, M., Miyagi, M., Kato, I. and Tsunasawa, S. (1998) Identification of the Catalytic Triad Residues of Porcine Liver Acylamino Acid-Releasing Enzyme. *Journal of Biochemistry* **123**, 924-931.

Miyagi, M., Sakiyama, F., Kato, I. and Tsunasawa, S. (1995) Complete Covalent Structure of Porcine Liver Acylamino Acid-Releasing Enzyme and Identification of Its Active Site Serine Residue. *Journal of Biochemistry* **118**, 771-779.

Monsky, W.L., Lin, C-Y., Aoyama, A., Kelly, T., Akiyama, S.K., Mueller, S.C. and Chen, W-T. (1994) A Potential Marker Protease of Invasiveness, Seprase, Is Localized on Invadopodia of Human Malignant Melanoma Cells, *Cancer Research*, **54**, 5702-5710.

Moriyama, A., Nakanishi, M. and Sasaki, M. (1988) Porcine Muscle Prolyl Endopeptidase and its Endogenous Substrates. *Journal of Biochemistry* **104**, 112-117.

Moriyama, A. and Sasaki, M. (1983) Porcine Liver Succinyltrialanine p-Nitroanilide Hydrolytic Enzyme. Its Purification and Characterization as a Post Proline Cleaving Enzyme. *Journal of Biochemistry* **94**, 1387-1397.

Morty, R.E., Fulop, V. and Andrews, N.W. (2002) Substrate Recognition Properties of Oligopeptidase B from *Salmonella enterica* Serovar Typhimurium. *Journal of Bacteriology* **184**(12), 3329-3337.

Morty, R.E., Lonsdale-Eccles, J.D., Morehead, J., Caler, E.V., Mentele, R., Auerswald, E.A., Coetzer, T.H.T., Andrews, N.W. and Burleigh, B.A. (1999) Oligopeptidase B from *Trypanosoma brucei*, a New Member of an Emerging Subgroup of Serine Oligopeptidases. *The Journal of Biological Chemistry* **274**(37), 26149-26156.

Morty, R.E., Lonsdale-Eccles, J.D., Mentele, R., Auerswald, E.A. and Coetzer, T.H.T. (2001) Trypanosome-Derived Oligopeptidase B Is Released into the Plasma of Infected Rodents, Where It Persists and Retains Full Catalytic Activity. *Infection and Immunity* **69**(4), 2757-2761.

Morty, R.E., Troeberg, L., Pike, R.N., Jones, R., Nickel, P., Lonsdale-Eccles, J.D. and Coetzer, T.H.T. (1998) A trypanosome oligopeptidase as a target for the trypanocidal agents pentamidine, diminazene and suramin. *FEBS Letters* **433**, 251-256.

**-N-**

Nagatsu, T., Hino, M., Fuyamada, H., Hayakawa, T. and Sakakibara, S. (1976) New chromogenic substrates for X-prolyl dipeptidyl aminopeptidases. *Analytical Biochemistry* **74**, 466-476.

Nakajima, T., Ono, Y., Kato, A., Maeda, J. and Ohe, T. (1992) Y-29794-a non-peptide prolyl endopeptidase inhibitor that can penetrate into the brain. *Neuroscience Letters* **141**, 156-160.

Nishikata, M. (1984) Trypsin-like protease from soybean seeds. Purification and some properties. *J Biochem (Tokyo)* **95**(4), 1169-1177.

Nomura, K. (1986) Specificity of Prolyl Endopeptidase. *FEBS Letters* **209**(2), 235-237.

Noula, C., Kokotos, G., Barth, T. and Tzougraki, C. (1997) New fluorogenic substrates for the study of secondary specificity of prolyl oligopeptidase *Journal of Peptide Research* **49**, 46-51.

**-O-**

Ogasawara, W., Ogawa, Y., Yano, K., Okada, H. and Morikawa, Y. (1996) Dipeptidyl Aminopeptidase IV from *Pseudomonas* sp. WO24. *Bioscience, Biotechnology and Biochemistry* **60**(12), 2032-2037.

Ogata, S., Misumi, Y. and Ikehara, Y. (1989) Primary Structure of Rat Liver Dipeptidyl Peptidase IV Deduced from its cDNA and Identification of the NH<sub>2</sub>-terminal Signal Sequence as the Membrane-anchoring Domain. *The Journal of Biological Chemistry* **264**(6), 3596-3601.

Ohkubo, I., Huang, K., Ochiai, Y., Takagaki, M. and Kani, K. (1994) Dipeptidyl peptidase IV from Porcine Seminal Plasma: Purification, Characterisation and N-Terminal Amino Acid Sequence. *Journal of Biochemistry* **116**, 1182-1186.

O'Leary, R.M. and O'Connor, (1995) Identification and localisation of a synaptosomal membrane prolyl endopeptidase from bovine brain. *European Journal of Biochemistry* **227**, 277-283.

O'Leary, R., Gallagher, S.P. and O'Connor, B. (1996) Purification and Characterization of a Novel Membrane-bound Form of Prolyl Endopeptidase from Bovine Brain. *International Journal of Biochemistry and Cell Biology* **28**(4), 441-449.

Oliveria, E.B., Martins, A.R. and Camargo, A.C.M. (1976) Isolation of Brain Endopeptidases: Influence of Size and Sequence of Substrates Structurally Related to Bradykinin. *Biochemistry* **15**(9), 1967-1974.

Orlowski, M., Wilk, E., Pearce, S. and Wilk, S. (1979) Purification and Properties of a Prolyl Endopeptidase from Rabbit Brain. *Journal of Neurochemistry* **33**(2), 461-469.

**-P-**

Pacaud, M. and Richaud, C. (1975) Protease II from *Escherichia coli*. Purification and Characterization. *Journal of Biological Chemistry* **250**(19), 7771-7779.

Park, J.E., Lentner, M.C., Zimmerman, R.N., Garin-Chesa, P., Old, L.J. and Rettig, W.J. (1999) Fibroblast activation protein, a dual specificity serine protease expressed in reactive tumour stromal fibroblasts. *The Journal of Biological Chemistry* **274**, 36505-36512.

Petit, A., Barelli, H., Morain, P. and Checler, F. (2000) Novel proline endopeptidase inhibitors do not modify A $\beta$ 40/42 formation and degradation by human cells expressing wild-type and Swedish mutated  $\beta$ -amyloid precursor protein. *British Journal of Pharmacology* **130**, 1613-1617.

Pineiro-Sanchez, M.L., Goldstein, L.A., Dodt, J., Howard, L., Yeh, Y. and Chen, W-T. (1997) Identification of the 170-kDa Melanoma Membrane-bound Gelatinase (Seprase) as a Serine Integral Membrane Protease. *The Journal of Biological Chemistry* **272**(12), 7595-7601.

Planchenault, T., Vidmar, S.L., Imhoff, J-M., Blondeau, X., Emod, I., Lottspeich, F and Keil-Dlouha, V. (1990) Potential Proteolytic Activity of Human Plasma Fibronectin: Fibronectin Gelatinase. *Biological Chemistry Hoppe-Seyler* **371**, 117-128.

Polgar, L. (1991) pH Dependant Mechanism in the Catalysis of Prolyl Endopeptidase from Pig Muscle. *European Journal of Biochemistry* **197**, 441-447.

Polgar, L. (1992a) Structural Relationship between Lipases and Peptidases of the Prolyl Oligopeptidase Family. *FEBS Letter* **311**(3), 281-284.

Polgar, L. (1992b) Prolyl Endopeptidase Catalysis: A Physical Rather Than a Chemical Step is Rate-Limiting. *Biochemical Journal* **283**(3), 647-648.

Polgar, L. (1994) Prolyl Oligopeptidase. *Methods in Enzymology* **244**, 189-215.

Polgar, L. (1997) A potential Processing Enzyme in Prokaryotes: Oligopeptidase B, a New Type of Serine Peptidase. *PROTEINS: Structure, Function and Genetics* **28**, 375-379.

Polgar, L. (1999) Oligopeptidase B: A New Type of Serine Peptidase with a Unique Substrate-Dependant Temperature Sensitivity. *Biochemistry* **38**, 15548-15555.

Polgar, L. (2002a) The Prolyl oligopeptidase family. *Cellular and Molecular Life Sciences* **59**, 349-362.

Polgar, L. (2002b) Structure-Function of Prolyl Oligopeptidase and its Role in Neurological Disorders. *Current Medicinal Chemistry - Central Nervous System Agents* **2**, 251-257.

Polgar, L., Kollat, E. and Hollosi, M. (1993) Prolyl oligopeptidase catalysis: Reactions with thiono substrates reveal substrate-induced conformational change to be the rate-limiting step. *FEBS Letters* **322**(3), 227-230.

Polgar, L. and Szabo, E. (1992) Prolyl Endopeptidase and Dipeptidyl Peptidase IV are Distantly Related Members of the Same Family of Serine Proteases. *Biological Chemistry Hoppe-Seyler* **373**, 361-366.

Pospisilik, J.A., Hinke, S.A., Pederson, R.A., Hoffman, T., Rosche, F., Schlenzig, D., Glund, K., Heiser, U., McIntosh, C.H.S. and Demuth, H-U. (2001) Metabolism of glucagons by dipeptidyl peptidase IV (CD26). *Regulatory Peptides* **96**, 133-141.

Puschel, G., Mentlein, R. and Heymann, E. (1982) Isolation and Characterization of Dipeptidyl Peptidase IV from Human Placenta. *European Journal of Biochemistry* **126**, 359-365.

#### **-R-**

Radhakrishna, G. and Wold, F. (1989) Purification and Characterization of an *N*-Acylaminoacyl-peptide Hydrolase from Rabbit Muscle. *The Journal of Biological Chemistry* **264**(19), 11076-11081.

Rahfeld, J., Schierhorn, M., Hartrodt, B., Neubert, K. and Heins, J. (1991) Are diprotin A (Ile-Pro-Ile) and diprotin B (Val-Leu-Pro) inhibitors or substrates of dipeptidyl peptidase IV?. *Biochimica et Biophysica Acta* **1076**, 314-316.

Raphel, V., Giardina, T., Guevel, L., Perrier, J., Dupuis, L., Guo, X-J. and Puigserver, A. (1999) Cloning, Sequencing and Further characterization of acylpeptide hydrolase from porcine intestinal mucosa. *Biochimica et Biophysica Acta* **1432**, 371-381.

Rasmussen, H.B., Branner, S., Wiberg, F.C. and Wagtmann, N. (2003) Crystal structure of human dipeptidyl peptidase IV/CD26 in complex with a substrate analog *Nature Structural Biology* **10**,19-25.

Rawlings, N.D. and Barrett, A.J. (1993) Evolutionary families of peptidases. *Biochemical Journal* **290**, 205-218.

Rawlings, N.D. and Barrett, A.J. (1994) Families of Serine Peptidases. *Methods in Enzymology* **244**, 19-61.

Rawlings, N.D., Polgar, L. and Barrett, A.J. (1991) A New Family of Serine-Type Peptidases Related to Prolyl Oligopeptidase. *Biochemical Journal* **279**, 907-911.

Reinhold, D., Bank, U., Buhling, F., Kahne, T., Kunt, D., Faust, J., Neubert, K. and Ansorge, S. (1994) Inhibitors of dipeptidyl peptidase IV (DPIV, CD26) specifically suppress proliferation and modulate cytokine production of strongly CD26 expressing U937 cells. *Immunobiology* **192**, 121-136.

Reinhold, D., Kahne, T., Steinbrecher, A., Wrenger, S., Neubert, K., Ansorge, S. and Brocke, S. (2002) The Role of Dipeptidyl peptidase IV (DP IV) Enzymatic Activity in T Cell Activation and Autoimmunity. *Biological Chemistry* **383**, 1133-1138.

Rennex, D., Hemmings, B.A., Hofsteenge, J. and Stone, S.R. (1991) cDNA Cloning of Porcine Brain Prolyl Endopeptidase and Identification of the Active-Site Seryl Residue. *Biochemistry* **30**, 2195-2203.

Richards, P.G., Johnston, M.K. and Ray, D.E. (2000) Identification of Acylpeptide Hydrolase as a Sensitive Site for Reaction with Organophosphorus Compounds and a Potential Target for Cognitive Enhancing Drugs. *Molecular Pharmacology* **58**, 577-583.



Robison, K.A., Bartley, D.A., Robb, F.T. and Schreier, H.J. (1995) A gene from the hyperthermophile *Pyrococcus furiosus* whose deduced product is homologous to members of the prolyl oligopeptidase family of proteases. *Gene* **152**, 103-106.

Roe, S. (1989) Separation Based on Structure, In: *Protein Purification Methods-A Practical Approach*. (Harris, E.L.V. and Angal, S. eds) IRL Press, Oxford. pp. 175-244.

Rosen, J., Tomkinson, B., Pettersson, G. and Zetterqvist, O. (1991) A Human Serine Endopeptidase, Purified with Respect to Activity Against a Peptide with Phosphoserine in the P<sub>1</sub>' Position, is Apparently Identical with Prolyl Endopeptidase. *The Journal of Biological Chemistry* **266**(6), 3827-3834.

Rupnow, J.H., Taylor, W.L., and Dixon, J.E. (1979) Purification and Characterization of a Thyrotropin-Releasing Hormone Deamidase from Rat Brain. *Biochemistry* **18**(7), 1206-1212.

-S-

Saito, M., Hashimoto, M., Kawaguchi, N., Shibata, H., Fukami, H., Tanaka, T. and Higuchi, N. (1991), Synthesis and Inhibitory Activity of Acyl-Peptidyl-Pyrrolidine Derivatives Toward Post Proline Cleaving Enzyme: A study of Subsite Specificity. *Journal of Enzyme Inhibition* **5**, 51-75.

Sattar Abdus, A.K.M., Yamamoto, N., Yoshimoto, T. and Tsuru, D. (1990) Purification and Characterization of an Extracellular Prolyl Endopeptidase from *Agaricus bispora*. *Journal of Biochemistry* **107**, 256-261.

Scaloni, A., Barra, D., Jones, W.M. and Manning, J.M. (1994) Human Acylpeptide Hydrolase. Studies on its thiol groups and mechanism of action. *The Journal of Biological Chemistry* **269**(21), 15076-15084.

Scaloni, A., Ingallinella, P., Andolfo, A., Jones, W., Marino, G. and Manning, J.M. (1999) Structural investigations on human erythrocyte acylpeptide hydrolase by mass spectrometric procedures. *Journal of Protein Chemistry* **18**(3), 349-360.

Scaloni, A., Jones, W.M., Barra, D., Pospischil, M., Sassa, S., Popowicz, A., Manning, L.R., Schneewind, O. and Manning J.M. (1992) Acylpeptide Hydrolase: Inhibitors and Some Active Site Residues of the Human Enzyme. *The Journal of Biological Chemistry* **267**(6), 3811-3818.

Schechter, I. and Berger, A. (1967) On the size of the active site in proteases. I. Papain. *Biochemical and Biophysical Research Communications* **27**, 157-162.

Schlabach, T.D. (1984) Postcolumn Detection of Serum Proteins with the Biuret and Lowry Reactions *Analytical Biochemistry* **139**, 309-315.

Schulz, I., Gerhartz, B., Neubauer, A., Holloschi, A., Heiser, U., Hafner, M. and Demuth, H.U. (2002) Modulation of inositol 1,4,5-triphosphate concentration by prolyl endopeptidase inhibition. *European Journal of Biochemistry* **269**, 5813-5820.

Sedo, A. and Malik, R. (2001) Dipeptidyl peptidase IV-like molecules: homologous proteins or homologous activities. *Biochimica and Biophysica Acta* **1550**, 107-116.

Shannon, J.D., Bond, J.S. and Bradley, S.G. (1982) Isolation and Characterization of an intracellular serine protease from *Rhodococcus erythropolis*. *Archives of Biochemistry and Biophysics* **219**(1), 80-88.

Shibuya-Saruta, H., Kasahara, Y. and Hashimoto, Y. (1996) Human Serum Dipeptidyl peptidase IV (DPPIV) and its unique properties. *Journal of Clinical Laboratory Analysis* **10**, 435-440.

Shinoda, M., Matsuo, A. and Toide, K. (1996) Pharmacological studies of a novel prolyl endopeptidase inhibitor, JTP-4819, in rats with middle cerebral artery occlusion. *European Journal of Pharmacology* **305**, 31-38.

Shinoda, M., Miyazaki, A. and Toide, K. (1999) Effects of a novel prolyl endopeptidase inhibitor, JTP-4819, on spatial memory and on cholinergic and peptidergic neurons in rats with ibotenate-induced lesions of the nucleus basalis magnocellularis. *Behavioural Brain Research* **99**, 17-25.

Shinoda, M., Toide, K., Ohsawa, I. and Kohsaka, S. (1997) Specific Inhibitor for Prolyl Endopeptidase Suppresses the Generation of Amyloid  $\beta$  Protein in NG108-15 Cells. *Biochemical and Biophysical Research Communication* **235**, 641-645.

Shirasawa, Y., Osawa, T. and Hirashima, A. (1994) Molecular Cloning and Characterization of Prolyl Endopeptidase from Human T cells. *Journal of Biochemistry* **115**, 724-729.

Smith, K.P., Krohn, K.I., Hermanson, G.T., Mallia, A.K., Gartner, F.H., Provenzano, M.D., Fujimoto, E.K., Gorke, N.M., Olson, B.J. and Klenk, D.C. (1985) Measurement of Protein Using Bicinchoninic Acid. *Analytical Biochemistry* **150**, 76-85.

Sokolik, C.W., Chyau Liang, T. and Wold, F. (1994) Studies on the specificity of acetylaminoacyl-peptide hydrolase. *Protein Science* **3**, 126-131.

Song, K.S. and Raskin, I. (2002) A Prolyl Endopeptidase-Inhibiting Benzofuran Dimer from *Polyozellus multiflex*. *Journal of Natural Products* **65**, 76-78.

Stone, S.R., Rennex, D., Wikstrom, P., Shaw, E. and Hofsteenge, J. (1991) Inactivation of Prolyl Endopeptidase by Peptidylchloromethane: Kinetics of Inactivation and Identification of Sites of Modification. *Biochemical Journal* **276**, 837-840.

Sudo, J. and Tanabe, T. (1985) Distributions of post-proline cleaving enzyme-, converting enzyme-, trypsin- and chymotrypsin-like activities in various nephron segments and in brush-border membranes isolated from rat kidney. *Chem Pharm Bull (Tokyo)* **33**(4), 1694-1702.

Szeltner, Z., Renner, V. and Polgar, L. (2000) Substrate- and pH-dependant contribution of oxyanion binding site to the catalysis of prolyl oligopeptidase, a paradigm of the serine oligopeptidase family. *Protein Science* **9**, 353-360.

Szeltner, Z., Renner, V. and Polgar, L. (2000) The Noncatalytic  $\beta$ -Propeller Domain of Prolyl Oligopeptidase Enhances the Catalytic Capability of the Peptidase Domain. *The Journal of Biological Chemistry* **275**(20), 15000-15005.

-T-

Tate, S.S. (1981) Purification and Properties of a Bovine Brain Thyrotropin-Releasing-Factor Deamidase: A Post-Proline Cleaving Enzyme of Limited Specificity. *European Journal of Biochemistry* **118**, 17-23.

Tirupathi, C., Miyamoto, Y., Ganapathy, V., Roesel, R.A., Whitford, G.M. and Leibach, F.H. (1990), Hydrolysis and Transport of Proline-containing Peptides in Renal Brush-border Membrane Vesicles from Dipeptidyl Peptidase IV-positive and Dipeptidyl IV-negative Rat Strains, *The Journal of Biological Chemistry*, **265**(3), 1476-1483.

Tiselius, A., Hjerten, S. and Levin, O. (1956) Protein Chromatography on Calcium Phosphate Columns. *Archives of Biochemistry and Biophysics* **65**, 132-155.

Toide, K., Iwamoto, Y., Fujiwara, T. and Abe, H. (1995a) JTP-4819: A Novel Prolyl Oligopeptidase Inhibitor with Potential as a Cognitive Enhancer. *Journal of Pharmacology and Experimental Therapeutics* **274**(3), 1370-1378.

Toide, K., Ohamiya, K., Iwamoto, Y. and Kato, T. (1995b) Effect of a Novel Prolyl Endopeptidase Inhibitor, JTP-4819, on Prolyl Endopeptidase Activity and Substance P-and Arginine-Vasopressin-Like Immunoreactivity in the Brains of Aged Rats. *Journal of Neurochemistry* **65**(1), 234-240.

Toide, K., Shinoda, M., Fujiwara, T. and Iwamoto, Y. (1997b) Effect of a Novel prolyl Endopeptidase Inhibitor, JTP-4819, on Spatial Memory and Central Cholinergic Neurons in Aged Rats. *Pharmacology Biochemistry and Behaviour* **56**(3), 427-434.

Toide, K., Shinoda, M., Iwamoto, Y., Fujiwara, T., Okamiya, K. and Uemura, A. (1997a) A novel prolyl endopeptidase inhibitor, JTP-4819, with potential for treating Alzheimer's disease. *Behavioural Brain Research* **83**, 147-151.

Troeberg, L., Pike, R.N., Morty, R.E., Berry, R.K., Coetzer, T.H.T. and Lonsdale-Eccles, J.D. (1996) Proteases from *Trypanosoma brucei brucei*. Purification, characterisation and interactions with host regulatory molecules. *European Journal of Biochemistry* **238**, 728-736.

Tsuda, M., Muraoka, Y., Nagai, M., Aoyagi, T. and Takeuchi, T. (1996) Postatin, a New Inhibitor of Prolyl Endopeptidase, VIII. Endopeptidase Inhibitory Activity of Non Peptidyl Postatin Analogues. *The Journal of Antibiotics* **49**(10), 1022-1030.

Tsuru, D. (1998) Oligopeptidase B. In: *Handbook of Proteolytic Enzymes*. (Barrett, A.J., Rawlings, N.D. and Woessner, J.F. eds.) Academic Press, London. pp. 375-376.

Tsuru, D. and Yoshimoto, T. (1994) Oligopeptidase B: Protease II from *Escherichia coli*. *Methods in Enzymology* **244**, 201-215,

Tsuru, D., Yoshimoto, T., Koryama, N. and Furukawa, S. (1988) Thiazolidine Derivatives as Potent Inhibitors Specific for Prolyl Endopeptidase. *Journal of Biochemistry* **104**, 580-568.

-W-

Wagner, L., Naude, R., Oelofsen, W., Naganuma, T. and Muramoto, K. (1999) Isolation and partial characterization of dipeptidyl peptidase IV from ostrich kidney. *Enzyme and Microbial Technology* **25**, 576-583.

Wallen, E.A.A., Christiaans, J.A.M., Forsberg, M.M., Venalainen, J.I., Mannisto, P.T. and Gynther, J. (2002) Dicarboxylic Acid bis (L-Prolyl-pyrrolidine) Amides as Prolyl Oligopeptidase Inhibitors. *Journal of Medicinal Chemistry* **45**(20), 4581-4584.

Walter, R. (1976) Partial Purification and Characterization of Post-Proline Cleaving Enzyme: Enzymatic Inactivation of Neurohypophyseal Hormones by Kidney Preparations of Various Species *Biochimica et Biophysica Acta* **422**, 138-158.

Walter, R. and Yoshimoto, T. (1978) Post-proline Cleaving Enzyme: Kinetic Studies of Size and Stereospecificity of its Active Site. *Biochemistry* **17**(20), 4139-4144.

Walter, R., Shlank, H., Glass, J.D., Schwartz, I.L. and Kerenyi, T.D. (1971) Leucylglycinamide Released from Oxytocin by Human Uterine Enzyme. *Science* **173**, 827-829.

Walter, R., Simmons, W.H. and Yoshimoto, T. (1980) Proline Specific Endo- and Exopeptidases. *Molecular and Cellular Biochemistry* **30**(2), 111-127.

Wilk, S. (1983) Prolyl Endopeptidase. *Life Sciences* **33**(22), 2149-2157.

Wilk, S. and Orłowski, M. (1983) Inhibition of Rabbit Brain Prolyl Endopeptidase by N-Benzoyloxycarbonyl Prolyl-Prolinal, A Transition State Aldehyde Inhibitor. *Journal of Neurochemistry* **41**, 69-75.

Wilk, S., Benuck, M., Orłowski, M. and Marks, N. (1979) Degradation of Luteinizing Hormone-Releasing Hormone (LHRH) by Brain Prolyl Endopeptidase with Release of Des-Glycineamide LHRH and Glycineamide. *Neuroscience Letters* **14**, 275-279.

Willand, N., Joossens, J., Gesquiere, J.C., Tartar, A.L., Michael Evans, D. and Roe, M.B. (2002) Solid and solution phase syntheses of the 2-cyanopyrrolidide DPP-IV inhibitor NVP-DPP728 *Tetrahedron* **58**, 5741-5746.

Willard, H., Merritt, L.L., Dean, J.A. and Settle, F.A. (1988) Fluorescence and phosphorescence spectrometry. In: *Instrumental Methods of Analysis*. Wadsworth Publishing Company, California. pp. 197-223.

Williams, R.S.B., Cheng, L., Mudge, A.W. and Harwood, A.J. (2002) A common mechanism of action for three mood stabilizing drugs. *Nature* **417**, 292-295.

Williams, R.S.B., Eames, M., Ryves, W.J., Viggars, J. and Harwood, A.J. (1999) Loss of a prolyl oligopeptidase confers resistance to lithium by elevation of inositol (1,4,5) trisphosphate. *The EMBO journal* **18**(10), 2734-2745.

Williams, R.S.B. and Harwood, A.J. (2000) Lithium therapy and signal transduction. *Tips* **21**, 61-64.

-Y-

Yokosawa, H., Nishikata, M. and Ishii, S. (1984) N-Benzyloxycarbonyl-Valyl-Proline, a potent Inhibitor of Post-Proline Cleaving Enzyme. *Journal of Biochemistry* **95**, 1819-1821.

Yoshimoto, T. and Tsuru, D. (1982) Proline-Specific Dipeptidyl Aminopeptidase from *Flavobacterium meningosepticum*. *Journal of Biochemistry* **91**, 1899-1906.

Yoshimoto, T. and Walter, R. (1977) Post-proline Dipeptidyl Aminopeptidase (Dipeptidyl Aminopeptidase IV) from Lamb Kidney. *Biochimica et Biophysica Acta* **485**, 391-401.

Yoshimoto, T., Abdus Sattar, A.K.M., Hirose, W. and Tsuru, D. (1987a) Studies on Prolyl Endopeptidase from Carrot (*Daucus carota*): Purification and Enzymatic Properties. *Biochimica et Biophysica Acta* **916**, 29-37.

Yoshimoto, T., Fischl, M. Orłowski, R.C. and Walter, R. (1978) Post-proline cleaving endopeptidase and post-proline dipeptidyl aminopeptidase. Comparison of two peptidases with high specificity for proline residues. *The Journal of Biological Chemistry* **253**, 3708-3716.

Yoshimoto, T., Kado, K., Matsubara, F., Koriyama, N., Kaneto, H. and Tsuru, D. (1987b) Specific Inhibitors for Prolyl Endopeptidase and their Anti-Amnesic effect. *J.Pharmacobio-Dyn.* **10**, 730-735.

Yoshimoto, T., Kanatani, A., Shimoda, T., Inaoka, T., Kokubo, T. and Tsuru, D. (1992) Prolyl Endopeptidase from *Flavobacterium meningsepticum*: Cloning and Sequencing of the Enzyme Gene. *Journal of Biochemistry* **110**, 873-878.

Yoshimoto, T., Miyozaki, K., Haraguchi, N., Kitazono, A., Kabashima, T. and Ita, K. (1997) Cloning and expression of the cDNA encoding prolyl oligopeptidase (PE) from bovine brain. *Biological Pharmacology Bulletin* **20**, 1047-1050.

Yoshimoto, T., Nishimura, T., Kita, T. and Tsuru, D. (1983) Post Proline Cleaving Enzyme (Prolyl Endopeptidase) from Bovine Brain. *Journal of Biochemistry* **94**, 1179-1190.

Yoshimoto, T., Ogita, K., Walter, R., Koida, M and Tsuru, D. (1979) Post Proline Cleaving Enzyme: Synthesis of a New Fluorogenic Substrate and Distribution of the Endopeptidase in Rat Tissues and Body Fluids of Man. *Biochimica et Biophysica Acta* **569**, 184-192.

Yoshimoto, T., Sattar, A.K.M.A., Hirose, W. and Tsuru, D. (1988) Studies of Prolyl Endopeptidase from Shakashimeji (*Lyophyllum cinerascens*): Purification and Enzymatic Properties. *Journal of Biochemistry* **104**, 622-627.

Yoshimoto, T., Simons, W.H., Kita, T. and Tsuru, D. (1981) Post-Proline Cleaving Enzyme from Lamb Brain. *Journal of Biochemistry* **90**, 325-334.

Yoshimoto, T., Tabira, J., Kabashima, T., Inoue, S. and Kiyoshi, I. (1995) Protease II from *Moraxella lacunata*: Cloning, Sequencing, and Expression of the Enzyme Gene, and Crystallization of the Expressed Enzyme. *Journal of Biochemistry* **117**, 654-660.



Yoshimoto, T., Walter, R. and Tsuru, D, (1980) Proline-Specific Endopeptidase from Flavobacterium: Purification and Properties. *The Journal of Biological Chemistry* **255**(10), 4786-4792.

## **APPENDIX**

## 6.0. APPENDIX

### 6.1. Enzyme Activity Quantification

One unit of enzyme activity is defined as the amount of enzyme, which releases 1 nanomole of AMC per minute at 37°C (unit = nmoles.min<sup>-1</sup>).

#### Derivation

$$\begin{aligned}\text{AMC released} &= X\mu\text{M} \\ &= X\mu\text{moles/L}^{-1}\end{aligned}$$

The assay uses 400 $\mu$ l Z-Gly-Pro-AMC and 100 $\mu$ l enzyme

$$\begin{aligned}\therefore \text{Enzyme activity} &= \frac{X(400 \times 10^{-6})}{(100 \times 10^{-6}) 60} \mu\text{moles.L}^{-2}.\text{L}.\text{min}^{-1} \\ &= \frac{X}{15} \mu\text{moles.L}^{-1}.\text{min}^{-1} \\ &= \frac{X(1000)}{15(1000)} \text{nmoles.ml}^{-1}.\text{min}^{-1} \\ &= \frac{X}{15} \text{nmoles.ml}^{-1}.\underline{\text{min}^{-1}} \\ &= \frac{X}{15} \text{units.ml}^{-1}\end{aligned}$$

Also: AMC released (X) is also defined as fluorescent intensity divided by the slope of the appropriate AMC standard curve so,

$$\begin{aligned}\therefore \text{Enzyme activity} &= \frac{\text{Fluorescent Intensity}}{\text{Slope of filtered std. curve} \times 15} \text{nmoles.min}^{-1}.\text{ml}^{-1} \\ &= \frac{\text{Fluorescent Intensity}}{\text{Slope of filtered std. curve} \times 15} \text{units.ml}^{-1}\end{aligned}$$

## 6.2. Purification Table Calculations

**Total activity (unit):** Units of enzyme activity, calculated from fluorescent intensity as described in section 6.1.

**Total protein (mg):** mg/ml of protein estimated from appropriate BSA standard curve x volume of sample in mls.

**Specific activity (unit/mg):** Total activity/Total protein.

**Purification factor:** Specific activity of sample/Specific activity of starting sample (serum).

**Recovery (%):** (Total activity of sample/Total activity of starting sample) x 100.

## 6.3. Error Bars

Error bars on all enzyme activity graphs represent the standard error of the mean of triplicate fluorescence values. The standard error (SE) of the mean is defined as:

$$SE = \sigma/\sqrt{n}$$

### Where:

$\sigma$  is the standard deviation i.e.  $\sqrt{\text{variance}}$  (variance =  $(a^2 + b^2 + c^2)/3$ , where a, b & c are the triplicate values).

n is the number of repeat values measured (three in this case).

## 6.4. Kinetic Analysis

### 6.4.1. $K_m$ Determination

The Michaelis constant, or  $K_m$  as it is usually known, is defined as the *substrate concentration which gives rise to a velocity equal to half the maximal velocity*. This constant can be analysed by measuring reaction velocity ( $V$ ) at various concentrations of substrate, the data giving rise to the well-known Michaelis-Menten hyperbola curve. Once an enzyme-catalysed reaction follows normal Michaelis-Menten kinetics, data can be applied to a number of kinetic models such as:

**Lineweaver-Burk:** Plot of  $1/\text{fluorescent intensity}$  versus  $1/\text{substrate concentration}$ . The intercept of the line on the y-axis gives a direct readout of  $1/V_{\max}$  and the intercept of the line on the x-axis gives  $-1/K_m$ . The slope of the line is equal to  $K_m/V$ .

**Eadie-Hofstee:** Plot of  $\text{fluorescent intensity}$  versus  $\text{fluorescent intensity}/\text{substrate concentration}$ . The intercept on the y-axis represents  $1/V_{\max}$ , while the slope is given as  $-K_m$ .

**Hanes-Woolf:** Plot of  $\text{substrate concentration}/\text{fluorescent intensity}$  versus  $\text{substrate concentration}$ . The intercept on the x-axis gives  $-K_m$ , and on the y-axis  $K_m/V_{\max}$ . The slope is  $1/V$ .

### 6.4.2. $K_i$ Determinations

$K_i$  or inhibition constant is the dissociation constant for the enzyme-inhibitor complex.  $K_i$  for competitive inhibition is calculated as follows,

$$K_i = \frac{K_m [I]}{K_m^{\text{app}} - K_m}$$

**Where:**

$K_i$  is the inhibition constant

$K_m$  is the Michaelis constant with no inhibitor present

$[I]$  is the inhibitor concentration

$K_m^{\text{app}}$  means the new or "apparent" value of  $K_m$  in the presence of  $I$ , the inhibitor.

Measured as for  $K_m$  (section 6.4.1.).

When inhibition is not competitive, the  $K_i$  value is calculated as follows,

$$K_i = \frac{V_{\max}^{\text{app}} [I]}{V_{\max} - V_{\max}^{\text{app}}}$$

**Where:**

$K_i$  is the inhibition constant

$V_{\max}$  is the maximum velocity with no inhibitor present

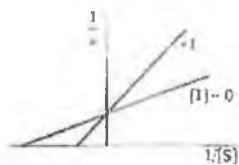
$[I]$  is the inhibitor concentration

$V_{\max}^{\text{app}}$  means the new or “apparent” value of  $V_{\max}$  in the presence of I, an uncompetitive or non-competitive inhibitor.

#### 6.4.3. Types of Reversible Inhibition

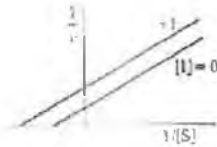
Inhibitors can be divided into two groups, reversible and irreversible. Reversible inhibition involves noncovalent forces that bind inhibitors to enzymes. There are several types of reversible inhibition: competitive, uncompetitive, non competitive and mixed. Distinguished, using the Lineweaver-Burk plot, by determining the effect of inhibitor on  $K_m$ ,  $V_{\max}$  and  $K_m/V_{\max}$ .

**Competitive Inhibition:** Involves the binding of an inhibitor to the enzyme forming an enzyme-inhibitor complex. The inhibitor bearing a structural and chemical similarity to the substrate binds to the active site thus competing with it for substrate.



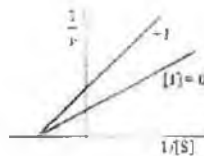
In competitive inhibition, the slope of the Lineweaver-Burk plot increases. The  $K_m$  value also increases but the  $V_{\max}$  value is unchanged. This type of inhibition is recognised by plots intersecting at a common point on the positive y-axis.

**Uncompetitive inhibition:** Involves binding only to the enzyme-substrate complex to prevent catalysis.



This type of inhibition causes a decrease in  $K_m$  and  $V_{max}$ . There is no change in the slope of the Lineweaver-Burk plot. It is identified by the presence of parallel lines in the Lineweaver-Burk plot.

**Non-competitive inhibition:** Involves binding equally to enzyme and enzyme-substrate complex.



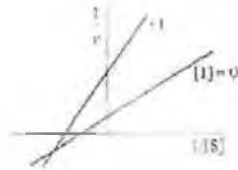
This type of inhibition causes a decrease in  $V_{max}$  along with  $K_m$  remaining the same. The slope of the Lineweaver-Burk plot increases and is recognisable by plots intersecting at a common point on the negative x-axis.

**Mixed Inhibition:** These inhibitors bind unequally to both enzyme and enzyme-substrate complex. There can be two cases with these inhibitors,

Mixed competitive-non-competitive increase  $K_m$  and decrease  $V_{max}$ . They cause an increase in the Lineweaver-Burk slope and are identified by plots intersecting above the negative portion of the x-axis.



Mixed non-competitive-uncompetitive decrease both  $K_m$  and  $V_{max}$ . The Lineweaver-Burk plot slope is increased and plots intersecting below the negative portion of the x-axis identify this type of inhibition.



#### 6.4.4. $IC_{50}$ Determination

The concentration of inhibitor that reduces enzyme velocity by 50% is known as the  $IC_{50}$  value. It can be determined graphically as shown below.

